PEGylated cationic polyacrylates for transfection : synthesis, characterization, DNA complexation and cytotoxicity

Maël Le Bohec

UNIVERSITE BRETAGNE LOIRE

Le Mans Université

Thèse de Doctorat

Maël LE BOHEC

Mémoire présenté en vue de l'obtention du
grade de Docteur de Le Mans Université
sous le sceau de l'Université Bretagne Loire

École doctorale : 3M

Discipline : *Chimie Moléculaire et Macromoléculaire, CNU33*
Spécialité : *Chimie et Physico-chime des polymères*
Unité de recherche : ***IMMM, UMR-CNRS6283***

Soutenue le 30 octobre 2017
Thèse N° : 2017LEMA1027

PEGylated cationic polyacrylates for transfection: synthesis, characterization, DNA complexation and cytotoxicity

JURY

Rapporteurs :	**Rachel O'REILLY**, Profesor, Warwick Univesity (U.K.) **Richard HOOGENBOOM,** Profesor, Ghent University (Belgium)
Examinateurs :	**Philippe GUEGAN,** Professeur, Université Pierre-Marie Curie (Paris 6, France)
Directeur de Thèse :	**Sagrario PASCUAL**, Maître de Conférence HDR, Le Mans Université (France)
Co-directeur de Thèse :	**Laurent FONTAINE**, Professeur, Le Mans Université (France)
Co-encadrant de Thèse :	**Sandie PIOGE**, Maître de Conférence, Le Mans Université (France)

Le Mans Université

DEMANDE D'AUTORISATION DE SOUTENANCE DE THÈSE

avec confidentialité du mémoire de thèse et/ou à huis clos

(article 19 de l'arrêté du 25 mai 2016)

Je, soussigné(e), Sagrario Pascual ..... , directeur de thèse de :

NOM : Le Bohec NOM d'usage :

Prénom : Maël

Sollicite, de Monsieur le chef d'établissement et de Monsieur le directeur de l'école doctorale,

☒ la confidentialité du mémoire de thèse pour une durée de : 9 mois.....

☐ l'autorisation de soutenir la thèse à huis clos[1] à la date prévue du : .....

Titre de la thèse : Polyacrylates cationiques PEGylés pour la transfection : synthèse, caractérisation, complexation avec de l'ADN et cytotoxicité

Motif(s) de la demande : Des résultats ne sont pas encore publiés et seront publiés au plus tard 9 mois après la soutenance de thèse. Par ailleurs, des stratégies de modification chimique de polymères, développées dans la thèse de Maël Le Bohec font l'objet d'une prospective industrielle..

.....

A Le Mans , le 29/09/2017

Signature du doctorant

Signature du directeur de thèse

Avis du directeur ou du directeur adjoint de l'école doctorale :	Le chef d'établissement :
☒ avis favorable ☒ à la confidentialité du mémoire ☐ à la soutenance à huis clos ☐ avis défavorable ☐ à la confidentialité du mémoire ☐ à la soutenance à huis clos Signature	☒ autorise ☒ la confidentialité du mémoire ☐ la soutenance de la thèse à huis clos ☐ n'autorise pas ☐ la confidentialité du mémoire ☐ la soutenance de la thèse à huis clos Signature

[1] Conformément à l'article 19 de l'arrêté du 25 mai 2016 relatif à la formation doctorale : *« la soutenance est publique, sauf dérogation accordée à titre exceptionnel par le chef d'établissement si le sujet de la thès présente un caractère confidentiel avéré. »*

“Neb a oar a gavo zeskift”

« Qui ne sait trouvera à s’instruire »

“Who doesn’t know will find to educate himself”

Proverbe Breton, Breton proverb

Acknowledgements

This work has been performed in the Institut des Molécules et Matériaux du Mans (IMMM)-UMRCNRS-6283 Laboratory in the Méthodologie et Synthèse des Polymères (MSP) team in Le Mans université. First, I would like to thanks the Collectivité Locales Sarthoises for the financial support.

Then, I would like to express my sincere gratitude to my supervisor the Dr Sagrario Pascual, to give me her trust for the PhD. I would like to apologize my-self for the numerous corrections of this work. Moreover I would like to thanks the Dr Sagrario Pascual for all the advices during my PhD and when I was a simple student, for her kindness, for her support, her understanding for the PhD and for everyday life.

I would like to thanks warmly my co-supervisor, Dr Sandie Piogé, to give me her trust for my Master 2 internship and the PhD. I would like to thanks the Dr Sandie Piogé to have pushed me during the Master 2 internship to improve myself, for her advices, all her encouraging words, her humor and her good mood.

I would like to give many grateful thanks to my co-supervisor, Pr Laurent Fontaine to welcome me in his laboratory. I would like to thanks him, for his advices, for his ideas and to trust me as a chemistry teacher. I would like to thanks him as the teacher to guide me in my career path.

I would like to express my sincere gratitude to the Pr. Rachel O'Reilly and the Pr Richard Hogenboom to report my PhD work. I am honored that they accepted to do this work.

I am really honored that the Pr. Philippe Guégan accepted to preside the evaluation comitee of my PhD. I would like to thanks him for his advices and his evaluation.

I would like to thanks warmly Dr. Nathalie Casse for her help for the gel retardation assay and her kindness.

Acknowledgements

I would like to express my sincere gratitude to the Dr Simona Mura, Stéphanie Denis and the Dr Julien Nicolas from the Galien institute for their warm welcome and their help for cell viability assays. I would like to thanks Pr Elias Fattal to allow me to perform cell viability assay within his team. I thank all the PhD student and interns for their welcome and their kindness.

I would like to give many grateful thanks to the Pr. Véronique Montembault for her help and for their advices for education. I would like to thanks the Dr. Pamela Passeto and the Dr. Arnaud Noury.

I would like to thanks Patricia Gangnery for HR-MS analyses and Corentin Jacquemmoz for NMR analyses. I would like to thanks warmly Emmanuelle Mebold for the numerous and difficult MALDI-TOF analyses and for the formation on SEC.

I would like to thank Dr Gwenaël Forcher and Alexandre Bénard for the azlactone syntheses. I would like to especially thank Alexandre Bénard for the advices for the chromatography column and for the invitations.

I would like to give grateful thanks to Anita Loiseau, Emilie Choppé, Aline Lamber and Clément Brière for their help and their kindness.

I would like to thanks Maud, my office co-worker, for the song contests and all the "stories" we talk about. I would like to thanks Clémence for all the work she done during her internship and all the discussions. I would like to thanks Joachim for his wisdom and his culture. I would like all the PhD student I met, Walailuk for all her stories, Cécile for all her journey, Nguyet for sweet potatoes, Lionel (Dr Lionel Lauber) for all politic debates, Julien and Héloïse for the association and Malika (Dr Malika Talantikite) for her humor.

I would like to thanks the interns who worked on this project: Kévin, Stève and Whenao.

Acknowledgements

I would like to thanks all the people I met during this PhD: Thomas, Sylvain, Flavien, Fabien, Kévin, Batiste, Justine, Kévin, Paul, Léo, Océane, Antoine… I forget many of them and I would like to thanks them too.

I would like to thanks all my good friends who support me and especially: Maxime, Ludovic, Jérémy (aka Djé), Matthieu, Vincent (aka Mouth) and Jéremy (aka Minidou).

I would like to thanks my family, my parents, André et Marie-Christine, my brother Erwan, my sister and her husband, Anne et Benoit, my step-father, Fabien and my nieces, Ninon and Maïlys, who help me to be in good spirit.

I would like to finish by thanking, the one who has support me the most during these three years, who has listen me, the one who give me her energy and courage. Thank you for all Laura.

Remerciements

Ce travail a été effectué au sein de l'Institut des Molécules et Matériaux du Mans (IMMM) – UMRCNRS-6283 dans l'équipe Méthodologie et Synthèse des Polymères (MSP) à l'Université du Mans et Laval. Je voudrais tout d'abord remercier les collectivités locales Sarthoises pour avoir financé ce doctorat.

Je souhaite ensuite remercier le Dr Sagrario Pascual, ma directrice de thèse, pour m'avoir accordé sa confiance pour le Master 2 et pour la thèse. Je tiens à présenter mes excuses pour les longues corrections de cette thèse. Mais je dois surtout remercier le Dr Sagrario Pascual pour tous les conseils qu'elle a pu me donner entant que doctorant ou simple étudiant. Je dois dire encore merci pour sa gentillesse, ses encouragements et sa compréhension pour la thèse et aussi dans la vie de tous les jours.

Je souhaite remercier tout aussi chaudement le Dr Sandie Piogé, ma co-encadrante de thèse, pour m'avoir accordé aussi sa confiance pour le Master 2 et la thèse, pour m'avoir poussé pendant le Master 2 pour donner le meilleur de moi-même. Je tiens aussi à remercier le Dr Piogé pour tous ses conseils, sa bonne humeur, son humour et toutes les paroles encourageantes qu'elle a pu me dire.

Je souhaite aussi remercier le Pr Laurent Fontaine, mon co-directeur de thèse, pour m'avoir accueilli tout d'abord dans son équipe puis dans son laboratoire. Je tiens aussi à le remercier en tant que co-directeur de thèse pour m'avoir conseillé, aiguillé dans mes choix, pour avoir donné de si bonnes idées et pour m'avoir fait confiance en tant qu'enseignant de chimie organique. Je tiens aussi à le remercier entant qu'enseignant pour avoir fait partie des personnes qui m'ont guidé vers la voie que j'ai choisi.

Je tiens aussi à remercier le Pr Rachel O'Reilly et le Pr Richard Hogenboom pour avoir accepté de rapporté ma thèse. Je dois aussi leur dire combien je suis honoré qu'ils aient effectué ce travail.

Remerciements

Je suis très honoré que le Pr. Philippe Guégan ait accepté de présider le comité d'évaluation ma thèse. Je me dois aussi de le remercier pour son évaluation et ses conseils.

Je dois aussi remercie le Dr Nathalie Casse pour son aide pour l'électrophorèse et sa gentillesse.

Je souhaite remercier grandement Stéphanie Denis, Dr Simona Mura et Dr Julien Nicolas de l'institut Galien pour leur accueil et leur aide pour les tests de cytotoxicité. Je souhaite aussi remercier le Pr Elias Fattal pour m'avoir accueilli au sein de son laboratoire. Je remercie aussi tous les doctorants et les stagiaires de l'institut qui ont su très bien m'accueillir

Je tiens à remercier le Pr. Véronique Montembault pour son accueil au sein de de l'équipe MSP et de m'avoir donné de précieux conseils pour l'enseignement. Je remercie aussi le Dr. Pamela Pasetto et le Dr. Noury

Je souhaite aussi remercier Patricia Gangnery pour les analyses de spectrométrie de masse, Corentin Jacquemmoz pour les analyses de spectrométrie RMN. Je souhaite aussi remercier grandement Emmanuelle Mebold pour les nombreuses spectrométries de masse MALDI-TOF parfois bien compliqués et de m'avoir formé à la SEC DMF.

Je dois aussi remercier le Dr Gwenaël Forcher et Alexandre Bénard pour la synthèse d'azlactone. Je tiens à remercier spécialement Alexandre pour les invitations et pour les conseils pour les colonnes de chromatographie.

Je souhaiterais aussi remercier Anita Loiseau, Emilie Choppé, Aline Lambert et M. Clément Brière pour leur aide et leur gentillesse.

Je dois aussi remercier Maud, ma collègue de bureau, merci pour les concours de chant et toutes les petites « histoires » qu'on a pu se raconter. Merci à Joachim pour sa sagesse et sa culture. Merci à Clémence Nicolas pour tout le travail qu'elle a pu faire pendant ses stages mais aussi à toutes les discussions qu'on a pu avoir. Je dois aussi remercier tous les autres doctorants,

Walailuk Inthavong et toutes ses histoires, Cécile Barthelet et ses voyages, Thi Nguyet Tran et ses patates douces, Lionel Lauber et les débats politiques, Julien Caille et Héloïse Fabre pour l'association et le Dr Malia Talantikite pour son humour.

Je remercie aussi les stagiaires qui ont travaillé sur ce projet : Kévin, Stève et Whenao

Je tiens aussi à remercier tous les autres personnes que j'ai rencontrées lors de cette thèse : Thomas,Sylvain, Flavien, Fabien, Kévin, Batiste, Justine, Kévin, Paul, Léo, Océane…J'en oublie certainement et je les remercie aussi.

Je remercie évidemment tous les amis qui m'ont soutenu et plus particulièrement Maxime, Ludovic, Jérémy (dit Djé), Matthieu, Vincent (dit Mouth) et Jérémy (dit Minidou).

Je souhaite remercier mes parents, André et Marie-Christine, mon frère Erwan, ma sœur Anne, mon beau-frère Benoit pour m'avoir soutenu et redonner le moral, Fabien, mon beau-père et mes nièces Ninon et Maïly qui ont tout le temps su me redonner le sourire.

Je finirais par remercier celle qui a su me supporter pendant ces trois ans, celle qui m'a le plus écouté. Merci Laura.

Abbreviations

A_{343nm}	Absorbance at 343 nm using UV spectrophotometry
ACVA	4,4-azobis-4-cyanolaveric acid
AEA	Aminoethyl acrylate
AEMA	Aminoethyl methacrylate
AHMA	Aminohexyl methacrylate
AIBN	2,2'-azobis(isobutyronitrile)
Alkyne-AZL	L-(4,4-dimethyl-5-oxo-4,5-dihydrooxazol-2-yl)ethylhex-5-ynoate
aPEO-CTA	α-alkynyl,ω-dodecyltrithiocarbonate PEO
$A_{t0,RI}$	SEC peak areas before reaction using RI detection
$A_{t0,UV}$	SEC peak areas before reaction using UV-vis detection at 309 nm
$A_{t,RI}$	SEC peak areas at a given time using RI detection
$A_{t,UV}$	SEC peak areas at a given time using UV-vis detection at 309 nm
ATRP	Atom Transfer Radical Polymerization
bPEI	Branched Poly(Ethylene Imine)
bPEO	Brush-like poly(ethylene oxide)
CbzLL	Carbobenzyloxy-*L*-Lysine
CDP	4-cyano-4-[(dodecylsulfanylthiocarbonyl)sulfanyl]pentanoic acid
C_{MPt18h}	Molar concentration of 2-mercaptopyridine after 18h of thiol-disulfide coupling reaction
COPYDC	2-cyano-5-oxo-5-(prop-2yn-1-ylamino)pentan-2-yl
CPADB	4-cyanopentanoic acid dithiobenzoate
CPDB	4-cyano-2-propyl dithiobenzoate

cPEI	Cyclic PEI
C_{PEOt0}	Initial molar concentration of α-pyridyldithio,ω-hydroxylPEO in the thiol-disulfide coupling reaction
$C_{PEOt18h}$	Molar concentration of α-pyridyldithio,ω-hydroxylPEO after 18h of thiol-disulfide coupling reaction
cRGD	Cyclic tripeptide arginine-glycine-aspartate
CTA	Chain Transfer Agent
DCC	Dicyclohexylcarbodiimide
DCTB	*Trans*-2-[3-(4-*tert*-butylphenyl)-2-methyl-2-propenylidene]malonitrile
DIC	Diisopropyl carbodiimide
DIT	Dithranol
DITH	DL-dithiothreitol
DLS	Dynamic light scattering
DMAEA	2-(*N,N*-dimethylamino)ethyl acrylate
DMAEMA	2-(*N,N*-dimethylamino)ethyl methacrylate
DMAP	4-(dimethylamino)pyridine
DMF	*N*,*N*-dimethyformamide
DMPP	Dimethylphenyl phosphine
DMSO	Dimethyl sulfoxide
DMT-MM	4-(4,6-dimethoxy-1,3,5-triazin-2-yl)-4-methylmorpholinium
DNA	Deoxyribonucleic acid
dPLL	Dendrimeric poly(L-Lysine)
$\overline{DP}_n$	Number-average degree of polymerization
$\overline{DP}_{n,MALDI}$	Number-average degree of polymerization calculated from MALDI-TOF spectrometry

E	Molar attenuation coefficient of 2-mercaptopyridine
EDCI	*N*-(3-dimethylaminopropyl)-*N'*-ethylcarbodiimide
EDTA	Ethylenediaminetetraacetic acid
eGFP	Green fluorescent protein
EO	Ethylene oxide unit
FDA	Food and Drugs Administration
f_{DMAEA}	Molar ratio of DMAEA in the comonomer feed
F_{DMAEA}	Molar ratio of DMAEA in the copolymer
FITC	Fluorescein Isothiocyanate
FT-IR	Fourier-Transform Infrared Spectroscopy
hbPBAE	Hyper branched poly(β-aminoester)
hbPLL	Hyper branched poly(L-lysine)
HOBT	1-hydroxybenzotriazole
HPLC	High Performance Liquid Chromatography
HR-MS	High Resolution Mass Spectrometry
IgG	Immunoglobulin G
k_p	Propagation rate constant
k_p^{app}	Apparent propagation rate constant
l	Length of the UV-vis cell
LL	L-Lysine
lPBAE	Linear poly(β-aminoester)
lPDMAEMA	Linear PDMAEMA
lPEI	Linear poly(ethylene imine)
lPEO	Linear poly(ethylene oxide)

List of Abbreviations

LPhe	*L*-phenylalanine-L-Lysine
lPLL	Linear poly(L-lysine)
lRGD	Linear RGD
MALDI-TOF	Matrix-assisted laser desorption-ionization-time of flight
M_{COPYDC}	Molar mass of COPYDC
M_{DMAEA}	Molar mass of DMAEA
$\overline{M_{n,NMR}}$	Number-average molar mass in ^{1}H NMR analysis of the purified polymer
$\overline{M_{n,SEC}}$	Number-average molar mass in SEC analysis
$\overline{M_{n,th}}$	Number-average molar mass in ^{1}H NMR analysis of the crude polymer determined with the monomer conversion
mPEO-CTA	α-methoxy,ω-dodecyltrithiocarbonate PEO
$M_{t\text{BocAEA}}$	Molar mass of *t*BocAEA
MTT	3-[4,5-dimethylthiazol-2-yl]-3,5-diphenyltetrazolium bromide
NaTFA	Sodium trifluroacetate
NMM	4-methylmorpholine
NMR	Nuclear magnetic resonance
OJ10 (SMOJ10)	*Sphingobacterium multivorum*
PAA	Poly(acrylic acid)
PBAE	Poly(β-amino ester)
PBS	Phosphate buffer solution
PCbzLL	Poly(carbobenzyloxy-*L*-Lysine)
pCMV-DsREd	pDNA coding for red fluorescent protein
pCMV-LacZ	Mammalian expression vector
pCMV-Luc	pDNA containing the firefly luciferase gene

PDEAEMA	Poly(2-(*N,N*-diethylamino)ethyl methacrylate)
PDMAEMA	Poly(2-(*N,N*-dimethylamino)ethyl methacrylate)
PDMAEMAm	Poly(2-(*N,N*-dimethylamino)ethyl methacrylamide)
PDMAPMA	Poly(3-(*N,N*-dimethylamino)propyl methacrylate)
PDMAPMAm	Poly(3-(*N,N*-dimethylamino)propyl methacrylamide)
pDNA	Plasmid deoxyribonucleic acid
PEI	Poly(ethylene imine)
PEGA	Oligo(ethylene glycol) acrylate
PEO	Poly(ethylene oxide)
PEO-CTA	Poly(ethylene oxide) macromolecular chain transfer agent
PLL	Poly(L-Lysine)
PNIPAM	Poly(*N*-isopropylacrylamide)
PPEGA	Poly(oligo(ethylene glycol) acrylate)
PPEGA-CTA	oligo(poly(ethylene glycol) acrylate) chain transfer agent
PPEGMA	Poly(oligo(ethylene glycol) methacrylate
PTMAEMA	Poly(2-(*N,N,N*-trimethylammonium)ethyl methacrylate)
PRSVlucDNA	Luciferase reporter gene obtained from cobra
PS	Polystyrene
RAFT	Reversible addition-fragmentation chain transfer
r_{DMAEA}	Reactivity ratio of DMAEA unit
RDRP	Reversible deactivation radical polymerization
RGD	Tripeptide arginine-glycine-aspartate
RI	Refractive index
ROP	Ring-opening polymerization

rPDMAEMA	Reducible poly(2-(*N,N*-dimethylamino)ethyl methacrylate)
$r_{t\text{BocAEA}}$	Reactivity ratio of *t*BocAEA unit
SEC	Size exclusion chromatography
sPDMAEMA-3	Star poly(2-(*N,N*-dimethylamino)ethyl methacrylate) with 3 arms
sPDMAEMA-5	Star poly(2-(*N,N*-dimethylamino)ethyl methacrylate) with 5 arms
SPDP	Succunimidyl 3-(2-pyridildithio)propionate
StA1	*Streptomyces albulus*
τ	Degree of functionalization of thiol-yne coupling reaction
*t*BocAEA	*N*-(*tert*-butoxycarbonyl)amino-ethyl acrylate)
*t*BocAEMA	*N*-(*tert*-butoxycarbonyl)aminoethyl methacrylate
*t*BocAHMA	*N*-(*tert*-butoxycarbonyl)aminohexyl methacrylate
TFA	Tritfluoroacetic acid
TGN	12-amino acid peptide: TGNYKALHPHNG
UV	Ultraviolet
UV-vis	Ultra-violet visible
ω	Total conversion of both DMAEA and *t*BocAEA

Cell lines

A431	Human epidermoid carcinoma epithelial cells
A-549	Adenocarcinoma human alveolar basal epithelial cells
B16F10	Mouse musculus melanoma cells
BCEC	Brain capillary endothelial cells
Bel7402	Human hepatocellular carcinoma cells

List of Abbreviations

BGC-823	Human gastric adenocarcinoma cells
C2C12	Mouse muscle embryoblast cells
CHO-DG44	Dihydrofolate reductase deficient Chinese Hamster Ovary cells
CHO-K1	Chinese hamster ovary epithelial like cells
COS-7	Cercopithecus aethiops kidney fibroblast
EA.hy926	Human somatic cell hybrid endothelial
HAE	Human aortic endothelial cells
HEK293	Human Embryonic Kidney cells
HeLa	Human Cervical cancer cells
Hep-G2	Human liver epithelial cells
HFF1	human foreskin fibroblast cells
HUVEC	Human umbilical vein endothelial cells
MDA-MB-231	Human breast carcinoma cells
MiaPaCa	Human pancreatic adenocarcinoma cells
NHK	Normal human keratinocytes cells
NIH-3T3	Mouse embryo fibroblast cells
OVCAR-3	Human ovary adenocarcinoma cells
RDEBK	Epidermolysis bullosa keratinocyte cells
SHSY-5Y	Human bone marrow neuroblastoma cells

Chapter 2: Synthesis and characterization of PEO macromolecular chain transfer agents

Chapter 3: Synthesis and characterization of (PEGylated) aminoethyl-based polyacrylates

Chapter 4: Chain-ends modification of (PEGylated) aminoethyl-based polyacrylates

Chapter 5: cationic (PEGylated) aminoethyl-based polyacrylates: pDNA complexation and cytotoxicity.

General Introduction

General Introduction

Gene therapy is a technique that uses genes to treat or prevent diseases due to genetic disorders. Such technique is based on the introduction of healthy or new genes into a patient's cells. Therefore, efficient delivery of exogenous genetic material is crucial in gene therapy.

Different strategies are available to achieve efficient gene delivery. Physical-based ones such as electroporation or sonoporation are not desirable because of complex protocols and the associated high tendency to induce cellular damage leading to necrosis.[1] Viral-based gene delivery systems including retroviruses and adenoviruses[2] have been employed. The first clinical trial was made in 1989 by Rosenberg *et al.*[3] to treat metastatic melanoma using retroviruses. Despite their high performance, the wide application of adenoviral and retroviral-mediated transfection for therapeutic purposes is limited by their toxicity and immunogenicity. The use of adenoviruses to treat partial ornithine transcarbamylase led to a patient death during a clinical trial in 1999.[4,5]

Consequently, the research and the development of synthetic non-viral gene delivery systems is strongly encouraged. Over time, cationic polymers have notably attracted keen attention, due to their ability to interact with cells more effectively and with higher stability compared to other chemically designed non-viral gene delivery systems, such as cationic lipids.[6–10] For instance, Escande and coworkers,[11] have shown that polymers enhanced gene delivery from the cytoplasm to the nucleus in comparison with cationic lipids and that transgene expression in the nucleus was prevented by complexation with cationic lipids but not with cationic polymers. Moreover, the easy control of the physical parameters (e.g., hydrophobicity, charge) of polymer systems represents an additional advantage over lipidic systems. Many reviews have been published on cationic polymeric systems for gene delivery and it appears that each system has its pros and cons to achieve a high transfection efficiency with a low cytotoxicity.[6–10] This is probably due to the fact that an efficient gene delivery necessitates a combination of numerous requirements (e.g., efficient deoxyribonucleic acid (DNA)

complexation, polyplex stability under physiological conditions, cell recognition, endosomal escape, cellular uptake, DNA release). For complexation, the positive charges of cationic polymers interact through electrostatic bindings with the anionic charges of DNA due to the phosphate groups of the backbone. The resulting DNA/polymer complex also named polyplex, has to overcome several barriers for an efficient gene delivery.(Scheme 1)[8,12–16]

First, the polyplex has to travel through the blood circulation. Indeed, a naked DNA can be uptaken by different cells as Kupffer hepatic macrophages cells, leading to the phagocytosis of DNA.[17] The cationic polymer allows to "hide" the negative charges of DNA and stop the uptake by macrophages cells.[17,18] Moreover, the polyplex has to be stable in the blood to avoid any accumulation in different tissues. The addition of a hydrophilic part such as poly(ethylene oxyde) (PEO) avoid any binding between the polyplex and specific proteins in the blood.[19] Such interactions lead to the opsonization of the polyplex. The opsonization is a major barrier to the transfection due to the coating of the polyplex by specific plasma proteins, leading to the clearance of the polyplex. Once the polyplex has gone through the blood, it has to go inside the cell.

The next barrier is the cell membrane which has to be penetrated. This step, named cellular uptake, occurs by endocytosis.[20] To go through the membrane, the cationic polymer has to form electrostatic interactions with anionic cell surface proteoglycans.[21] The interaction of the cationic polymer with specific proteins leads to the internalization of the polyplex *via* endocytosis. Indeed, it has been shown that a poly(L-Lysine) (PLL) cannot transfect Raji cells, as such cells do not possess proteoglycans proteins.[22] This pathway is specific to the cationic polymers which do not get recognition ligands. Such recognition ligands are able to bind the polyplex to specific receptors on the cell surface. This binding allows the polyplex to be internalized by clathrin-dependent endocytosis pathway. In this pathway, the polyplex is trapped in the endocytic vesicles which fuse with the endosome.[23] Then, the polyplex escapes

from the endosome to go to the cytoplasm. Once in the cytoplasm, the DNA has to be released from the cationic polymer to enter the nucleus. The polyplex can be dissociated thanks to specific enzymes and partially in the endosome.[13] To improve the DNA release, degradable cationic polymers can be used, such as polymers containing biodegradable bonds or hydrolysable bonds. Furthermore, a better elimination of the cationic polymer by the cell is targeted when using degradable cationic polymers.

Based on previous studies,[6–10] the key structural parameters to overcome all requirements to target a high transfection efficiency and a low cytotoxicity are: (i) cationic amine entities for DNA complexation and endosomal escape, (ii) PEGylation to achieve a high polyplex stability and to hinder the reticuloendothelial recognition allowing longer circulation, (iii) ligands capable to target specific cell membrane receptors for an efficient cell recognition and cellular uptake and (iv) degradable polymers for efficiently release DNA and to reduce cytotoxicity. Many studies have evaluated some of the previously mentioned key structural parameters from many different polymers.[6–10] However, the adequate combination of all these structural parameters in a unique polymer scaffold has not been reported yet.

In this context, the aim of this research work is to synthesize one single polymer chain containing both cationic amines and degradable entities by using aminoethyl-based polyacrylates, a covalently linked PEO chain and specific chain-ends to anchor recognition ligands. The interest of such polymer is its aptitude to efficiently complex DNA, its self-degradation capacity and its ability to react with recognition ligands.

The emergence of controlled/living polymerizations including radical deactivation chain transfer polymerization (RDRP) techniques and versatile strategies for polymer chain-ends modification constitutes a scientific breakthrough for polymer chemists.[28,29] The reversible addition-fragmentation transfer (RAFT) polymerization, the thiol-disulfide exchange reaction

and the thiol-yne coupling reaction able to be performed under mild conditions have been applied to synthesize our multi-structural single polymer chain.[30–32] The structure/complexation and the structure/cells viability relationships have been investigated during this work.

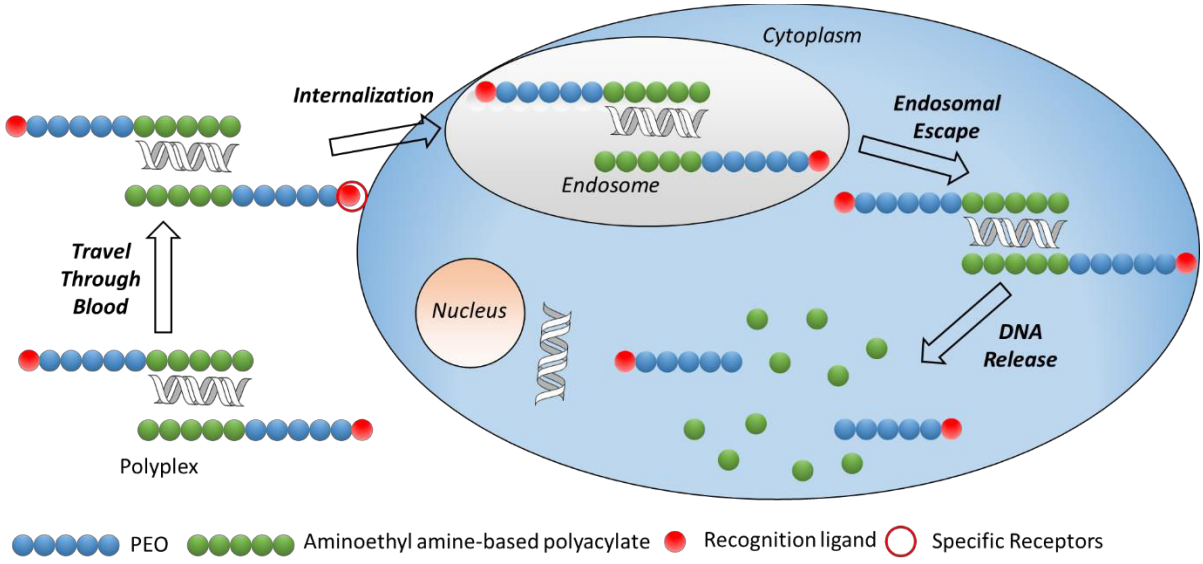

Scheme 1. Barriers to overcome and key structural parameters on a polymer for an efficient gene delivery.

This Ph. D manuscript is organized in five chapters.

The first chapter is a bibliographic study on cationic polymers used for DNA delivery. Their synthesis, their efficiency to deliver DNA into cells and their cytotoxicity are discussed.

The second chapter describes the synthesis of macromolecular chain transfer agents based on linear PEO (lPEO) and brushed-like PEO (bPEO). A heterofunctional lPEO with thiol reactive functions at the α-position and a trithiocarbonate chain transfer agent moiety at the ω-position have been synthesized and fully characterized using different strategies. A heterofunctional bPEO has been synthesized by RAFT polymerization using a new alkyne-based chain transfer agent.

The third chapter describes the RAFT copolymerization of two aminoethyl acrylates using a lPEO and a bPEO macromolecular chain transfer agents, and an alkyne-based chain transfer agent. Then, the cationization of the repeating units to form the PEGylated cationic copolymers is discussed.

The fourth chapter describes the trithiocarbonate removal reaction using thermal- and photochemical-activation and the thiol-yne and disulfide exchange coupling reactions to functionalize the PEGylated cationic copolymer using thiol-based molecules.

The fifth chapter describes the pDNA complexation and the cytotoxicity of cationic polymers according to the PEO architectures, the trithiocarbonate removal and the molar composition of cationic copolymers.

References

(1) Mehier-Humbert, S.; Guy, R. H. Physical Methods for Gene Transfer: Improving the Kinetics of Gene Delivery into Cells. *Advanced Drug Delivery Reviews* **2005**, *57* (5), 733–753.

(2) Misra, S. Human Gene Therapy: A Brief Overview of the Genetic Revolution. *Journal of the Association of Physicians of India* **2013**, *61* (2), 127–33.

(3) Rosenberg, S. A.; Aebersold, P.; Cornetta, K.; Kasid, A.; Morgan, R. A.; Moen, R.; Karson, E. M.; Lotze, M. T.; Yang, J. C.; Topalian, S. L.; Merino, M. J.; Culver, K.; Miller, A. D.; Blaese, R. M.; Anderson, W. F. Gene Transfer into Humans — Immunotherapy of Patients with Advanced Melanoma, Using Tumor-Infiltrating Lymphocytes Modified by Retroviral Gene Transduction. *New England Journal of Medicine* **1990**, *323* (9), 570–578.

(4) Baum, C. Side Effects of Retroviral Gene Transfer into Hematopoietic Stem Cells. *Blood* **2003**, *101* (6), 2099–2113.

(5) Lehrman, S. *Virus Treatment Questioned after Gene Therapy Death*; Nature Publishing Group, **1999**.

(6) Lalani, J.; Misra, A. 4 - Gene Delivery Using Chemical Methods. In *Challenges in Delivery of Therapeutic Genomics and Proteomics*; Elsevier: London, **2011**; pp 127–206.

(7) Yue, Y.; Wu, C. Progress and Perspectives in Developing Polymeric Vectors for in Vitro Gene Delivery. *Biomaterials Science* **2013**, *1* (2), 152–170.

(8) Nguyen, D. N.; Green, J. J.; Chan, J. M.; Langer, R.; Anderson, D. G. Polymeric Materials for Gene Delivery and DNA Vaccination. *Advanced Materials* **2009**, *21* (8), 847–867.

(9) Samal, S. K.; Dash, M.; Van Vlierberghe, S.; Kaplan, D. L.; Chiellini, E.; van Blitterswijk, C.; Moroni, L.; Dubruel, P. Cationic Polymers and Their Therapeutic Potential. *Chemical Society Reviews* **2012**, *41* (21), 7147-7194.

(10) J Tiera, M.; Shi, Q.; M Winnik, F.; C Fernandes, J. Polycation-Based Gene Therapy: Current Knowledge and New Perspectives. *Current Gene Therapy* **2011**, *11* (4), 288–306.

(11) Pollard, H.; Remy, J.-S.; Loussouarn, G.; Demolombe, S.; Behr, J.-P.; Escande, D. Polyethylenimine but Not Cationic Lipids Promotes Transgene Delivery to the Nucleus in Mammalian Cells. *Journal of Biological Chemistry* **1998**, *273* (13), 7507–7511.

(12) Zhang, X.-X.; McIntosh, T. J.; Grinstaff, M. W. Functional Lipids and Lipoplexes for Improved Gene Delivery. *Biochimie* **2012**, *94* (1), 42–58.

(13) Pouton, C. W.; Seymour, L. W. Key Issues in Non-Viral Gene Delivery. *Advanced Drug Delivery Reviews* **1998**, *34* (1), 3–19.

(14) Mintzer, M. A.; Simanek, E. E. Nonviral Vectors for Gene Delivery. *Chemical Reviews* **2009**, *109* (2), 259–302.

(15) Al-Dosari, M. S.; Gao, X. Nonviral Gene Delivery: Principle, Limitations, and Recent Progress. *The American Association of Pharmaceutical Scientits Journal* **2009**, *11* (4), 671–681.

(16) Zhang, Y.; Satterlee, A.; Huang, L. In Vivo Gene Delivery by Nonviral Vectors: Overcoming Hurdles. *Molecular Therapy* **2012**, *20* (7), 1298–1304.

(17) Hashida, M.; Mahato, R. I.; Kawabata, K.; Miyao, T.; Nishikawa, M.; Takakura, Y. Pharmacokinetics and Targeted Delivery of Proteins and Genes. *Journal of Controlled Release* **1996**, *41* (1), 91–97.

(18) Suk, J. S.; Xu, Q.; Kim, N.; Hanes, J.; Ensign, L. M. PEGylation as a Strategy for Improving Nanoparticle-Based Drug and Gene Delivery. *Advanced Drug Delivery Reviews* **2016**, *99*, 28–51.

(19) Kolate, A.; Baradia, D.; Patil, S.; Vhora, I.; Kore, G.; Misra, A. PEG — A Versatile Conjugating Ligand for Drugs and Drug Delivery Systems. *Journal of Controlled Release* **2014**, *192*, 67–81.

(20) Mellman, I. Ensocytosis and Molecular Sorting. *Annual Review of Cell and Developmental Biology* **1996**, *12* (1), 575–625.

(21) Iozzo, R. V. Matrix Proteoglycans: From Molecular Design to Cellular Function. *Annual Review of Biochemistry* **1998**, *67* (1), 609–652.

(22) Mounkes, L. C.; Zhong, W.; Cipres-Palacin, G.; Heath, T. D.; Debs, R. J. Proteoglycans Mediate Cationic Liposome-DNA Complex-Based Gene Delivery *in Vitro* and *in Vivo*. *Journal of Biological Chemistry* **1998**, *273* (40), 26164–26170.
(23) Stoorvogel, W.; Strous, G. J.; Geuze, H. J.; Oorschot, V.; Schwartzt, A. L. Late Endosomes Derive from Early Endosomes by Maturation. *Cell* **1991**, *65* (3), 417–427.
(24) Cotanda, P.; Wright, D. B.; Tyler, M.; O'Reilly, R. K. A Comparative Study of the Stimuli-Responsive Properties of DMAEA and DMAEMA Containing Polymers. *Journal of Polymer Science Part A: Polymer Chemistry* **2013**, *51* (16), 3333–3338.
(25) Truong, N. P.; Jia, Z.; Burgess, M.; Payne, L.; McMillan, N. A. J.; Monteiro, M. J. Self-Catalyzed Degradable Cationic Polymer for Release of DNA. *Biomacromolecules* **2011**, *12* (10), 3540–3548.
(26) Truong, N. P.; Jia, Z.; Burges, M.; McMillan, N. A. J.; Monteiro, M. J. Self-Catalyzed Degradation of Linear Cationic Poly(2-Dimethylaminoethyl Acrylate) in Water. *Biomacromolecules* **2011**, *12* (5), 1876–1882.
(27) Ho, H. T.; Pascual, S.; Montembault, V.; Casse, N.; Fontaine, L. Innovative Well-Defined Primary Amine-Based Polyacrylates for Plasmid DNA Complexation. *Polymer Chemistry* **2014**, *5* (19), 5542-5545.
(28) Akeroyd, N.; Klumperman, B. The Combination of Living Radical Polymerization and Click Chemistry for the Synthesis of Advanced Macromolecular Architectures. *European Polymer Journal* **2011**, *47* (6), 1207–1231.
(29) Lunn, D. J.; Discekici, E. H.; Read de Alaniz, J.; Gutekunst, W. R.; Hawker, C. J. Established and Emerging Strategies for Polymer Chain-End Modification. *Journal of Polymer Science Part A: Polymer Chemistry* **2017**, *55* (18), 2903–2914.
(30) Ahmed, M.; Narain, R. Progress of RAFT Based Polymers in Gene Delivery. *Progress in Polymer Science* **2013**, *38* (5), 767–790.
(31) Hoogenboom, R. Thiol-Yne Chemistry: A Powerful Tool for Creating Highly Functional Materials. *Angewandte Chemie International Edition* **2010**, *49* (20), 3415–3417.
(32) Lin, C.; Engbersen, J. F. The Role of the Disulfide Group in Disulfide-Based Polymeric Gene Carriers. *Expert Opinion on Drug Delivery* **2009**, *6* (4), 421–439.

Chapter 1: Bibliographic Study

Introduction

Cationic polymers containing amines such as polyethyleneimine (PEI),[1] PLL,[2] poly(β-amino ester)s (PBAEs)[3] and amine-based vinylic polymers are commonly used and well characterized concerning their DNA delivery potential.[4] Modified cationic polymers have been studied in order to satisfy and meet all the following requirements e.g. good DNA complexation, serum stability, cellular uptake, endosomal escape and DNA release with a high transfection efficiency and with minimal cytotoxicity.

The shielding of the cationic polymer by PEO, also named PEGylation, tends to protect it from blood components and to increase its circulation time. PEO possesses many unique physical and biological properties including non-toxicity and excellent biocompatibility.[5–7] It has been confirmed that PEGylation increases nuclease resistance of complexed pDNA in serum supplemented physiological saline, providing steric protection against DNAse degradation to entrapped pDNA and reduces non-specific interactions between polyplexes and endogenous biomolecules.[5–7] Two main strategies have been developed to target PEGylated cationic polymers: the "PEO grafting onto" and the "PEO grafting from".

Although PEGylation will reduce cytotoxicity and endow polyplexes with stealth properties, it often leads to decreased transfection efficiency, likely due to interference with the polyplex-cell interactions[8] and thus to a reduced cellular uptake.[9] Therefore, the introduction of several recognition ligands (tripeptide arginine-glycine-aspartate (RGD), folate, anisamide, etc.) has been considered to achieve targeted uptake of polyplexes through receptor-mediated endocytosis.[10,11] The covalent linkage of recognition ligand is mediated through their reactive amine and thiol entities. Amine and thiol-chemistry reactions are performed in soft conditions (room temperature, aqueous solution) to keep the integrity of the recognition ligand.

Other structural parameters such as degradable linkages have been introduced within cationic polymers used for DNA delivery.[12] Depending on their position within the cationic polymer, in the backbone or in the pendant groups, such degradable linkages will either decrease the polymer cytotoxicity or either increases the transfection efficiency. The degradable linkages used for DNA delivery are either hydrolyzable groups or either biodegradable groups. The hydrolyzable linkages are generally ester function. Peptide linkage and disulfide linkage can be reduced by bioactivity.

In this chapter, the synthesis of PEI, PLL, PBAEs and amine-based vinylic polymers and the strategies, reported in the literature, to target PEGylated cationic polymers, to introduce recognition ligands and degradable moieties on cationic ligands have been described. The influence of the chemical structure of cationic polymer together with the addition of a PEO, of recognition ligands onto cationic polymers and the presence of degradable moieties within the cationic polymers on the polyplexes transfection efficiency and cytotoxicity will be discussed.

I. Cationic polymers for DNA delivery

As PEI,[1] PLL,[2] PBAEs and vinylic polymers widely studied in the literature as synthetic cationic polymers for gene delivery,[1,3,4] their synthesis together with their transfection efficiency and cytotoxicity will be described in this chapter.

A. Poly(ethylene imine) (PEI)

The PEI is called "the gold standard" of synthetic cationic polymers for DNA delivery as it is the most used and widely studied.[1,13] PEIs are classified into three categories depending on their architectures: linear PEI (lPEI), cyclic PEI (cPEI) and branched PEI (bPEI).

lPEIs are synthesized by a two steps reaction. The first step is the cationic Ring-Opening Polymerization (ROP) of 2-ethyl-2-oxazoline mostly initiated by methyl *p*-toluenesulfonate to form the poly(2-ethyl-2-oxazoline) and the second step is the hydrolysis, in acidic media, of amide functions (Scheme I. 1(A)).[14,15] The polymer backbone is based on protonable secondary amines which pKa values varied from 7.9 to 8.4.[14,16]

cPEIs can be formed by an intramolecular Huisgen click reaction of the α-alkynyl-ω-azidopoly(2-ethyl-2-oxazoline) followed by the hydrolysis of the resulting cyclic poly(2-ethyl-2-oxazoline) using hydrochloric acid (Scheme I. 1(B)).[15]

bPEI is synthesized *via* an acid-catalyzed ROP of aziridine.[17] Independently of its number-average molar mass, bPEI contains protonable primary (25 %), secondary (50 %) and tertiary amines (25 %) with pKa values equal to 4.5, 6.7 and 11.6, respectively.[18]

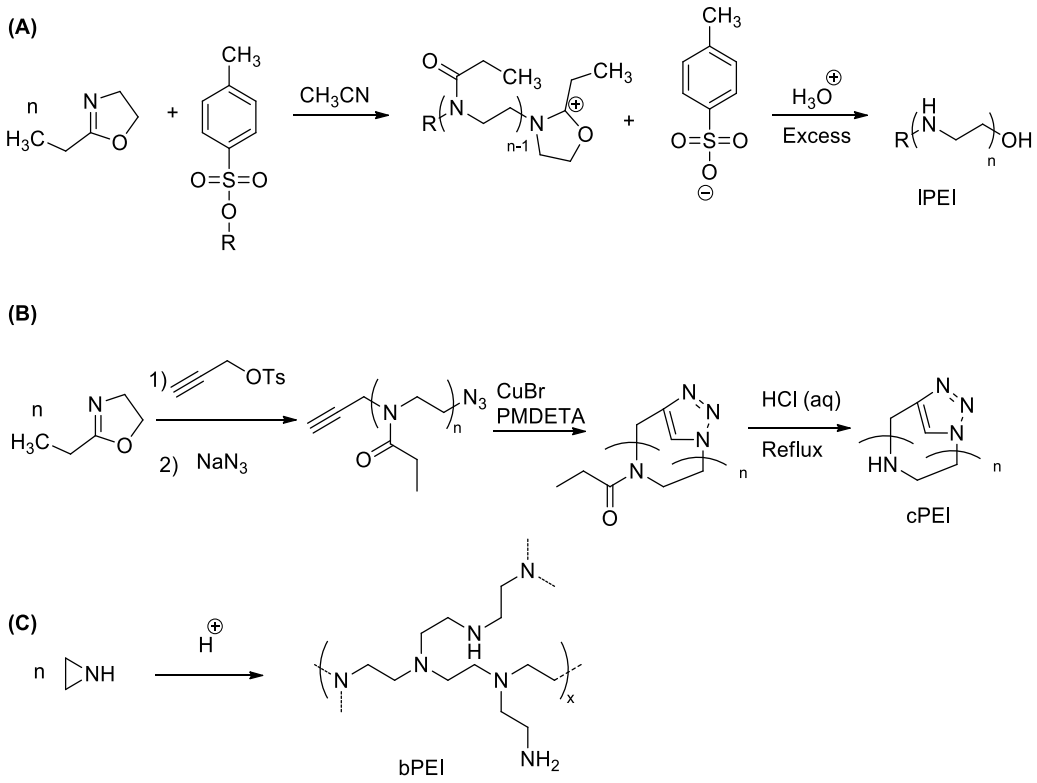

Scheme I. 1. Synthesis of (A) a lPEI as described by Brissault *et al.*[14], (B) a cPEI as described by Cortez *et al.*[15] and (C) a bPEI described by Zhuk *et al.*[17]

It has been shown that several PEI macromolecular characteristics such as number-average molar mass and architecture are important to control the transfection efficiency and cytotoxicity of such polymers.

It is well-known that PEIs with number-average molar masses below 5 kDa are insufficient in polyplex formation and stability.[19] However, for polymers with number-average molar masses above 5 kDa, Remy and co-workers[20] compared three lPEIs with different number-average molar masses (22 kDa, 88 kDa and 220 kDa) and resulting polyplexes with a nitrogen (N from PEI) to phosphorus (P from DNA) ratio (N/P) of 10/1. They showed a better transfection efficiency of pCMV-Luc, a plasmid DNA containing the firefly luciferase gene reporter, with the 22 kDa PEI to transfect NIH-3T3 cells, fibroblasts cells from mouse embryo.

The second important factor for DNA delivery using PEI is its architecture. Even if the comparison of lPEI, cPEI and bPEI with similar number-average molar masses is difficult as amines substitution, charge density or structural flexibility are different, some studies compared them. Cortez *et al.*[15] have compared lPEI and cPEI. They synthesized a range of lPEI and cPEI with the same number-average polymerization degree ranging from 21 to 84. They tested these polymers with different N/P ratios on transfection efficiency of pCMV-DsREd-express, a pDNA coding for red fluorescent protein on HAE and HFF1 cells, human aortic endothelial and human foreskin fibroblast, respectively. In all cases, cPEI seems to have better transfection efficiency than lPEI with similar number-average polymerization degree. The increase of transfection efficiency is explained by the increase of the charge density due to the more compact conformation of cPEI than the lPEI one.[15]

As transfection efficiency, PEI's cytotoxicity depends strongly of its number-average molar mass and architecture. A comparison between two lPEIs with different number-average polymerization degrees, 70 and 84, shows the increase of cytotoxicity with the increase of polymer number-average molar mass on HAE cells.[15] The same result was obtained with two cPEI with two different number-average polymerization degrees, 70 and 84. These results can be explained by the increase of charge density with increasing number-average molar mass of polymers. Indeed, the cationic charges are able to disrupt cell membrane.

However, a study on bPEI showed that the cytotoxicity of polymers can changed with different cell lines. Okon *et al.*[21] showed that an 800 Da bPEI is less toxic with HeLa cells, cell line derived from human cervical cancer and a 25 kDa bPEI is less toxic with Vero cells, kidney epithelial cells from an African green monkey. Thus, cytotoxicity depends of the physiology of cells too. The comparison of a lPEI and a bPEI with the same number-average molar mass (25 kDa) shows a lower cytotoxicity of lPEI than bPEI to transfect A431 cells, cell line derived from human epidermoid carcinoma, due to the decrease of the charge density. Indeed, the zeta

potential analysis of bPEI shows a charge density almost twice greater than lPEI: 28.7 mV for bPEI and 15.7 mV for lPEI.[22]

B. Poly(L-lysine) (PLL)

The protonable PLL with different architectures (linear PLL-lPLL, hyperbranched PLL-hbPLL and dendrimeric PLL-dPLL, (Scheme I. 2)) has been employed for DNA delivery thanks to its ability to complex easily DNA with strong electrostatic interactions.[23] PLL is a synthetic polyamide which owns cationic primary amines at neutral pH. lPLLs can be divided in two categories: the α-PLL and the ε-PLL (Scheme I. 2).

lPLLs can be synthesized using an easy reaction: thermal condensation of L-Lysine in bulk or in aqueous solution. However this reaction leads to a mixture of α- and ε-PLL.[24] To avoid such mixture, Kushwaha *et al.*[25] proposed to synthesize a linear ε-PLL using N_α-Butoxylcarbonyl-N_ε-Carbobenzyloxy-L-Lysine (N_α-Boc-N_ε-Cbz-L-Lysine). The polymerization is made step by step, repeat unit by repeat unit. However the process is harsh, using Lindlar palladium, and with several step, leading to a decrease of yield.[25] Another method to form linear ε-PLL avoiding the use of protecting groups has been reported. To synthesize only the ε-PLL, Ho *et al.*[26] used *N*-(3-dimethylaminopropyl)-*N'*-ethylcarbodiimide (EDCI). When the *N,N'*-dicyclohexylcarbodiimide (DCC) was used, only the α-PLL was formed.[27]

hbPLL is synthesized by heating L-Lysine (LL) at high temperature under basic medium and with several metalorganics catalysts as $Zr(O_nBu)_4$, $Ti(O_nBu)_4$, $Sb(OEt)_3$. These conditions lead to the amidification of the carboxylic acid with the amine of L-lysine.[28]

The synthesis of dPLL needs several steps. First step is the protection of amine functions of LL. In the second step, the protected LL reacts by amidification with hexylene diamine using coupling agents. Finally, the amines are deprotected to generate the first generation dPLL. The formation of the next generations follows the same reactions with same conditions.[29]

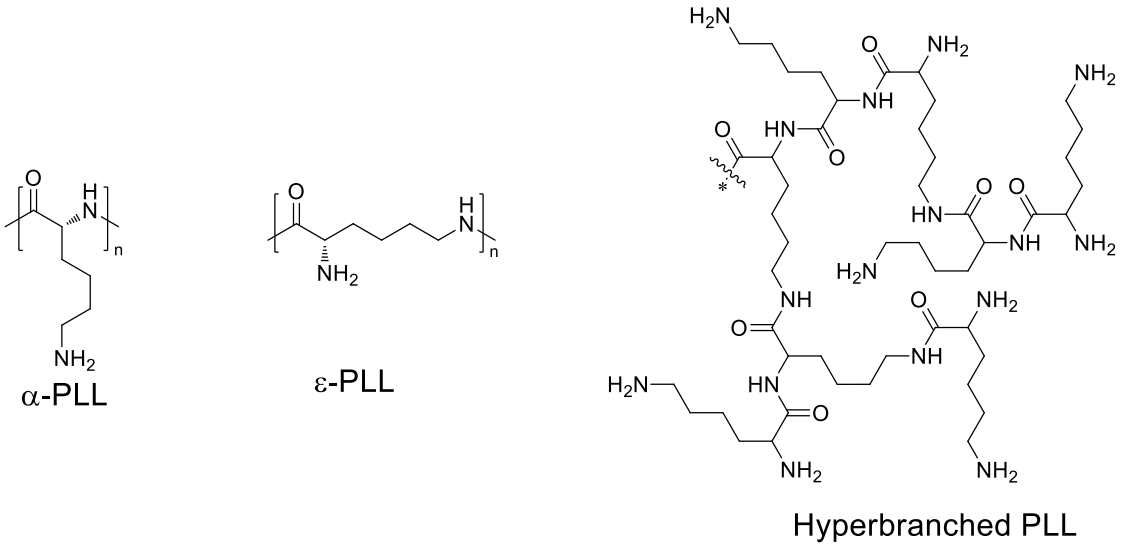

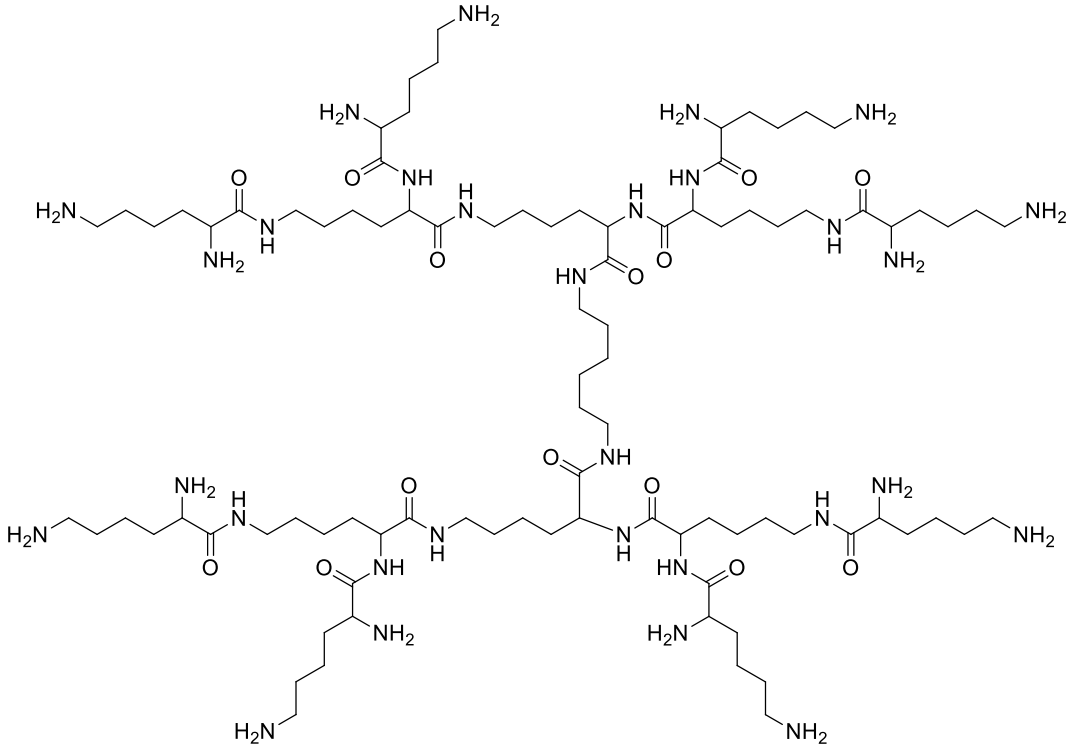

Scheme I. 2. Chemical structures of linear α-PLL and ε-PLL, hyperbranched PLL and dentritic PLL.[26–29]

As for PEI, the transfection efficiency is correlated to the number-average molar mass and the architecture of PLL. Kadlecova *et al.*[30] compared the transfection efficiency of PLLs depending on their number-average molar mass and their architecture on CHO DG44 cells,

chinese hamster ovary cells, by measuring a green fluorescent protein, eGFP, expression and IgG production, immunoglobulin G. For a same architecture, they proved the increase of transfection efficiency with the number-average molar mass on lPLL, hbPLL or dPLL. For example, with a N/P = 3/1, the green fluorescence is five times higher, representing the internalization of lPLL in CHO DG44 cells when the lPLL number-average molar mass increases from 800 to 19600 Da. These results show a better binding of lPLL on extracellular membrane with a higher number-average molar mass. Similar results have been obtained for hbPLL and dPLL. Moreover, Kadlecova *et al.*[30] compared the transfection efficiency according to the architecture keeping a comparable number-average molar mass. The hbPLL shows a higher transfection efficiency than dPLL and lPLL. Authors explained this result because hbPLL has the best binding affinity with the cell membrane due to the highest pH buffering effect.

Moreover, PLL number-average molar mass and architecture have an impact also on cytotoxicity. Kadlecova *et al*[29] compared the effect of number-average molar mass and architecture of PLL cytotoxicity on CHO DG44 cells. For a specific architecture, when the number-average molar mass of PLL increases, the cell viability decreases. When PLL number-average molar mass increases, the PLL interactions with cell membranes increase. These interactions lead to disruption of cell membranes by increasing the cationic group of polymer.

As for PEI, PLL architecture plays a key role in cytotoxicity. In the same study, Kadlecova *et al.*[29] showed the effect of different architectures, lPLL, hbPLL and dPLL. With comparable number-average molar mass, the lPLL seems to be five times less toxic than hbPLL and dPLL. The comparison of hbPLL and dPLL doesn't show a significant difference. They showed the complete degradation of a lPLL with trypsin after 8 hours, a peptidase found in gastric acid, and a partial degradation of hbPLL and dPLL. This degradation can explain the lower cytotoxicity of lPLL.[30] Moreover, there is a difference between the two linear analogues,

α-PLL and ε-PLL. Indeed, De Vries *et al.*[31] shows that the α-PLL is toxic for mice, guinea pig, rabbits and human kind and causes unacceptable damages to lungs, and membrane cells due to the too high charge of cationic primary amines which react with negatively charged membrane of lungs or kidney.[32] The high solubility of ε-PLL in water, compared to the α-PLL, is a great asset for bio-application indeed the lack of solubility in water can lead to aggregation and block arteries leading to necrosis and heart attack.[27] However, the ε-PLL polyplex is very stable which avoid destabilization of polyplex leading to the DNA release.

C. Poly(*β*-amino ester) (PBAE)

PBAE has been studied for DNA delivery as they got the advantage of being protonable due to the amine group and of being biodegradable due to the ester function.[3] The first study of PBAE used for DNA delivery has been made by the team of Langer in 2000.[33] In this work, they prove the efficiency to form several linear PBAEs (lPBAE)s synthesized through Michael addition (Scheme I. 3(A)) able to complex DNA efficiently. In a recent work, a hyper branched poly(β-aminoester) (hbPBAE) was synthesized using a trialkene monomer as a crosslinker in a one-pot Michael addition (Scheme I. 3(B)).[34]

The number-average molar mass of PBAE plays a key role on transfection efficiency. Akinc *et al.*[35] studied two lPBAEs (Scheme I. 3(C)) with different number-average molar masses (5 and 15 kDa) complexing a pDNA containing luciferase on COS-7 cell line, fibroblast from monkey kidney tissue. The results show the increase of transfection efficiency with the increase of lPBAE number-average molar masses. Like PEI or PLL, this increase is really significant. The values of transfection efficiency for a lPBAE of 5 kDa are nearly 0 ng per well as for a lPBAE with a number-average molar mass twice higher the transfection efficiency is around 50 ng per well, for a polymer/pDNA ratio of 80 (w/w %) (this has been explained by the absence of polyplexes formation with the low number-average molar mass lPBAE as it was not able to retard pDNA on a gel agarose assay).

The effect of PBAE architecture on transfection efficiency has also been studied. Cutlar *et al.*[34] compared the transfection efficiency of a hbPBAE and a lPBAE with comparable number-average molar masses (hPBAE and lPBAE4 Scheme I. 3(B)). They found that hbPBAE has a better transfection efficiency than lPBAE with HeLa cells and RDEBK cells, keratinocyte cell lines derivated from epidermolysis bullosa. The authors explained this result by the strong interactions of hbPBAE/DNA polyplexes with cells as shown by gluciferase activity in different cell lines. Moreover, the hbPBAE protects more DNA against DNAse, an enzyme able to degrade DNA, than lPBAE.

As compared to PEI and PLL, PBAE number-average molar mass has an influence on cytotoxicity. The comparison of lPBAE and hbPBAE with similar number-average molar masses shows that lPBAE is less toxic than hbPBAE on HeLa, human cervical cancer cells, NHK, normal human keratinocytes cells, and RDEBK, epidermolysis bullosa keratinocyte cells, because of the poor interaction between the lPBAE/DNA polyplex and the cell membrane and the better hydrophilicity of lPBAE. Unlike PEI and PLL, cytotoxicity tests of hbPBAE of different number-average molar masses showed an increase of cell viability with the number-average molar mass on HeLa cells and SHSY-5Y cells, cells of human bone marrow suffering from neuroblastoma.[36] However, Eltoukhy *et al.*[37] showed no significant difference on cytotoxicity of lPBAE on HeLa cells with different molar masses. The authors explain this result with the increase of number-average molar mass, the size of polyplexes decrease which leads to the decrease of cytotoxicity. Moreover the extremities of PBAEs have also an effect on cytotoxicity.[35] It has been shown that an hydroxyl-terminated PBAE is less toxic than an acrylate-terminated PBAE on COS-7 cells (Scheme I. 3(C))

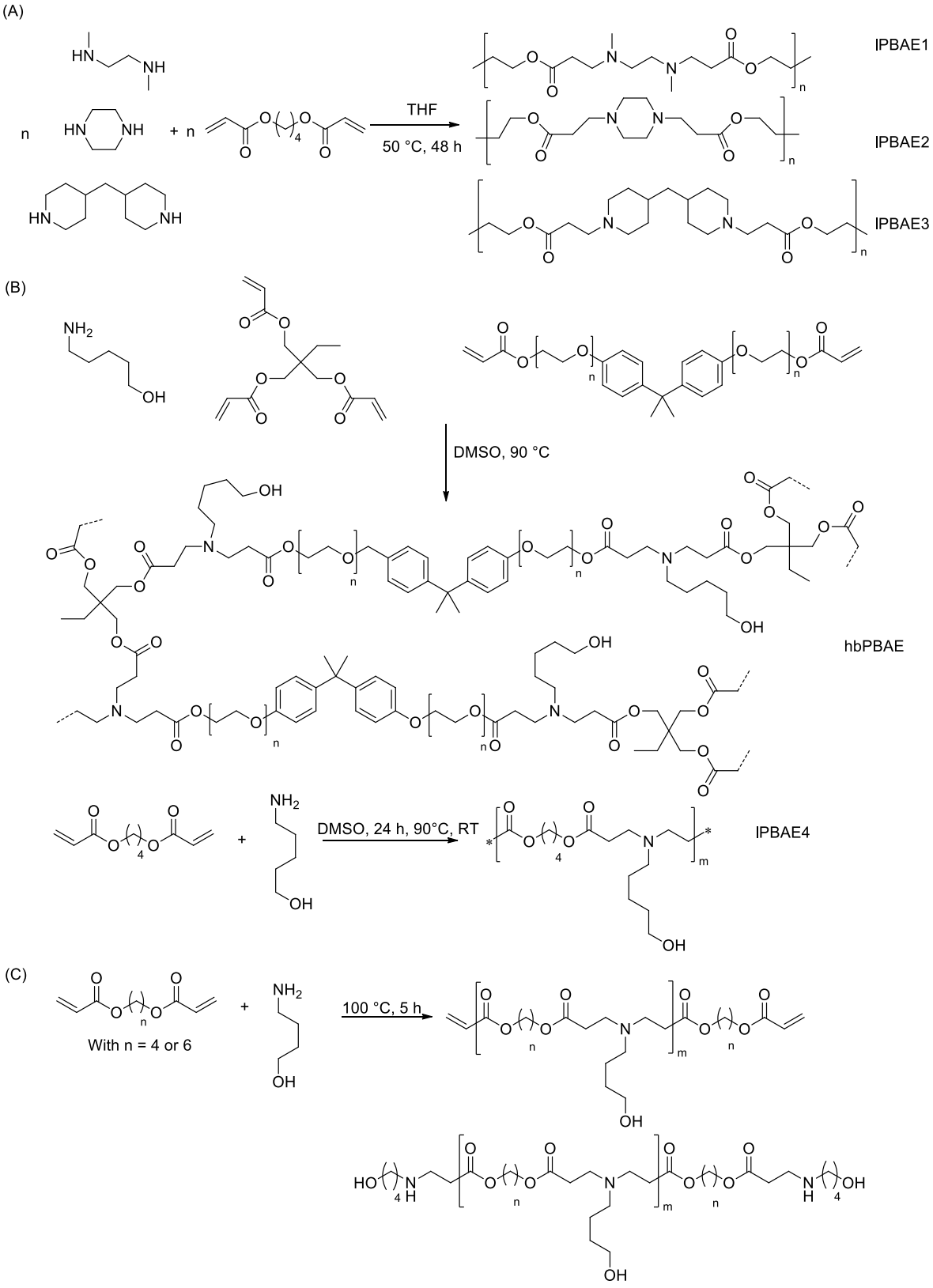

Scheme I. 3. Synthesis (A) of lPBAEs by Lynn *et al.*[33], (B) of hbPBAE and lPBAE by Cutlar *et al.*[34] and (C) of lPBAEs by Akinc *et al.*[35]

D. Cationic vinylic polymers

Cationic polymers based on vinyl monomers such as (meth)acrylates and (meth)acrylamides have been developed as potential transfecting agents.[13,38,39] Van de Wetering *et al.*[40] studied different cationic amine-based polymers (Scheme I. 4) on transfection efficiency on OVCAR-3 using pCMV-LacZ, a pDNA containing a mammalian expression vector. They showed that the transfection efficiency is better with (meth)acrylates than with (meth)acrylamides due to the polymer-polymer interactions between amide functions that stabilizes the polyplex and disturbs the DNA release. They showed that the best transfection efficiency was obtained with poly(2-(*N,N*-dimethylamino)ethyl methacrylate) (PDMAEMA) compared to the other vinylic monomers due to its pKa of 7.5. At this physiological pH, the polymer is partially protonated leading, as PEI, to an efficient endosomal escape. PDMAEMA is one of the most studied amine-based polymethacrylate.[39]

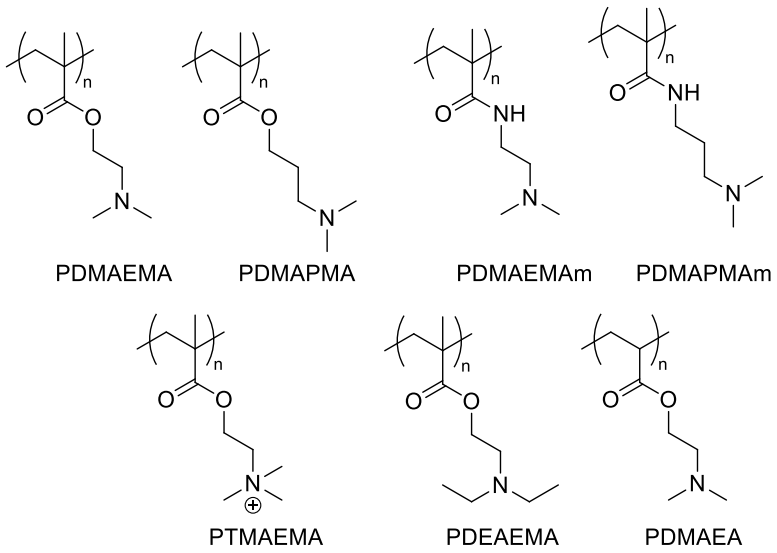

Scheme I. 4. Cationic amine-based polymers studied on transfection efficiency by Van de Wetering *et al.*[40], PDMAEMA, poly(3-(*N,N*-dimethylamino)propyl methacrylate) (PDMAPMA), poly(2-(*N,N*-dimethylamino)ethyl methacrylamide) (PDMAEMAm), poly(3-(*N,N*-dimethylamino)propyl methacrylamide) (PDMAPMAm), poly(2-(*N,N,N*-

trimethylammonium)ethyl methacrylate) (PTMAEMA), poly(2-(*N,N*-diethylamino)ethyl methacrylate) (PDEAEMA), poly(2-(*N,N*-dimethylamino)ethyl acrylate) (PDMAEA).

The first synthesis of linear PDMAEMA (lPDMAEMA) made by RDRP methods was performed using Atom Transfer Radical Polymerization (ATRP) by Matyjaszewski's group in different conditions (Scheme I. 5(A)).[41] Furthermore, Synatschke *et al*.[42] synthesized two stars PDMAEMA with three (sPDMAEMA-3) and five arms (sPDMAEMA-5), using sugar based macroinitiators (Scheme I. 5(B)).

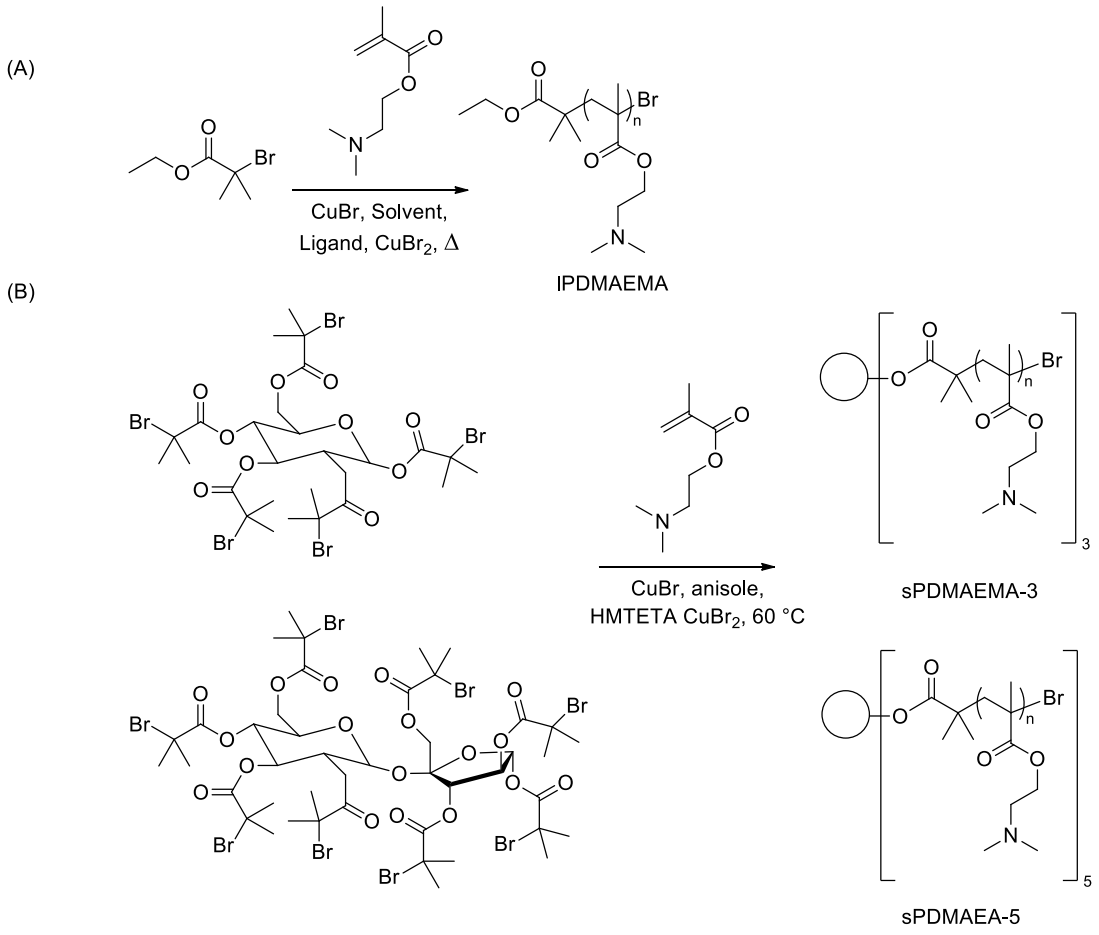

Scheme I. 5. (A) Synthesis of a lPDMAEMA by ATRP using different solvents, ligands and temperatures by Zhang *et al.*[41] (B) Synthesis of stars PDMAEMA (sPDMAEMA-3 and sPDMEMA-5) by ATRP using different sugar-based macroinitiators by Synatschke *et al.*[42]

Among the RDRP methods, RAFT polymerization has been also employed to synthesize PDMAEMA. The RAFT polymerization of 2-(*N,N*-dimethylamino)ethyl methacrylate (DMAEMA) can occurs in organic solvent,[43] in water, [44] by heating or UV-exposition.[4,45,46] As an example, Sahnoun *et al.*[43] studied the RAFT polymerization of DMAEMA in 1,4-dioxane using 2,2'-azobis(isobutyronitrile) (AIBN) and 4-cyano-2-propyl dithiobenzoate (CPDB) using different ratios of $[CPDB]_0/[AIBN]_0$ and of $[DMAEMA]_0/[CPDB]_0$. For all conditions, they reached well-controlled polymerizations with relatively low dispersity (values) (Đ = 1.09-1.4) and they reached high DMAEMA conversions (93 %).

The effect of the architecture of PDMAEMA has been studied on transfection efficiency by Müller and co-workers.[42] They compared lPDMAEMA with two stars PDMAEMA, the sPDMAEMA-3 and the sPDMEMA-5. They transfected CHO-K1 cells with a pDNA containing a green fluorescent protein. At comparable number-average molar mass and N/P = 2, the lPDMAEMA is more effective than the two stars and the sPDMAEMA-5 is more effective than the sPDMAEMA-3. When the ratio N/P is increases to 20, there are no significant differences between the architectures. The authors explain this result by the difficulty of DNA to reach the nitrogen in the core of stars polymers.

The effect of lPDMAEMA number-average molar masses on transfection efficiency of pCMV-LacZ a mammalian expression vector was investigated in two different cell lines, COS-7 and OVCAR-3, epithelial cells from human ovary suffering from adenocarcinoma.[47] In OVCAR-3 cells, the transfection efficiency increases with the lPDMAEMA number-average molar mass from 4 to 817 kDa. In COS-7 cells, the transfection efficiency increases with the number-average molar mass to a limit value (300 kDa) then the transfection efficiency decreases. The increase is due to the free cationic polymers (non-complexed chains) which destabilize the endosomal membrane and help the transfection. Above a number-average molar mass of 300 kDa, the high number of free cationic polymers can limit the transfection by

destabilizing directly the cell membrane. Such behavior has a similar impact on cytotoxicity. When the number-average molar mass increases until 63 kDa for COS-7 cells and 27 kDa for OVCAR-3 cells, the cell viability decreases. Then, for a number-average molar mass around 300 kDa, a plateau is reached and the cell viability at this plateau is around 50 % for both cell-lines.

The effect of PDMAEMA architecture on cytotoxicity has been studied by Müller and co-workers too.[42] The sPDMAEMA-3 and sPDMAEMA-5 shows a lower cytotoxicity than a lPDMAEMA on CHO-K1 cells. The authors explained this result because of the charge density. In the star polymers sPDMAEMA-3 and sPDMAEMA-5, the charge density is hiding in the core of the stars. As for PEI and PLL,[22] the increase of the charge density leads to the decrease of cell viability.

In 2010, Zhu *et al.* proposed to synthesize a statistical copolymer by RAFT copolymerization of DMAEMA with *N*-(*tert*-butoxycarbonyl)aminoethyl methacrylate (*t*BocAEMA) or with *N*-(*tert*-butoxycarbonyl)aminohexyl methacrylate (*t*BocAHMA). After amine deprotection under acidic medium, leading to aminoethyl methacrylate (AEMA) and aminohexyl methacrylate (AHMA) using *t*BocAEMA and *t*BocAHMA, respectively, the P(DMAEMA-*co*-AEMA) and P(DMAEMA-*co*-AHMA) contain ammonium groups from primary and tertiary amines (Scheme I. 6(A)).[48] Such copolymers were employed to transfect COS-7 cells using the pDNA pCMV-Luc as a reporter gene. They compared several molar ratios of primary and tertiary amines for both copolymers, P(DMAEMA-*co*-AEMA) and P(DMAEMA-*co*-AHMA). The results show the decrease of the buffer capacity with the increase of primary amine ratios due to the higher pKa. However the increase of primary amine ratio allows improving the DNA condensation as shown on the gel agarose retardation assay. They showed the better efficiency of P(DMAEMA-*co*-AHMA) than P(DMAEMA-*co*-AEMA) to transfect pCMV-Luc on COS-7 cells. The authors explained this result from: (i) the smallest

size of P(DMAEMA-*co*-AHMA)/pDNA complex than P(DMAEMA-*co*-AEMA)/pDNA complex, (ii) higher charge density of P(DMAEMA-*co*-AHMA) and (iii) a better association of P(DMAEA-*co*-AHMA) with cell membrane due to the hydrophobic interactions of AHMA units. As for the other cationic polymers, transfection efficiency has to be linked with cytotoxicity. The study of the effect of primary amine amount on cell viability didn't show any significant differences with P(DMAEMA-*co*-AHMA) at different DMAEMA/AHMA molar ratio. However, the P(DMAEMA-*co*-AEMA) shows a better cell viability with a higher DMAEMA/AEMA molar ratio due to the lower charge density.

Moreover, the acrylate associated monomers have been used because of their efficiency to self-degrade. Monteiro and co-workers synthesized by RAFT polymerization a poly(2-(*N,N*-dimethylamino)ethyl acrylate) (PDMAEA) using the methyl 2-(butylthiocarbonothioylthio)propanoate (MCEBTTC) as the chain transfer agent and AIBN as the radical initiator in 1,4-dioxane at 60°C (Scheme I. 6(B)).[49] Authors compared the transfection efficiency and the cytotoxicity of PDMAEA with number-average molar mass ranging from 3000 to 8600 $g.mol^{-1}$ on Hela-cells with fluorescein isothiocyanate (FITC)-labeled oligoDNA. Authors showed the increase of transfection with the increase of number-average molar mass for PDMAEA (from 10 % to 80 % of transfected cells in 4 hours). The PDMAEA of 8600 $g.mol^{-1}$ showed interesting results with a high transfection efficiency in just 4 hours. Furthermore, the DNA/PDMAEA polyplexes formed with PDMAEAs of low number-average molar mass (from 3000 to 5000 $g.mol^{-1}$) can be dissociated easily to release DNA as shown by gel retarding assay. For PDMAEA with a number-average molar mass ranging from 6900 to 8600 $g.mol^{-1}$, a partial dissociation has been observed. The study on cytotoxicity showed the same behavior between PDMAEA with low number-average molar masses and with high number-average molar masses. Indeed, authors showed the non-cytotoxicity of PDMAEA with a number-average molar mass equal or below 5600 $g.mol^{-1}$.

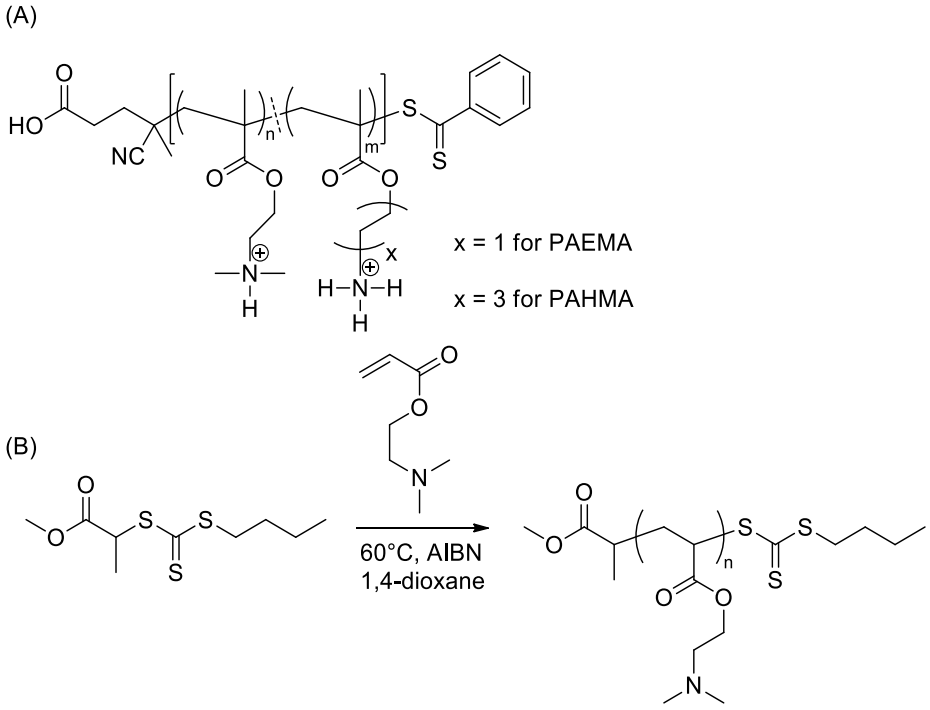

Scheme I. 6. (A) Chemical structures of P(DMAEA-*co*-AEMA) and P(DMAEMA-*co*-AHMA) copolymers obtained by RAFT polymerization and studied by Zhu *et al.*[48] (B) RAFT polymerization of 2-(*N,N*-dimethylamino)ethyl acrylate (DMAEA) mediated through MCETTC as the chain transfer agent and AIBN as the initiator in 1,4-dioxane at 60°C as described by Monteiro and co-workers.[49]

Cationic polymers (PEI, PLL, PBAE and vinylic polymers) showed high charge density inducing cytotoxicity. To overcome this issue many reports have been made on the PEGylation of cationic polymers.

II. PEGylation

PEGylation is based on the covalent linkage of PEO on molecules, most tipically peptides, proteins and antibody fragments. PEO possesses many unique properties including non-cytotoxicity, non-immunogenesis, non-antigenicity, excellent biocompatibility and miscibility with many solvent.[4,50] Therefore, the clinical value of PEGylation is well established: increases stability, enhanced protection from proteolytic degradation, extended circulating life,…[50,51] The

addition of PEO on a non-viral DNA delivery system has been reported, on PEI,[52] on PLL,[54,55] on PBAE,[55,56] and mostly on cationic vinylic polymers.[57–59]

A. How to target PEGylated cationic polymers?

Two main strategies have been developed to covalently attach PEO to a cationic polymer. The first strategy is based on the linkage of the PEO to a preformed cationic polymer. This strategy will be called "PEO grafted onto". The second strategy is to build the cationic polymer from a PEO; such strategy will be called "PEO grafted from".

The "PEO grafted onto" strategy needs the use of very reactive functions to target an efficient coupling reaction. For example, isocyanate-functionalized PEO has proved to be reactive towards amines and allows to PEGylate a lPEI (Scheme I. 7(A)).[60] Unfortunately, this strategy has led to a very low functionalization as only 15 % of lPEI has been attached to the PEO. Recently, Pezzoli *et al.*[52] used an α-*N*-hydroxysuccinimide,ω-maleimide PEO (Scheme I. 7 (B)) to react with primary amines of a bPEI. From 0.36 % to 5.58 % of primary amines have been grafted with PEO. A PEO was also grafted onto an α-PLL by reacting a *N*-hydrosuccinimide-PEO onto an α-PLL (Scheme I. 7(C)).[61] This reaction doesn't need harsh conditions and allows tuning easily the grafting ratio of PEO onto the α-PLL from 4.4 % to 45 %. The versatile "click-chemistry" has also been employed to covalently attach PEO to a cationic polymer.[62,63] Kim *et al.*[55] used the thiol-ene coupling reaction to link a diacrylate-based PEO on a lPBAE (Scheme I. 7(D)). The thiol-ene reaction has been made using soft conditions, at room temperature in basic conditions with a total conversion of the diacrylate-based PEO as determined by ^{1}H nuclear magnetic resonance (NMR) spectroscopy.

Apart from the thiol-ene coupling reaction such "PEO grafted onto" strategy is generally limited to low attachment efficiency probably due the incompatibility of polymers and also to

the accessibility of the chain-end. The PEGylation of cationic vinylic polymers is mostly based on the second strategies: the "PEO grafted from".

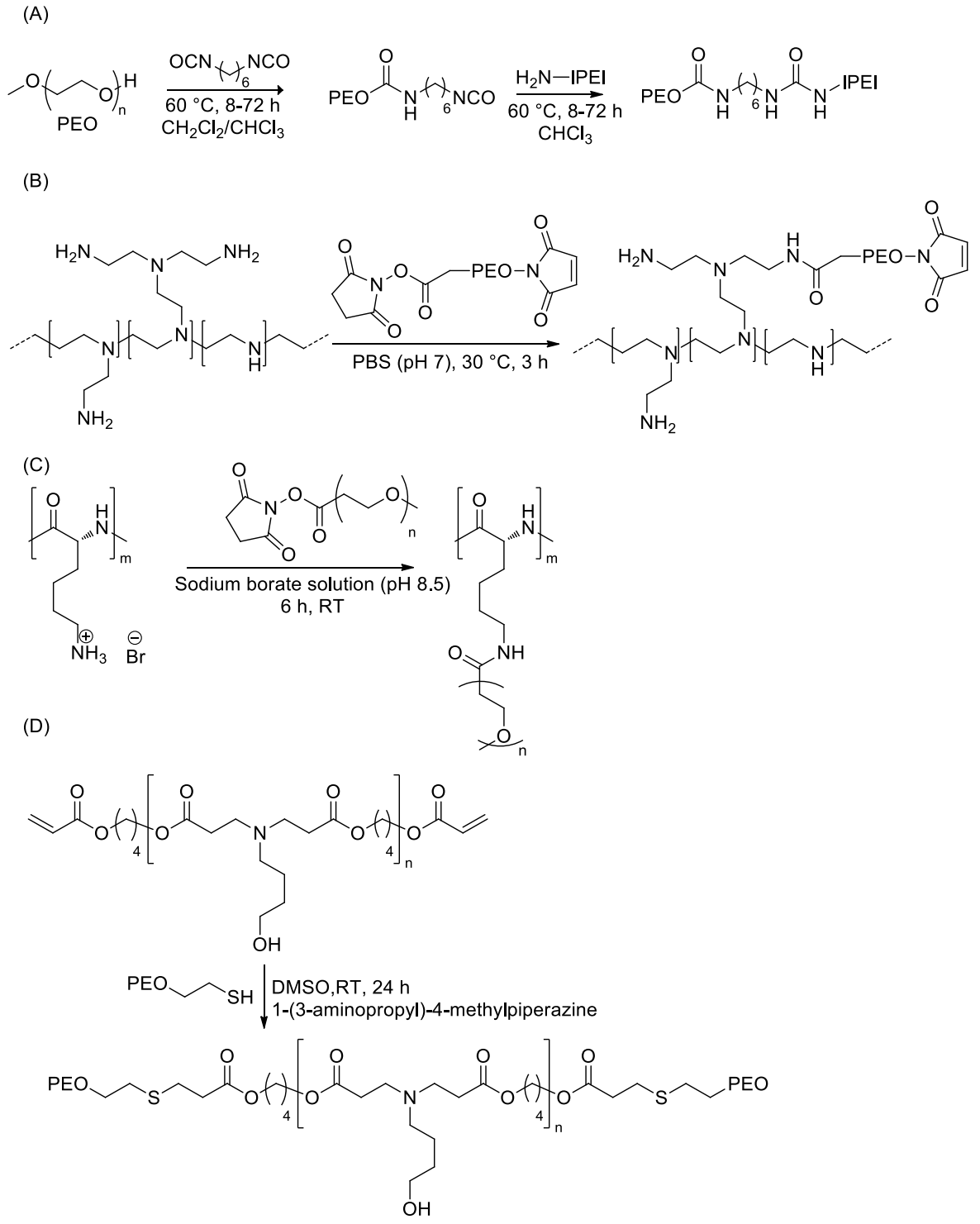

Scheme I. 7. Covalent linkage of PEO using the grafted-onto strategy on (A) a lPEI thanks to a diisocyanate reagent;[60] (B) a bPEI thanks to a *N*-hydroxy-succinimide,ω-maleimide-PEO;[52]

(C) a α-PLL using a α-*N*-hydroxysuccinimide-PEO[60] and (D) a PBAE by thiol-ene coupling reaction.[55]

Such "PEO grafted from" strategy has been possible thanks to RDRPs or living polymerization techniques. Usually the chemical chain-end modification of PEO with a low number-average molar mass molecule is performed in order to introduce initiating group or a chain transfer agent moiety. Such chemical modification is quantitative and leads to target fully PEGylated cationic polymers. ATRP, RAFT polymerization and ROP have been widely employed to synthesize cationic polymers from functionalized PEO and resulting copolymers have been tested for gene delivery.[53,64,65]

For instance, to process ATRP, Välimäki *et al.*[64] first quantitavely synthesized an α-methoxy-ω-bromo-PEO macroinitiator by reacting an ω-hydroxyl-PEO on the 2-bromoisobutyrylbromide. Such macroinitiator was then employed to perform the ATRP of DMAEMA using a copper complex (Scheme I. 8(A)). To avoid the use of copper, RAFT polymerization is more and more employed for the "PEO grafted from" strategy. Venkataraman *et al.* fixed a 4-cyanopentanoic acid dithiobenzoate (CPADB) onto a hydroxyl-PEO by esterification using a diisopropyl carbodiimide (DIC) as a coupling agent in dichloromethane (Scheme I. 8(B)). They used the resulting PEO as a macromolecular RAFT agent to perform the RAFT polymerization of DMAEMA in 1,4-dioxane using 4,4-azobis-4-cyanolaveric acid (ACVA) as the initiator. They obtained a PEO-*b*-PDMAEMA copolymer of 10100 g.mol^{-1} with Đ value of 1.18. The PEO "grafted from" strategy has also been used with ROP. Choi *et al.*[53] have polymerized the carbobenzyloxy-*L*-Lysine (CbzLL) and *L*-phenylalanine-*L*-Lysine (LPheLL) by ROP using an α-methoxy,ω-amino-PEO of 2000 g.mol^{-1} as an initiator to form a PEO-*b*-P(LPheLL-*co*-CbzLL). They performed the amine deprotection of the poly(carbobenzyloxy-*L*-Lysine) (PCbzLL) using acidic conditions to target PEO-*b*-P(LPheLL-

co-LL) copolymers with number-average molar masses ranging from 31300 g.mol^{-1} to 37700 g.mol^{-1} and ratios of *L*-Lysine to LPheLL ranging from 10/0 to 6/4.

This method can also be used to link a branched PEO. Venkatamaran *et al.*[65] synthesized a poly(oligo(ethylene glycol) methacrylate) (PPEGMA) by RAFT polymerization using the CPADB as the chain transfer agent at 70°C using ACVA to generate radical initiators in 1,4-dioxane (Scheme I. 8(D)). Then thanks the remaining dithioester group on the PPEGMA block, a PDMAEMA block has been synthesized to finally obtain a PPEGMA-*b*-PDMAEMA with a number-average molar mass of 11800 g.mol^{-1} and a dispersity value of 1.25.

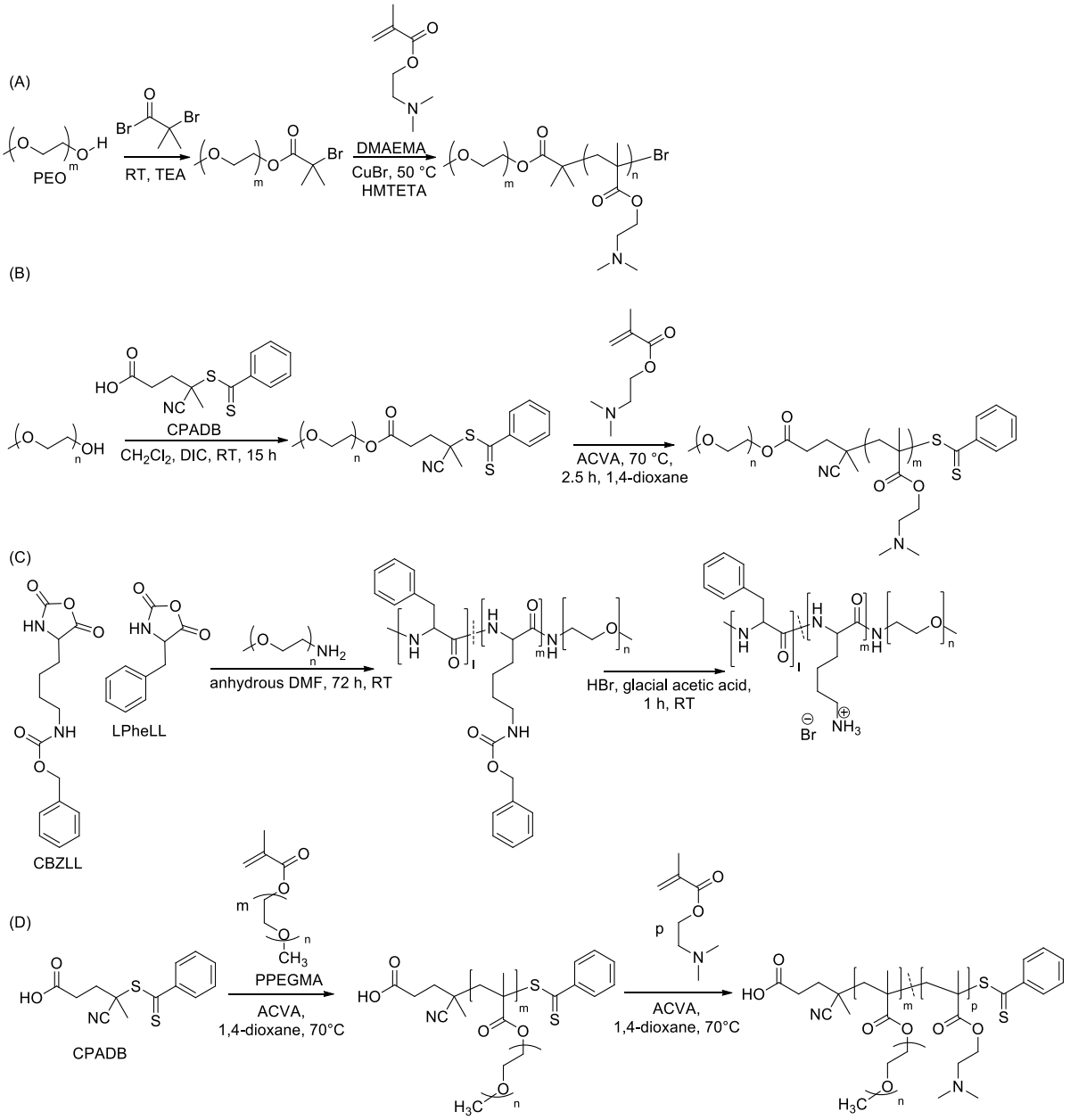

Scheme I. 8. Covalent linkage of PEO using the "PEO grafted-from" strategy using (A) ATRP of DMAEMA as reported by Välimäki *et al.*[64] (B) RAFT polymerization of DMAEMA as reported by Venkataraman *et al.*[65] (C) ROP of LPheLL and CbzLL and subsequent amine deprotection reported by Choi *et al.*[53] and (D) successive RAFT polymerization of oligo(ethylene glycol) acrylate (PEGA) and DMAEMA as reported by Venkataraman *et al*.[65]

B. Impact of PEGylation on transfection efficiency and cytotoxicity

Zhang *et al*.[66] studied the PEGylation effect of a bPEI of 25 kDa on transfection efficiency and cytotoxicity on HeLa cells with a plasmid pEGFP-C1, a plasmid containing the enhanced green fluorescent protein. They have shown that with a low grafting ratio (1.89 mole of PEO of 2 kDa for one mole of bPEI or 0.66 mole of PEO of 5 kDa for one mole of bPEI), the transfection efficiency is higher with PEO than without PEO due to the increase of the polyplexes stability. However, a decrease of the transfection efficiency has been observed for a higher grafting ratio (4.17 moles of PEO of 2 kDa for one mole of PEI or 1.67 mole of PEO of 5 kDa for one mole of PEI). This has been explained by the decrease of zeta potential (from 20 mV to 3 mV) with the increase of grafting ratios leading to a decrease of interactions with the cell membrane.[66] Moreover, Zhang *et al*. studied the effect of the number-average molar mass of the grafted PEO on Hela cells. Two PEOs with number-average molar masses of 2 kDa and 5 kDa have been compared. They have shown that the transfection with a PEO of 5 kDa is less effective than with a PEO of 2 kDa. Indeed the zeta potential of the cationic polymer is lowest with the 5 kDa than with the 2 kDa PEO. This result leads to a lower binding affinity with the membrane cell. Moreover, these two factors, grafting ratio and number-average molar mass, play a role on cytotoxicity. At low concentrations of cationic polymer, ranging from 1 $\mu g.mL^{-1}$ and 10 $\mu g.mL^{-1}$, there are no significant differences between PEGylated bPEI and a bPEI. The addition of PEO leads to a decrease of cytotoxicity for concentrations higher than 10 $\mu g.mL^{-1}$. This fall of the cytotoxicity goes on with the number of PEOs unit. Indeed, when the number-average molar mass of the PEO increases the cell viability increases. This phenomenon has been explained by the decrease of charge density with the increase of the PEO number-average molar mass. Similar result has been obtained by Fitzsimmons *et al.*[67] on HEK293 cells, Human Embryonic Kidney cells.

Other studies have been reported on the PEGylation effect of PDMAEMA on transfection efficiency. Similar conclusions than previous studies with the bPEI have been obtained. The PEGylation of PDMAEMA decreases both transfection efficiency and cytotoxicity. The comparison between PDMAEMA and PEO-*b*-PDMAEMA proved the better transfection efficiency of PDMAEMA than of PEO-*b*-PDMAEMA on A-549 cell line,[57] adenocarcinoma human alveolar basal epithelial cells with PRSVlucDNA, containing luciferase reporter gene obtained from cobra. The authors explained these results by a steric hindrance due to the PEO acting like a shield leading to a decrease of interaction of the polyplex with the cell membrane.

The PEO architecture can also influence the transfection efficiency and the cytotoxicity. Indeed the poly(oligo(ethylene glycol) acrylate) (PPEGA) is a brush-like PEO. Venkataraman *et al.*[65] studied the effect of the architecture of PEO on transfection efficiency of pCMV-Luc, a plasmid containing the firefly luciferase gene, on Hep-G2 (human liver cell lines) and HEK-293 cells lines and on cytotoxicity by comparing a PDMAEMA-*b*-PEO and a PDMAEMA-*b*-PPEGA. They synthesized these two copolymers by ATRP. The results of transfection efficiency don't show any significant differences in the different cell lines on HEK 293 cell lines but, authors shown the better transfection efficiency of PDMAEMA-*b*-PEO on Hep-G2 cell lines than PDMAEMA-*b*-PPEGA due to the better cellular uptake of PDMAEMA-*b*-PEO than PDMAEMA-*b*-PPEGA. However, the architecture of the PEO doesn't play a key role on cytotoxicity. Indeed, the authors didn't show any significant differences between the two copolymers.

The positive influence of PEGylation on the cellular viability to the detriment of transfection efficiency has been shown. However, a promising strategy to overcome the decrease of transfection efficiency due to the PEGylation of cationic polymers is the addition of a recognition ligand.

III. Recognition ligands addition

Some diseases, as cancers, lead to a production of specific protein on the cell membrane. These specific proteins can be targeted with a recognition ligand.[68] Several targeting ligands are used including antibodies and peptides.[69] The recognition ligand has to be added on the cationic polymer by versatile, efficient reactions that can be proceed at room temperature in water to maintain the integrity of ligands.

A. Incorporation of recognition ligand onto cationic polymers

There are different methods to add several kinds of recognition ligands on cationic polymers. For example, Pezzoli *et al.*[52] reported the anchoring of a cyclic tripeptide arginine-glycine-aspartate (cRGD) and a linear RGD (lRGD) on a PEGylated *b*-bPEI (Scheme I. 9 (A)). RGD is able to target several integrins as, $\alpha_5\beta_1$, $\alpha_8\beta_1$, $\alpha_{IIb}\beta_3$, $\alpha_V\beta_3$, $\alpha_{5V}\beta_5$, $\alpha_V\beta_6$ and $\alpha_V\beta_8$.[70,71] First, the authors grafted a maleimide and a *N*-hydroxysuccinimide-functionalized PEO onto a bPEI through nucleophilic substitution. Then, they added the amine-based cRGD or lRGD onto maleimide moieties of the PEGylated bPEI through nucleophilic addition. The complete addition of the cRGD and lRGD was checked by the titration of unreacted RGD with Ellman's test after purification by ultra-filtration. The degrees of functionalization was from 0.36 to 5.58 %.

Suh *et al.*[72] grafted an antibody on a PLL of 20 kDa containing thiol units through a disulfide coupling exchange between PLL units functionalized by a thiol and an antibody functionalized by a pyridyl disulfide bound (Scheme I. 9(B)). They finally obtained a statistical copolymer containing LL units and LL-*grafted*-antibody units with a number-average molar ratio of 98.5/1.5, respectively. The degree of functionalization was equal to 68 %.

Moreover, a recognition ligand can be added on the chain-end of linear cationic polymer. Qian *et al.*[73] synthesized a PEO-*b*-PDMAEMA by ATRP with an α-maleimide,ω-bromide PEO

used as the macroinitiator (Scheme I. 9(C)). Then they finally added a 12-amino acids peptide, TGNYKALHPHNG (TGN), by nucleophilic addition on the maleimide with a thiolated TGN. They obtained a complete conversion determined by ^{1}H NMR spectroscopy.

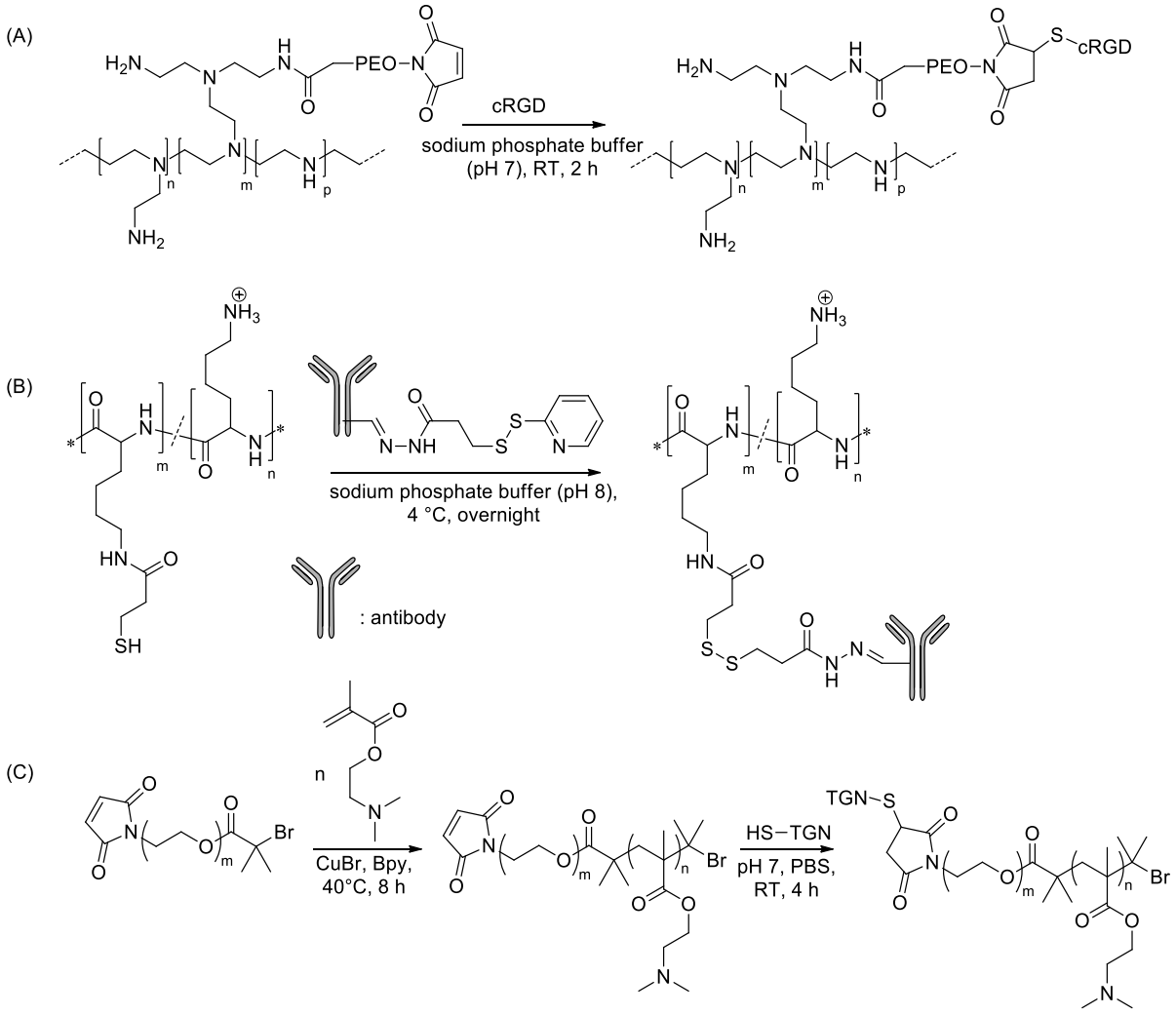

Scheme I. 9. (A) cRGD functionalization of a PEO-*b*-bPEI as described by Pezzoli *et al.*[52] (B) antibody functionalization of a PLL by disulfide coupling exchange as reported by Suh *et al.*[72] and (C) TGN functionalization of a PEO-*b*-PDMAEMA as described by Qian *et al.*[73]

B. Impact of recognition ligand on transfection efficiency of polyplexes

The addition of a recognition ligand onto cationic polymers has an impact on their transfection efficiency through the recognition of some proteins on cell membrane.

Oba *et al.*[74] studied the impact of the addition of cRGD on PEGylated-*b*-PLL on transfection efficiency of pCAcc+Luc, a pDNA containing the luciferase firefly gene on HeLa and HEK293 cells. cRGD is able to target $\alpha_V\beta_3$ and $\alpha_V\beta_5$ integrins. The authors showed, by flow cytometric analysis, that HEK293 cells don't expressed the $\alpha_V\beta_3$ and expressed a little amount of $\alpha_V\beta_5$ while the HeLa cells expressed both of integrins. The comparison of transfection efficiency between the cRGD-PEO-*b*-PLL and PEO-*b*-PLL on HeLa cells showed the better transfection efficiency of polymer functionalized by cRGD. Moreover, the comparison on 293T cells didn't show any significant differences between cRGD-PEO-*b*-PLL and PEO-*b*-PLL. These results showed the ability of cRGD to target $\alpha_V\beta_3$ and $\alpha_V\beta_5$ integrins and the better transfection efficiency of polymers with a recognition ligand.

The work of Qian *et al.*[73] on TGN-PEO-*b*-PDMAEMA showed the effect of the recognition ligand on transfection efficiency. This ligand is able to target brain cells. The authors showed the best transfection efficiency of TGN-PEO-*b*-PDMAEMA of pGL2 pDNA on brain capillary endothelial cells, BCECs compared to a PEO-*b*-PDMAEMA. Moreover, the authors showed not significant differences of cell viability on BCECs. Therefore, as PEGylation, the addition of a recognition ligand has no effect on cytotoxicity.

IV. Cationic polymers degradability and its effect on transfection efficiency and cytotoxicity

Degradable linkages have been introduced within cationic polymers used for DNA delivery. Depending on their position within the cationic polymer, in the backbone or in the pendant groups, such degradable linkages either decrease the polymer cytotoxicity or either increases the transfection efficiency. The degradable linkages used for DNA delivery are either hydrolyzable groups or either biodegradable groups. The hydrolyzable linkages are generally ester function. Peptide linkage and disulfide linkage can be reduced by bioactivity.

A. Hydrolyzable functions

Hydrolyzable ester functions are present within the pendant groups of amine-based poly(meth)acrylate, they can be introduced on a non-degradable polymer as PEI and in the PBAEs backbone

The PDMAEMA with pendant esters functions can be hydrolyzed depending on the pH. Van de Wetering *et al.*[75] have studied the hydrolytic stability of polyplexes based-on pCMV-LacZ etiher PDMAEMA of a number-average molar mass of 17000 $g.mol^{-1}$ or with PDMAEA of a number-average of 9000 $g.mol^{-1}$, at different pH. After 6 months of incubation at 37°C, authors didn't observe traces of the degradation products by high performance liquid chromatography (HPLC). To increase the hydrolysis rate, they increased the temperature. They showed that the hydrolysis rate of PDMAEA is 50 % at pH 7 and 80 % at pH 1 in 12 days. The hydrolysis rate of PDMAEMA is lower than the hydrolysis rate of PDMAEA as 45 % at pH 1 and less than 10 % at pH 7 in 12 days. This is probably due to a better solubility of PDMAEA in water than PDMAEMA. Therefore, Monteiro and co-workers studied more deeply the hydrolysis of PDMAEA leading to the formation of poly(acrylic acid) (PAA) and 2-*N,N*-dimethylaminoethanol (Scheme I. 10 (A)).[76] PAA is a non-toxic polymer already used in oral chemotherapy.[77] Several PDMAEAs have been synthesized with number-average molar mass ranging from 3300 to 8600 $g.mol^{-1}$. In 200 hours, all PDMAEAs reached 80 % of degradation whatever the pH (pH = 5.1 and 7.4).

Hydrolyzable ester functions have been added on non-degradable 800 Da bPEI-NH_2 (800 Da) by Forrest *et al.*[78]. The nucleophilic addition of a bPEI-NH_2 onto a diacrylate has been performed (Scheme I. 10(B)) and has led to bPEI with higher number-average molar masses, 14 kDa (named P1) and 30 kDa (named P2), which are more effective to transfect pDNA containing luciferase gene on MDA-MB-231, human breast carcinoma cell line and C2C12, murine myoblast cell line than a bPEI with lower number-average molar mass.[20] Forrest *et al.*[78]

showed the degradation of 40 % of ester linkages at pH 5.1 and 80 % at pH 7.4 for P1 and P2. Such P1 and P2 have been compared with a non-degradable bPEI of 25 kDa in terms of transfection efficiency and of cytotoxicity.[78] They tested the transfection efficiency of such polymers using pGL3, a pDNA containing a luciferase gene onto two cell lines, MDA-MB-231 and C2C12. P2 is more efficient to transfect MDA-MB-231 cells lines at low N/P ratios, 4/1, but at higher N/P, from 8/1 to 12/1 ratios, P1 is more efficient. With C2C12 cells, both polymers don't show any significant difference. Moreover, P1 and P2 showed higher transfection efficiency than bPEI (from 2 fold to 6 fold for MDA-MB-231 and 9 fold to 16 fold for C2C12).[78] The authors explained these results by a better pDNA release with degradable P1 and P2. Moreover, all bPEIs (degradable and non-degradable) don't show any significant cytotoxicity on MDA-MB-231 cells. But with C2C12 cells, P1 and P2 showed a lower cytotoxicity than non-degradable bPEI.

Hydrolyzable ester functions which are present within the PBAEs backbone can be easily degraded at 37°C in less than 40 hours at pH 5.1 and in less than 70 hours at pH 7.4.[33] The degradation has been followed by size exclusion chromatography (SEC) and the resulting by-products were identified by ^{1}H NMR spectroscopy and were non-toxic. PBAEs showed a very low cytotoxicity.

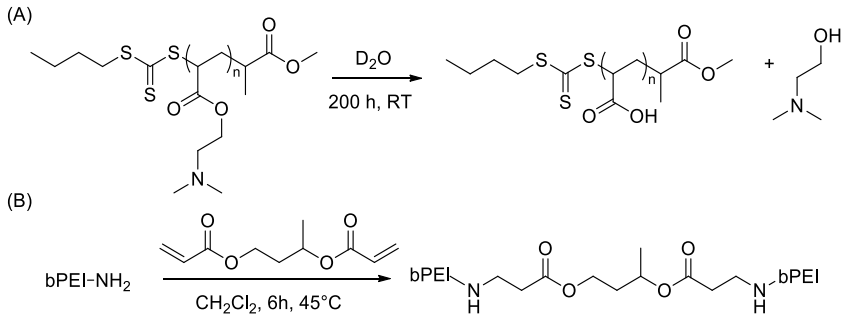

Scheme I. 10. (A) Degradation of PDMAEA PAA[75] and (B) synthesis of degradable bPEI with ester functions by nucleophilic addition on a diacrylate by Forrest *et al.*[78]

B. Biodegradable linkages

The disulfide bounds can be reduced by glutathione, an enzyme found in the cytoplasm.[79] You *et al.*[80] synthesized a reducible PDMAEMA (named rPDMAEMA) and compared it to a usual PDMAEMA. An α,ω-dithiobenzoate PDMAEMA synthesized by RAFT polymerization (Scheme I. 11). The rPDMAEMA was synthesized thanks to the coupling between two α,ω-dithiolPDMAEMAs (HS-PDMAEMA-SH) resulting from the aminolysis of α,ω-dithiobenzoate PDMAEMA. Then the transfection efficiency of rPDMAEMAs with a number-average molar mass of 16700 $g.mol^{-1}$ (rPDMAEMA1) and with a number-average molar mass of 53000 $g.mol^{-1}$ (rPDMAEMA2) was compared with PDMAEMAs with a number-average molar mass of 13000 $g.mol^{-1}$ (PDMAEMA1) and with a number-average molar mass of 26000 $g.mol^{-1}$ (PDMAEMA2), respectively. The transfection efficiency was measured, on B16F10 cells, cells from mouse muscle with gWiz^{TM}, with high-expression luciferase pDNA. The authors showed the best transfection efficiency of rPDAEMA1 compared to PDMAEMA1. The cytotoxicity of PDMAEMAs and rPDMAEMAs was also compared at different concentrations (from 10 to 50 $\mu g.mL^{-1}$). At a concentration of 10 $\mu g.mL^{-1}$, the different polymers don't show any significant differences. For a concentration of 20 $\mu g.mL^{-1}$, the two rPDMAEMAs did not show any cytotoxic contrary to PDMAEMAs showed a cytoxicity towards human endothelial EA.hy926 cells and human pancreatic adenocarcinoma MiaPaCa cells. The authors explained such results by the degradation of rPDMAEMA leading to PDMAEMA with low number-average molar masses.

Peptide linkages are very stable and can't be hydrolyzed at room temperature but there are sensitive to enzymatic degradation.[81] Kito *et al.*[82,83] measured the degradation of ε-PLL (number-average molar mass around 4000 $g.mol^{-1}$) with two enzymes, *Streptomyces albulus* (StAl) and *Sphingobacterium multivorum* OJ10 (SMOJ10) by HPLC. They showed that the ε-

PLL degradation leads to the formation of LL with both enzyme and a complete degradation of PLL is achieved in one hour.

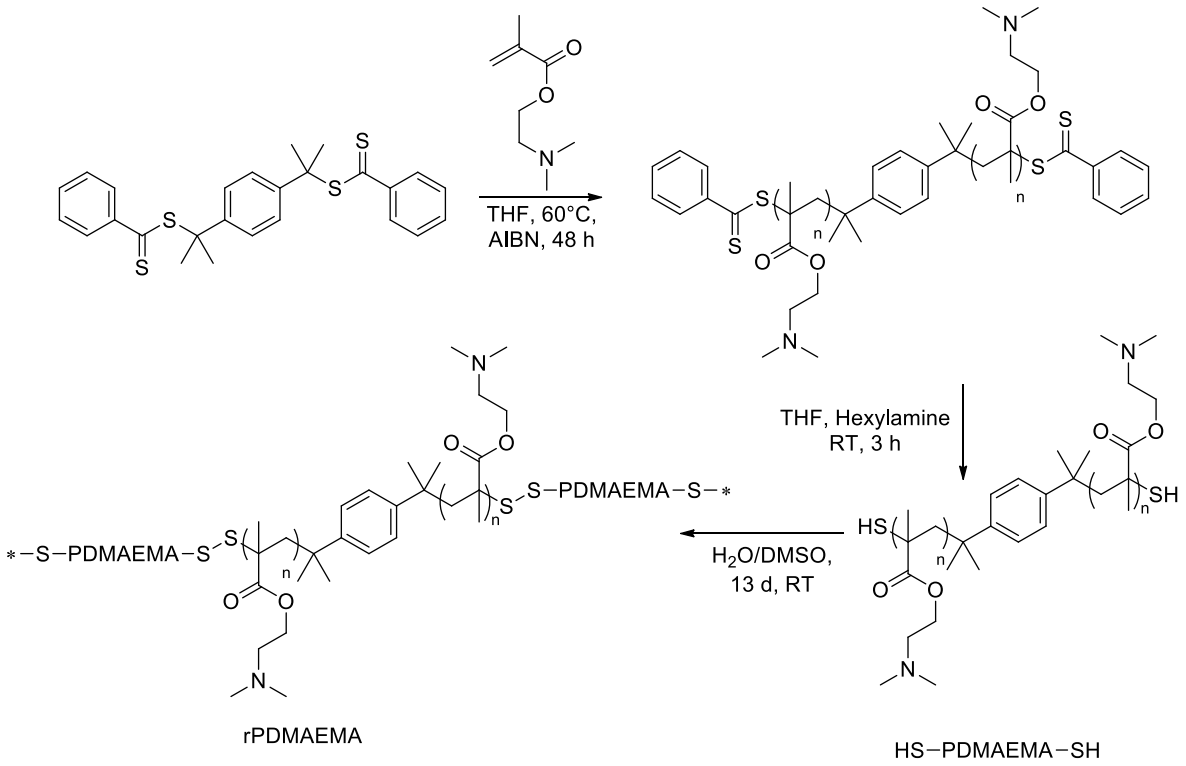

Scheme I. 11. Synthesis of reducible PDMAEMA by RAFT polymerization followed by an aminolysis and oxidation reduction by You *et al.*[80]

Conclusions

Cationic polymers have been studied for gene delivery in order to replace the adenovirus systems which are known to be toxics. The PEI, the PLL, the PBAE and cationic vinylic polymers are the most synthetic cationic polymers studied till now to transfect DNA. Each of them has its pros and cons. The PEI and the PLL showed high transfection but higher cytotoxicity. The PBAE did not show a high transfection efficiency but the degradability leads to a very low cytotoxicity. The cationic vinylic polymers are easily designed and tunable. Among the cationic vinylic polymers, the cationic acrylate-based copolymers present hydrolysable functions which allow high transfection efficiency and low cytotoxicity.

The PEGylation of cationic polymers is one step further to decrease cytotoxicity by decreasing the charge density and increasing the hydrophilicity. Moreover, the linkage of recognition-ligands onto cationic polymers increases transfection efficiency by improving the cellular uptake. The degradation of cationic polymers, by addition of biodegradable or hydrolyzable linkages, increases the transfection efficiency by helping the DNA release.

In our work, following the literature to obtain a high transfection efficiency and a low cytotoxicity of polyplex we developed a new cationic copolymer. A cationic acrylate-based polymer containing primary amine and tertiary amines has been chosen. The coupling of tertiary and primary amines allows to tune the charge density to improve the cell binding affinity, the endosomal escape and cytotoxicity.[48] Moreover, the acrylate functions are hydrolysable leading to a decrease of cytotoxicity and an increase of the transfection efficiency.[49,76] The PEGylation of cationic polymer has been realized by RAFT using the "PEO grafting from" process. The addition of a PEO allows to decrease the cytotoxicity and increase the polyplex stability.[66] This PEO was functionalized with reactive functions to add a thiol-based RGD recognition ligand. The addition of a recognition ligand allows to increase the transfection efficiency by increasing the cellular uptake and to target specific cells.[68]

References

(1) Pandey, A. P.; Sawant, K. K. Polyethylenimine: A Versatile, Multifunctional Non-Viral Vector for Nucleic Acid Delivery. *Materials Science and Engineering: C* **2016**, *68*, 904–918.
(2) Yoshida, T.; Nagasawa, T. ε-Poly-L-Lysine: Microbial Production, Biodegradation and Application Potential. *Applied Microbiology and Biotechnology* **2003**, *62* (1), 21–26.
(3) Zugates, G. T.; Little, S. R.; Anderson, D. G.; Langer, R. Poly(ß-Amino Ester)s for DNA Delivery. *Israel Journal of Chemistry* **2005**, *45* (4), 477–485.
(4) Xu, F. J.; Yang, W. T. Polymer Vectors via Controlled/Living Radical Polymerization for Gene Delivery. *Progress in Polymer Science* **2011**, *36* (9), 1099–1131.
(5) Higuchi, A.; Sugiyama, K.; Yoon, B. O.; Sakurai, M.; Hara, M.; Sumita, M.; Sugawara, S.; Shirai, T. Serum Protein Adsorption and Platelet Adhesion on Pluronic™-Adsorbed Polysulfone Membranes. *Biomaterials* **2003**, *24* (19), 3235–3245.
(6) Chen, H.; Brook, M. A.; Sheardown, H. Silicone Elastomers for Reduced Protein Adsorption. *Biomaterials* **2004**, *25* (12), 2273–2282.

(7) Lan, S.; Veiseh, M.; Zhang, M. Surface Modification of Silicon and Gold-Patterned Silicon Surfaces for Improved Biocompatibility and Cell Patterning Selectivity. *Biosensors and Bioelectronics* **2005**, *20* (9), 1697–1708.
(8) Verbaan, F. J.; Oussoren, C.; Snel, C. J.; Crommelin, D. J. A.; Hennink, W. E.; Storm, G. Steric Stabilization of poly(2-(Dimethylamino)ethyl Methacrylate)-Based Polyplexes Mediates Prolonged Circulation and Tumor Targeting in Mice. *Journal of Gene Medicine* **2004**, *6* (1), 64–75.
(9) Lee, Y.; Miyata, K.; Oba, M.; Ishii, T.; Fukushima, S.; Han, M.; Koyama, H.; Nishiyama, N.; Kataoka, K. Charge-Conversion Ternary Polyplex with Endosome Disruption Moiety: A Technique for Efficient and Safe Gene Delivery. *Angewandte Chemie* **2008**, *120* (28), 5241–5244.
(10) Fernandez, C. A.; Rice, K. G. Engineered Nanoscaled Polyplex Gene Delivery Systems. *Molecular Pharmaceutics* **2009**, *6* (5), 1277–1289.
(11) Li, S.-D.; Chono, S.; Huang, L. Efficient Gene Silencing in Metastatic Tumor by siRNA Formulated in Surface-Modified Nanoparticles. *Journal of Controlled Release* **2008**, *126* (1), 77–84.
(12) Luten, J.; van Nostrum, C. F.; De Smedt, S. C.; Hennink, W. E. Biodegradable Polymers as Non-Viral Carriers for Plasmid DNA Delivery. *Journal of Controlled Release* **2008**, *126* (2), 97–110.
(13) O'Rorke, S.; Keeney, M.; Pandit, A. Non-Viral Polyplexes: Scaffold Mediated Delivery for Gene Therapy. *Progress in Polymer Science* **2010**, *35* (4), 441–458.
(14) Brissault, B.; Kichler, A.; Guis, C.; Leborgne, C.; Danos, O.; Cheradame, H. Synthesis of Linear Polyethylenimine Derivatives for DNA Transfection. *Bioconjugate Chemistry* **2003**, *14* (3), 581–587.
(15) Cortez, M. A.; Godbey, W. T.; Fang, Y.; Payne, M. E.; Cafferty, B. J.; Kosakowska, K. A.; Grayson, S. M. The Synthesis of Cyclic Poly(ethylene Imine) and Exact Linear Analogues: An Evaluation of Gene Delivery Comparing Polymer Architectures. *Journal of the American Chemical Society* **2015**, *137* (20), 6541–6549.
(16) Rinkenauer, A. C.; Schubert, S.; Traeger, A.; Schubert, U. S. The Influence of Polymer Architecture on in Vitro pDNA Transfection. *Journal of Material Chemistry B* **2015**, *3* (38), 7477–7493.
(17) Zhuk, D. S.; Gembitskii, P. A.; Kargin, V. A. Advances in the Chemistry of Polyethyleneimine (Polyaziridine). *Russian Chemical Reviews* **1965**, *34* (7), 515-527.
(18) Demadis, K. D.; Paspalaki, M.; Theodorou, J. Controlled Release of Bis(phosphonate) Pharmaceuticals from Cationic Biodegradable Polymeric Matrices. *Industrial & Engineering Chemistry Research* **2011**, *50* (9), 5873–5876.
(19) Rinkenauer, A. C.; Vollrath, A.; Schallon, A.; Tauhardt, L.; Kempe, K.; Schubert, S.; Fischer, D.; Schubert, U. S. Parallel High-Throughput Screening of Polymer Vectors for Nonviral Gene Delivery: Evaluation of Structure–Property Relationships of Transfection. *American Chemical Society Combinatorial Science* **2013**, *15* (9), 475–482.
(20) Remy, J.-S.; Abdallah, B.; Zanta, M. A.; Boussif, O.; Behr, J.-P.; Demeneix, B. Gene Transfer with Lipospermines and Polyethylenimines. *Advanced Drug Delivery Reviews* **1998**, *30* (1), 85–95.
(21) Edet Uwem Okon; Gihan Hammed; Poussy Abu El Wafa; Opetiti Abraham; Nicole Case; Elecia Henry. In-Vitro Cytotoxicity of Polyethyleneimine on HeLa and Vero Cells. *International Journal of Innovation and Applied Studies* **2014**, *5* (3), 192–199.
(22) Kafil, V.; Omidi, Y. Cytotoxic Impacts of Linear and Branched Polyethylenimine Nanostructures in A431 Cells. *BioImpacts* **2011**, *1* (1), 23–30.
(23) Wu, G. Y.; Wu, C. H. Receptor-Mediated in Vitro Gene Transformation by a Soluble DNA Carrier System. *Journal of Biological Chemistry* **1987**, *262* (10), 4429–4432.
(24) Heinrich, M. R.; Rohlfing, D. L.; Bugna, E. The Effect of Time of Heating on the Thermal Polymerization of L-Lysine. *Archives of Biochemistry and Biophysics* **1969**, *130*, 441–448.
(25) Kushwaha, D. R. S.; Mathur, K. B.; Balasubramanian, D. Poly(ε-L-lysine): Synthesis and Conformation. *Biopolymers* **1980**, *19* (2), 219–229.
(26) Ho, C. H.; Odermatt, E.; Berndt, I.; Tiller, J. C. Ways of Selective Polycondensation of L-lysine towards Linear A- and ε-poly-L-lysine. *Journal of Polymer Science Part A: Polymer Chemistry* **2008**, *46* (15), 5053–5063.

(27) Shukla, S. C.; Singh, A.; Pandey, A. K.; Mishra, A. Review on Production and Medical Applications of Ɛ-Polylysine. *Biochemical Engineering Journal* **2012**, *65*, 70–81.
(28) Scholl, M.; Nguyen, T. Q.; Bruchmann, B.; Klok, H.-A. The Thermal Polymerization of Amino Acids Revisited; Synthesis and Structural Characterization of Hyperbranched Polymers fromL-Lysine. *Journal of Polymer Science Part A: Polymer Chemistry* **2007**, *45* (23), 5494–5508.
(29) Kadlecova, Z.; Baldi, L.; Hacker, D.; Wurm, F. M.; Klok, H.-A. Comparative Study on the In Vitro Cytotoxicity of Linear, Dendritic, and Hyperbranched Polylysine Analogues. *Biomacromolecules* **2012**, *13* (10), 3127–3137.
(30) Kadlecova, Z.; Rajendra, Y.; Matasci, M.; Baldi, L.; Hacker, D. L.; Wurm, F. M.; Klok, H.-A. DNA Delivery with Hyperbranched Polylysine: A Comparative Study with Linear and Dendritic Polylysine. *Journal of Controlled Release* **2013**, *169* (3), 276–288.
(31) de Vries, A.; Feldman, J. D.; Stein, O.; Stein, Y.; Katchalski, E. Effects of Intravenously Administered Poly-D L-Lysine in Rats. *Experimental Biology and Medicine* **1953**, *82* (2), 237–240.
(32) Sela, M.; Katchalski, E. Biological Properties of Poly-α- Amino Acids. *Advances in Protein Chemistry* **1959**, *14*, 391–478.
(33) Lynn, D. M.; Langer, R. Degradable Poly(β-Amino Esters): Synthesis, Characterization, and Self-Assembly with Plasmid DNA. *Journal of American Chemical Society* **2000**, *122* (44), 10761–10768.
(34) Cutlar, L.; Zhou, D.; Gao, Y.; Zhao, T.; Greiser, U.; Wang, W.; Wang, W. Highly Branched Poly(β-Amino Esters): Synthesis and Application in Gene Delivery. *Biomacromolecules* **2015**, *16* (9), 2609–2617.
(35) Akinc, A.; Anderson, D. G.; Lynn, D. M.; Langer, R. Synthesis of Poly(β-Amino Ester)s Optimized for Highly Effective Gene Delivery. *Bioconjugate Chemistry* **2003**, *14* (5), 979–988.
(36) Gao, Y.; Huang, J.-Y.; O'Keeffe Ahern, J.; Cutlar, L.; Zhou, D.; Lin, F.-H.; Wang, W. Highly Branched Poly(β-Amino Esters) for Non-Viral Gene Delivery: High Transfection Efficiency and Low Toxicity Achieved by Increasing Molecular Weight. *Biomacromolecules* **2016**, *17* (11), 3640–3647.
(37) Eltoukhy, A. A.; Siegwart, D. J.; Alabi, C. A.; Rajan, J. S.; Langer, R.; Anderson, D. G. Effect of Molecular Weight of Amine End-Modified Poly(β-Amino Ester)s on Gene Delivery Efficiency and Toxicity. *Biomaterials* **2012**, *33* (13), 3594–3603.
(38) Jin, L.; Zeng, X.; Liu, M.; Deng, Y.; He, N. Current Progress in Gene Delivery Technology Based on Chemical Methods and Nano-Carriers. *Theranostics* **2014**, *4* (3), 240–255.
(39) Agarwal, S.; Zhang, Y.; Maji, S.; Greiner, A. PDMAEMA Based Gene Delivery Materials. *Materials Today* **2012**, *15* (9), 388–393.
(40) Van de Wetering, P.; Moret, E. E.; Schuurmans-Nieuwenbroek, N. M. E.; van Steenbergen, M. J.; Hennink, W. E. Structure−Activity Relationships of Water-Soluble Cationic Methacrylate/Methacrylamide Polymers for Nonviral Gene Delivery. *Bioconjugate Chemistry* **1999**, *10* (4), 589–597.
(41) Zhang, X.; Xia, J.; Matyjaszewski, K. Controlled/"Living" Radical Polymerization of 2-(Dimethylamino)ethyl Methacrylate. *Macromolecules* **1998**, *31* (15), 5167–5169.
(42) Synatschke, C. V.; Schallon, A.; Jérôme, V.; Freitag, R.; Müller, A. H. E. Influence of Polymer Architecture and Molecular Weight of Poly(2-(Dimethylamino)ethyl Methacrylate) Polycations on Transfection Efficiency and Cell Viability in Gene Delivery. *Biomacromolecules* **2011**, *12* (12), 4247–4255.
(43) Sahnoun, M.; Charreyre, M.-T.; Veron, L.; Delair, T.; D'Agosto, F. Synthetic and Characterization Aspects of Dimethylaminoethyl Methacrylate Reversible Addition Fragmentation Chain Transfer (RAFT) Polymerization. *Journal of Polymer Science Part A: Polymer Chemistry* **2005**, *43* (16), 3551–3565.
(44) Xiong, Q.; Ni, P.; Zhang, F.; Yu, Z. Synthesis and Characterization of 2-(Dimethylamino)ethyl Methacrylate Homopolymers via Aqueous RAFT Polymerization and Their Application in Miniemulsion Polymerization. *Polymer Bulletin* **2004**, *53* (1), 1–8.
(45) Yuan, J.; Peng, J.; Li, J.; Ju, X.; Zhai, M. Synthesis of Poly(dimethylaminoethyl Methacrylate) with High Cloud Point by RAFT Polymerization under γ-Irradiation. *Radiation Physics and Chemistry* **2015**, *108*, 95–101.

(46) Wu, W.; Wang, W.; Li, J. Star Polymers: Advances in Biomedical Applications. *Progress in Polymer Science* **2015**, *46*, 55–85.
(47) Van de Wetering, P.; Cherng, J.-Y.; Talsma, H.; Hennink, W. E. Relation between Transfection Efficiency and Cytotoxicity of Poly (2-(Dimethylamino) Ethyl Methacrylate)/Plasmid Complexes. *Journal of Controlled Release* **1997**, *49* (1), 59–69.
(48) Zhu, C.; Jung, S.; Si, G.; Cheng, R.; Meng, F.; Zhu, X.; Park, T. G.; Zhong, Z. Cationic Methacrylate Copolymers Containing Primary and Tertiary Amino Side Groups: Controlled Synthesis via RAFT Polymerization, DNA Condensation, and in Vitro Gene Transfection. *Journal of Polymer Science Part A: Polymer Chemistry* **2010**, *48* (13), 2869–2877.
(49) Truong, N. P.; Jia, Z.; Burgess, M.; Payne, L.; McMillan, N. A. J.; Monteiro, M. J. Self-Catalyzed Degradable Cationic Polymer for Release of DNA. *Biomacromolecules* **2011**, *12* (10), 3540–3548.
(50) Kolate, A.; Baradia, D.; Patil, S.; Vhora, I.; Kore, G.; Misra, A. PEG — A Versatile Conjugating Ligand for Drugs and Drug Delivery Systems. *Journal of Controlled Release* **2014**, *192*, 67–81.
(51) C. Campa and S. P. Harding. Anti-VEGF Compounds in the Treatment of Neovascular Age Related Macular Degeneration. *Current Drug Targets* **2011**, *12* (2), 173–181.
(52) Pezzoli, D.; Tarsini, P.; Melone, L.; Candiani, G. RGD-Derivatized PEI-PEG Copolymers: Influence of the Degree of Substitution on the Targeting Behavior. *Journal of Drug Delivery Science and Technology* **2017**, *37*, 115–122.
(53) Choi, Y.-R.; Chae, S. Y.; Ahn, C.-H.; Lee, M.; Oh, S.; Byun, Y.; Rhee, B. D.; Ko, K. S. Development of Polymeric Gene Delivery Carriers: PEGylated Copolymers of L-Lysine and L-Phenylalanine. *Journal of Drug Targeting* **2007**, *15* (6), 391–398.
(54) Thiersch, M.; Rimann, M.; Panagiotopoulou, V.; Öztürk, E.; Biedermann, T.; Textor, M.; Lühmann, T. C.; Hall, H. The Angiogenic Response to PLL-G-PEG-Mediated HIF-1α Plasmid DNA Delivery in Healthy and Diabetic Rats. *Biomaterials* **2013**, *34* (16), 4173–4182.
(55) Kim, J.; Kang, Y.; Tzeng, S. Y.; Green, J. J. Synthesis and Application of Poly(ethylene Glycol)-Co-Poly(β-Amino Ester) Copolymers for Small Cell Lung Cancer Gene Therapy. *Acta Biomaterialia* **2016**, *41*, 293–301.
(56) Mastorakos, P.; da Silva, A. L.; Chisholm, J.; Song, E.; Choi, W. K.; Boyle, M. P.; Morales, M. M.; Hanes, J.; Suk, J. S. Highly Compacted Biodegradable DNA Nanoparticles Capable of Overcoming the Mucus Barrier for Inhaled Lung Gene Therapy. *Proceedings of the National Academy of Sciences* **2015**, *112* (28), 8720–8725.
(57) Rungsardthong, U.; Deshpande, M.; Bailey, L.; Vamvakaki, M.; Armes, S. P.; Garnett, M. C.; Stolnik, S. Copolymers of Amine Methacrylate with Poly(ethylene Glycol) as Vectors for Gene Therapy. *Journal of Controlled Release* **2001**, *73* (2–3), 359–380.
(58) Lin, D.; Huang, Y.; Jiang, Q.; Zhang, W.; Yue, X.; Guo, S.; Xiao, P.; Du, Q.; Xing, J.; Deng, L.; Liang, Z.; Dong, A. Structural Contributions of Blocked or Grafted poly(2-Dimethylaminoethyl Methacrylate) on PEGylated Polycaprolactone Nanoparticles in siRNA Delivery. *Biomaterials* **2011**, *32* (33), 8730–8742.
(59) Lai, J.; Xu, Z.; Tang, R.; Ji, W.; Wang, R.; Wang, J.; Wang, C. PEGylated Block Copolymers Containing Tertiary Amine Side-Chains Cleavable via Acid-Labile Ortho Ester Linkages for pH-Triggered Release of DNA. *Polymer* **2014**, *55* (12), 2761–2771.
(60) Petersen, H.; Fechner, P. M.; Fischer, D.; Kissel, T. Synthesis, Characterization, and Biocompatibility of Polyethylenimine-Graft-Poly(ethylene Glycol) Block Copolymers. *Macromolecules* **2002**, *35* (18), 6867–6874.
(61) Pasche, S.; Textor, M.; Meagher, L.; Spencer, N. D.; Griesser, H. J. Relationship between Interfacial Forces Measured by Colloid-Probe Atomic Force Microscopy and Protein Resistance of Poly(ethylene Glycol)-Grafted Poly(L -Lysine) Adlayers on Niobia Surfaces. *Langmuir* **2005**, *21* (14), 6508–6520.
(62) Kolb, H. C.; Finn, M. G.; Sharpless, K. B. Click Chemistry: Diverse Chemical Function from a Few Good Reactions. *Angewandte Chemie International Edition* **2001**, *40* (11), 2004–2021.
(63) Hoyle, C. E.; Lowe, A. B.; Bowman, C. N. Thiol-Click Chemistry: A Multifaceted Toolbox for Small Molecule and Polymer Synthesis. *Chemical Society Reviews* **2010**, *39* (4), 1355.

(64) Välimäki, S.; Khakalo, A.; Ora, A.; Johansson, L.-S.; Rojas, O. J.; Kostiainen, M. A. Effect of PEG–PDMAEMA Block Copolymer Architecture on Polyelectrolyte Complex Formation with Heparin. *Biomacromolecules* **2016**, *17* (9), 2891–2900.

(65) Venkataraman, S.; Ong, W. L.; Ong, Z. Y.; Joachim Loo, S. C.; Rachel Ee, P. L.; Yang, Y. Y. The Role of PEG Architecture and Molecular Weight in the Gene Transfection Performance of PEGylated Poly(dimethylaminoethyl Methacrylate) Based Cationic Polymers. *Biomaterials* **2011**, *32* (9), 2369–2378.

(66) Zhang, X.; Pan, S.-R.; Hu, H.-M.; Wu, G.-F.; Feng, M.; Zhang, W.; Luo, X. Poly(ethylene Glycol)-Block-Polyethylenimine Copolymers as Carriers for Gene Delivery: Effects of PEG Molecular Weight and PEGylation Degree. *Journal of Biomedical Materials Research Part A* **2008**, *84A* (3), 795–804.

(67) Fitzsimmons, R. E. B.; Uludağ, H. Specific Effects of PEGylation on Gene Delivery Efficacy of Polyethylenimine: Interplay between PEG Substitution and N/P Ratio. *Acta Biomaterialia* **2012**, *8* (11), 3941–3955.

(68) Sergeeva, A.; Kolonin, M.; Molldrem, J.; Pasqualini, R.; Arap, W. Display Technologies: Application for the Discovery of Drug and Gene Delivery Agents. *Advanced Drug Delivery Reviews* **2006**, *58* (15), 1622–1654.

(69) Park, J.; Singha, K.; Son, S.; Kim, J.; Namgung, R.; Yun, C. O.; Kim, W. J. A Review of RGD-Functionalized Nonviral Gene Delivery Vectors for Cancer Therapy. *Cancer gene therapy* **2012**, *19* (11), 741–748.

(70) Takagi, J. Structural Basis for Ligand Recognition by RGD (Arg-Gly-Asp)-Dependent Integrins. *Biochemical Society Transactions* **2004**, *32* (3), 403–406.

(71) Plow, E. F.; Haas, T. A.; Zhang, L.; Loftus, J.; Smith, J. W. Ligand Binding to Integrins. *Journal of Biological Chemistry* **2000**, *275* (29), 21785–21788.

(72) Suh, W.; Chung, J.-K.; Park, S.-H.; Kim, S. W. Anti-JL1 Antibody-Conjugated Poly (L-Lysine) for Targeted Gene Delivery to Leukemia T Cells. *Journal of controlled release* **2001**, *72* (1), 171–178.

(73) Qian, Y.; Zha, Y.; Feng, B.; Pang, Z.; Zhang, B.; Sun, X.; Ren, J.; Zhang, C.; Shao, X.; Zhang, Q.; Jiang, X. PEGylated poly(2-(Dimethylamino) Ethyl Methacrylate)/DNA Polyplex Micelles Decorated with Phage-Displayed TGN Peptide for Brain-Targeted Gene Delivery. *Biomaterials* **2013**, *34* (8), 2117–2129.

(74) Oba, M.; Fukushima, S.; Kanayama, N.; Aoyagi, K.; Nishiyama, N.; Koyama, H.; Kataoka, K. Cyclic RGD Peptide-Conjugated Polyplex Micelles as a Targetable Gene Delivery System Directed to Cells Possessing $\alpha_v\beta_3$ and $\alpha_v\beta_5$ Integrins. *Bioconjugate Chemistry* **2007**, *18* (5), 1415–1423.

(75) Van de Wetering, P.; Zuidam, N. J.; van Steenbergen, M. J.; van der Houwen, O. A. G. J.; Underberg, W. J. M.; Hennink, W. E. A Mechanistic Study of the Hydrolytic Stability of Poly(2-(Dimethylamino)ethyl Methacrylate). *Macromolecules* **1998**, *31* (23), 8063–8068.

(76) Truong, N. P.; Jia, Z.; Burges, M.; McMillan, N. A. J.; Monteiro, M. J. Self-Catalyzed Degradation of Linear Cationic Poly(2-Dimethylaminoethyl Acrylate) in Water. *Biomacromolecules* **2011**, *12* (5), 1876–1882.

(77) Bromberg, L. Polymeric Micelles in Oral Chemotherapy. *Journal of Controlled Release* **2008**, *128* (2), 99–112.

(78) Forrest, M. L.; Koerber, J. T.; Pack, D. W. A Degradable Polyethylenimine Derivative with Low Toxicity for Highly Efficient Gene Delivery. *Bioconjugate Chemistry* **2003**, *14* (5), 934–940.

(79) Lin, C.; Engbersen, J. F. The Role of the Disulfide Group in Disulfide-Based Polymeric Gene Carriers. *Expert Opinion on Drug Delivery* **2009**, *6* (4), 421–439.

(80) You, Y.-Z.; Manickam, D. S.; Zhou, Q.-H.; Oupický, D. Reducible poly(2-Dimethylaminoethyl Methacrylate): Synthesis, Cytotoxicity, and Gene Delivery Activity. *Journal of Controlled Release* **2007**, *122* (3), 217–225.

(81) Islam, M. A.; Park, T.; Singh, B.; Maharjan, S.; Firdous, J.; Cho, M.-H.; Kang, S.-K.; Yun, C.-H.; Choi, Y.; Cho, C.-S. Major Degradable Polycations as Carriers for DNA and siRNA. *Journal of Controlled Release* **2014**, *193*, 74–89.

(82) Kito, M.; Takimoto, R.; Yoshida, T.; Nagasawa, T. Purification and Characterization of an ε-Poly- L -Lysine-Degrading Enzyme from an ε-Poly- L -Lysine-Producing Strain of Streptomyces Albulus. *Archives of Microbiology* **2002**, *178* (5), 325–330.

(83) Kito, M.; Onji, Y.; Yoshida, T.; Nagasawa, T. Occurrence of ε -Poly-L-Lysine-Degrading Enzyme in ε-Poly-L-Lysine-Tolerant Sphingobacterium Multivorum OJ10: Purification and Characterization. *FEMS Microbiology Letters* **2002**, *207* (2), 147–151.

Chapter 2: Synthesis and characterization of PEO macromolecular chain transfer agents

Introduction

PEO is a commercial water soluble, non-toxic and biocompatible polymer widely used in several applications such as cosmetic or biology and it has been approved by the food and drugs administration (FDA).[1–4] PEO is used in biopharmaceuticals processes to increase the circulating half-life of drugs.[2] The addition of a PEO on a molecule or a polymer is named PEGylation.

In gene therapy, the PEGylation of cationic polymers was studied on PEI,[5] PLL,[6,7] PBAE,[8,9] or cationic vinylic polymers.[10–12] It has been shown that the PEGylation decreases cytotoxicity of cationic polymers by decreasing the charge density.[13,14] Moreover, this decrease of the charge density leads to a lower binding affinity with cell membrane leading to a decrease of transfection efficiency.[13] However, with a low grafting ratio of PEO on polyplex, the transfection efficiency increases due to the better stability of the polyplex. The PEO acts like a "shield" to protect the polyplex from destabilization, opsonization and rapid clearance due to the salts, proteins of macrophages in the blood.[3,4,15,16]

As reported in the literature chapter (Chapter I-§A), there are two strategies to covalently attach a linear PEO onto a cationic polymer to target block copolymers: either the "PEO grafted onto" or either the "PEO grafted from". The "PEO grafted onto" strategy based on the covalent linkage between the PEO block and the second cationic polymer block, leads too low yields and partial functionalization due the incompatibility of both polymer blocks. In this work, the "PEO grafting from" strategy was employed. It consists in the formation of the second polymer block by the direct polymerization of appropriate monomer(s) from a first PEO block used as a macromolecular initiator or a macromolecular chain transfer agent. It is well-known that such "PEO grafting from" strategy allows a high PEO functionalization with good yields. As the versatile RAFT polymerization has been chosen in our study to synthesize cationic amine-based

polyacrylates, a linear PEO (lPEO) and a bPEO macromolecular chain transfer agents are aimed in this work. The influence of the POE architecture will be studied on the polyplex formation and the cationic polymer cytotoxicity. Moreover, in order to introduce a recognition ligand, heterofunctionalized PEOs are targeted.

In this chapter, the first part is devoted to the heterofunctionalization of lPEO. The chosen recognition ligand possesses a thiol group. A pyridyldithio group and an alkyne group able to react with thiol functionalizd recognition ligand under mild conditions, have been added on the α-position of the lPEO. The thiol function of the recognition ligand can be added to the lPEO by disulfide echange reaction or by thiol-yne coupling reaction with the pyridyldithio group and the alkyne group, respectively.[17–20] On the ω-position of the lPEO has been a trithiocarbonate group, by nucleophilic substitution using different methods. Trithiocarbonate allows to control the RAFT polymerization of aminoethyl acrylate[21]. The trithiocarbonate has been chose because of its better stability and lower toxicity than dithioesters.[22,23]

In a second part, the heterofunctionalization of the bPEO has been studied by RAFT polymerization of PEGA using an alkyne-based chain transfer agent.

A wide range of groups can be introduced and monitored at the a-position of the RAFT synthesized polymer by carefully choosing the R-group of the initial chain transfer agent. The direct RAFT polymerization using a clickable functionalized RAFT agent allows the thiol-yne reaction to functionalize the α-position of a polymer by alkyne-click chemistry.[11,24–26] This chain-transfer agent contains an alkyne R-group and a trithiocarbonate Z-group. The alkyne group is linked via an amide function. The stability of the alkyne bond could avoid side reactions during the polymerization, and the amide group is a robust functionality that can resist hydrolysis in view of further (biological) applications in aqueous media. The alkyne group can react with a thiol by thiol-yne coupling reaction to functionalize the α-position of the PPEGA.

I. Synthesis of an heterofuntional linear poly(ethylene oxide) (lPEO) for PEGylation of cationic copolymers

On the α chain-end of the lPEO, reactive groups including pyridyldisulfide or alkyne will allow the incorporation of thiol-based recognition ligand through disulfide exchange reaction and thiol-yne coupling reaction, respectively.[17–20] Such reactions have been chosen because they could be performed under mild conditions in order to preserve the recognition ligand. Then, on the ω chain-end, a trithiocarbonate group will permit to control the RAFT copolymerization of aminoethyl acrylate.

A. Synthesis of an α-pyridyldithio,ω-hydroxylPEO

The α-pyridyldithio,ω-hydroxylPEO was synthesized through the nucleophilic substitution of the succinimidyl 3-(2-pyridyldithio)propionate (SPDP) by the α-amino,ω-hydroxylPEO with a number-average molar mass determined by matrix-assisted laser desorption-ionization-time of flight (MALDI-TOF) mass spectrometry (number-average degree of polymerization determined by MALDI-TOF, $\overline{DP_{n,MALDI}}$ = 64) of 2970 g.mol^{-1} (Scheme II. 1). The reaction was performed using 1.2 equivalents of SPDP and 1 equivalent of α-amino,ω-hydroxylPEO in acetonitrile during 5 hours at room temperature. The final polymer was purified by dialysis in ultra-pure water. After freeze-drying, the polymer was obtained with a yield of 89 % and analyzed by Fourier-transform infrared (FT-IR) spectroscopy, MALDI-TOF mass spectrometry, ^{1}H NMR spectroscopy and SEC.

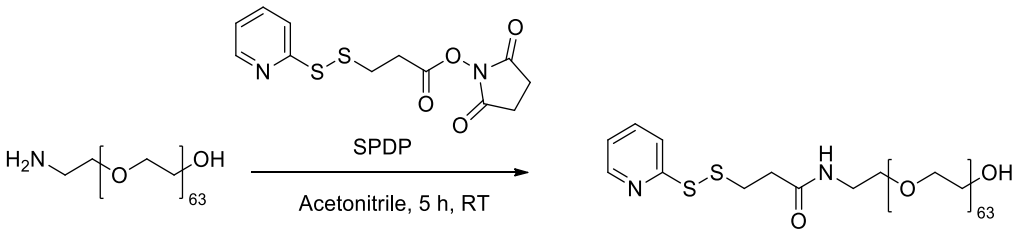

Scheme II. 1. Synthesis of an α-pyridyldithio,ω-hydroxylPEO.

The comparison between the FT-IR spectra of α-amino,ω-hydroxylPEO and α-pyridyldithio,ω-hydroxylPEO shows the appearance of signals at 1569 cm^{-1} and at 1662 cm^{-1} relative to the N-H amide bending band and to the C-O amide stretching band, respectively (Figure II. 1).

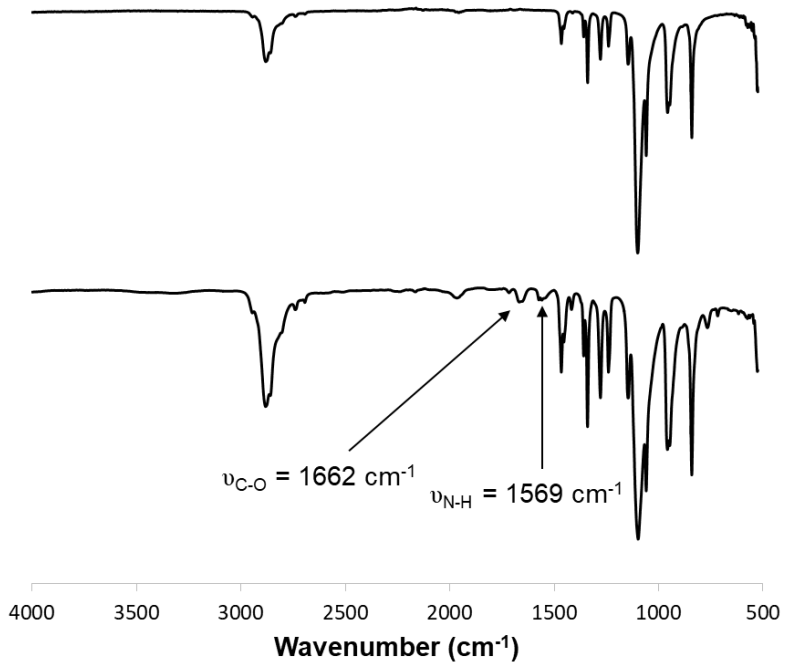

Figure II. 1. Comparison of FT-IR spectra of α-amino,ω-hydroxylPEO (top) and α-pyridyldithio,ω-hydroxylPEO (bottom).

The MALDI-TOF mass spectrum (Figure II. 2) shows a single series of peaks separated by a m/z_{exp} = 44.026 Da characteristic of the molar mass of ethylene oxide (EO) unit (m/z_{calc} = 44.026 Da). The main peak at m/z_{exp} = 3054.466 Da on the spectrum corresponds to 64 EO repeating unit, a pyridyldithio-propanoxo moiety at one chain-end, a hydroxyl moiety at the other chain-end and a sodium atom responsible of the ionization (calculated value m/z_{calc} = 3054.690 Da). A number-average degree of polymerization ($\overline{DP_n}$) of 64 for the α-pyridyldithio,ω-hydroxylPEO has been determined by MALDI-TOF mass spectrometry.

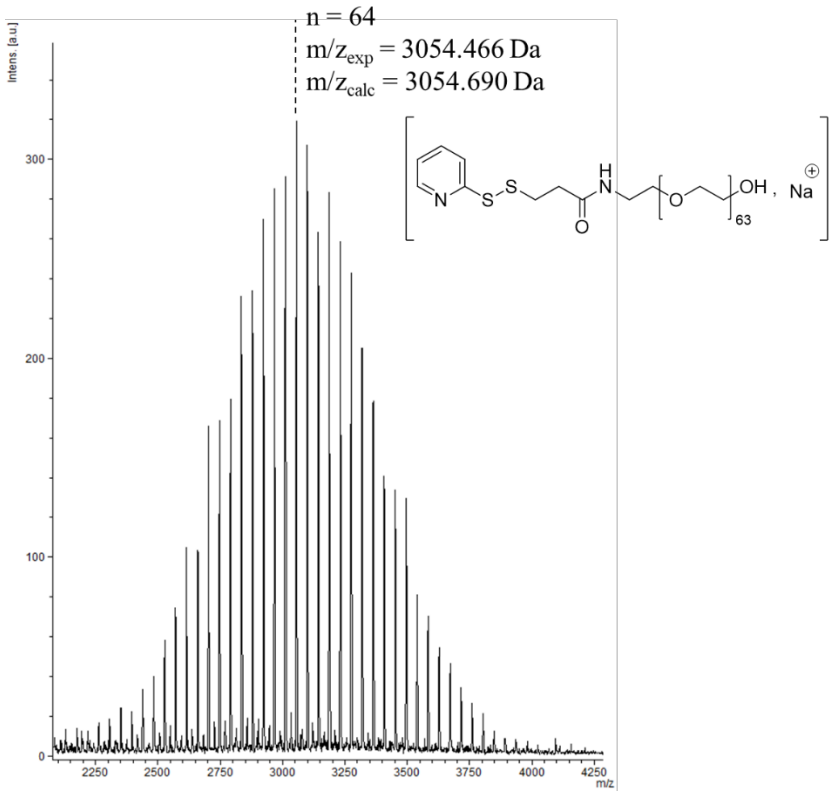

Figure II. 2. MALDI-TOF mass spectrum of an α-pyridyldithio,ω-hydroxylPEO. Matrix: dithranol (DIT), salt: sodium trifluoroacetate (NaTFA).

The ^{1}H NMR spectrum of purified polymer (Figure II. 3) shows the characteristic signals of C*H*$_2$C*H*$_2$*O* of EO unit at 3.65 ppm (labeled h in Figure II. 3) and the characteristic signals of aromatic protons of pyridyl group between 7.10 and 8.49 ppm (labeled a, b, c and d in Figure II. 3). Moreover, two triplets are also observed at 3.09 and 2.62 ppm characteristics of the SSC*H*$_2$CH$_2$C(=O)NH and of the SSCH$_2$C*H*$_2$CONH (labeled e and f in Figure II. 3), respectively. The degree of functionalization was calculated by comparing the integration areas of the C*H*$_2$C*H*$_2$O signal of PEO at 3.65 ppm, (256 protons corresponding to a $\overline{DP_n}$ = 64, determined by MALDI-TOF mass spectrometry, labeled h in Figure II. 3) and of the SSCH$_2$C*H*$_2$CONH at 2.62 ppm (1.90 protons, labeled f in Figure II. 3). The functionalization degree is equal to 95 %.

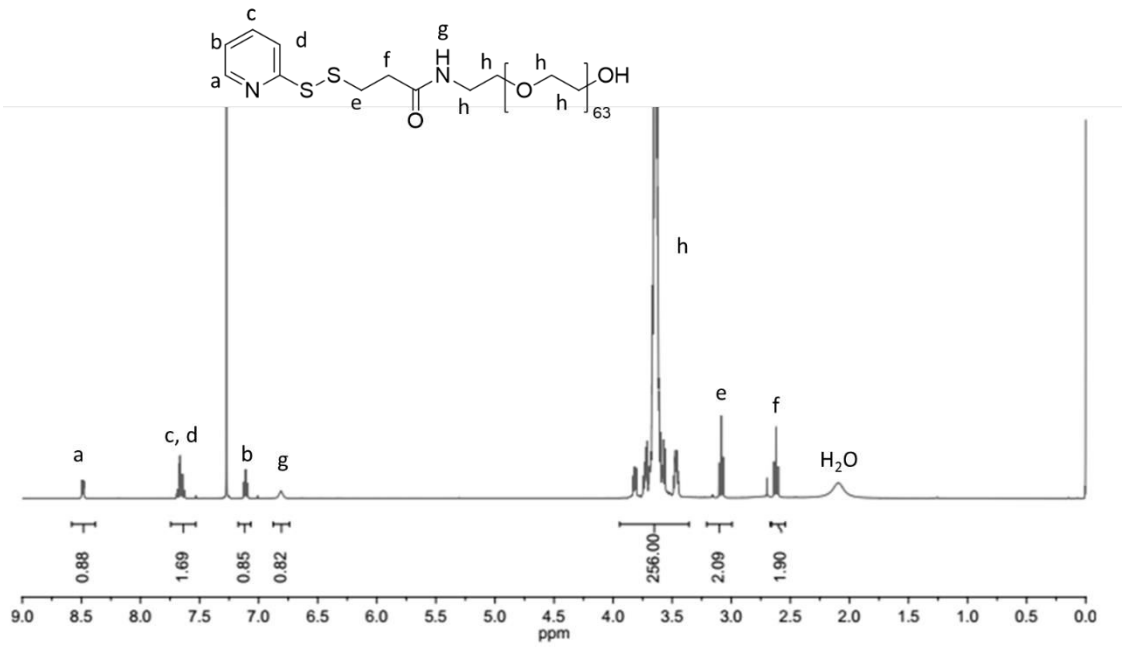

Figure II. 3. ^{1}H NMR spectrum (400 MHz, $CDCl_3$) of the α-pyridyldithio,ω-hydroxylPEO.

The final polymer was also analyzed by SEC in *N,N*-dimethylformamide (DMF, LiBr, 1 $g.L^{-1}$) using refractive index (RI) detection and ultra-violet-visible (UV-vis) detection at 281.6 nm (corresponding to the maximum wavelength of the pyridyl group, Figure II. 4). The SEC traces show a bimodal signal using RI detection and an unimodal signal using UV-vis detection. The signal observed using RI detection at low elution volume corresponds to a PEO with a double molar mass, inherent to the commercial α-amino,ω-hydroxylPEO. The unimodal trace observed using UV-vis detection at 281.6 nm corresponds to the PEO containing the pyridyldithio group (number-average molar mass determined by SEC ($\overline{M_{n,SEC}}$) = 8800 $g.mol^{-1}$, polystyrene (PS) equivalents, $Đ$ = 1.07).

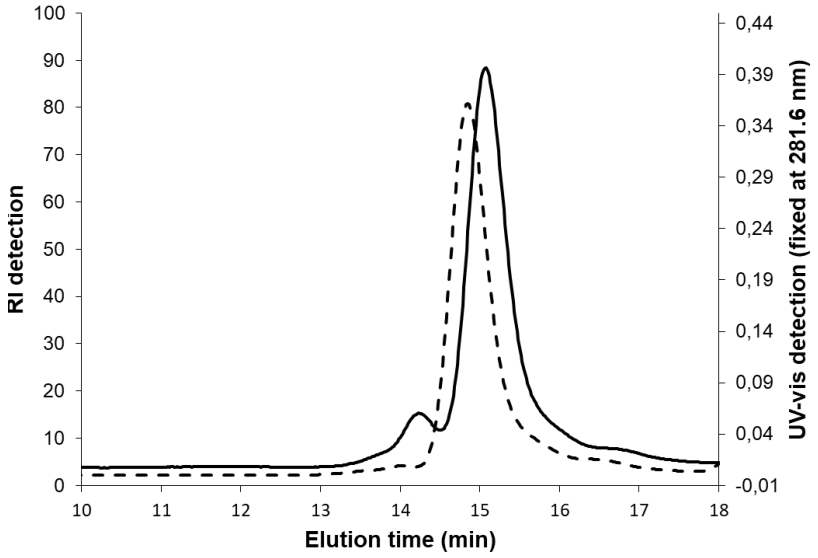

Figure II. 4. Overlaid SEC traces of purified α-pyridyldithio,ω-hydroxylPEO (solid line: RI response, dash line: UV-vis response at 281.6 nm).

All FT-IR and ^{1}H NMR spectroscopies, MALDI-TOF mass spectrometry and SEC characterizations confirmed the successful synthesis and purification of the α-pyridyldithio,ω-hydroxylPEO.

B. Synthesis of an α-alkynyl,ω-hydroxylPEO

Two different strategies have been explored to introduce an alkyne group on the α position of a PEO: the first one is based on the nucleophilic substitution of the propargyl bromide using the α,ω-dihydroxylPEO under basic condition (Williamson reaction) and the second one is based on the nucleophilic addition of the α-amino,ω-hydroxyPEO on L-(4,4-dimethyl-5-oxo-4,5-dihydrooxazol-2-yl)ethylhex-5-ynoate, an azlactone-based linker containing the alkyne group (named alkyne-AZL).

1. Using the propargyl bromide

An α,ω-dihydroxylPEO with a number-average molar mass determined by MALDI-TOF mass spectrometry ($\overline{DP}_{n,MALDI\text{-}TOF}$ = 44) of 1938 g.mol^{-1} was employed as starting PEO. The reaction was performed using 1 equivalent of α,ω-dihydroxylPEO, 1.9 equivalent of potassium

hydroxide and 1.3 equivalent of propargyl bromide in toluene during 7 days at 70°C (Scheme II. 2). The final product was purified by precipitation in cold diethyl ether and dried under vacuum. The resulting polymer was obtained with a yield of 87 % and was analyzed by ^{1}H NMR spectroscopy and MALDI-TOF mass spectrometry.

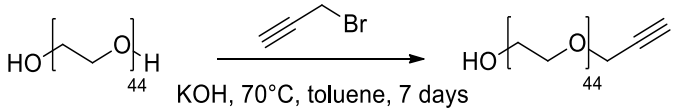

Scheme II. 2. Synthesis of an α-alkynyl,ω-hydroxylPEO using the propargyl bromide.

The ^{1}H NMR spectroscopy (Figure II. 5) shows the characteristic signals of C*H*$_2$C*H*$_2$O of EO repeating unit at 3.65 ppm (labeled b in Figure II. 5) and two signals characteristics of the propargyl moiety at 4.20 ppm for the methylene protons of HC≡CC*H*$_2$O (labeled c in Figure II. 5) and at 2.40 ppm for the methine proton of *H*C≡CCH$_2$O (labeled d in Figure II. 5). The degree of functionalization was calculated by comparing the integration areas of the C*H*$_2$C*H*$_2$O signals of EO unit at 3.65 ppm (176 protons, corresponding to a $\overline{DP_n}$ = 44 determined by MALDI-TOF mass spectrometry, labeled b in Figure II. 5) and of the *H*C≡CCH$_2$O signal of the methine proton at 2.40 ppm (0.78 proton, labeled d in Figure II. 5). The degree of functionalization is equal to 78 %.

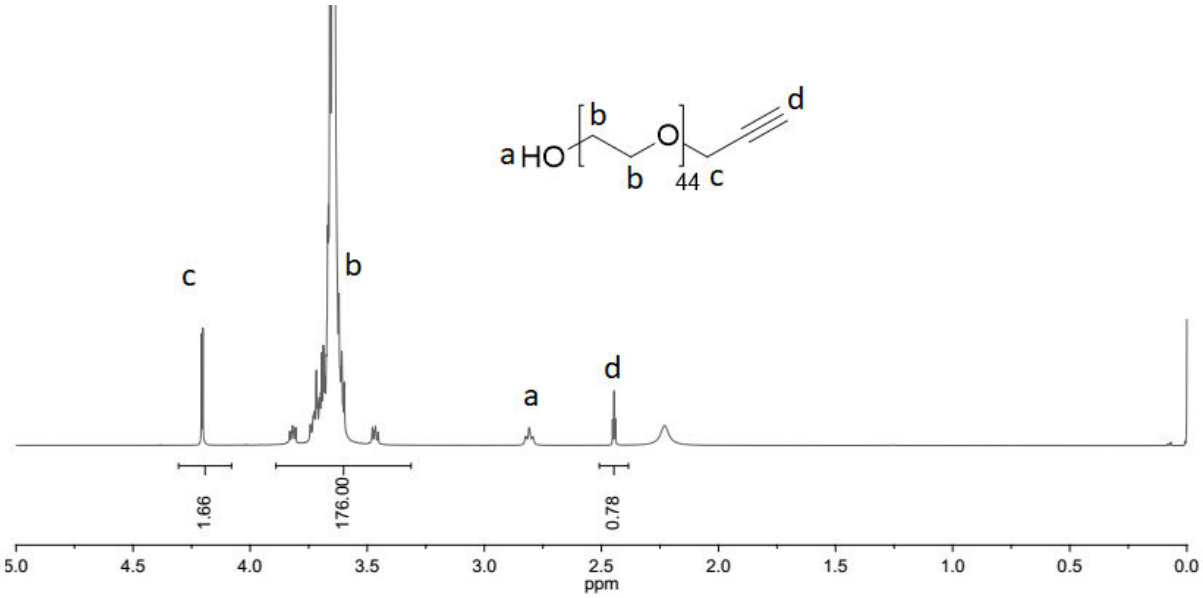

Figure II. 5. ^{1}H NMR spectrum (400 MHz, $CDCl_3$) of the α-alkynyl,ω-hydroxylPEO synthesized using the propargyl bromide.

This reaction leads to an uncomplete functionalization, which was further confirmed by MALDI-TOF mass spectrometry (Figure II. 6). The MALDI-TOF mass spectrum shows three populations: (A) α-alkynyl,ω-potassium hydroxylate PEO, (B) α-alkynyl,ω-hydroxylPEO and (C) α,ω-dihydroxylPEO which were clearly identified. This result shows that this reaction is not selective and the difficulty comes probably from the homofunctional α,ω-dihydroxylPEO. Therefore, the heterofunctional α-amino,ω-hydroxylPEO will be employed for our follow-up work.

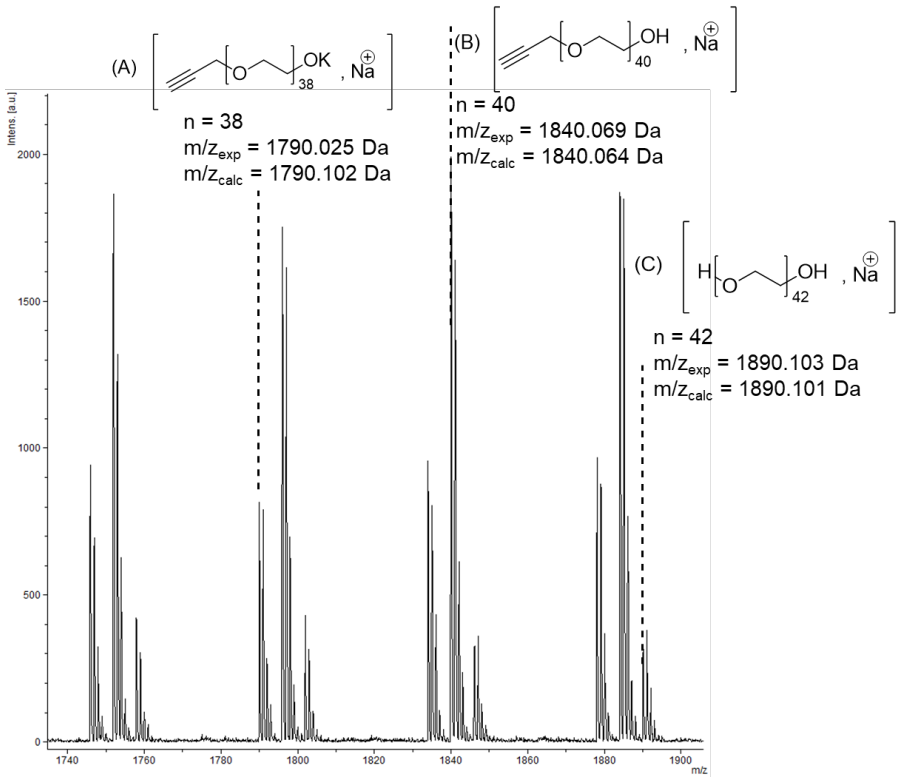

Figure II. 6. MALDI-TOF spectrum between m/z of 1740 and 1900 Da of purified polymer obtained after reaction of α,ω-dihydroxylPEO with propargyl bromide and KOH in toluene at 70 °C during 7 days. Matrix: *trans*-2-[3-(4-butylphenyl)-2-methyl-2-propenylidene]malono-nitrile (DCTB), salt: NaTFA.

2. Using the L-(4,4-dimethyl-5-oxo-4,5-dihydrooxazol-2-yl) ethyl hex-5-ynoate (named alkyne-AZL)

The azlactone (also named oxazolidin-5-one) is an electrophilic heterocycle which can react easily with amines through a ring-opening reaction. This reaction leads to complete conversion without the formation of by-products and can be performed in organic solvent or water.[27,28] In this work, the alkyne-AZL has been chosen as a linker to modify the α-amino,ω-hydroxylPEO to target the α-alkynyl,ω-hydroxylPEO. The alkyne-AZL was synthesized according to the reported procedure from our laboratory.[28] One equivalent of α-amino,ω-hydroxylPEO was added to 1.1 equivalent of alkyne-AZL previously solubilized in dichloromethane (CH_2Cl_2). The reaction was performed at room temperature for 24 hours

(Scheme II. 3). The final polymer was separated and purified by one precipitation in cold diethyl ether. After purification, a white powder was obtained with a yield of 99 % and was analyzed by MALDI-TOF mass spectrometry and ^{1}H and ^{13}C NMR spectroscopies.

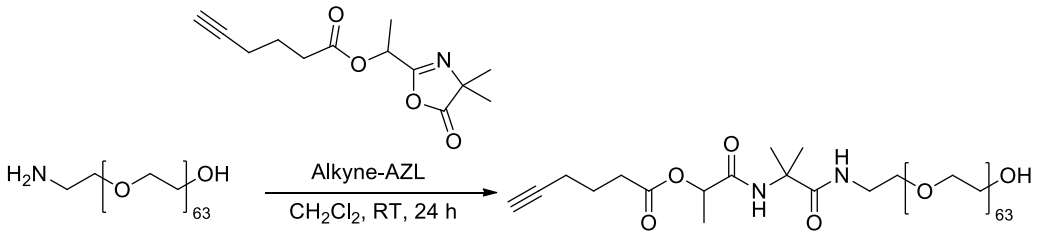

Scheme II. 3. Synthesis of an α-alkynyl,ω-hydroxylPEO using the alkyne-AZL.

The purified polymer was first analyzed by MALDI-TOF mass spectrometry (Figure II. 7). The spectrum shows a single series of peaks separated by 44.023 Da, corresponding to the molar mass of the EO repeating unit (calculated value: 44.026 Da). The peak at 3108.780 Da corresponds to a polymer chain with 64 EO unit, an alkynyl moiety at one chain-end, a hydroxyl group at the other chain-end, and a sodium entity as the atom responsible of the ionization (calculated value: 3108.809 Da). A $\overline{DP_n}$ of 64 has been determined by MALDI-TOF mass spectrometry.

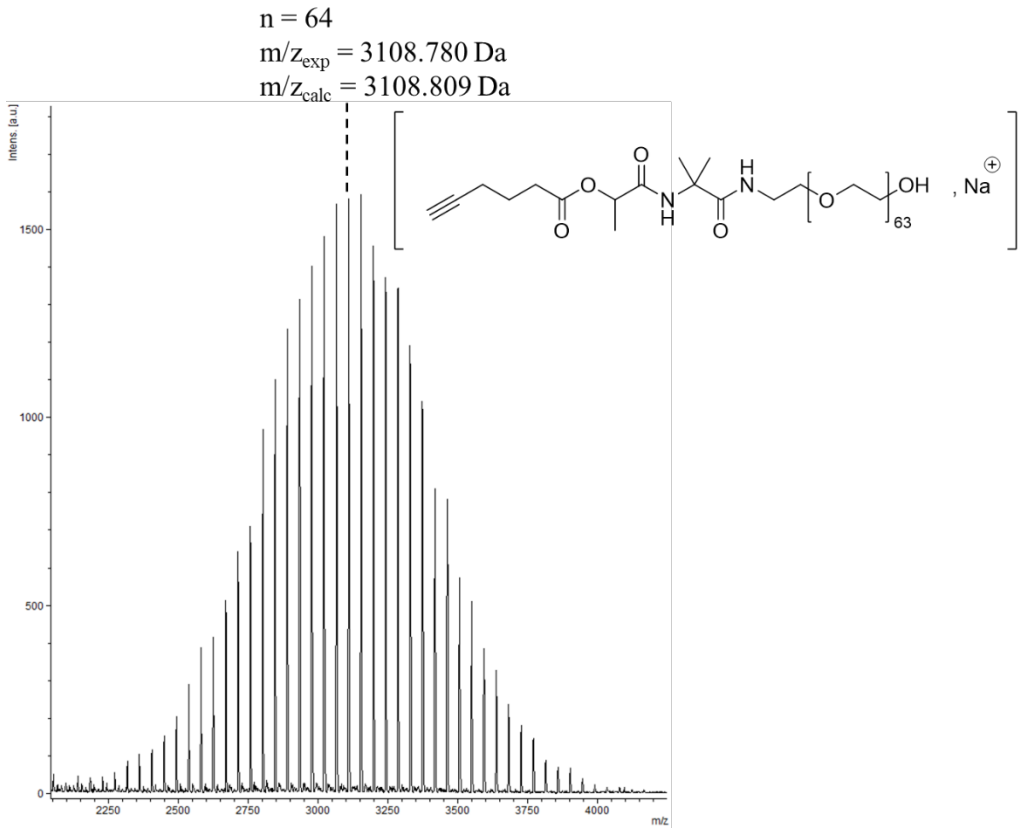

Figure II. 7. MALDI-TOF mass spectrometry of α-alkynyl,ω-hydroxylPEO obtained by ring-opening reaction of the alkyne-AZL by α-amino,ω-hydroxylPEO in CH_2Cl_2 at room temperature during 24 hours. Matrix: DIT, salt: NaTFA.

The ^{1}H NMR spectrum (Figure II. 8) shows a signal at 3.65 ppm corresponding to the methylene protons C*H*$_2$C*H*$_2$O of EO unit (labeled j in Figure II. 8) together with a triplet at 2.01 ppm corresponding to the methine *H*C≡CCH$_2$ proton of the alkyne group (labeled a in Figure II. 8). Moreover, one doublet at 1.46 and two singlets at 1.62 ppm characteristics of the two methyl groups of the azlactone precursor appear (labeled f and h in Figure II. 8, respectively). The degree of functionalization was calculated by comparing the integration areas signal corresponding to the C*H*$_2$C*H*$_2$O of the repeating unit of PEO (labeled j in Figure II. 8, 256 protons, corresponding to a $\overline{DP_{n,MALDI}}$ = 64, determined by MALDI-TOF mass spectrometry) and of the CH$_3$C*H*C(=O)NH of the azlactone precursor at 5.11 ppm (1.03 proton, labeled e in Figure II. 8). The calculated conversion rate was 100 %.

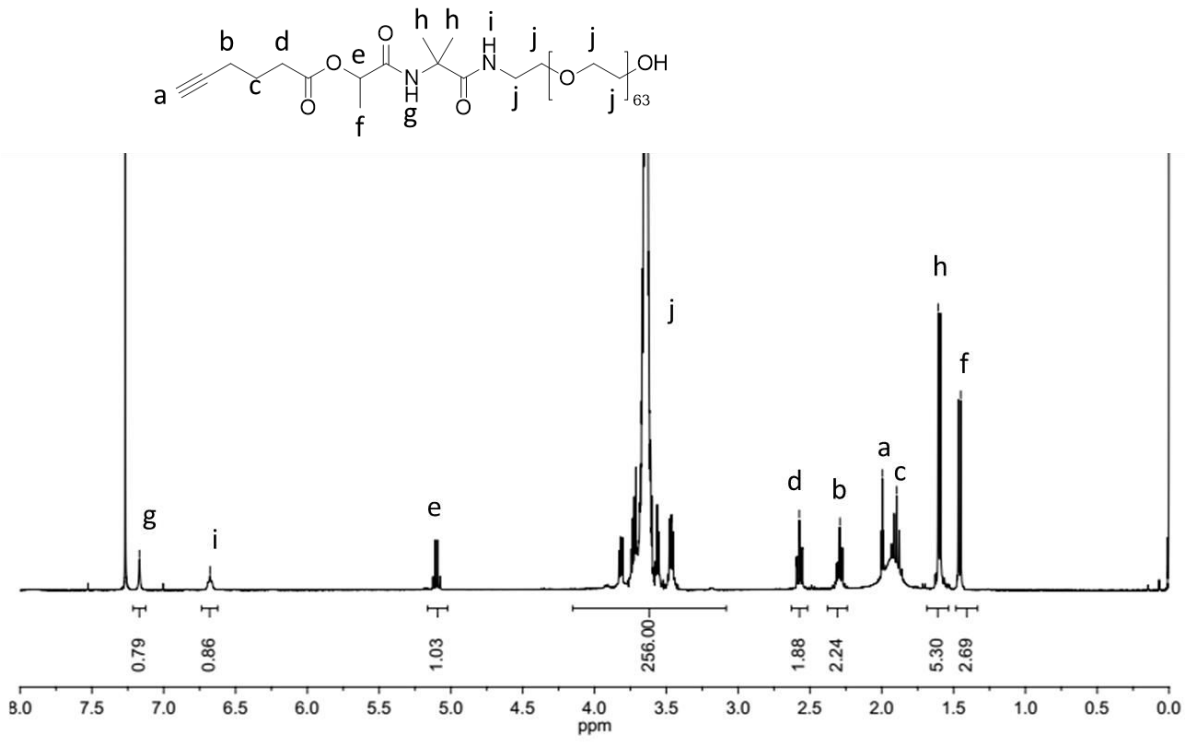

Figure II. 8. ^{1}H NMR spectrum (400 MHz, $CDCl_3$) of α-alkynyl,ω-hydroxylPEO obtained by ring-opening reaction of the alkyne-AZL with α-amino,ω-hydroxylPEO in CH_2Cl_2 at room temperature during 24 hours.

The ^{13}C NMR spectrum of the purified polymer (Figure II. 9) shows the presence of the *C*=O of the ester at 172 ppm (labeled f in Figure II. 9), of the *C*=O of the amides at 170 ppm and 175 ppm (labeled l and i in Figure II. 9). These signals are correlated with the presence of the signal of CH_2CH_2O of EO unit at 70 ppm (labeled n in Figure II. 9).

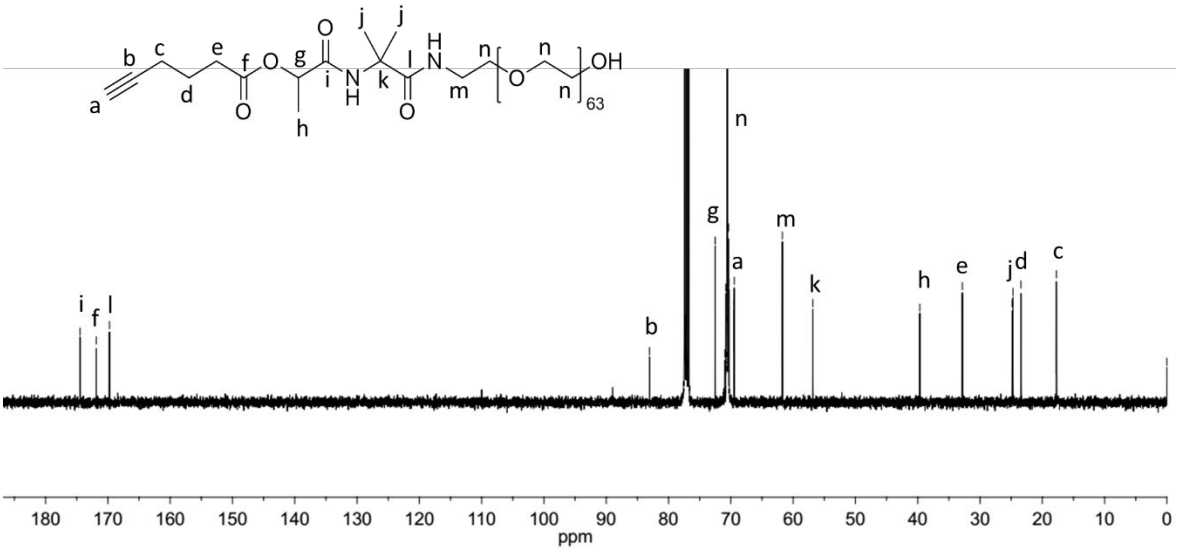

Figure II. 9. ^{13}C NMR spectrum (100 MHz, $CDCl_3$) of α-alkynyl,ω-hydroxylPEO obtained by ring-opening reaction of the alkyne-AZL with α-amino,ω-hydroxylPEO in CH_2Cl_2 at room temperature during 24 hours.

All NMR spectroscopies and MALDI-TOF mass spectrometry characterizations confirmed the successful synthesis and purification of the α-alkynyl,ω-hydroxylPEO using the alkyne-AZL linker.

The effective synthesis of the α-pyrydyldithio,ω-hydroxylPEO and the α-alkynyl,ω-hydroxylPEO will allow the incorporation of thiol-based recognition ligand through disulfide exchange reaction and thiol-yne coupling reaction under mild conditions, respectively. Then, a trithiocarbonate will be attached to the ω-position of both PEOs in order to be able to use them as macromolecular chain transfer agents to mediate the RAFT copolymerization of aminoethyl acrylates.

C. Synthesis of a linear PEO macromolecular chain transfer agent (named PEO-CTA)

The synthesis of the PEO-CTA is based on the esterification of the α-pyridyldithio,ω-hydroxylPEO and of the α-alkynyl,ω-hydroxylPEO previously synthesized and the 4-cyano-4-[(dodecylsulfanylthiocarbonyl)sulfanyl]pentanoic acid (CDP).

Several activation methods have been used to process the esterification. The first one is based on the esterification of α-pyridyldithio,ω-hydroxylPEO mediated through the acyl chloride derived from CDP.

1. Esterification of α-pyridyldithio,ω-hydroxylPEO

a) Esterification mediated through acyl chloride

To perform the esterification through the acyl chloride from CDP, one equivalent of CDP is previously modified with 5 equivalents of oxalyl chloride in anhydrous CH_2Cl_2 at 50°C under argon (Scheme II. 4(A)). After three hours of reaction the unreacted oxalyl chloride was evaporated under vacuum. Then a solution of one equivalent of α-pyridyldithio,ω-hydroxylPEO in CH_2Cl_2 was added slowly under argon at room temperature (Scheme II. 4(B)). The reaction was launched for 24 hours. The product was purified by precipitation in cold diethyl ether and analyzed by ^1H NMR spectroscopy and SEC in DMF (LiBr 1 $g.L^{-1}$).

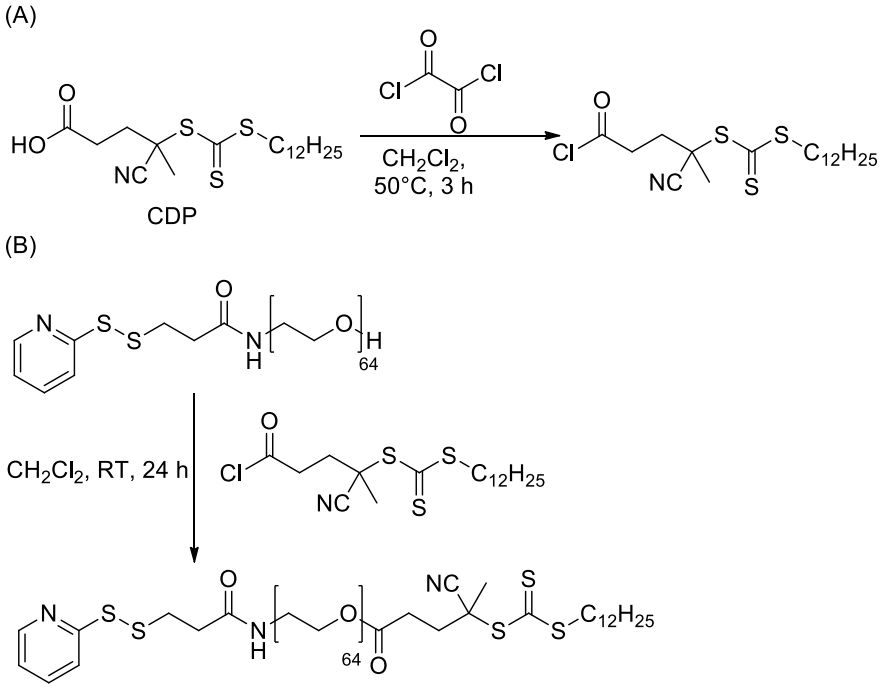

Scheme II. 4. Synthesis of (A) the acyl chloride derived from CDP and (B) the α-pyridyldithio,ω-dodecyltrithiocarbonate PEO by esterification using the acyl chloride based CDP in CH_2Cl_2 at room temperature during 24 hours.

The ^{1}H NMR spectroscopy (Figure II. 10) shows the characteristic signals of the CH_2CH_2O of EO repeating unit between 3.65 ppm (labeled h in Figure II. 10), a triplet at 0.88 ppm characteristic of the methyl protons $SCH_2(CH_2)_{10}CH_3$ of the dodecyl moiety (labeled p in Figure II. 10) and a triplet at 4.25 ppm characteristic of the $CH_2CH_2OC(=O)$ at the α- position of the ester bond created during the esterification (labeled i in Figure II. 10). The degree of functionalization was calculated by comparing integration areas of the methylene CH_2CH_2O of the repeating unit at 3.65 ppm (254 protons, corresponding to a $\overline{DP_n}$ = 64, determined by MALDI-TOF mass spectrometry) and the methylene signal of the $CH_2CH_2OC(=O)$ (0.84 proton, labeled i in Figure II. 10). The conversion rate is equal to 42 %. A surprising feature has been observed when comparing the integration areas of the CH_2CH_2O signal of the repeating units at 3.65 ppm (254 protons, labeled h in Figure II. 10) and of the CHC*H*NCSS aromatic signals at 8.49 ppm (0.49 proton, labeled a in Figure II. 10). The degree of

functionalization with the pyridyl group decreases to 30 %. This decrease may be due to a cleavage of the disulfide bond. Further investigations have been performed by SEC analysis in DMF (LiBr 1 $g.L^{-1}$).

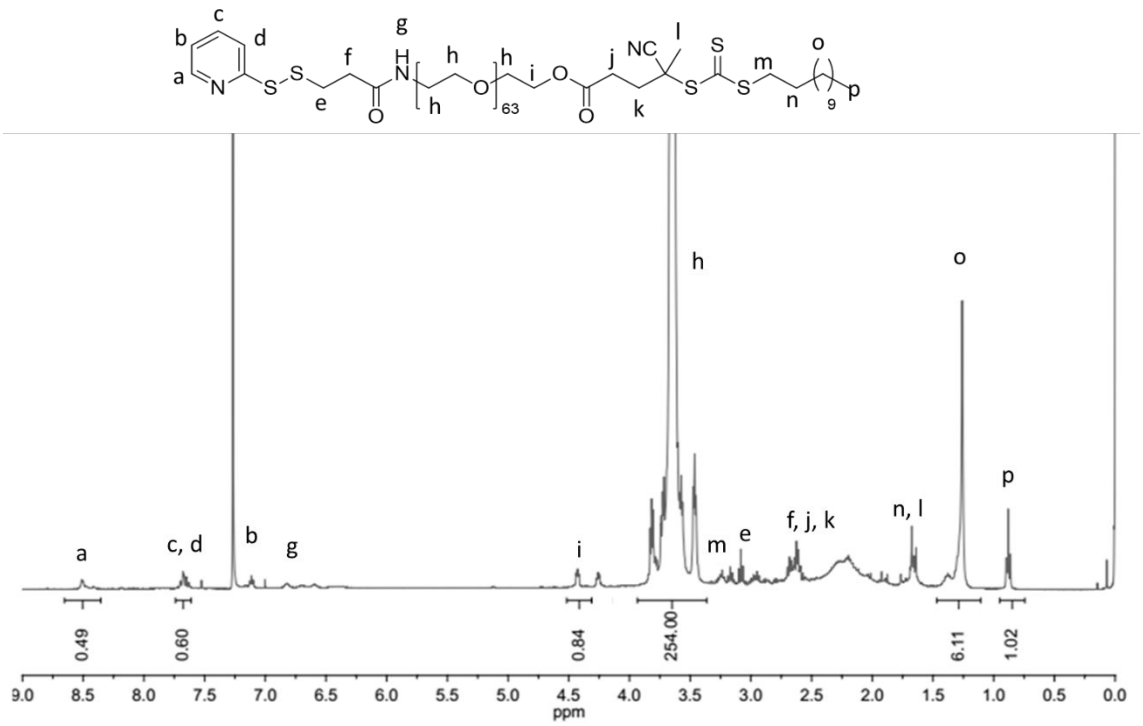

Figure II. 10. ^{1}H NMR spectrum (400 MHz, $CDCl_3$) of α-pyridyldithio,ω-dodecyl trithiocarbonate PEO obtained by esterification of α-pyridyldithio,ω-hydroxylPEO with the acyl chloride based on CDP.

The SEC traces of the final purified compound using RI detection show two populations (Figure 11). These two populations also absorb at 309 nm which is the characteristic wavelength of trithiocarbonate group. The signal at higher elution time show the functionalization of α-pyridyldithio,ω-hydroxylPEO with the trithiocarbonate. The signal at lower elution time can be explained by the coupling of two PEOs due to the cleavage of the disulfide bond.

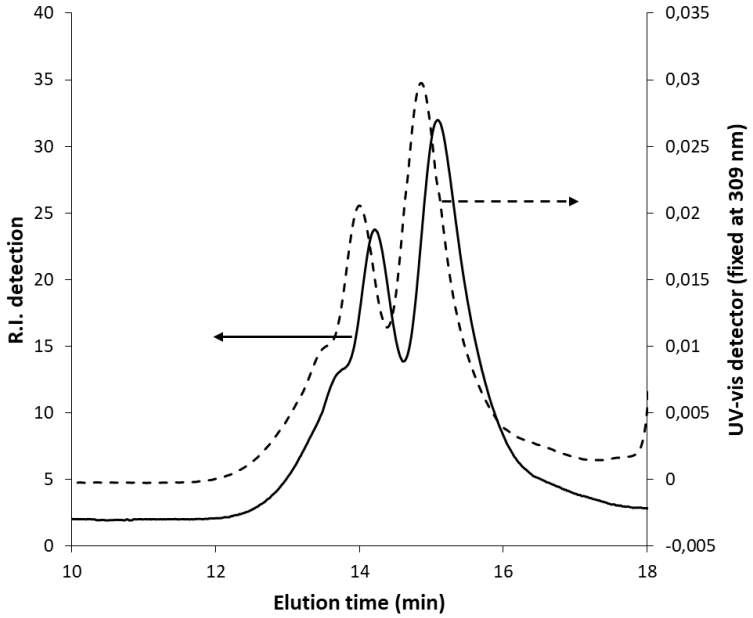

Figure II. 11. Overlaid SEC traces of purified α-pyridyldithio,ω-dodecyltrithiocarbonate PEO using RI detection (solid line) and UV-vis detection at 309 (dash line) obtained by esterification of α-pyridyldithio,ω-hydroxylPEO with acyl chloride based on CDP.

The coupling of two PEOs has been highlighted by reducing the disulfide bond with DL-dithiothreitol (DITH) (Scheme II. 5). The crude product was analyzed by SEC in DMF (LiBr 1 $g.L^{-1}$).

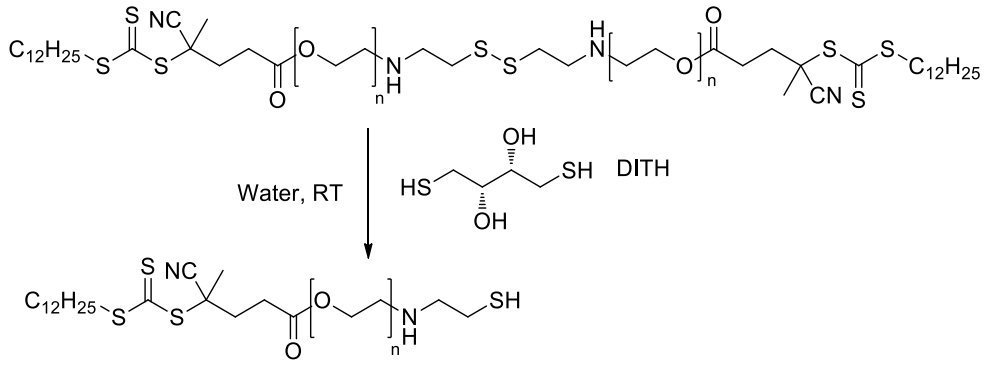

Scheme II. 5. Reduction of the disulfide bond of two coupled PEO with DITH.

The SEC trace (Figure II. 12) of α-pyridyldithio,ω-dodecyltrithiocarbonate PEO after reduction shows a decrease of the population at lower elution time. This confirms that the

population with the lower time has a reducible disulfide bond. The hypothesis of coupled PEOs obtained by disulfide exchange has been confirmed.

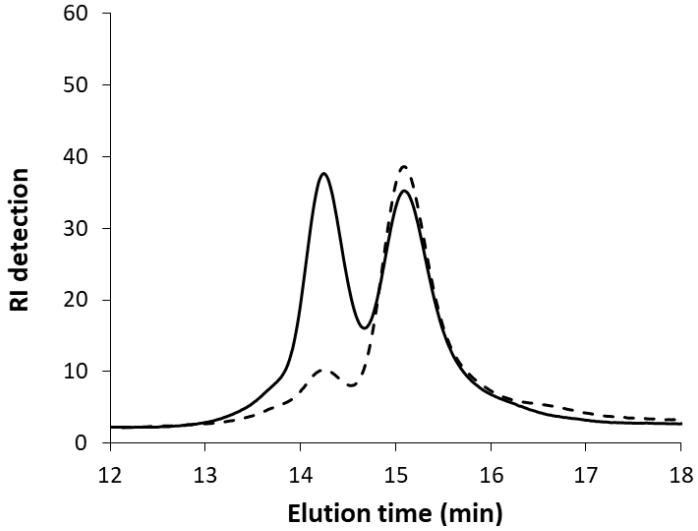

Figure II. 12. Overlaid of SEC traces using RI detection of α-pyridyldithio,ω-dodecyltrithiocarbonate PEO before (solid line) and after (dash line) reduction with DITH.

^{1}H NMR spectroscopy shows a low degree of functionalization (42 %). SEC shows the coupling of PEOs. Therefore, other methods were studied to covalently link a dodecyltrithiocarbonate on the α-pyridyldithio,ω-hydroxylPEO.

b) Esterification mediated through DMT-MM

4-(4,6-dimethoxy-1,3,5-triazin-2-yl)-4-methylmorpholinium chloride (DMT-MM) has been reported to be an efficient activating agent for esterification in basic media.[29] Therefore, 3 equivalents of DMT-MM were added slowly to a solution with 1 equivalent of α-pyridyldithio,ω-hydroxylPEO, 1 equivalent of CDP and 3 equivalents of 4-methylmorpholine (NMM) in tetrahydrofuran (THF) (Scheme II. 6). The reaction was launched during 24 hours at room temperature. The crude product was washed three times with a saturated solution of NaCl and precipitated in cold diethyl ether. The polymer purified was analyzed by ^{1}H NMR spectroscopy and SEC in DMF (LiBr 1 g.L^{-1}).

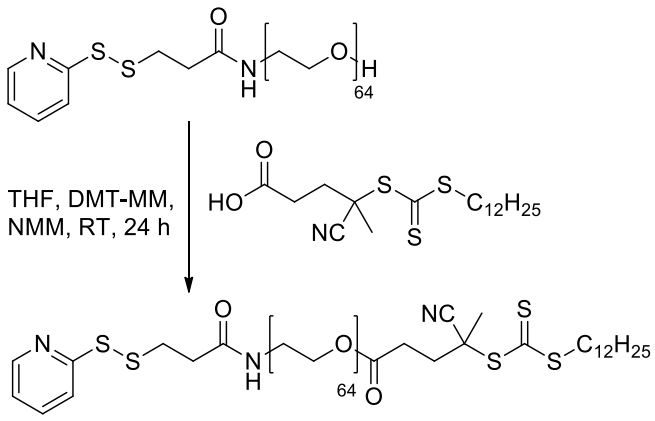

Scheme II. 6. Synthesis of the α-pyridyldithio,ω-dodecyltrithiocarbonate PEO by esterification of the α-pyridyldithio,ω-hydroxylPEO with CDP using DMT-MM and NMM at room temperature in THF during 24 hours.

The ^{1}H NMR spectrum (Figure II. 13) shows the characteristic signals of the C*H*$_2$C*H*$_2$O of the repeating unit at 3.65 ppm (labeled h in Figure II. 13), of the aromatic signals of the pyridyldithio moiety at 8.49, 7.67 and 7.10 ppm (labeled a, c and d, and b in Figure II. 13, respectively), of the methyl protons SCH$_2$(CH$_2$)$_{10}$C*H*$_3$ of the dodecyl group at 0.88 ppm (labeled p in Figure II. 13) and of the methylene protons CH$_2$C*H*$_2$OC(=O) at 4.25 ppm (labeled i in Figure II. 13). The degree of functionalization was calculated by comparing the integration areas of the C*H*$_2$C*H*$_2$O of the repeating unit (254 protons, corresponding to a PEO with $\overline{DP}_n$ of 64 as determined by MALDI-TOF mass spectrometry) and the intensity of the CH$_2$C*H*$_2$OC(=O) (1.38 proton, labeled i in Figure II. 13). The degree of functionalization is equal to 69 %. Again, a decrease of integration area of the CHC*H*NCSS aromatic signal at 8.49 ppm (labeled a in Figure II. 13) in comparison to the C*H*$_2$C*H*$_2$O signal at 3.65 ppm of the repeating unit (labeled h in Figure II. 13). A SEC in DMF (LiBr 1 g.L^{-1}) has been performed to investigate such feature.

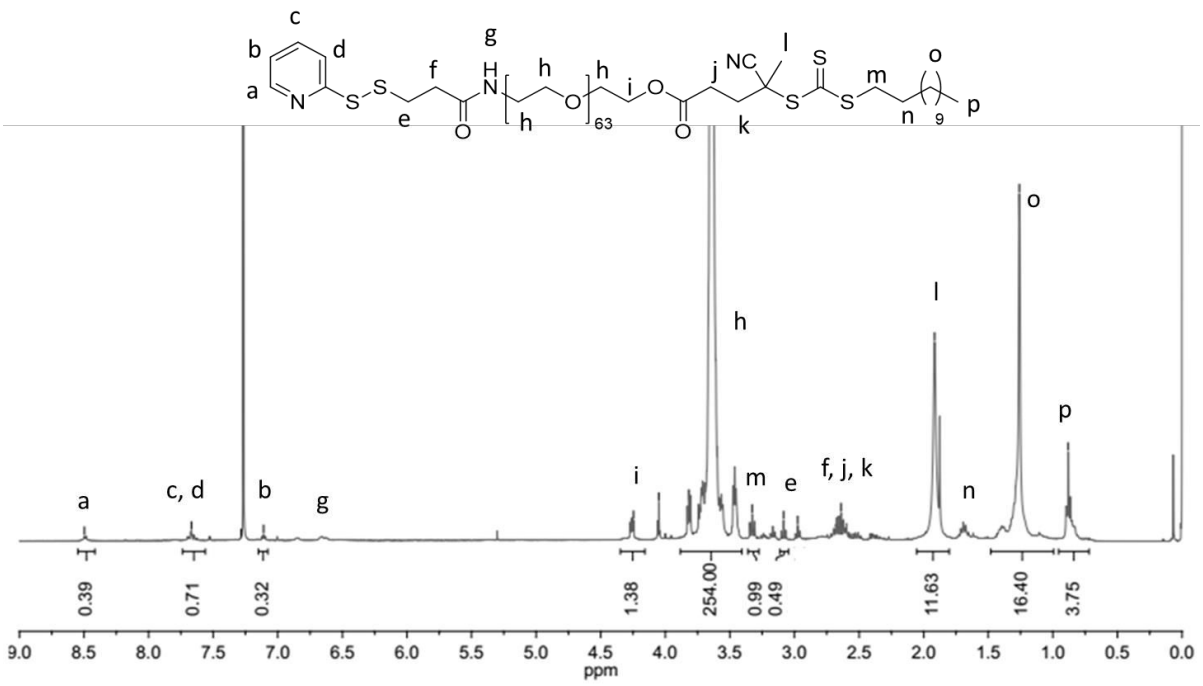

Figure II. 13. ^{1}H NMR spectrum (400 MHz, $CDCl_3$) of α-pyridyldithio,ω-dodecyltrithiocarbonate PEO obtained by esterification of α-pyridyldithio,ω-hydroxylPEO and CDP with DMT-MM in basic media.

The SEC traces using the RI detection and UV-vis detection at 309 nm show two populations (Figure II. 14). As for the esterification mediated through acyl chloride of CDP, this behavior can be explained by the cleavage of the disulfide bond leading to a coupling of two PEOs.

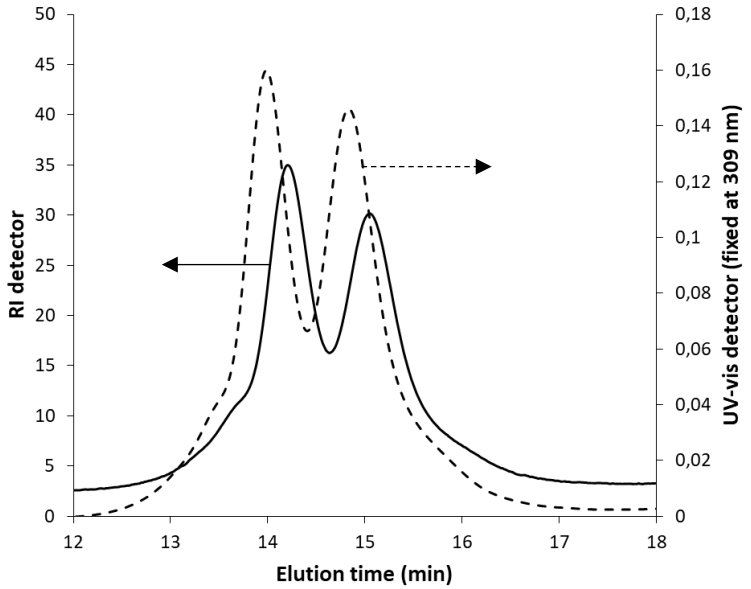

Figure II. 14. Overlaid SEC traces of purified α-pyridyldithio,ω-dodecyltrithiocarbonate PEO using RI detection (solid line) and UV-vis detection at 309 nm (dash line) obtained by esterification of α-pyridyldithio,ω-hydroxylPEO with CDP using DMT-MM.

The ^{1}H NMR spectrum and the SEC trace obtained with the UV-vis detector (fixed at 309 nm) prove the addition of the dodecyltrithiocarbonate group on the α-pyridyldithio,ω-hydroxylPEO. However the degree of functionalization calculated by ^{1}H NMR is still low, 69 %, and the SEC trace, obtained with the RI detector, shows disulfide exchange reaction.

c) Esterification mediated through DCC/DMAP

DCC is a coupling agent used with 4-(dimethylamino)pyridine (DMAP) to improve esterification.[30] A solution of 1 equivalent of DCC in anhydrous CH_2Cl_2 was added slowly at 0°C to a solution containing 1 equivalent of α-pyridyldithio,ω-hydroxylPEO, 2 equivalents of CDP and 0.2 equivalent of DMAP in anhydrous CH_2Cl_2 (Scheme II. 7). The reaction was launched during 4 days at room temperature. The solution was filtered and evaporated. The crude polymer purified by dialysis and liophilized. The product was obtained with a yield of 57.7 %. The pure product was analyzed by ^{1}H NMR spectroscopy and SEC.

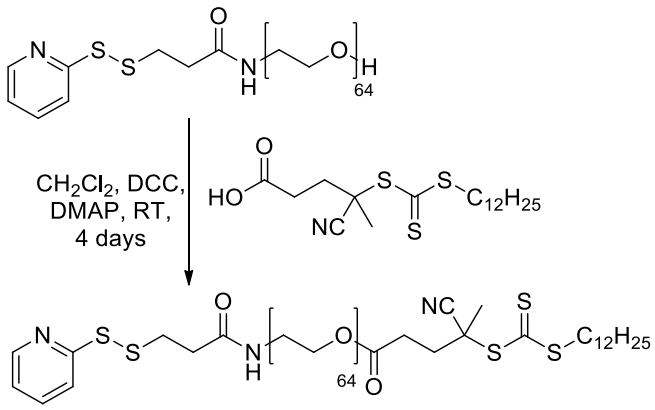

Scheme II. 7. Synthesis of α-pyridyldithio,ω-dodecyltrithiocarbonate PEO by esterification of α-pyridyldithio,ω-hydroxylPEO with CDP mediated through DCC and DMAP at room temperature in CH_2Cl_2 during 4 days.

The ^{1}H NMR spectrum (Figure II. 15) shows the characteristic signals of the C*H*$_2$C*H*$_2$O of the repeating unit at 3.65 ppm (labeled h in Figure II. 15) and of the aromatic signals at 8.49, 7.67 and 7.10 ppm (labeled a, c, d and b in Figure II. 15). The functionalization is confirmed by the presence of the methyl protons signal of the $SCH_2(CH_2)_{10}CH_3$ moiety at 0.88 ppm (labeled p in Figure II. 15) and of the methylene protons signal of the $CH_2CH_2OC(=O)$ at 4.25 ppm (labeled i in Figure II. 15). The degree of functionalization was calculated by comparing the integrations areas of the C*H*$_2$C*H*$_2$O repeating unit at 3.65 ppm (254 protons, labeled h in Figure II. 15 corresponding to a $\overline{DP_{n,MALDI}}$ = 64 as determined by MALDI-TOF mass spectrometry) and of the $CH_2CH_2OC(=O)$ protons (1.06 protons, labeled i in Figure II. 15). The degree of functionalization is equal to 53 %. Interestingly, integration areas of the aromatic protons of the pyridyldithio moiety after esterification mediated through DCC/DMAP are still in agreement with the integration areas of the aromatic protons of the pyridyldithio moiety

before esterification. Further investigation has been performed by SEC analysis in DMF (LiBr 1 $g.L^{-1}$).

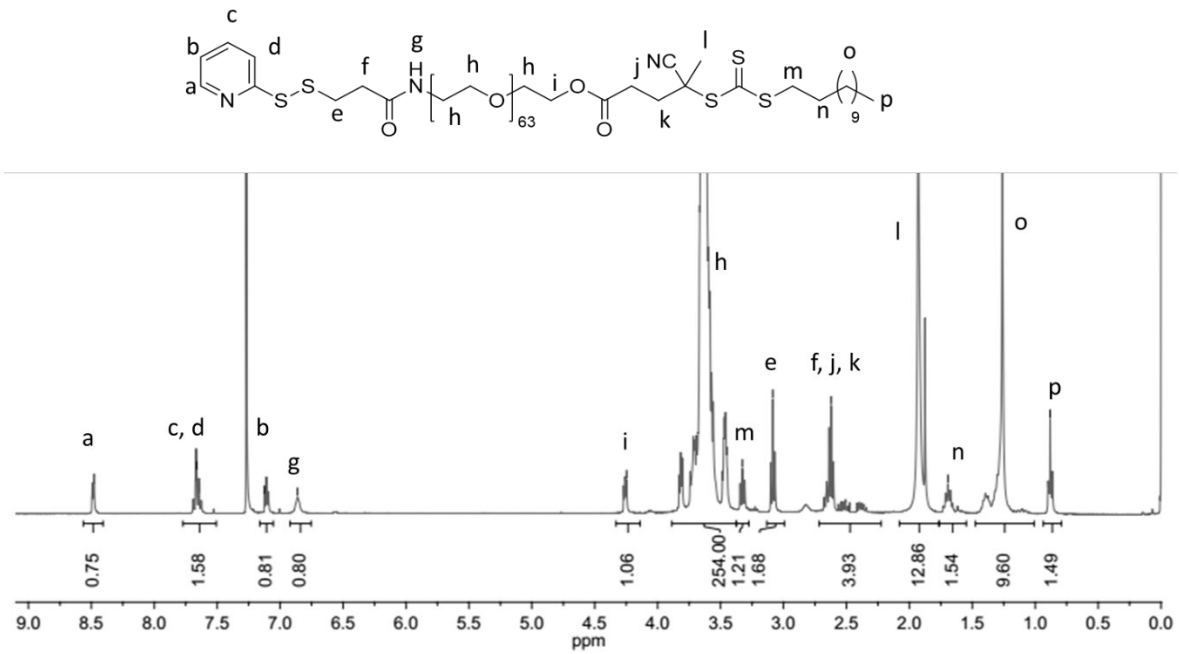

Figure II. 15. ^{1}H NMR spectrum (400 MHz, $CDCl_3$) of the α-pyridyldithio,ω-dodecyltrithiocarbonate PEO obtained by esterification of the α-pyridyldithio,ω-hydroxylPEO and CDP mediated through DCC and DMAP.

The SEC traces using a RI detection and UV-vis detection at 309 nm show a bimodal signal (Figure II. 16). The population at lower elution time using both of detections corresponds to a PEO with a double molar mass inherent to the commercial α-amino,ω-hydroxylPEO. Using both detection the signal observed at higher elution time is related to the successful esterification of the α-pyridyldithio,ω-hydroxylPEO as 309 nm is the characteristic wavelength of the trithiocarbonate group ($\overline{M_{n,SEC}}$ = 8500 $g.mol^{-1}$ (PS equivalent) and $Đ$ = 1.10).

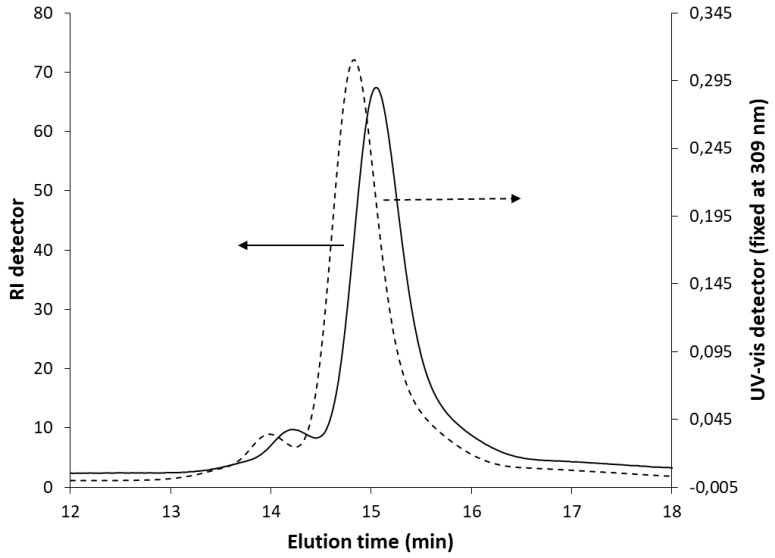

Figure II. 16. Overlaid SEC traces of purified α-pyridyldithio,ω-dodecyl trithiocarbonate PEO using RI detection (solid line) and UV-vis detection at 309 nm (dash line) obtained by esterification of the α-pyridyldithio,ω-hydroxylPEO with CDP mediated through DCC/DMAP.

^{1}H NMR spectrum and SEC traces showed the addition of covalent linkage of the dodecyltrithiocarbonate group on the α-pyridyldithio,ω-hydroxylPEO and the absence of any coupling reactions.

Even if the degree of functionalization is not quantitative (53 %), the esterification of the α-pyridyldithio,ω-hydroxylPEO with CDP mediated through DCC/DMAP is the best choice as there is no evidence of coupling reactions between two PEOs.

2. Esterification of α-alkynyl,ω-hydroxylPEO

a) Esterification mediated through acyl chloride

To perform the esterification through the acyl chloride from CDP, the same conditions were used than for the synthesis of the α-pyridyldithio,ω-dodecyltrithiocarbonate PEO (Chapter II-§C-1-a, Scheme II. 8). The polymer was characterized by ^{1}H NMR spectroscopy and SEC in DMF (LiBr 1 g.L^{-1}).

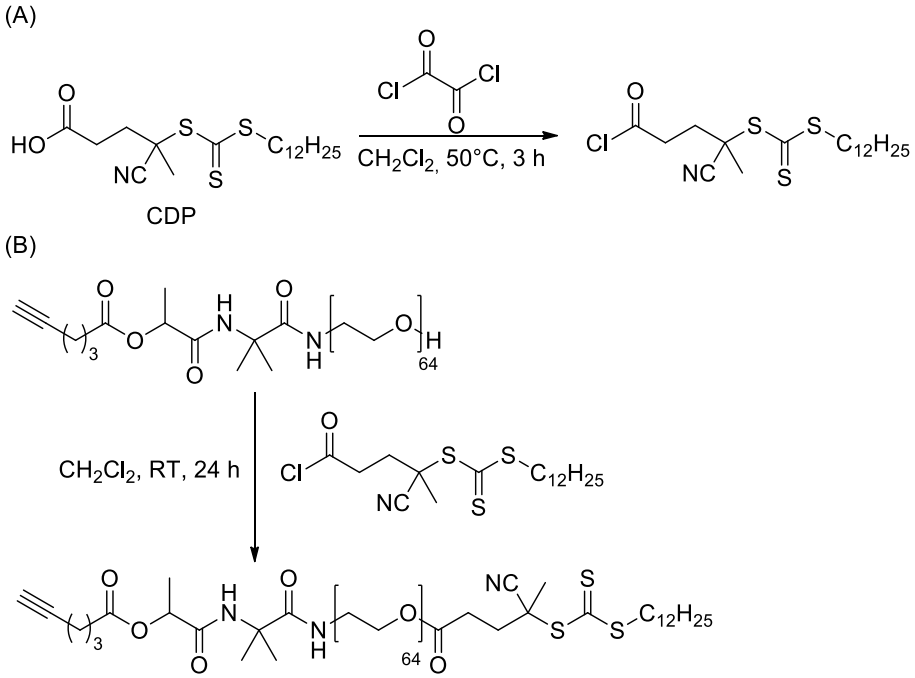

Scheme II. 8. Synthesis of (A) the acyl chloride derived from CDP and (B) the α-alkynyl,ω-dodecyltrithiocarbonate PEO by esterification using the acyl chloride based CDP in CH_2Cl_2 at room temperature during 24 hours.

The ^{1}H NMR spectrum shows the characteristic signals of the C*H*$_2$C*H*$_2$O of EO unit at 3.65 ppm (labeled j in Figure II. 17), the quadruplet of the $CH_3CHC(=O)NH$ at 5.10 ppm (labeled e in Figure II. 17) and the triplet at 3.12 ppm characteristic to the $SCH_2(CH_2)_{10}CH_3$ (labeled o in Figure II. 17). The integration values ratio was calculated by comparing the intensity areas of methylene protons C*H*$_2$C*H*$_2$O of the repeating unit (labeled j in Figure II. 17) and of the methylene proton $CH_2CH_2OC(=O)$ (labeled k in Figure II. 17). The integration values ratio is equal to 254/0.26 corresponding to a degree of functionalization of 13 %.

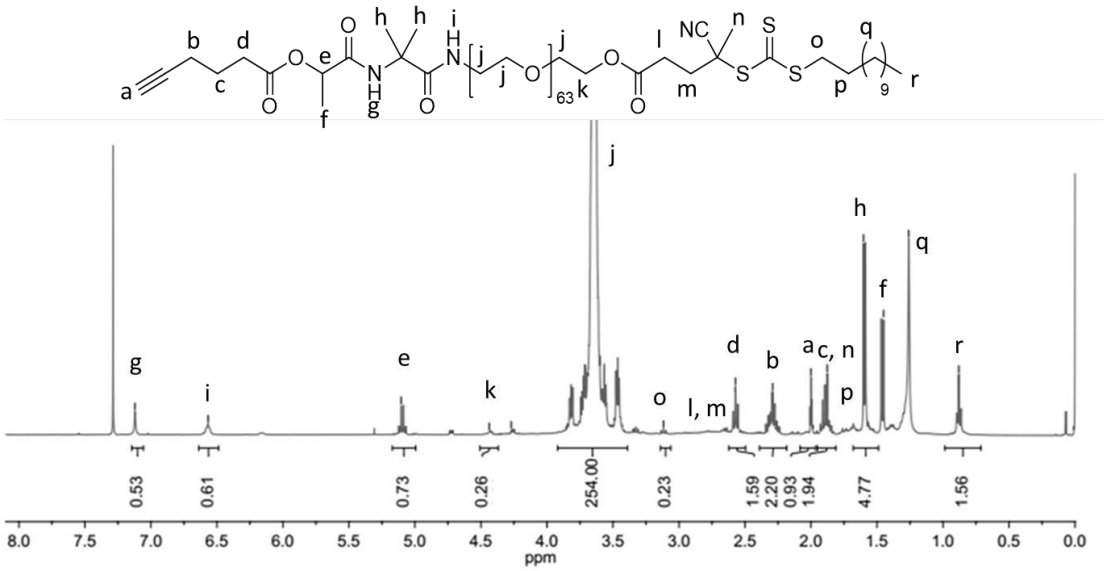

Figure II. 17. ^{1}H NMR spectrum (400 MHz, $CDCl_3$) of the α-alkynyl,ω-dodecyltrithiocarbonate PEO obtained through the esterification between the acyl chloride derived from CDP and the α-alkynyl,ω-hydroxylPEO in anhydrous CH_2Cl_2 at room temperature for 24 hours.

The final polymer was also analyzed by SEC in DMF (LiBr 1 $g.L^{-1}$) using RI detection and UV-vis detection at 309 nm (Figure II. 18). The SEC traces show a bimodal signal using both detections. The signals observed at lower elution time using both detections corresponds to a PEO with a double molar mass, inherent to the commercial α-amino,ω-hydroxyPEO. Using both detection, the signal observed at higher elution time is related to the successful esterification of α-alkynyl,ω-hydroxylPEO with acyl chloride derivated from CDP as 309 nm is the wavelength characteristic to the trithiocarbonate group ($\overline{M_{n,SEC}}$= 9300 $g.mol^{-1}$, PS equivalents, $Đ$ = 1.13).

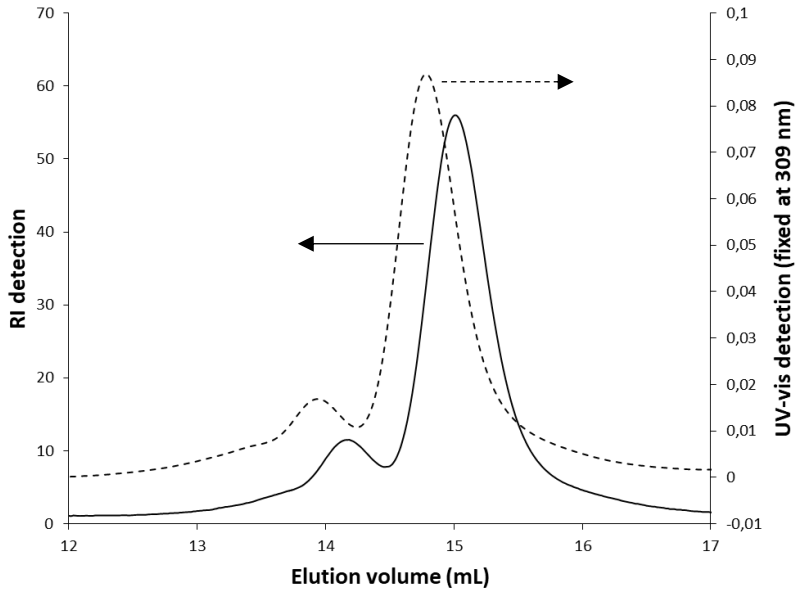

Figure II. 18. Overlaid SEC traces of purified α-alkynyl,ω-dodecyltrithiocarbonate PEO using RI detection (solid line) and UV-vis detection at 309 nm (dash line) obtained by esterification of the α-alkynyl,ω-hydroxylPEO with acyl chloride derived from CDP.

^{1}H NMR spectroscopy confirmed the low degree of functionalization (13 %) of the α-alkynyl,ω-hydroxylPEO using acyl chloride derived from CDP as it was shown during the esterification of the α-pyridyldithio,ω-hydroxylPEO. Therefore, the esterification of the α-alkynyl,ω-hydroxylPEO was performed using the best conditions highlighted for the esterification of the α-pyridyldithio,ω-hydroxylPEO with CDP mediated through DCC/DMAP.

b) Esterification mediated through DCC/DMAP

To perform the esterification, a solution of 2 equivalents of DCC in anhydrous CH_2Cl_2 was added slowly to a cold solution containing 1 equivalent of α-alkynyl,ω-hydroxylPEO, 0.2 equivalent of DMAP and 2 equivalents of CDP. After 4 days at room temperature, the polymer has been purified by several washes and by chromatography column. The product was analyzed by SEC in DMF, ^{1}H and ^{13}C spectroscopies and MALDI-TOF mass spectrometry.

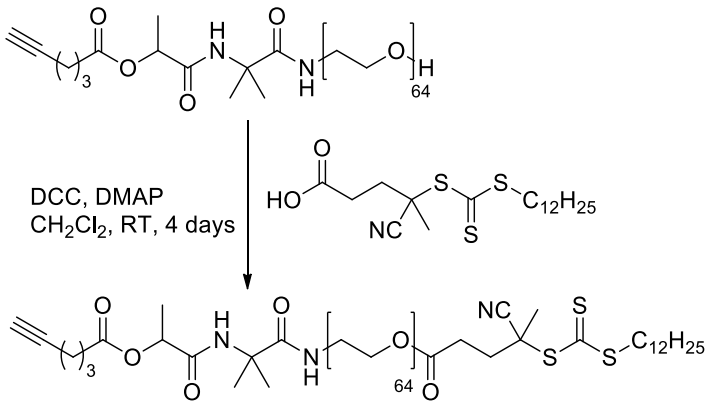

Scheme II. 9. Synthesis of an α-alkynyl,ω-dodecyltrithiocarbonate PEO by esterification between the α-alkynyl,ω-hydroxylPEO and CDP using DCC and DMAP as a coupling agents in CH_2Cl_2 at room temperature during 4 days.

The SEC trace using UV-vis detection fixed at 309 nm of the polymer before purification shows a signal at higher elution time due to the CDP (Figure II. 19). After purification the SEC trace using UV-vis detector shows the complete disapearance of the CDP signal. The signal at lower elution time is narrow and unimodal ($\overline{M_{n,SEC}}$ = 8200 g.mol^{-1} (PS equivalent) and $Đ$ = 1.13).

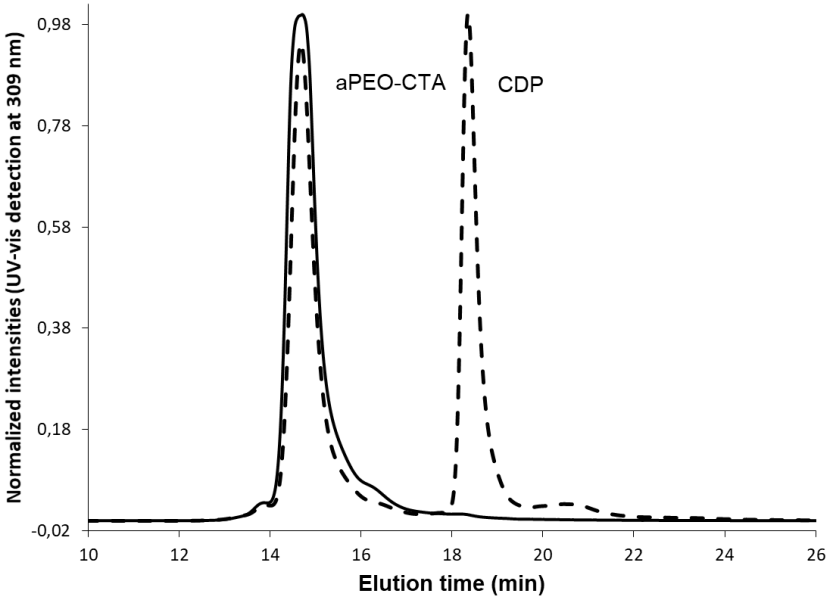

Figure II. 19. Overlaid of SEC traces using a UV-vis detection fixed at 309 nm of α-alkynyl,ω-dodecyltrithiocarbonate PEO (aPEO-CTA) before (dash line) and after (solid line) purification by chromatography column.

The ^{1}H NMR spectrum (Figure II. 20) shows the characteristic signals of the methylene protons C*H*$_2$C*H*$_2$O of the EO repeating unit at 3.65 ppm (labeled j in Figure II. 20). The triplet at 0.88 ppm corresponding to the SCH$_2$(CH$_2$)$_{10}$C*H*$_3$, the triplet at 3.34 ppm corresponding to the methylene protons SC*H*$_2$(CH$_2$)$_{10}$CH$_3$ and the triplet at 4.27 ppm corresponding to the methylene protons CH$_2$C*H*$_2$OC(=O) (labeled r, o and k in Figure II. 20, respectively) prove the covalent linkage of the dodecyltrithiocarbonate group on the PEO. The degree of functionalization was calculated to be equal to 100 % by comparing the integration areas of C*H*$_2$C*H*$_2$O of the repeating units (254 protons, corresponding to a $\overline{DP_n}$ = 64, determined by MALDI-TOF mass spectrometry, labeled j in Figure II. 20) and of the CH$_2$C*H*$_2$OC(=O) methylene protons (2.15 protons labeled k in Figure II. 20).

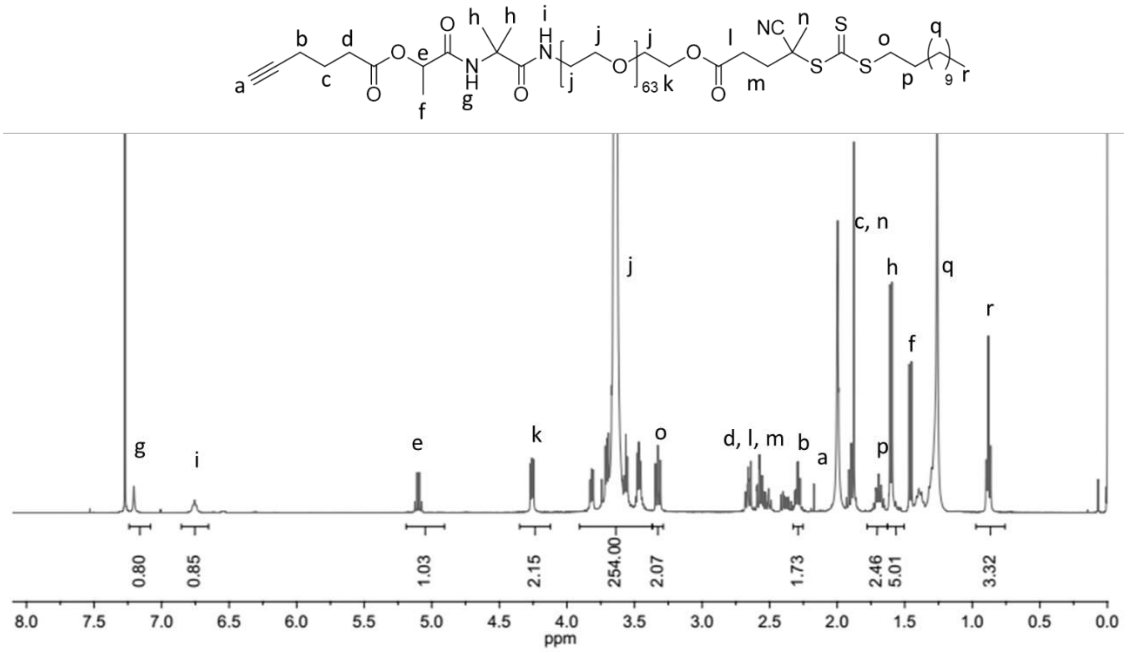

Figure II. 20. ^{1}H NMR spectrum (400 MHz, $CDCl_3$) of the α-alkynyl,ω-dodecyltrithiocarbonate PEO obtained by esterification of the α-alkynyl,ω-hydroxylPEO with CDP using DCC and DMAP.

The ^{13}C NMR spectrum (Figure II. 21) shows the characteristic signal of the CH_2CH_2O of the EO repeating unit at 71 ppm (labeled n in Figure II. 21), of the $HC{\equiv}CCH_2$ at 69 ppm (labeled a in Figure II. 21), of the $HC{\equiv}CCH_2$ at 83 ppm (labeled b in Figure II. 21) and the S*C*(=S)S at 217 ppm (labeled v in Figure II. 21). Such signals are relevant with the effective addition of the trithiocarbonate group.

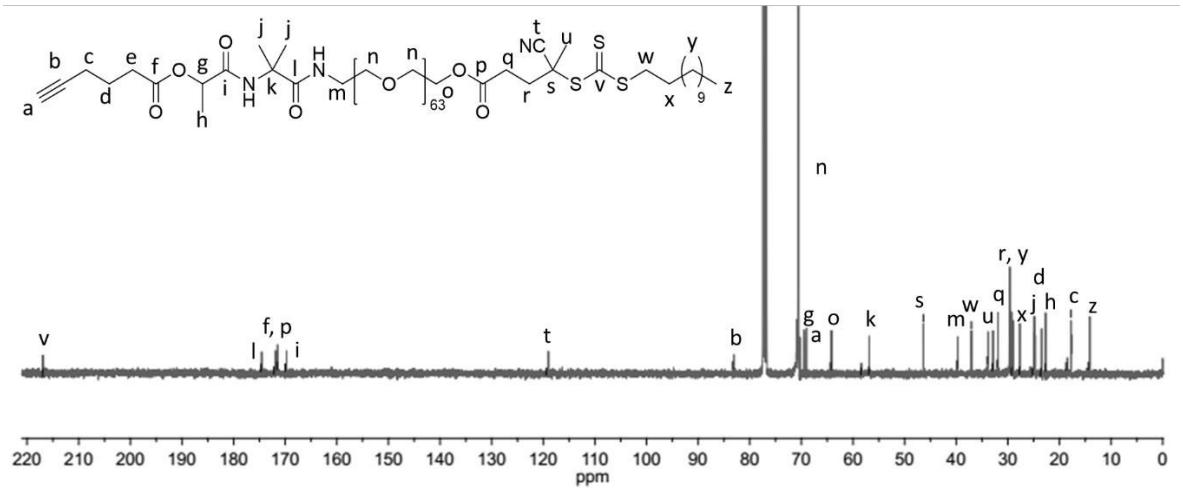

Figure II. 21. ^{13}C NMR spectrum (100 MHz, $CDCl_3$) of the α-alkynyl,ω-dodecyltrithiocarbonate PEO obtained by esterification of the α-alkynyl,ω-hydroxylPEO with CDP mediated through DCC and DMAP.

Furthermore, the final polymer was analyzed by MALDI-TOF mass spectrometry (Figure II. 22). The spectrum shows one series of peaks separated by an average m/z_{exp} equal to 44.087 Da corresponding to the molar mass of the EO repeat unit (m/z_{calc} = 44.023 Da). The peak at m/z_{exp} = 3538.038 Da on the spectrum corresponds to a PEO with 65 repeating units, a alkyne mediated through azlactone moiety at one chain-end, a hydroxyl moiety at the other chain-end and a sodium atom responsible of the ionization (calculated value m/z_{calc} = 3537.991 Da).

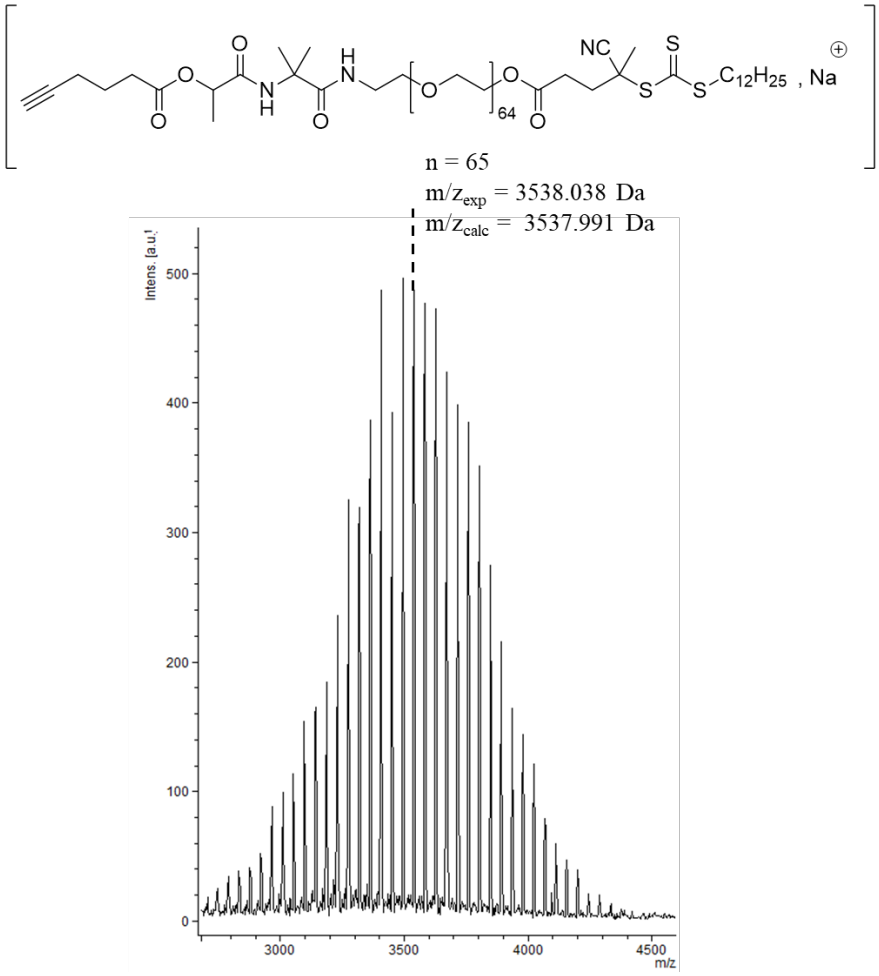

Figure II. 22. MALDI-TOF mass spectrometry of the α-alkynyl,ω-dodecyltrithiocarbonate PEO obtained by esterification of the α-alkynyl,ω-hydroxylPEO with CDP mediated through DCC and DMAP. Matrix: DCTB, salt: NaTFA.

The SEC in DMF, the ^{1}H and ^{13}C NMRs spectroscopies and MALDI-TOF mass spectrometry analyses showed the efficiency of the esterification and purification.

The combination between the addition of an alkyne with an azlactone group and the esterification using DCC and DMAP, allows to obtained a well-defined α-alkynyl,ω-dodecyltrithiocarbonate PEO (aPEO-CTA). This polymer can be used as a macromolecular chain transfer agent to perform RAFT polymerizations.

II. Synthesis of an heterofuntional brush-like PEO (bPEO) for PEGylation of cationic copolymers

The role of PEO architecture has been already studied on PDMAEMA.[31] In our work, two main architectures are studied: the lPEO and the bPEO. bPEO is synthesized through the polymerization of the PEGA for instance. In this work, the synthesis of PPEGA by RAFT polymerization has been studied using a new alkyne-based chain transfer agent: the 2-cyano-5-oxo-5-(prop-2-yn-1-ylamino)pentan-2-yldodecyltrithiocarbonate (COPYDC). Such chain transfer agent will lead to bPEO containing an alkyne group at α-chain-end position and a trithiocarbonate at the ω-chain-end position.

A. Synthesis of 2-cyano-5-oxo-5-(prop-2-yn-1-ylamino)pentan-2-yldodecyltrithiocarbonate (COPYDC)

The synthesises of various alkyne-terminated chain transfer agents have been previously reported.[25,26,32] In contrast with previous studies, our contribution relies on the presence of an amide group, known to be more stable than the ester group to hydrolysis and less sensitive to side reactions during thiol-yne reaction.[33] The alkyne-based chain transfer agent was synthesized through the nucleophilic substitution of the CDP with propargyl amine as shown in Scheme II. 10. The reaction was performed with 1 equivalent of CDP, 1 equivalent of propargyl amine, 1 equivalent of EDCI and 0.98 equivalent of 1-hydroxybenzotriazole (HOBT) in CH_2Cl_2 and *N,N*-dimethylformamide (DMF) at room temperature. The crude oil was purified by column chromatography and the product was obtained with a yield of 70 %. It was

[‡] Le Bohec, M.; Pascual, S.; Piogé, S.; Fontaine, L.: Heterofunctional RAFT-derived PNIPAM *via* cascade trithiocarbonate removal and thiol-yne click coupling reaction. *Journal of Polymer Science Part A: Polymer Chemistry* **2017**, accepted manuscript

characterized by ^{1}H and ^{13}C NMR, FT-IR spectroscopies and high-resolution mass spectrometry (HR-MS).

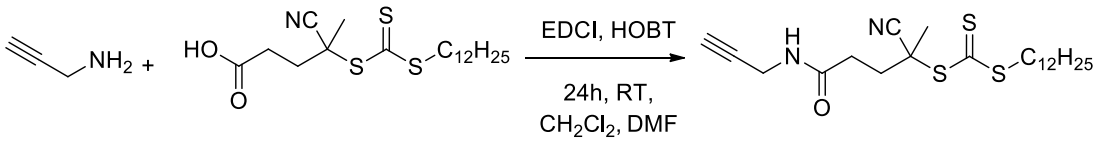

Scheme II. 10. Synthesis of COPYDC by amidification of CDP with propargyl amine in CH_2Cl_2 and DMF at room temperature during 24 hours

The FT-IR spectrum of COPYDC (Figure II. 23) shows the presence of the N-H stretching band at 3292 cm^{-1}, C-H stretching band at 2919 cm^{-1}, the C≡N stretching band at 2232 cm^{-1} characteristics of alkyne function, the C=O stretching band at 1651 cm^{-1}, the N-H bending band at 1537 cm^{-1} characteristics of the amide function, and the C=S stretching band at 1064 cm^{-1} characteristics of the trithiocarbonate group.

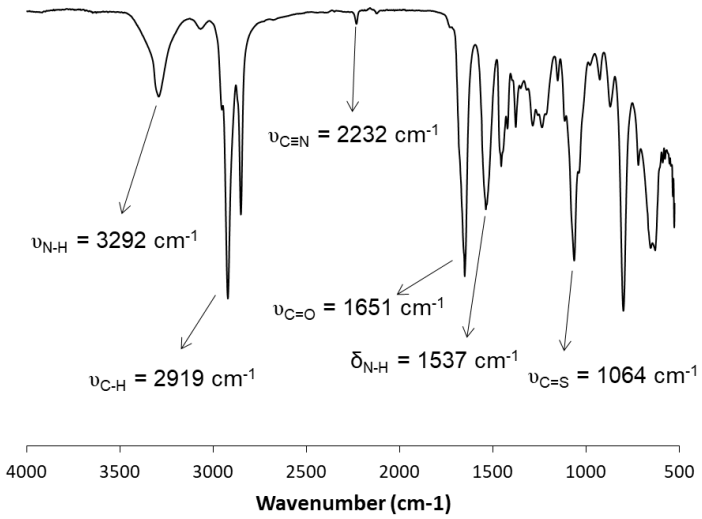

Figure II. 23. FT-IR spectrum of 2-cyano-5-oxo-5-(prop2-yn-1-ylamino)pentan-2-yldodecylcarbonotrithioate (COPYDC).

The comparison of ^{1}H NMR spectra of the CDP and the purified compound (Figure II. 24) shows the appearance of a signal at 2.25 ppm (labeled q, Figure II. 24) corresponding to the methine proton of the alkyne group, of a signal at 4.05 ppm (labeled o, Figure II. 24)

corresponding to the methylene protons of HC≡CC*H*$_2$NH and finally of a signal at 6.02 ppm corresponding to the CH$_2$N*H* proton (labeled n, Figure II. 24). The key peak integral area values of the methyl protons corresponding to the dodecyl chain (labeled a, Figure II. 24), of the methylene protons directly attached to the trithiocarbonate moiety (labeled f, Figure 1), and of the methylene protons of HC≡CC*H*$_2$NH (labeled o, Figure II. 24) are 3.0, 1.9 and 2.0 respectively, which correlates well with the theoretical values.

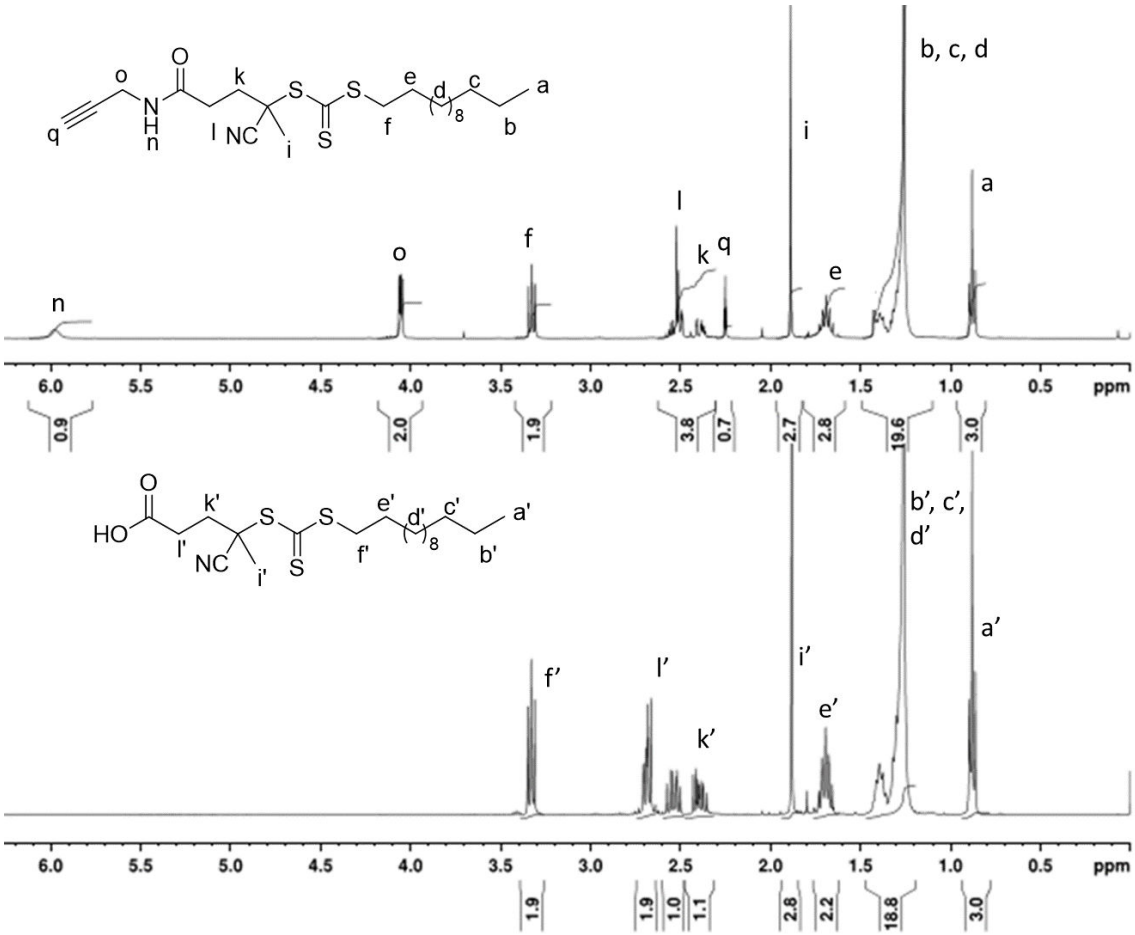

Figure II. 24. Superposition of ^{1}H NMR spectra (400 MHz, $CDCl_3$) of COPYDC (top) and CDP (bottom).

The ^{13}C NMR spectrum of the COPYDC (Figure II. 25) shows a signal at 170 ppm corresponding to the carbon of the *C*=O amide (labeled m, Figure II. 25) and the presence of

the trithiocarbonate entity is confirmed by the signal of the thiocarbonyl S(*C*=S)S at 217 ppm (labeled g, Figure II. 25).

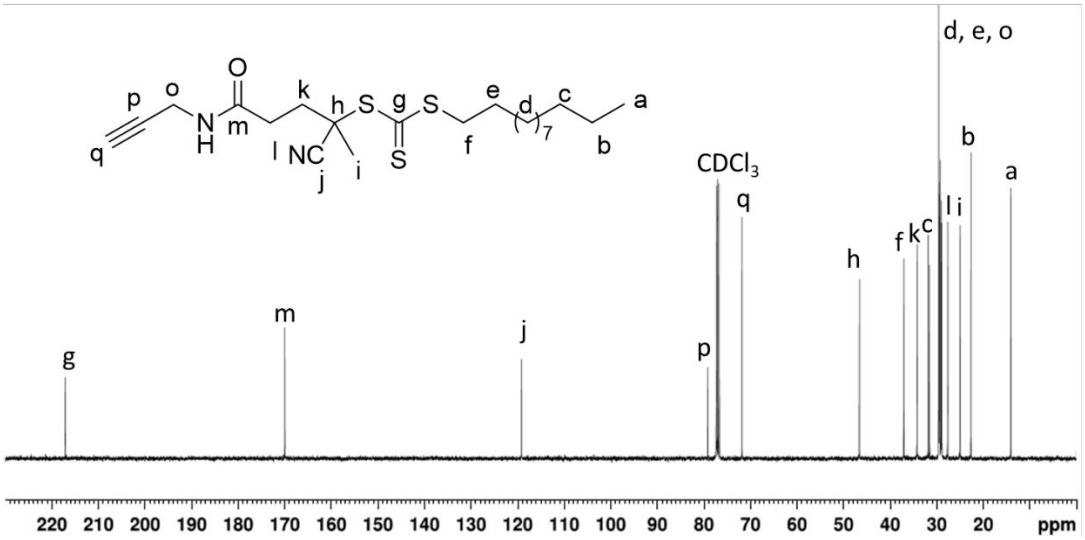

Figure II. 25. ^{13}C NMR spectrum (100 MHz, $CDCl_3$) of COPYDC.

Finally, the HR-MS analysis also confirms the identity of the alkyne-based chain transfer agent (calculated value for $[C_{22}H_{36}N_2OS_3 + Na]^+ = 463.1888$ Da, experimental = 463.1869 Da).

The analysis of FT-IR, ^1H and ^{13}C NMR spectroscopies and of HR-MS spectrometry showed the efficient synthesis and purification of the COPYDC which could be used as an alkyne-based chain transfer agent to mediate the RAFT polymerization of PEGA.

B. RAFT polymerization of PEGA using COPYDC

Several conditions have been already used to perform the RAFT polymerization of PEGA. Boyer *et al.*[34] synthesized a PPEGA by RAFT polymerization using AIBN in acetonitrile. Song *et al*.[35] synthesized a PPEGA by RAFT polymerization using AIBN but in 1,4-dioxane. Qiao *et al*.[36] recently synthesized a PPEGA in acetate buffer (pH = 5.2) using ACVA a water soluble initiator. In our hands, several studied have been performed on the RAFT polymerization of PEGA using, ACVA or AIBN as the initiator and 1,4-dioxane, toluene

and DMF as the solvent. The best conditions were obtained using ACVA and DMF. Moreover, ACVA and DMF are water-soluble and water-miscible respectively and they can be eliminated together easily by dialysis with the remaining PEGA. A study has been performed to find the best conditions to target well-defined PPEGA by RAFT polymerization and different $[PPEGA]_0/[COPYDC]_0/[ACVA]_0$ initial molar ratios were studied for the RAFT polymerizations of PEGA at 70°C (Scheme II. 11).

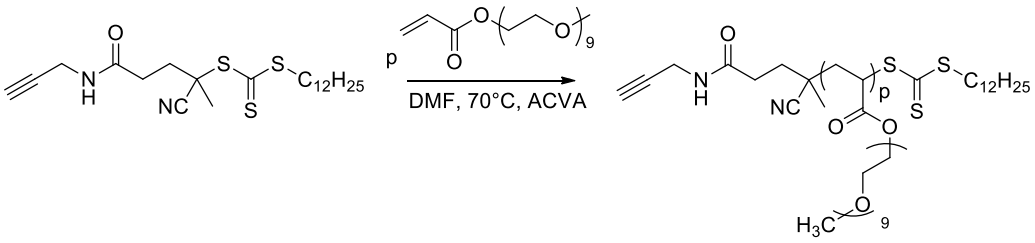

Scheme II. 11. RAFT polymerization of PEGA using COPYDC as the chain transfer agent, ACVA as the initiator in DMF at 70°C.

During RAFT polymerizations, aliquots have been taken to determine the PEGA conversion by ^{1}H NMR spectroscopy, $\overline{M_{n,SEC}}$ and $Đ$ values by SEC in DMF (LiBr 1 g.L^{-1}). The influence of the $[COPYDC]_0/[ACVA]_0$ and of the $[PEGA]_0/[COPYDC]_0$ initial molar ratios were studied on polymerization kinetics and on the evolution of $\overline{M_n}$ and $Đ$ with conversion.

1. Influence of the $[COPYDC]_0/[ACVA]_0$ initial molar ratio

RAFT polymerizations of PEGA were performed using a constant $[PEGA]_0/[COPYDC]_0$ ratio ($[PEGA]_0/[COPYDC]_0 = 150$) and changing the $[COPYDC]_0/[ACVA]_0$ ratio from 1/0.5 to 1/0.1.

The Figure II. 26 shows the evolution of $\ln([M]_0/[M]_t)$ *versus* time for both $[COPYDC]_0/[ACVA]_0$ ratios. In both cases, a short inhibition period (30 minutes) is observed. Such inhibition period is well-known to be dependent on the structure and concentration chain transfer agent and is related to the establishment of the addition-fragmentation equilibrium.[24] Moreover, the slope of the $\ln([M]_0/[M]_t)$ versus time is higher using the $[COPYDC]_0/[ACVA]_0$

ratio of 1/0.5 in comparison with the $[COPYDC]_0/[ACVA]_0$ ratio of 1/0.1. Such behavior is relevant with an apparent propagation rate constant ($k_p^{app} = k_p[P^\bullet]$) higher using the $[COPYDC]_0/[ACVA]_0$ ration of 1/0.5. Same behavior has been observed by Wood *et al.*[37] when they studied the influence of initiator concentration on RAFT polymerization of methacrylate. At PEGA conversions above 70 % (for $[COPYDC]_0/[ACVA]_0$ = 150/1/0.5) and 75% (for $[COPYDC]_0/[ACVA]_0$ = 150/1/0.1), a decrease of the apparent propagation rate constant is observed due to a decrease of the propagating radicals concentration due to the presence of irreversible termination reactions.

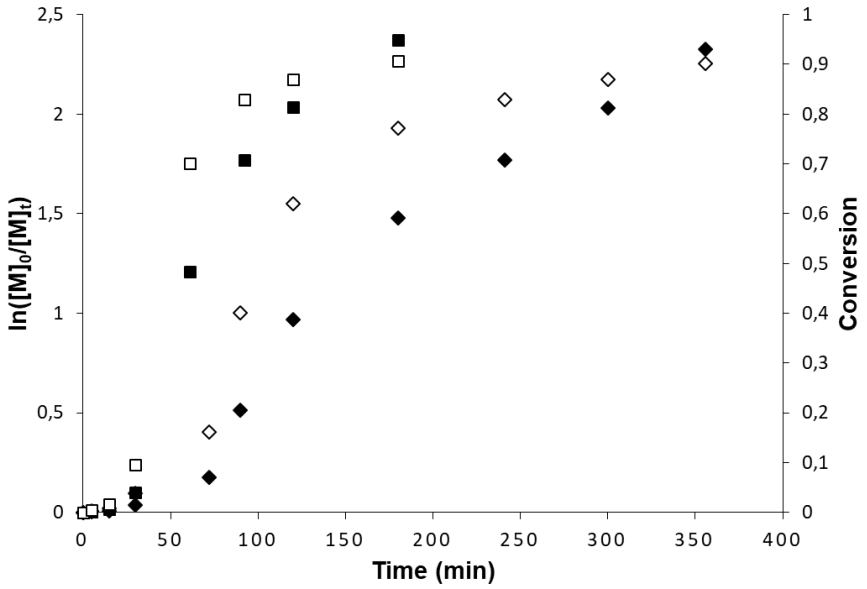

Figure II. 26. Evolution of $\ln([M]_0/[M]_t)$ and conversion *versus* time of RAFT polymerization of PEGA using COPYDC and ACVA at 70°C in DMF (◆,◇ $[PEGA]_0/[COPYDC]_0/[ACVA]_0$ = 150/1/0.1 and ■,□ $[PEGA]_0/[COPYDC]_0/[ACVA]_0$ = 150/1/0.5)

Table II. 1 and table II. 2 show the monomer conversion and macromolecular characteristic of RAFT polymerization of PEGA using $[PEGA]_0/[COPYDC]_0/[ACVA]_0$ = 150/1/0.1 and $[PEGA]_0/[COPYDC]_0/[ACVA]_0$ = 150/1/0.5, respectively. The two tables show the increase of the number-average molar masses with time and conversion. However, the dispersities are high at low conversion ($Đ$ = 1.46 at 40.1 % of conversion, Table II.1). These

results show the initial molar ratio $[COPYDC]_0/[ACVA]_0$ = 1/0.1 or 1/0.5 doesn't play a key role in the control of RAFT polymerization. Indeed, in both cases the RAFT polymerization show a poor control of the RAFT polymerization.

Table II. 1. Monomer conversion and macromolecular characteristics of polymers obtained by RAFT polymerization of PEGA with COPYDC as chain transfer agent and ACVA as the initiator in DMF at 70°C. $[PEGA]_0/[COPYDC]_0/[ACVA]_0$ = 150/1/0.1

Time (min)	Conv. (%) [a]	$\overline{M_{n,SEC}}$ (g.mol^{-1}) [b]	Đ [b]	$\overline{M_{n,NMR}}$ (g.mol^{-1})[c]
0	0	1300	1.12	440
30	3.8	13300	1.13	3200
72	16.2	17300	1.28	12000
90	40.1	24700	1.46	29300
120	62.0	33500	1.48	45100
241	83.0	35200	1.83	60200
300	86.7	36600	1.87	63000
356	90.2	40900	1.74	65400

[a] Determined by ^{1}H NMR spectroscopy (400 MHz, $CDCl_3$) by comparing the integration values of the formamide proton of DMF at 8.02 ppm and of the alkene protons of PEGA between 5.7 and 6.5 ppm. [b] Determined by SEC in DMF (LiBr 1 g.L^{-1}) using PS equivalents. [c] $\overline{M_{n,NMR}} = \frac{[PEGA]_0}{[ACVA]_0} \times conv \times \overline{M_{n,PEGA}} + M_{COPYDC}$ where conv is the conversion, $\overline{M_{n,PEGA}}$ is the number-average molar mass of PEGA ($\overline{M_{n,PEGA}}$ = 480 g.mol^{-1}) and M_{COPYDC} is the molar mass of COPYDC (M_{COPYDC} = 440 g.mol^{-1}).

Table II. 2. Monomer conversion and macromolecular characteristics of polymers obtained by RAFT polymerization of PEGA with COPYDC as chain transfer agent and ACVA as the initiator in DMF at 70°C. $[PEGA]_0/[COPYDC]_0/[ACVA]_0 = 150/1/0.5$

Time (min)	Conv. (%) [a]	$\overline{M_{n,SEC}}$ (g.mol^{-1}) [b]	Đ [b]	$\overline{M_{n,NMR}}$ (g.mol^{-1})[c]
0	0	1320	1.12	440
15	1.7	1330	1.13	1700
30	9.5	12900	1.27	7300
61	70.1	40300	1.47	51000
92	83.0	42200	1.73	60200
120	87.0	42500	1.79	63100

[a] Determined by ^{1}H NMR spectroscopy (400 MHz, $CDCl_3$) by comparing the integration values of the formamide proton of DMF at 8.02 ppm and of the alkene protons of PEGA between 5.7 and 6.5 ppm. [b] Determined by SEC in DMF (LiBr 1 g.L^{-1}) using PS equivalents. [c] $\overline{M_{n,NMR}} = \frac{[PEGA]_0}{[ACVA]_0} \times conv \times \overline{M_{n,PEGA}} + M_{COPYDC}$ where conv is the conversion, $\overline{M_{n,PEGA}}$ is the number-average molar mass of PEGA ($\overline{M_{n,PEGA}}$ = 480 g.mol^{-1}) and M_{COPYDC} is the molar mass of COPYDC (M_{COPYDC} = 440 g.mol^{-1}).

To get a better control, the influence $[PEGA]_0/[COPYDC]_0$ initial molar ratio on the RAFT polymerization will be studied. The chosen $[COPYDC]_0/[ACVA]_0$ initial molar ratio is equal to 1/0.1. The literature shows the increase of the control of RAFT polymerization by decreasing the chain transfer agent initiator initial molar ratio.[24,37]

2. Influence of the $[PEGA]_0/[COPYDC]_0$ initial molar ratio

RAFT polymerizations of PEGA were performed in DMF at 70°C using a constant initial concentration of PEGA, a constant $[COPYDC]_0/[ACVA]_0$ initial molar ratio of 1/0.1 and changing the $[PEGA]_0/[COPYDC]_0$ ratios (150/1, 50/1, and 30/1).

The Figure II. 27 shows the comparison of the evolution of $\ln([M]_0/[M]_t)$ *versus* time of three RAFT polymerizations of PEGA. The inhibition period increases with the decrease of the $[PEGA]_0/[COPYDC]_0$ initial molar ratio: from 30 minutes for 150/1 to 90 minutes for 30/1. This result is well-known and is called "the initialization" effect.[38] Moreover, the apparent propagation rate constant decreases with the decrease of the $[PEGA]_0/[COPYDC]_0$ ratios. This phenomenon is known as the "retardation"effet.[38] As shown by the decrease of the slope of $\ln([M]_0/[M]_t)$ *versus* time at high conversions, a loss of control is observed for a PEGA conversion of 70 % for $[PEGA]_0/[COPYDC]_0$ = 150/1, of 80 % for $[PEGA]_0/[COPYDC]_0$ = 50/1 and of 85 % for $[PEGA]_0/[COPYDC]_0$ = 30/1.

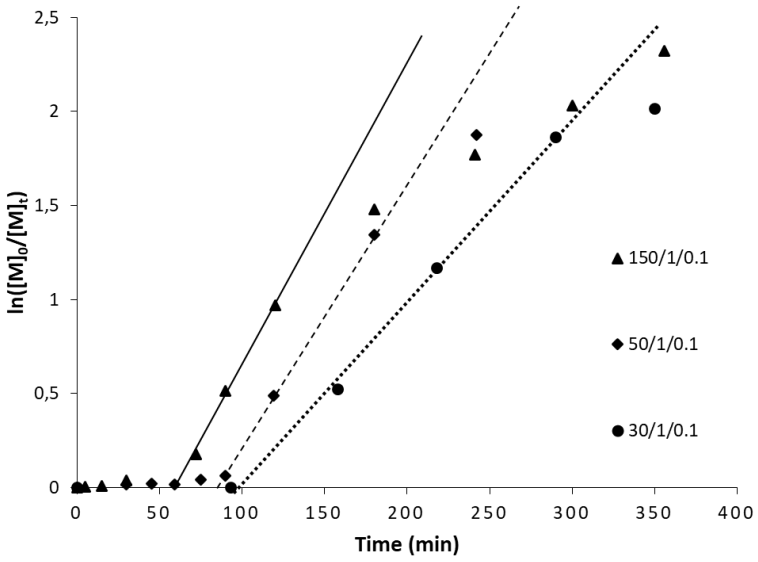

Figure II. 27. Evolution of $\ln([M]_0/[M]_t)$ *versus* time during the RAFT polymerizations of PEGA mediated through ACVA and COPYDC in DMF at 70°C.

$[PEGA]_0/[COPYDC]_0/[ACVA]_0$: 150/1/0.1 (▲, solid line), 50/1/0.1 (◆, dash line) and 30/1/0.1 (●, point line).

The Figure II. 28 shows the evolution of the $\overline{M_{n,SEC}}$ and *Đ versus* PEGA conversion. Increasing the concentration of PEGA relative to COPYDC increases the number-average molar masses but such molar masses are not close to the theory. Moreover, dispersity values are high ($1.12 < Đ < 1.89$). Interestingly, the number-average molar masses are close to theory for a lower $[PEGA]_0/[COPYDC]_0$ initial molar ratio ($[PEGA]_0/[COPYDC]_0 = 30/1$), possibly because of a high concentration of COPYDC to give a better control of the system. Moreover, the dispersity value remains low ($Đ = 1.19$) at high conversion.

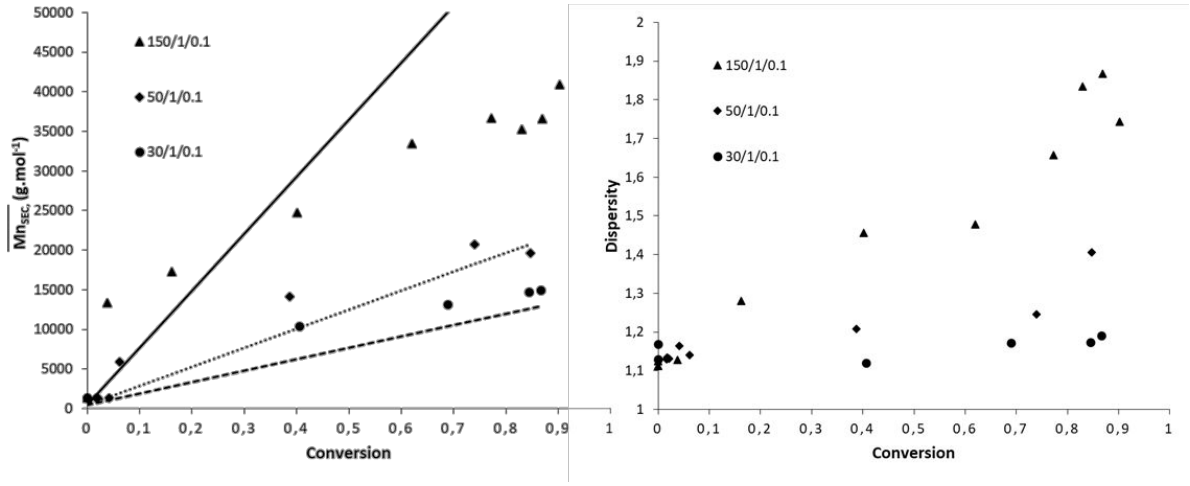

Figure II. 28. Evolution of $\overline{M_{n,SEC}}$, $\overline{M_{n,NMR}}$ (lines) and *Đ versus* conversion of RAFT polymerizations of PEGA mediated through ACVA and COPYDC in DMF at 70°C. $[PPEGA]_0/[COPYDC]_0/[ACVA]_0$: 150/1/0.1 (▲, solid line), $[PPEGA]_0/[COPYDC]_0/[ACVA]_0$: 50/1/0.1 (◆, point line), and $[PEGA]_0/[COPYDC]_0/[ACVA]_0$: 30/1/0.1 (●, dash line).

Among all these RAFT polymerization conditions, the $[PEGA]_0/[COPYDC]_0$ ratio of 30/1 together with the $[COPYDC]_0/[ACVA]_0$ ratio of 1/0.1 gave the best results in terms of kinetics, molar masses and dispersity values ($Đ < 1.2$). Indeed, using such conditions, a good control of the RAFT polymerization of PEGA allowed to target well-defined heterofunctional α-alkynyl,ω-dodecyltrithiocarbonatePPEGA.

3. Synthesis of a high amount of α-alkynyl,ω-dodecyltrithiocarbonate PPEGA

To target a high amount of well-defined heterofunctional α-alkynyl,ω-dodecyltrithiocarbonate PPEGA, the optimal experimental conditions previously defined for the RAFT polymerization of PEGA were used on a larger initial amount of PEGA ($[PEGA]_0/[COPYDC]_0/[AVCA]_0 = 30/1/0.1$ in DMF at 70°C). The reaction was launched and several aliquots were taken to follow the reaction by SEC in DMF (LiBr 1g.L^{-1}, Figure II. 29). The SEC traces show the decrease of the intensity of the PEGA signal at higher elution time corresponding to the remaining PEGA concentration and the shift of the PPEGA signal to the higher elution time due to the increase of the number-average molar mass with time. The final PEGA conversion, determined by ^{1}H NMR spectroscopy was equal to 52 %. The polymer was purified by several dialysis in pure water and lyophilized. The pure product was analyzed by SEC in DMF (LiBr 1 g.L^{-1}) and ^{1}H NMR spectroscopy.

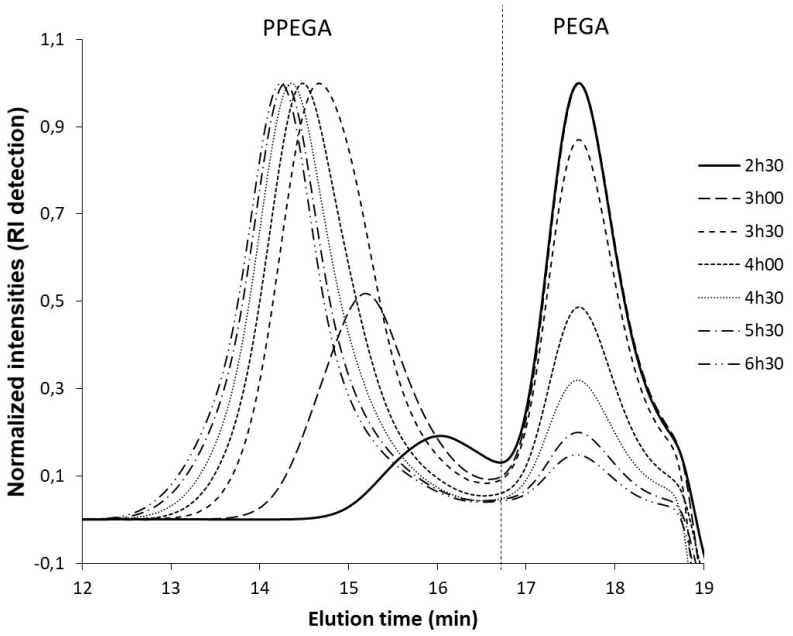

Figure II. 29. Overlaid of SEC traces using RI detection of the crude mixture of the RAFT polymerization of PEGA using COPYDC and ACVA in DMF at 70°C $[PEGA]_0/[COPYDC]_0/[ACVA]_0$ = 30/1/0.1 at different times of reaction.

The SEC trace of the purified polymer obtained using the RI detection shows a unimodal and narrow signal with a number-average molar mass determined by SEC ($\overline{M_{n,SEC}}$) = 14700 g.mol^{-1} (PS equivalents) and a $Đ$ = 1.26 (Figure II. 30). The SEC trace using the UV-vis detector fixed at 309 nm (Figure II. 30, characteristic wavelength of the trithiocarbonate group) shows that the resulting PPEGA absorbs at this wavelength. Such result is characteristic to PPEGA chain with $\overline{M_n}$ = 14700 g.mol^{-1} (PS equivalents) and a $Đ$ = 1.26 terminated by a trithiocarbonate group.

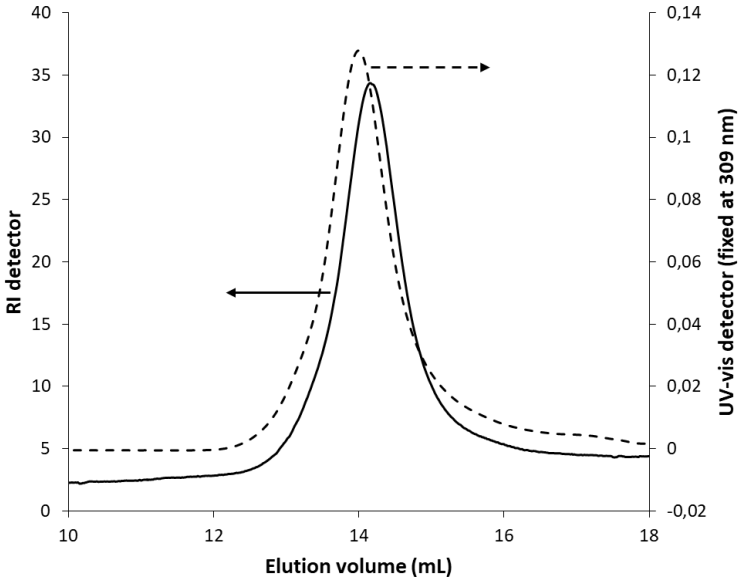

Figure II. 30. Overlaid SEC traces of purified α-alkynyl,ω-dodecyltrithiocarbonate PPEGA using RI detection (solid line) and UV-vis detection at 309 nm (dash line) obtained by RAFT polymerization of PEGA using ACVA and COPYDC ($[PEGA]_0/[COPYDC]_0/[ACVA]_0$ = 30/1/0.1).

The ^{1}H NMR spectrum (Figure II. 31) shows the characteristic signals of the CH_2CH_2O of the EO repeating unit at 3.65 ppm (labeled e and f in Figure II. 31, respectively). The singlet at 3.38 ppm corresponds to the methyl protons $(CH_2CH_2O)_9CH_3$ of the repeating units of PPEGA (labeled g in Figure II. 31). The triplet at 0.88 ppm is characteristic of the methyl protons of the dodecyl chain (labeled a in Figure II. 31). The $\overline{DP_n}$ of PEO was calculated by comparing the methyl protons $SCH_2(CH_2)_{10}CH_3$ of the dodecyl chains (3 protons, labeled a in Figure II. 31) with the methylene protons C(=O)OCH_2CH_2O$(CH_2CH_2O)_9$ and the methylene protons HC≡CCH_2NH (26.10 protons, labeled d and h in Figure II. 31, respectively). The $\overline{DP_n}$ is equal to 12.

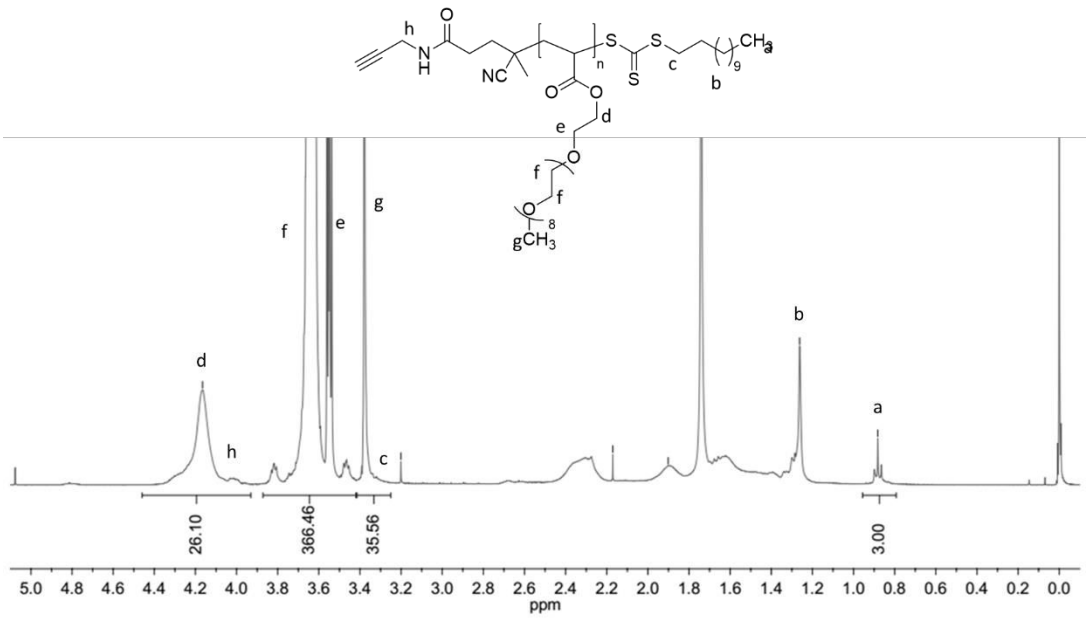

Figure II. 31. ^{1}H NMR spectrum (400 MHz, $CDCl_3$) of PPEGA synthesized by RAFT polymerization of PEGA with ACVA and COPYDC ($[PEGA]_0/[COPYDC]_0/[ACVA]_0$ = 30/1/0.1) in DMF at 70°C.

The SEC and the ^{1}H NMR spectrum and the SEC showed the efficiency of RAFT polymerization to target well-defined α-alkynyl,ω-dodecyltrithiocarbonatePPEGAs able to be used as macromolecular chain transfer agents for the copolymerization of aminoethyl acrylate.

Conclusion

Different pathways have been used to target well-defined heterofunctional lPEO and bPEO containing reactive function which can react with a thiol group at the α-position and a chain transfer agent moiety able to control a RAFT polymerization at the ω-position.

Two different thiol-reactive groups have been added on the α-position of lPEO: a pyridyldithio group able to react with a thiol group by disulfide exchange and an alkyne group able to react with a thiol group by thiol-yne coupling reaction. The addition of the pyridyldithio group moiety was efficient with a high degree of functionalization (95 %) using SPDP. The

addition of the alkyne on the lPEO has been studied using two different strategies. The nucleophilic substitution of the propargyl bromide using α,ω-dihydroxylPEO led to low degree of functionalization (78 %) meanwhile the nucleophilic addition of α-amino, ω-hydroxylPEO onto the alkyne-AZL led to complete functionalization under mild conditions.

Several strategies have been studied to functionalize the ω-position of the lPEO with a trithiocarbonate. The esterification of α-pyridyldithio,ω-hydroxylPEO with CDP has been mediated through acyl chloride based CDP, DMT-MM and DCC. The esterification using the acyl chloride based CDP and DMT-MM lead to low degree of functionalization (42 and 69 %, respectively) and polymer-polymer coupling. The esterification of α-pyridyldithio,ω-hydroxylPEO with CDP mediated through DCC/DMAP led to a low degree of functionalization (53 %) under mild conditions but doesn't lead to polymer-polymer coupling. The esterification of α-alkynyl,ω-hydroxylPEO with CDP has been mediated through acyl chloride based CDP and DCC. The addition of the trithiocarbonate group using the acyl chloride based CDP led to low conversion (13 %) meanwhile the esterification of α-alkynyl,ω-hydroxylPEO with CDP using DCC led to the synthesis of a well-defined α-alkynyl,ω-dodecyltrithiocarbonate PEO fully functionalized as shown by FT-IR, ^{1}H and ^{13}C NMRs spectroscopies, SEC and MALDI-TOF mass spectrometry.

The bPEO, PPEGA, has been synthesized by RAFT polymerization using an alkyne-based chain transfer agent the COPYDC. The influence of the $[COPYDC]_0/[ACVA]_0$ and $[PEGA]_0/[COPYDC]_0$ initial molar ratios have been studied. The best conditions was $[PEGA]_0/[COPYDC]_0/[ACVA]_0$: 30/1/0.1 to form an α-alkynyl,ω-dodecyltrithiocarbonate PPEGA ($\overline{M_{n,SEC}}$ = 14700 g.mol^{-1}, $Đ$ = 1.26).

Experimental part

A. Reagents

All reagents were purchased from Sigma-Aldrich unless otherwise noted. Sodium trifluoroacetate (NaTFA, ≥ 98 %), *trans*-2-[3-(4-*tert*-butylphenyl)-2-methyl-2propenylidene]malononitrile (DCTB, ≥ 98 %), dithranol (DIT, 97 %) DL-dithiothreitol (DITH, ≥ 98 %), dicyclohexylcarbodiimide (DCC, 99%), 4-(dimethylamino)pyridine (DMAP, 99 %) 4-cyano-4-[(dodecylsulfanylthiocarbonyl)sulfanyl]pentanoic acid (CDP, 97 %), *N*-(3-dimethylaminopropyl)-*N'*-ethylcarbodiimide hydrochloride (EDCI, ≤ 97 %), oxalyl chloride (99 %); 4-(4,6-dimethoxy-1,3,5-triazin-2-yl)-4-methylmorpholinium chloride (DMT-MM, 96 %), 4-methylmorpholine (NMM, 99 %), propargyl bromide (80 % in toluene), 4,4-azobis(4-cyanolaveric acid) (ACVA, 98 %), sodium carbonate (Na_2CO_3, 99,5 %), hydrochloric acid (HCl, 37 %), *N,N*-dimethylformamide (DMF), toluene (99.5 %), acetonitrile (99.8 %), succinimidyl 3-(2-Pyridyldithio)propionate (SPDP, ≥ 95 %), phosphorus pentoxide (P_2O_5, ≥ 99.8 %), aluminum oxide (basic activated), α-amino,ω-hydroxylpoly(ethylene oxide) ($\overline{DP}_{n,MALDI}$ = 64 pure, Rapp polymers), α,ω-dihydroxylpoly(ethylene oxide) ($\overline{DP}_{n,MALDI}$ = 44, pure, Rapp polymers), magnesium sulfate ($MgSO_4$, laboratory reagent grade, Fischer), cyclohexane (99.8 %, Quaron), diethyl ether (99.8 %, Carlo Erba), methanol (99.8 %, Carlo Erba), ethyl acetate (pure, Carlo Erba), propargyl amine (≥ 99 %, Acros Organics), 1-hydroxybenzotriazole (HOBT, 98 %, Acros-Organics), potassium hydroxide (KOH, Acros-Organics, 85 %), sodium chloride (NaCl, Acros-Organics, 99.5 %) and silica gel for chromatography (SiO_2, 0.035 - 0.070 mm, 60 Å, Acros Organics). Dichloromethane (CH_2Cl_2, HPLC grade, Fisher Chemical) and tetrahydrofuran (THF, 99.9 %) were dried over dry solvent stations GT S100. Oligo(ethylene glycol) acrylate (PEGA, pure, sigma Aldrich) was passed through a column of aluminum oxide prior to polymerization. The L-(4,4-dimethyl-5-oxo-4,5-dihydrooxazol-2-yl) ethyl hex-5-ynoate (alkyne-AZL) have been synthesized following a

reported procedures.[28] Ultra-pure water was obtained from a Millipore Direct Q system and had a conductivity of 18.2 MΩcm at 25°C. All the deuterated solvents are purchased from Euriso-top

B. General Characterization

Nuclear Magnetic Resonance (NMR) spectra were recorded on a Bruker AC-400 spectrometer for ^{1}H NMR (400 MHz) and ^{13}C NMR (100 MHz). Chemical shifts are reported in ppm relative to the deuterated solvent resonances.

The average molar masses (number-average molar mass $\overline{M_{n,SEC}}$, weight-average molar mass $\overline{M_{w,SEC}}$ and dispersity ($Đ = \overline{M_{w,SEC}}/\overline{M_{n,SEC}}$) values were measured by Size Exclusion Chromatography (SEC) using DMF-LiBr (1 $g.L^{-1}$) as an eluent and carried out using a system equipped with a guard column (Polymer Laboratories, PL Gel 5 µm) followed by two columns (Polymer Laboratories, 2 PL gel 5 µm MIXED-D columns) and with a Waters 410 differential refractometer (RI) and a Waters 481 UV-Visible detector. The instrument operated at a flow rate of 1.0 $mL.min^{-1}$ at 60°C and was calibrated with narrow linear polystyrene (PS) standards ranging in molar mass from 580 $g.mol^{-1}$ to 483 000 $g.mol^{-1}$. Molar masses and dispersities were calculated using Waters EMPOWER software.

FT-IR spectra of polymers were recorded using a Nicolet iS5 FT-IR spectrometer operating with an attenuated total reflection (iD5 ATR Diamond) gate. Spectra were analyzed with OMNIC software.

High-resolution Mass Spectra (HR-MS) were recorded on a Bruker MicroTOF-QIII (ESI^{+}).

MALDI-TOF Mass Spectrometry analyses were performed on a Bruker UltraFlex II instrument equipped with a nitrogen laser operating a 337 nm, pulsed ion extraction source and reflectron. Spectra were recorded in the reflectron mode with an acceleration voltage of 25 kV

and a delay of 300 ns, 500 single shot aquisitions were summed to give the spectra and the data were analyzed using Bruker FlexAnalysis and Polytools softwares. Samples were prepared by dissolving the matrix (DCTB or DIT) in the solvent (CH_2Cl_2, 30 mg.mL^{-1}) and mixing with the polymer (10 mg.mL^{-1}) in the ratio 1:10 (v/v). 1 µL was spotted directly onto a thin layer of NaTFA in acetone (concentration 19 mg.mL^{-1}) that had been deposited to act as a cationizing agent.

C. Synthesis of an α-pyridyldithio,ω-hydroxylPEO

In a round bottom flask a magnetic stir bar was carged together with α-amino,ω-hydroxylPEO (50 mg, 0.016 mmol) and SPDP (6 mg, 0.019 mmol) and acetonitrile (4 mL). The reaction was launched at room temperature during 5 hours. The solution was concentrated and the solid obtained was dissolved in 10 mL of ultra-pure water. The solution was filtered onto a nylon filter with a porosity of 0.22 µm. The solution was dialyzed with a 10 kDa membrane during 24 hours. The solution was lyophilized and the solid obtained was dried under vacuum with P_2O_5. The solid was obtained with a yield of 89 % (m = 44.5 mg).

FT-IR (ν in cm^{-1}): 2875 (C-H), 1662 (C-O amide), 1569 (C=C aromatic and C-N amide), 1100 (C-O ether).

^{1}H NMR (400 MHz, $CDCl_3$), δ (ppm): 2.62 (t, $SSCH_2CH_2C(=O)NH$, 1.90 H), 3.09 (t, $SSCH_2CH_2C(=O)NH$, 2.09 H), 3.65 (m, $(CH_2CH_2O)_{64}$, 256 H), 6.98 (m, $C(=O)NHCH_2CH_2$, 0.82 H), 7.10 (m, CHCHNC(S), 0.85 H), 7.67 (m, CHCHC(S), 1.69 H), 8.49 (m, CHCHNC(S), 0.88 H).

SEC in DMF: $\overline{M_{n,SEC}}$ = 8800 g.mol^{-1} (PS equivalent), $Đ$ = 1.07

D. Synthesis of an α-alkynyl,ω-hydroxylPEO

1. Using the propargyl bromide

α,ω-dihydroxylPEO (10.0504 g, 5.186 mmol) was previously purified by azeotropic distillation in toluene. After complete water removal, the temperature was decreased to 70°C and a dried powder of KOH (0.5500 g, 9.980 mmol) was added to the solution. The mixture was stirred during 1 hour at 70°C and propargyl bromide (0.8248 g, 6.933 mmol) was injected through a syringe previously degassed. The solution was stirred at 70°C during 7 days. Toluene is removed by evaporation and the residual mixture was dissolved in CH_2Cl_2. The organic phase is washed three times with a solution of HCl (3N) and three times with a saturated solution of NaCl. The organic phase was concentrated and precipitated three times in cold diethyl ether. The mass obtained was 8.8339 g with a yield of 87 %.

^{1}H NMR (400 MHz, $CDCl_3$), δ (ppm): 2.40 (t, *H*C≡CCH_2O, 0.78 H), 2.81 (t, *H*O(CH_2CH_2O)$_{44}$), 3.65 (m, (C*H*$_2$C*H*$_2$O)$_{44}$, 176 H), 4.20 (d, HC≡CC*H*$_2$O, 1.66 H)

2. Using the L-(4,4-dimethyl-5-oxo-4,5-dihydrooxazol-2-yl) ethyl hex-5-ynoate (named alkyne-AZL)

In a round bottom flask were charged α-alkynyl,ω-hydroxylPEO (2,301 g, 0.764 mmol), alkyne-AZL (222.9 mg, 0.888 mmol) and CH_2Cl_2 (50 mL). The reaction was launched during 24 hours at room temperature. The solution was concentrated and precipitated once in cold diethyl ether. The solid obtained was dried under vacuum in the presence of P_2O_5. The final product was obtained with a yield of 99 %.

FT-IR (ν in cm^{-1}): 3196 (C-H), 2239 (C≡C), 1737 (C=O, ester), 1660 ($\nu_{(C=O)}$, amide), 1517 (N-H, amide), 1100 (C-O, ether)

^{1}H NMR (400 MHz, $CDCl_3$), δ (ppm): 1.46 (d, C*H*$_3$CHC(=O)NH, 2.69 H), 1.62 (2 s, (C*H*$_3$)$_2$CC(=O)NH, 5.30 H), 1.90 (tt, C*H*$_2$CH$_2$C(=O)O), 2.01 (t, *H*C≡CCH_2), 2.30 (td,

HC≡CC*H*$_2$, 2.24 H), 2.58 (t, $CH_2CH_2C(=O)O$, 1.88 H), 3.65 (m, $(CH_2CH_2O)_{64}$, 256 H), 5.11 (q, $CH_3CHC(=O)NH$, 1.03 H), 6.74 (m, $NH(CH_2CH_2O)_{64}$, 0.86 H), 7.22 (m, $NHC(CH_3)_2$, 0.79 H).

^{13}C NMR (100 MHz, $CDCl_3$), δ (ppm): 17 ($CH{\equiv}CCH_2$), 23 ($CH_2CH_2C(=O)O$), 25 ($(CH_3)_2CC(=O)NH$), 33 ($CH_2CH_2C(=O)O$), 40 ($CH_3CHC(=O)NH$), 57 ($(CH_3)_2CC(=O)NH$), 62 ($NHCH_2CH_2O(CH_2CH_2O)_{63}$), 69 ($CH{\equiv}CCH_2$), 70 ($NHCH_2CH_2(OCH_2CH_2)_{63}$), 72 ($CH_3CHC(=O)NH$), 83 ($CH{\equiv}CCH_2$), 170 ($(CH_3)_2CC(=O)NH$), 172 ($CH_2CH_2C(=O)O$, 175 ($CH_3CHC(=O)NH$)

SEC (DMF): $\overline{M_{n,SEC}}$ = 8900 g.mol^{-1} (PS equivalent), Đ = 1.13

E. Synthesis of a linear PEO macromolecular chain transfer agent (named PEO-CTA)

1. Esterification of α-pyridyldithio,ω-hydroxylPEO

a) Esterification mediated through acyl chloride

Esterification mediated through acyl chloride A solution of CDP (8.3 mg, 0.02 mmol) in 0.25 mL of anhydrous $CH_2Cl_2$was degassed under argon for 15 minutes. Oxalyl chloride (13 mg, 0.1 mmol) was added to the solution. The mixture was heated to reflux at 50°C during 3 hours. CH_2Cl_2 and oxalyl chloride were removed under vacuum. Then after, a solution of α-pyridyldithio,ω-hydroxylPEO (68 mg, 0.021 mmol) in 0.5 mL of anhydrous CH_2Cl_2 was added under argon. The solution was kept during 24 hours at room temperature. The solution was evaporated and the solid obtained was dissolved in a minimum of CH_2Cl_2 and was precipitated in cold diethyl ether. The solid obtained was dried under vacuum in the presence of P_2O_5. The mass obtained was 38 mg.

^{1}H NMR (400 MHz, $CDCl_3$), δ (ppm): 0.88 (t, $SCH_2(CH_2)_{10}CH_3$, 1.02 H) , 1.25 (m, -$SCH_2CH_2(CH_2)_{10}CH_3$, 6.11 H), 1.55-1.95 (m, $CH_2CH_2C(CN)(CH_3)$, $SCH_2CH_2(CH_2)_{10}CH_3$),

1.88 (m, 2.62 (m, $CH_2CH_2C(=O)NH$, $CH_2CH_2C(CN)$), 3.08 (t, $SSCH_2CH_2$), 3.24 (t, $SCH_2(CH_2)_{10}CH_3$), 3.65 (m, CH_2CH_2O, 254 H), 4.27 (t, $CH_2CH_2OC(=O)$, 0.84 H), 6.83 (m, $C(=O)NHCH_2$), 7.11 (m, CHCHNC), 7.67 (m, CHCHCSS, 0.60 H), 8.51 (m, CHCHNCSS, 0.49 H).

b) Esterification mediated through DMT-MM

A solution of CDP (8.2 mg, 0.02 mmol), α-pyridyldithio,ω-hydroxylPEO (67.0 mg, 0.02 mmol) and NMM (6.1 mg, 0.06 mmol) in 0.5 mL of anhydrous THF was stirred at room temperature for 10 minutes. The DMT-MM (16.6 mg, 0.06 mmol) was added and the mixture was stirred at room temperature for 24 hours. Solvent was evaporated and the residual mixture was dissoled in CH_2Cl_2. The solution was filtered and washed 3 times by a NaCl saturated solution. The organic phase was dried on $MgSO_4$ and filtered. The solution was concentrated and the residual mixture was precipitated in cold diethyl ether. The solid was dried under vacuum in the presence of P_2O_5.

^{1}H NMR (400 MHz, $CDCl_3$), δ (ppm) : 0.88 (t, $SCH_2(CH_2)_{10}CH_3$, 3.75 H) , 1.26 (m, $SCH_2CH_2(CH_2)_9CH_3$, 16.40 H), 1.69 (m, $SCH_2CH_2(CH_2)_9CH_3$), 1.92 (m, $C(CH_3)(CN)SC(=S)$, 11.63 H), 2.15-2.76 (m, $CH_2CH_2C(=O)NH$, $CH_2CH_2C(CN)$), 3.08 (t, $SSCH_2CH_2$, 0.49 H), 3.33 (t, $SCH_2(CH_2)_{10}CH_3$, 0.99 H), 3.65 (m, CH_2CH_2O, 254 H), 4.25 (t, $CH_2CH_2OC(=O)$, 1.38 H), 6.87 (m, $C(=O)NHCH_2$-), 7.10 (m, CHCHNC, 0.32 H), 7.67 (m, CHCHCSS, 0.71 H), 8.49 (m, CHCHNCSS, 0.39 H).

c) Esterification mediated through DCC/DMAP

In a round bottom flask a stirred bar was charged together with CDP (17.1 mg, 0.043 mmol) and DCC (8.9 mg, 0.043 mmol). Under argon, were added 0.4 mL of a solution of DMAP (6.0 mg, 0.049 mmol) in 4 mL of anhydrous CH_2Cl_2. At 0°C and under argon was added a solution of α-pyridyldithio,ω-hydroxylPEO (72.6 mg, 0.022 mmol) in 0.6 mL of anhydrous

CH_2Cl_2. After complete addition, the solution was stirred at 0°C during 6 hours and at room temperature during 4 days. The solution was filtered and concentrated. The product was dialyzed into ethanol during 24 hours with a membrane of 1kDa, dried, solubilized in a minimum of CH_2Cl_2 and precipitated three times in cold diether. The solid obtained was dried under vacuum in the presence of P_2O_5. The solid was obtained with a yield of 47 % (30 mg).

^{1}H NMR (400 MHz, $CDCl_3$), δ (ppm) : 0.88 (t, $SCH_2(CH_2)_{10}CH_3$, 1.49 H) , 1.25 (m, $SCH_2CH_2(CH_2)_9CH_3$, 9.60 H), 1.69 (m, $SCH_2CH_2(CH_2)_9CH_3$, 1.54 H), 1.93 (m, $C(CH_3)(CN)SC(=S)$), 2.25-2.75 (m, $CH_2CH_2C(=O)NH$, $CH_2CH_2C(CN)$, 3.93 H), 3.09 (t, $SSCH_2CH_2$, 1.68 H), 3.31 (t, $SCH_2CH_2(CH_2)_9CH_3$, 1.21 H), 3.65 (m, CH_2CH_2O, 254 H), 4.25 (t, $CH_2CH_2OC(=O)$, 1.06 H), 6.86 (m, $C(=O)NHCH_2$, 0.80 H), 7.10 (m, CHCHNC, 0.81 H), 7.67 (m, CHCHCSS, 1.58 H), 8.49 (m, CHCHNCSS, 0.75 H).

SEC in DMF (LiBr 1 g.L^{-1}): $\overline{M_{n,SEC}}$ = 8500 g.mol^{-1} and $Đ$ = 1.10.

2. Esterification of α-alkynyl,ω-hydroxylPEO

a) Esterification mediated through acyl chloride

A solution of CDP (68.3 mg, 0.170 mmol) in 2.1 mL of anhydrous CH_2Cl_2 was degassed under argon for 30 minutes and oxalyl chloride (108.0 mg, 0.850 mmol) was added to the solution. The mixture was heated to reflux during 3 hours at 50°C. CH_2Cl_2 and oxalyl chloride were removed under vacuum and under argon was added α-alkynyl,ω-hydroxylPEO (500.0 mg, 0.154 mmol) in 6.4 mL of anhydrous CH_2Cl_2. The solution was agitated during 24 hours at room temperature. The solution was evaporated and the solid was precipitated in cold diethyl ether and dried under vacuum.

^{1}H NMR (400 MHz, $CDCl_3$), δ (ppm): 0.88 (t, $S(CH_2)_{11}CH_3$, 1.56 H), 1.26 (m, $SCH_2CH_2(CH_2)_9CH_3$), 1.45 (d, $CH_3CHC(=O)NH$), 1.60 (d, $(CH_3)_2CC(=O)NH$, 4.77 H), 1.70 (m, $SCH_2CH_2(CH_2)_9CH_3$), 1.88 (m, $HC{\equiv}CCH_2CH_2$, $C(CH_3)(CN)S$, 1.94 H), 2.00 (t,

*H*C≡CCH$_2$, 0.93 H), 2.29 (td, HC≡CC*H$_2$*, 2.20 H), 2.57 (t, CH$_2$C*H$_2$*C(=O)OCH, 1.59 H), 2.65 (m, C*H$_2$*C*H$_2$*C(CN)(CH$_3$)), 3.12 (t, -SC*H$_2$*(CH$_2$)$_{10}$CH$_3$, 0.23 H), 3.65 (m, (C*H$_2$*C*H$_2$*O)$_{64}$, 254 H), 4.27 (t, CH$_2$C*H$_2$*OC(=O), 0.26 H), 5.10 (q, CH$_3$C*H*C(=O)NH, 0.73 H), 6.57 (m, N*H*CH$_2$CH$_2$O, 0.61 H), 7.12 (m, N*H*C(CH$_3$)$_2$, 0.53 H).

SEC in DMF (Libr 1 g.L^{-1}): $\overline{M_{n,SEC}}$ = 9300 g.mol^{-1}, Đ = 1.13

b) Esterification mediated through DCC/DMAP

In a round bottom flask was charged a stir bar together with α-alkynyl,ω-hydroxylPEO (2190 mg, 0.674 mmol), DMAP (17.6 mg, 0.144 mmol), and CDP (543.1 mg, 1.34 mmol). 10 mL of anhydrous CH_2Cl_2 were added under argon. In another round bottom flask, DCC (302.4 mg, 1.47 mmol) was solubilized in 7 mL of anhydrous CH_2Cl_2 under argon. The solution of DCC was injected dropwise into the first solution *via* a syringe. The solution became trouble. The solution was degassed during 10 minutes and the reaction was launched at room temperature for 4 days. Organic phase was washed twice with a solution of HCl 3 M and twice with a saturated solution of NaCl. The organic phase was evaporated and the residual mixture was kept in ice. Aliquots of 500 mg of the crude product were purified using a silica column (15 mL of silica) with CH_2Cl_2/MeOH mixture (from 100/0 to 90/10 in volume). The solvent was evaporated and the product was dried under vacuum at 40°C.

^{1}H NMR (400 MHz, $CDCl_3$), δ (ppm): 0.88 (t, SCH$_2$(CH$_2$)$_{10}$C*H$_3$*, 3.32 H), 1.26 (m, SCH$_2$CH$_2$(C*H$_2$*)$_9$CH$_3$), 1.45(d, C*H$_3$*CHC(=O)NH), 1.59 (2 s, (C*H$_3$*)$_2$CC(=O)NH, 5.01 H), 1.70 (m, SCH$_2$C*H$_2$*(CH$_2$)$_9$C*H$_3$*, 2.46 H), 1.87 (m, HC≡CCH$_2$C*H$_2$*, CH$_2$CH$_2$C(C*H$_3$*)(CN)), 2.00 (s, *H*C≡CCH$_2$), 2.29 (td, CH≡CC*H$_2$*, 1.73 H), 2.70-2.30 (m, CH$_2$C*H$_2$*C(=O)OCH, C*H$_2$*C*H$_2$*C(CH$_3$)(CN)), 3.34 (t, SC*H$_2$*(CH$_2$)$_{10}$CH$_3$, 2.07 H), 3.65 (m, (C*H$_2$*C*H$_2$*O)$_{63}$, 254 H), 4.27 (t, CH$_2$C*H$_2$*OC(=O), 2.15 H), 5.10 (q, CH$_3$C*H*C(=O)NH, 1.03 H), 6.72 (m, N*H*CH$_2$CH$_2$O, 0.85 H), 7.12 (m, N*H*C(CH$_3$)$_2$, 0.80 H)

^{13}C NMR (100 MHz, $CDCl_3$), δ (ppm): 14 ($SCH_2(CH_2)_{10}\mathit{C}H_3$), 18 ($HC{\equiv}C\mathit{C}H_2$), 23 ($\mathit{C}H_3CHC(=O)NH$), 24 ($\mathit{C}H_2CH_2C(=O)O$), 25 (($\mathit{C}H_3)_2CC(=O)NH$), 28 ($SCH_2\mathit{C}H_2(CH_2)_9CH_3$), 29 ($CH_2\mathit{C}H_2C(CH_3)(CN)S$, $SCH_2CH_2(C\mathit{H_2})_9CH_3$), 32 ($\mathit{C}H_2CH_2C(CH_3)(CN)$), 33 ($\mathit{C}H_2C(=O)OCHCH_3$), 34 ($CH_2CH_2C(\mathit{C}H_3)(CN)$), 37 ($SC(=S)S\mathit{C}H_2$), 40 ($\mathit{C}H_2NHC(=O)C(CH_3)_2$), 46 ($CH_2CH_2\mathit{C}(CH_3)(CN)$), 57 ($\mathit{C}(CH_3)_2NH$), 64 ($\mathit{C}H_2OC(=O)CH_2$), 69 ($H\mathit{C}{\equiv}CCH_2$), 70 ($CH_3\mathit{C}HC(=O)NH$), 71 (($\mathit{C}H_2\mathit{C}H_2O)_{64}$), 83 ($HC{\equiv}\mathit{C}CH_2$), 120 ($CH_2CH_2C(CH_3)(\mathit{C}N)$), 170 ($\mathit{C}(=O)NHC(CH_3)_2$), 172 ($\mathit{C}(=O)OCH(CH_3)$ and $\mathit{C}(=O)CH_2CH_2C(CN)(CH_3)$), 175 ($\mathit{C}(=O)NH(CH_2CH_2O)_{64}$), 217 (SC(=S)S),

SEC in DMF: $\overline{M_{n,SEC}}$ = 8200 g.mol^{-1} (PS equivalent), Đ = 1.13

F. Synthesis of an heterofuntional brush-like PEO (bPEO) for PEGylation of cationic copolymers

1. Synthesis of 2-cyano-5-oxo-5-(prop2-yn-1-ylamino)pentan-2-yldodecylcarbonotrithioate (COPYDC)

HOBT (0.7479 g, 4.88 mmol) and EDCI (0.7740 g, 4.99 mmol) were charged with a stir bar in a 100 mL round bottom flask. Under argon at 0°C were added DMF (2.8 mL) and anhydrous CH_2Cl_2 (5 mL). In another round bottom flask, CDP (2.0004 g, 4.96 mmol) was weighted and 15 mL of anhydrous CH_2Cl_2 were added. This second solution was degassed under argon during 10 minutes and was transferred in the first round bottom flask with a double-tipped needle under argon. Propargyl amine (0.2764 g, 5.02 mmol) was added with a degassed syringe under argon. The final mixture was degassed under argon during 10 minutes. The ice bath was removed and the reaction was launched for 24 hours at room temperature. The reaction was stopped by opening it to air. The solution was dissolved in 200 mL of CH_2Cl_2 and the organic phase was washed with 600 mL of a saturated solution of Na_2CO_3 and 600 mL of 1M HCl solution. The organic phase was dried with $MgSO_4$ and evaporated. The crude product was

purified using a silica gel column with cyclohexane/ethyl acetate mixture (2/1 by volume) as the eluent. A brown oil was obtained in a yield of 70 %.

^{1}H NMR (400 MHz, $CDCl_3$), δ (ppm): 0.88 (t, 3H, $SCH_2(CH_2)_{10}CH_3$, 3.0 H), 1.28 (m, $SCH_2CH_2(CH_2)_9CH_3$, 19.6 H), 1.70 (quint, $SCH_2CH_2(CH_2)_9CH_3$, 2.8 H), 1.88 (s, $CH_2CH_2C(CH_3)(CN)$, 2.7 H), 2.25 (t, $HC{\equiv}CCH_2NH$, 0.7 H), 2.30-2.70 (m, $CH_2CH_2C(CH_3)(CN)$, 3.8 H), 3.26 (t, $SCH_2(CH_2)_{10}CH_3$, 1.9 H), 4.05 (dd, $HC{\equiv}CCH_2NH$, 2 H), 6.02 (m, CH_2NH, 0.9 H).

^{13}C NMR (400 MHz, $CDCl_3$), δ (ppm): 15 ($SCH_2(CH_2)_{10}CH_3$), 23 ($S(CH_2)_{10}CH_2CH_3$), 25 ($CH_2CH_2C(CH_3)(CN)S$), 27 ($CH_2CH_2C(CH_3)(CN)$), 29 ($HC{\equiv}CCH_2NH$, $SCH_2CH_2(CH_2)_9CH_3$), 32 ($SCH_2(CH_2)_8CH_2CH_2CH_3$), 34 ($CH_2C(CH_3(CN))$), 37 ($SCH_2CH_2$), 47 ($C(CN)(CH_3)S$), 72 ($HC{\equiv}CCH_2$), 80 ($HC{\equiv}CCH_2$), 119 ($N{\equiv}C$), 170 ($C{=}O$), 217 ($SC(=S)S$)

FT-IR (ν in cm^{-1}): 3292 (N-H), 2919 (C-H, CH_2). 2232 (C≡N), 1651 (C=O, amide), 1532 (N-H), 1453 (C-H, CH_2), 1375 (C-H, CH_3), 1275-1230 (C-N), 1064 (C=S).

HRMS: $[M+Na]^+_{exp}$ = 463.1869 Da, $[M+Na]^+_{theo}$ = 463.1888 Da.

2. RAFT polymerization of PEGA using COPYDC

General procedure of RAFT polymerization of PEGA using COPYDC:

In a typical successful RAFT polymerization procedure, a magnetic stir bar was charged to a schlenk flask together with ACVA, COPYDC and PEGA in DMF. The solution was degassed with argon for 20 minutes and immersed in an oil bath thermostated at 70°C. Aliquots were withdrawn every 30 minutes and are analyzed by ^{1}H NMR spectroscopy to determine PEGA conversion and SEC in DMF to determine the $\overline{M_{n,SEC}}$ and the $Đ$. The reaction was stopped after 300 minutes by opening the reaction to the air and cooling the schlenk flask in liquid nitrogen.

Conversion of PEGA was determined by ^{1}H NMR spectroscopy by comparing the integration area values of the vinylic protons signals of PEGA between 5.7 and 6.5 ppm and of the formamide proton signal of DMF used at internal standard at 8.02. The DMF was removed under vacuum and the product was dialyzed in water during 3 days. The solution was lyophilized and the solid obtained was dried under vacuum in the presence of P_2O_5. The final product was analyzed by ^{1}H NMR spectroscopy and SEC in DMF (LiBr 1g.L^{-1}).

$\overline{DP}_{n,PEGA}$ was calculated by comparing the integration area values of the signal at 0.88 ppm corresponding to the methyl protons $S(CH_2)_{11}C\mathit{H}_3$ and of the signal at 4.17 ppm corresponding to the methylene protons $CH{\equiv}CC\mathit{H}_2NHC(=O)$ and $C(=O)OC\mathit{H}_2CH_2(OCH_2CH_2)_8$.

^{1}H NMR (400 MHz, $CDCl_3$), δ (ppm): 0.88 (t, $SCH_2(CH_2)_{10}C\mathit{H}_3$), 1.10-2.00 (m, $CH_2CH_2C(C\mathit{H}_3)(CN)S$, $(C\mathit{H}_2C\mathit{H})_n$, $SCH_2(C\mathit{H}_2)_{10}$), 2.00-2.60 (m, $C\mathit{H}_2C(=O)NH$, $C\mathit{H}_2C\mathit{H}_2C(CH_3)(CN)$, $C\mathit{H}{\equiv}CCH_2$), 3.38 (m, $(CH_2CH_2O)_9C\mathit{H}_3$, $SC(=S)SC\mathit{H}_2$), 3.65 (m, $C\mathit{H}_2C\mathit{H}_2O$), 4.17 (m, $HC{\equiv}CC\mathit{H}_2$, $C\mathit{H}_2CH_2O(CH_2CH_2O)_8CH_3$).

For the large amount of PPEGA:

A magnetic stir bar was charged, to a schlenk flask together with ACVA (8.5 mg, 0.030 mmol), COPYDC (134.2 mg, 0.305 mmol) and PEGA (4.3275 g, 9.02 mmol) in 4 mL of DMF. The solution was homogeneized, and degassed with argon during 30 minutes. The reaction was launched at 70°C during 1h30. The reaction was stopped by freezing the schlenk in liquid nitrogen and opening it to the air. Conversion of PEGA was determined to be 52 % by ^{1}H NMR spectroscopy by comparing the integration area values of the formamide proton of DMF at 8.00 ppm and the vinylic protons of PEGA between 5.7 and 6.5 pppm. The crude polymer was purified with several dialysis in pure water, lyophilized and dried under vacuum in the presence

of P_2O_5. The pure product was analyzed by ^{1}H NMR spectroscopy and SEC in DMF (LiBr g.L^{-1}).

$\overline{DP}_{n,PEGA}$ = 12 was calculated by comparing the integration area values of the signal at 0.88 ppm corresponding to the methyl protons $S(CH_2)_{11}CH_3$ and of the signal at 4.17 ppm corresponding to the methylene protons $CH{\equiv}CCH_2NHC(=O)$ and $CH_2CH_2O(CH_2CH_2O)_8CH_3$.

^{1}H NMR (400 MHz, $CDCl_3$), δ (ppm): 0.88 (t, $SCH_2(CH_2)_{10}CH_3$, 3.00 H), 1.10-2.00 (m, $CH_2CH_2C(CH_3)(CN)S$, $(CH_2CH)_n$, $SCH_2(CH_2)_{10}$), 2.00-2.60 (m, $CH_2C(=O)NH$, $CH_2CH_2C(CH_3)(CN)$, $CH{\equiv}CCH_2$), 3.38 (m, $(CH_2CH_2O)_9CH_3$, $SC(=S)SCH_2$, 35.56 H), 3.65 (m, $(CH_2CH_2O)_8$, 366.46 H), 4.17 (m, $HC{\equiv}CCH_2$, $CH_2CH_2O(CH_2CH_2O)_8CH_3$, 26.10 H).

SEC in DMF (LiBr 1 g.L^{-1}): $\overline{M_{n,SEC}}$ = 14700 g.mol^{-1}, $Đ$ = 1.26

References

(1) C. Campa and S. P. Harding. Anti-VEGF Compounds in the Treatment of Neovascular Age Related Macular Degeneration. *Current Drug Targets* **2011**, *12* (2), 173–181.

(2) Turecek, P. L.; Bossard, M. J.; Schoetens, F.; Ivens, I. A. PEGylation of Biopharmaceuticals: A Review of Chemistry and Nonclinical Safety Information of Approved Drugs. *Journal of Pharmaceutical Sciences* **2016**, *105* (2), 460–475.

(3) Kolate, A.; Baradia, D.; Patil, S.; Vhora, I.; Kore, G.; Misra, A. PEG ? A Versatile Conjugating Ligand for Drugs and Drug Delivery Systems. *Journal of Controlled Release* **2014**, *192*, 67–81.

(4) Kavitha, K.; BhalaMurugan, G. L. A Review on PEG-Ylationin Anti-Cancer Drug Delivery Systems. *Int J Pharm Biomed Sci* **2013**, *4*, 296–304.

(5) Pezzoli, D.; Tarsini, P.; Melone, L.; Candiani, G. RGD-Derivatized PEI-PEG Copolymers: Influence of the Degree of Substitution on the Targeting Behavior. *Journal of Drug Delivery Science and Technology* **2017**, *37*, 115–122.

(6) Choi, Y.-R.; Chae, S. Y.; Ahn, C.-H.; Lee, M.; Oh, S.; Byun, Y.; Rhee, B. D.; Ko, K. S. Development of Polymeric Gene Delivery Carriers: PEGylated Copolymers of L-Lysine and L-Phenylalanine. *Journal of Drug Targeting* **2007**, *15* (6), 391–398.

(7) Thiersch, M.; Rimann, M.; Panagiotopoulou, V.; Öztürk, E.; Biedermann, T.; Textor, M.; Lühmann, T. C.; Hall, H. The Angiogenic Response to PLL-G-PEG-Mediated HIF-1α Plasmid DNA Delivery in Healthy and Diabetic Rats. *Biomaterials* **2013**, *34* (16), 4173–4182.

(8) Kim, J.; Kang, Y.; Tzeng, S. Y.; Green, J. J. Synthesis and Application of Poly(ethylene Glycol)-Co-Poly(β-Amino Ester) Copolymers for Small Cell Lung Cancer Gene Therapy. *Acta Biomaterialia* **2016**, *41*, 293–301.

(9) Mastorakos, P.; da Silva, A. L.; Chisholm, J.; Song, E.; Choi, W. K.; Boyle, M. P.; Morales, M. M.; Hanes, J.; Suk, J. S. Highly Compacted Biodegradable DNA Nanoparticles Capable of Overcoming the Mucus Barrier for Inhaled Lung Gene Therapy. *Proceedings of the National Academy of Sciences* **2015**, *112* (28), 8720–8725.

(10) Rungsardthong, U.; Deshpande, M.; Bailey, L.; Vamvakaki, M.; Armes, S. P.; Garnett, M. C.; Stolnik, S. Copolymers of Amine Methacrylate with Poly(ethylene Glycol) as Vectors for Gene Therapy. *Journal of Controlled Release* **2001**, *73* (2–3), 359–380.
(11) Lin, D.; Huang, Y.; Jiang, Q.; Zhang, W.; Yue, X.; Guo, S.; Xiao, P.; Du, Q.; Xing, J.; Deng, L.; Liang, Z.; Dong, A. Structural Contributions of Blocked or Grafted poly(2-Dimethylaminoethyl Methacrylate) on PEGylated Polycaprolactone Nanoparticles in siRNA Delivery. *Biomaterials* **2011**, *32* (33), 8730–8742.
(12) Lai, J.; Xu, Z.; Tang, R.; Ji, W.; Wang, R.; Wang, J.; Wang, C. PEGylated Block Copolymers Containing Tertiary Amine Side-Chains Cleavable via Acid-Labile Ortho Ester Linkages for pH-Triggered Release of DNA. *Polymer* **2014**, *55* (12), 2761–2771.
(13) Zhang, X.; Pan, S.-R.; Hu, H.-M.; Wu, G.-F.; Feng, M.; Zhang, W.; Luo, X. Poly(ethylene Glycol)-Block-Polyethylenimine Copolymers as Carriers for Gene Delivery: Effects of PEG Molecular Weight and PEGylation Degree. *Journal of Biomedical Materials Research Part A* **2008**, *84A* (3), 795–804.
(14) Fitzsimmons, R. E. B.; Uludag, H. Specific Effects of PEGylation on Gene Delivery Efficacy of Polyethylenimine: Interplay between PEG Substitution and N/P Ratio. *Acta Biomaterialia* **2012**, *8* (11), 3941–3955.
(15) Pouton, C. W.; Seymour, L. W. Key Issues in Non-Viral Gene Delivery. *Advanced Drug Delivery Reviews* **1998**, *34* (1), 3–19.
(16) Mintzer, M. A.; Simanek, E. E. Nonviral Vectors for Gene Delivery. *Chemical Reviews* **2009**, *109* (2), 259–302.
(17) Lin, C.; Engbersen, J. F. The Role of the Disulfide Group in Disulfide-Based Polymeric Gene Carriers. *Expert Opinion on Drug Delivery* **2009**, *6* (4), 421–439.
(18) Meng, F.; Hennink, W. E.; Zhong, Z. Reduction-Sensitive Polymers and Bioconjugates for Biomedical Applications. *Biomaterials* **2009**, *30* (12), 2180–2198.
(19) Hoogenboom, R. Thiol-Yne Chemistry: A Powerful Tool for Creating Highly Functional Materials. *Angewandte Chemie International Edition* **2010**, *49* (20), 3415–3417.
(20) Hoyle, C. E.; Lowe, A. B.; Bowman, C. N. Thiol-Click Chemistry: A Multifaceted Toolbox for Small Molecule and Polymer Synthesis. *Chemical Society Reviews* **2010**, *39* (4), 1355.
(21) Cotanda, P.; Wright, D. B.; Tyler, M.; O'Reilly, R. K. A Comparative Study of the Stimuli-Responsive Properties of DMAEA and DMAEMA Containing Polymers. *Journal of Polymer Science Part A: Polymer Chemistry* **2013**, *51* (16), 3333–3338.
(22) Chang, C.-W.; Bays, E.; Tao, L.; Alconcel, S. N. S.; Maynard, H. D. Differences in Cytotoxicity of poly(PEGA)s Synthesized by Reversible Addition-Fragmentation Chain Transfer Polymerization. *Chemical Communications* **2009**, No. 24, 3580–3582.
(23) Fairbanks, B. D.; Gunatillake, P. A.; Meagher, L. Biomedical Applications of Polymers Derived by Reversible Addition-Fragmentation Chain-Transfer (RAFT). *Advanced Drug Delivery Reviews* **2015**, *91*, 141–152.
(24) *Handbook of RAFT Polymerization*; Barner-Kowollik, C., Ed.; Wiley-VCH: Weinheim, 2008.
(25) Moad, G.; Rizzardo, E.; Thang, S. H. Living Radical Polymerization by the RAFT Process ? A Third Update. *Australian Journal of Chemistry* **2012**, *65* (8), 985.
(26) Mansfeld, U.; Pietsch, C.; Hoogenboom, R.; Becer, C. R.; Schubert, U. S. Clickable Initiators, Monomers and Polymers in Controlled Radical Polymerizations – a Prospective Combination in Polymer Science. *Polymer Chemistry* **2010**, *1* (10), 1560.
(27) Levere, M. E.; Ho, H. T.; Pascual, S.; Fontaine, L. Stable Azlactone-Functionalized Nanoparticles Prepared from Thermoresponsive Copolymers Synthesized by RAFT Polymerization. *Polymer Chemistry* **2011**, *2* (12), 2878-2887.
(28) Fontaine, L.; Ho, T. H.; Pascual, S.; Montembault, V. Multifunctional Coupling Reagents Having an Azlactone Function. EP 2909185 A1, August 26, 2015.
(29) Kunishima, M.; Kawachi, C.; Iwasaki, F.; Terao, K.; Tani, S. Synthesis and Characterization of 4-(4,6-Dimethoxy-1,3,5-Triazin-2-Yl)-4-Methylmorpholinium Chloride. *Tetrahedron Letters* **1999**, *40* (29), 5327–5330.

(30) Gilon, C.; Klausner, Y.; Hassner, A. A Novel Method for the Facile Synthesis of Depsipeptides. *Tetrahedron Letters* **1979**, *20* (40), 3811–3814.
(31) Venkataraman, S.; Ong, W. L.; Ong, Z. Y.; Joachim Loo, S. C.; Rachel Ee, P. L.; Yang, Y. Y. The Role of PEG Architecture and Molecular Weight in the Gene Transfection Performance of PEGylated Poly(dimethylaminoethyl Methacrylate) Based Cationic Polymers. *Biomaterials* **2011**, *32* (9), 2369–2378.
(32) Luo, K.; Yang, J.; Kopečková, P.; Kopeček, J. Biodegradable Multiblock Poly[*N* -(2-Hydroxypropyl)methacrylamide] via Reversible Addition−Fragmentation Chain Transfer Polymerization and Click Chemistry. *Macromolecules* **2011**, *44* (8), 2481–2488.
(33) Robinson, B. A.; Tester, J. W. Kinetics of Alkaline Hydrolysis of Organic Esters and Amides in Neutrally-Buffered Solution. *International Journal of Chemical Kinetics* **1990**, *22* (5), 431–448.
(34) Boyer, C.; Whittaker, M. R.; Luzon, M.; Davis, T. P. Design and Synthesis of Dual Thermoresponsive and Antifouling Hybrid Polymer/Gold Nanoparticles. *Macromolecules* **2009**, *42* (18), 6917–6926.
(35) Song, Z.; Xu, Y.; Yang, W.; Cui, L.; Zhang, J.; Liu, J. Graphene/Tri-Block Copolymer Composites Prepared via RAFT Polymerizations for Dual Controlled Drug Delivery via pH Stimulation and Biodegradation. *European Polymer Journal* **2015**, *69*, 559–572.
(36) Qiao, M.; Wu, S.; Wang, Y.; Ran, Q. Brush-like Block Copolymer Synthesized via RAFT Polymerization for Graphene Oxide Aqueous Suspensions. *Royal Society of Chemistry Advances* **2017**, *7* (8), 4776–4782.
(37) Wood, M. R.; Duncalf, D. J.; Findlay, P.; Rannard, S. P.; Perrier, S. Investigation of the Experimental Factors Affecting the Trithiocarbonate-Mediated RAFT Polymerization of Methyl Acrylate. *Australian Journal of Chemistry* **2007**, *60* (10), 772–778.
(38) Perrier, S.; Barner-Kowollik, C.; Quinn, J. F.; Vana, P.; Davis, T. P. Origin of Inhibition Effects in the Reversible Addition Fragmentation Chain Transfer (RAFT) Polymerization of Methyl Acrylate. *Macromolecules* **2002**, *35* (22), 8300–8306.

Chapter 3: Synthesis and Characterization of (PEGylated) aminoethyl-based polyacrylates.

Introduction

Interest in cationic polymers results from their potential to mediate transfection *via* the condensation of nucleic acids, to provide protection from enzymatic degradation and to facilitate cellular uptake and endosomal escape.[1–4]

Such feature is provided by the charge density of the cationic polymer.[1–4] The charge density is driven by the pKa of cationic amine groups which can be protonated to form polyplexes with negatively charged nucleic acids through electrostatic interactions. Amine groups with a high pKa allow efficient DNA complexation and protection whereas amine groups with a low pKa facilitate endosomal escape. Several works showed the addition of primary amine allows to increase the charge density and the transfection efficiency.[5,6] The incorporation of protonatable tertiary amine within the copolymer reduces its cellular toxicity.[7] It has been shown that the combination of both primary and tertiary amines with a wide buffer range rise to modulate transfection efficiency and cytotoxicity.[8,9] Zhu *et al.*[6] synthesized polymethacrylates containing tertiary amines DMAEMA units, and primary amine groups, AEMA units. Authors studied the effect of DMAEMA/AEMA molar ratios on transfection efficiency and cytotoxicity. They showed that the decrease of DMAEMA/AEMA molar ratio from 91/9 to 70/30 led to the increase of the complexation of pDNA and a better transfection efficiency together with a decrease of cell viability.

In our work, polyacrylates containing primary and tertiary amines group are targeted. The interest of polyacrylates in comparison with polymethacrylates for gene delivery is their high water solubility and self-catalyzed hydrolyzation leading to a lower cytotoxicity.[10,11] Therefore, *N*-aminoethyl acrylate (AEA) and 2-(*N,N*-dimethylamino)ethyl acrylate (DMAEA) were chosen as repeating units. Recent studies dealing with block copolymers *versus* statistical copolymers with similar composition, showed that statistical copolymers lead to greater cell viabilities and gene expression, in the presence and absence of serum, as compared to diblock

copolymers, even if diblock copolymers form polyplexes with a higher colloidal stability.[12–14] Therefore, statistical copolymers based on DMAEA and AEA units are studied on this work as they are supposed to be better candidates for transfection than block copolymers. The RAFT polymerization has been chosen as it paves the way for the synthesis of polymers not only with defined molar mass, narrow molar mass distribution but also with homogeneous chain composition and monomer sequences.[15] The RAFT polymerization of aminoethyl acrylates is well-known and have been previously described.[10,11,16] Furthermore, the synthesis and the RAFT polymerization of *N*-(*tert*-butoxycarbonyl)aminoethyl acrylate (*t*BocAEA) has been described for the first time by our group.[17] In such study,[17] to avoid any aminolysis of chain transfer agent moiety in the presence of primary amine-derived AEA, the protected *t*BocAEA was used as a precursor for the RAFT polymerization.

The RAFT copolymerizations of DMAEA and *t*BocAEA mediated through an α-alkynyl,ω-dodecyltrithiocarbonate PEO (aPEO-CTA), an α-alkynyl,ω-dodecyltrithiocarbonate PPEGA (PPEGA-CTA) and the COPYDC was studied to target: aPEO-*b*-P(DMAEA-*co*-*t*BocAEA), PPEGA-*b*-P(DMAEA-*co*-*t*BocAEA) and P(DMAEA-*co*-*t*BocAEA) copolymers, respectively. These copolymers with lPEO and bPEO blocks have been synthesized with different DMAEA/*t*BocAEA molar ratios. The associated cationic copolymers was obtained by cationization and deprotection of *t*BocAEA repeating unit in acidic media. In our study, the influence of the PEO architecture and the DMAEA/AEA molar ratio onto pDNA complexation and onto resulting polyplexes cytotoxicity will be highlighted.

I. Copolymers based on DMAEA and *t*BocAEA units.

A. Determination of DMAEA and *t*BocAEA reactivity ratios[‡]

In conventional free radical copolymerization, if reactivities of two monomers are different, chains formed at different times in the process have different composition and the final polymer is a mixture of chains with different microstructures. In a RAFT copolymerization, since all chains grow at the same time, the composition drift takes place at the same extent in each single chain. The copolymer composition is influenced by the reactivity ratios. Several methods are currently used to determine reactivity ratios among which the Fineman–Ross method,[18] the Mayo–Lewis terminal model,[19] and the Kelen–Tüdos method.[20] Usually, in conventional free radical copolymerization, monomers reactivity ratios are measured by fitting the copolymer composition at low conversion as a function of initial monomer feed composition. However, in RDRPs, the copolymer chain composition at low conversion could be affected by the initiation step considering that different reactivities are usually detected.[21] Therefore, to obtain reliable results, it is necessary to measure the cumulative copolymer composition from 10% to high conversion. The extended Kelen–Tüdos method is the right choice to calculate both monomer reactivity ratios (r_{DMAEA} and $r_{tBocAEA}$) because higher conversions could be considered.[22] The extended Kelen-Tüdos equation is expressed by the following equations:

$$\eta = \left(r_{DMAEA} + \frac{r_{tBocAEA}}{\alpha}\right)\xi - \frac{r_{tBocAEA}}{\alpha} \quad \text{Equation (III. 1)}$$

[‡]Ho, H.T.; Bohec, M. L.; Frémaux, J.; Piogé, S.; Casse, N. ; Fontaine L.; Pascual, S. Tuning the molar composition of «charge-shifting» cationic copolymers based on 2-(N,N-dimethylamino) ethyl acrylate. *Macromolecular Rapid Communications* **2017**, *38* (5), 1600641-600646

With: $\eta = \frac{G}{\alpha+F}$ Equation (III. 2)

$G = \frac{y-1}{z}$ Equation (III. 3)

$\alpha = \sqrt{F_{min} \times F_{max}}$ Equation (III. 4)

$\xi = \frac{F}{\alpha+F}$ Equation (III. 5)

$F = \frac{y}{z^2}$ Equation (III. 6)

$y = \frac{F_{DMAEA}}{1-F_{DMAEA}}$ Equation (III. 7)

$$z = \frac{\log(1 - \xi_{DMAEA})}{\log(1 - \xi_{tBocAEA})}$$ Equation (III. 8)

$\xi_{DMAEA} = \xi_{tBocAEA} \frac{y}{x_0}$ Equation (III. 9)

$\xi_{tBocAEA} = \omega \frac{\mu+x_0}{\mu+y}$ Equation (III. 10)

$\mu = \frac{M_{DMAEA}}{M_{tBocAEA}}$ Equation (III. 11)

$x_0 = \frac{f_{DMAEA}}{1-f_{DMAEA}}$ Equation (III. 12)

where, f_{DMAEA} is the molar ratio of DMAEA in the comonomer feed, F_{DMAEA} is the molar ratio in the copolymer, M_{DMAEA} is the molar mass of DMAEA (143.2 g.mol^{-1}), $M_{tBocAEA}$ is the molar mass of *t*BocAEA (215.2 g.mol^{-1}), ω represents the total conversion of both DMAEA and *t*BocAEA monomers and α = 1.04323.

To determine such parameters, several RAFT copolymerizations of DMAEA and *t*BocAEA were carried out (Table III. 1)

Table III. 1. Data for the RAFT (co)polymerizations of DMAEA and *t*BocAEA at different loadings using mPEO-CTA as macromolecular chain transfer agent and ACVA as the initiator in 1,4-dioxane using ($[DMAEA]_0/[tBocAEA]_0$)/$[mPEO\text{-}CTA]_0/[ACVA]_0$ = 100/1/0.2

Run	$[DMAEA]_0/[tBocAEA]_0$	Time (h)	Conv (%)[a]	$\overline{DP}_{n,PDMAEA}$[b]	$\overline{DP}_{n,PtBocAEA}$[b]	$\overline{M_{n,NMR}}$ (g.mol^{-1})[c]	$\overline{M_{n,SEC}}$ (g.mol^{-1})[d]	Đ[d]
1	100/0[e]	8	44	23	0	5690	8900	1.07
2	50/50[e]	18	22	10	10	5980	9400	1.16
3	70/30[e]	12	24	18	9	6910	9600	1.17
4	0/100[f]	4	14	0	14	5410	9400	1.15

[a] Total monomers conversion determined by ^{1}H NMR spectroscopy (400 MHz, $CDCl_3$) comparing the peak area of the vinylic protons of DMAEA and *t*BocAEA at 5.81-6.46 ppm with the peak area of the CH of DMF (used at internal standard) at 8.02 ppm. [b] Determined by ^{1}H NMR spectroscopy (400 MHz in $CDCl_3$) [c] $\overline{M_{n,NMR}} = \overline{M_{n,mPEO\text{-}CTA}} + \overline{DP}_{n,PDMAEA} \times M_{DMAEA} + \overline{DP}_{n,PtBocAEA} \times M_{tBocAEA}$ with $\overline{M_{n,mPEO\text{-}CTA}}$ = 2400 g.mol^{-1}, M_{DMAEA} = 143.2 g.mol^{-1} and $M_{tBocAEA}$ = 215.2 g.mol^{-1}. [d] Determined by SEC in DMF (LiBr g.L^{-1}, PS equivalents). [e] Solvent: 1,4-dioxane and T = 70°C [f] Solvent: N,N-dimethylformamide and T = 90 °C

RAFT (co)polymerizations were performed at 70°C in organic solvents such as 1,4-dioxane in which DMAEA and *t*BocAEA are stable.[10,11,17,23] RAFT agents bearing a 4-cyanopentanoic acid as a R leaving group have previously been used with success for RAFT polymerizations involving DMAEA and *t*BocAEA.[17] Therefore, statistical RAFT copolymerization of DMAEA and *t*BocAEA were carried out a PEO bearing a 4-cyanopentanoic acid (also called mPEO-CTA) as a model macromolecular chain transfer agent,

ACVA as a generator of radicals and a $[mPEO\text{-}CTA]_0/[ACVA]_0$ molar ratio equal to 1/0.2 in order to allow the control of the copolymerizations (Scheme III. 1).

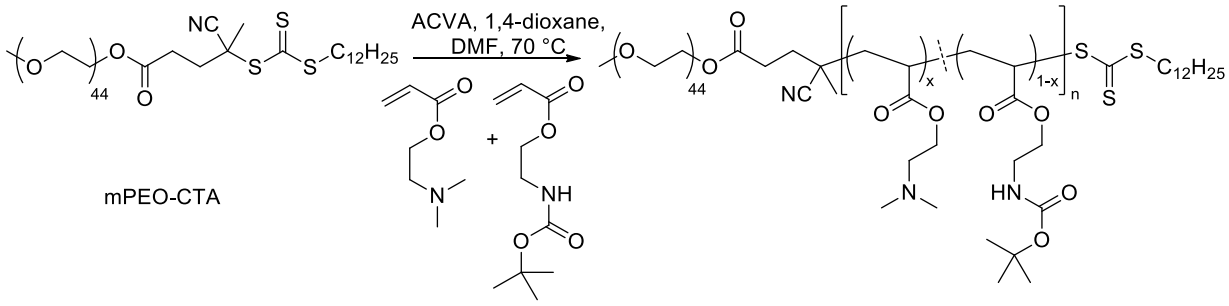

Scheme III. 1. RAFT copolymerization of *t*BocAEA and DMAEA mediated through ACVA used as the initiator and α-methoxy,ω-dodecyltrithiocarbonate PEO (mPEO-CTA) used as the macromolecular chain transfer agent in 1,4-dioxane and DMF at 70°C $([DMAEA]_0+[t\text{BocAEA}]_0)/[mPEO\text{-}CTA]_0/[ACVA]_0 = 100/1/0.2$.

The $[monomer(s)]_0/[mPEO\text{-}CTA]_0$ molar ratio was fixed at 100/1 with different molar ratios of both monomers $[DMAEA]_0/[t\text{BocAEA}]_0$. The total DMAEA and *t*BocAEA conversions were determined by ^1H NMR spectroscopy analysis of crude mixtures by comparing the integration values of vinylic protons of monomers between 5.81 and 6.46 ppm (labeled b, c, d, e, f and g in Figure III. 1) and of the methine proton of DMF (used as internal standard) at 8.02 ppm (labeled a in Figure III. 1).

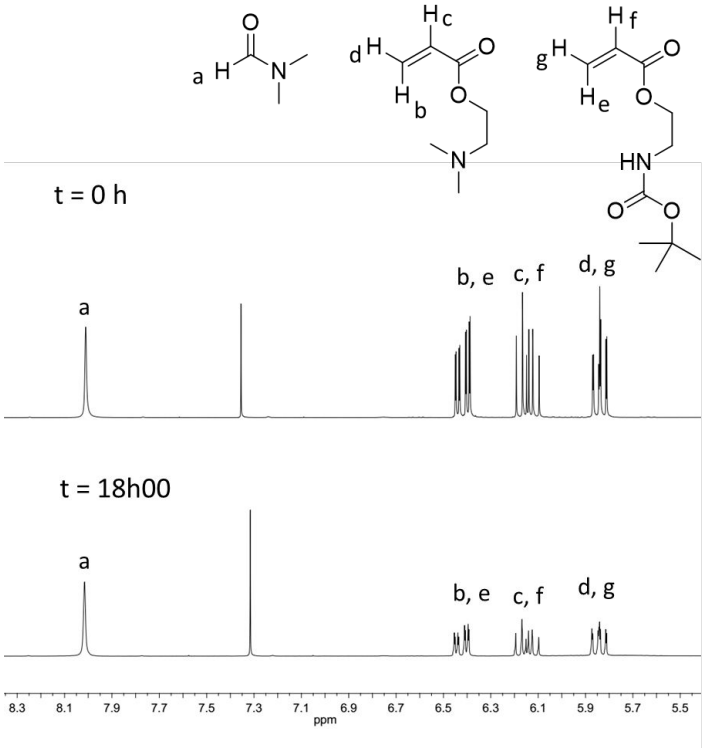

Figure III. 1. Overlaid ^{1}H NMR spectra (400MHz, $CDCl_3$) of crude solutions obtained from RAFT copolymerization of tBocAEA and DMAEA using mPEO-CTA, ACVA at 70°C in 1,4-dioxane at t = 0h and t = 18h using $[DMAEA]_0/[t\text{BocAEA}]_0/[\text{mPEO-CTA}]_0/[ACVA]_0$ = 50/50/1/0.2 (Run 2, Table III. 1).

The number-average polymerization degrees of DMAEA ($\overline{DP}_{n,,PDMAEA}$) and *t*BocAEA ($\overline{DP}_{n,PtBocAEA}$) were determined by ^{1}H NMR spectroscopy analysis of purified copolymers. Figure III. 2 shows a typical ^{1}H NMR spectrum obtained from the precipitated copolymer without any trace of unreacted monomer. The resonance of the methylene protons CH_2CH_2O of EO units appears at 3.65 ppm (labeled b in Figure III. 2), of the methylene protons $OCH_2CH_2NH(C=O)$ corresponding to the *t*BocAEA units appears at 3.38–3.40 ppm (labeled h in Figure III. 2), and the one from the methylene protons $CH_2CH_2OC(=O)$, $OCH_2CH_2N(CH_3)_2$ of the DMAEA units and $OCH_2CH_2NH(C=O)$ of *t*BocAEA units appear at 4.15 ppm (labeled c, d and g in Figure III. 2, respectively). By taking into account the number of protons and the

integration of those peaks, the number-average molar masses of copolymers were calculated (Table III. 1).

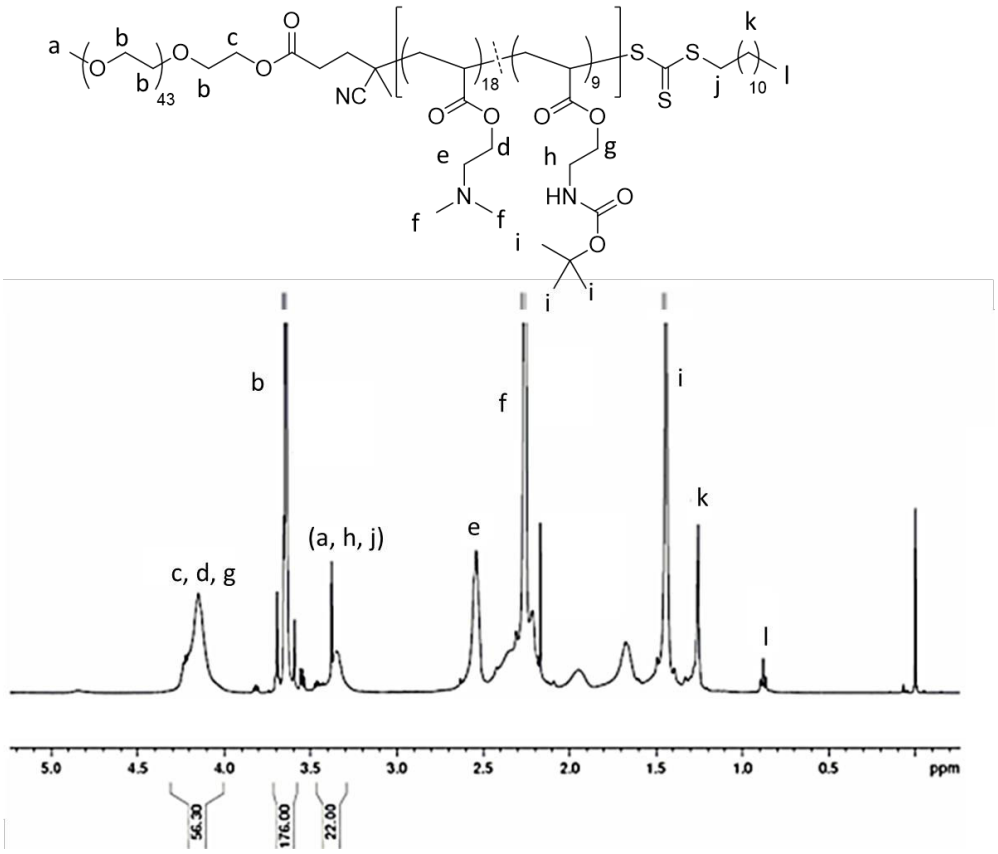

Figure III. 2. ^{1}H NMR spectrum (400 MHz, $CDCl_3$) of purified mPEO-*b*-P(DMAEA-*co*-*t*BocAEA) synthesized by RAFT copolymerization of DMAEA and *t*BocAEA using mPEO-CTA as the macromolecular chain agent, ACVA as the initiator in 1,4-dioxane at 70°C during 12 hours using $[DMAEA]_0/[tBocAEA]_0/[mPEO\text{-}CTA]_0/[ACVA]_0 = 70/30/1/0.2$ (Run 3; Table III. 1).

SEC analysis were performed on purified copolymers. Results obtained from SEC analysis (Figure III. 3) shows shifted SEC traces to higher retention times for copolymers in

comparison with the SEC trace for mPEO-CTA, indicating the formation of block copolymers based on a PEO first block and a P(DMAEA-*co*-*t*BocAEA) second block.

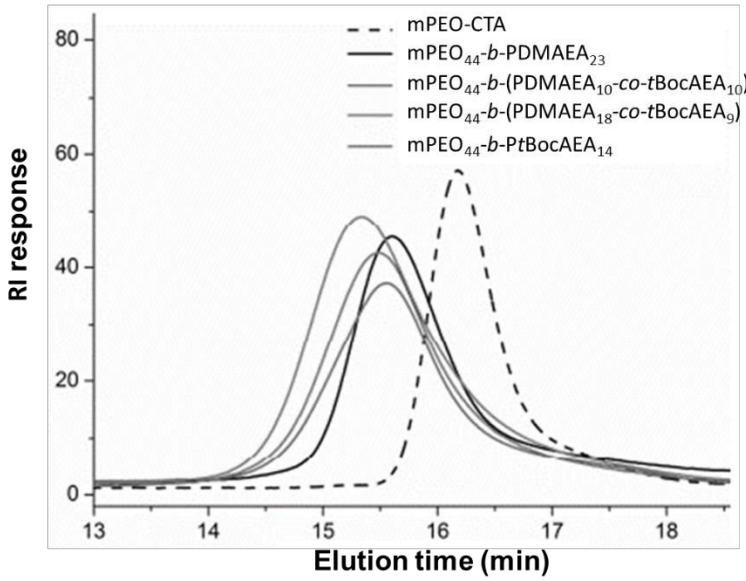

Figure III. 3. Overlaid SEC traces using RI detection of the PEO macromolecular chain transfer agent (mPEO-CTA) and copolymers based on EO, DMAEA and tBocAEA units.

DMAEA and *t*BocAEA molar fractions in the copolymer were determined by ^{1}H NMR spectroscopy analysis of purified copolymers from relative areas of peaks C*H*$_2$C*H*$_2$O (EO units) at 3.65 ppm (labeled b in Figure III. 2), OCH$_2$C*H*$_2$NHC(=O) (*t*BocAEA units) between 3.38-3.40 ppm (labeled h in Figure III. 2) and of OC*H*$_2$CH$_2$N(CH$_3$)$_2$ at 4.15 ppm (labeled d in Figure III. 2). According of these analyses, several parameters were determined to assess the reactivities ratios by extended Kelen-Tüdos method (Table III. 2).

Table III. 2. Extended Kelen-Tüdos parameters for the RAFT copolymerizations of DMAEA and *t*BocAEA at different loadings mediated by mPEO-CTA used as a macromolecular chain transfer agent and ACVA used as generator of radicals in 1,4-dioxane at 70°C ($\alpha = 1.04323$).

f_{DMAEA}	F_{DMAEA}	ω	x_0	jY	ξ_2	ξ_1	z	F	G	η	ξ
0.10	0.10	0.12	0.11111	0.11111	0.00120	0.00120	1.0000	0.11110	-0.88889	-0.92718	0.11159
0.33	0.31	0.17	0.49553	0.44927	0.00177	0.00161	0.91209	0.54005	-0.60380	-0.43513	0.38918
0.41	0.38	0.16	0.69491	0.61290	0.00165	0.00145	0.88190	0.78805	-0.43894	-0.26836	0.48180
0.50	0.50	0.22	1.00000	1.00000	0.00220	0.00220	1.00000	1.00000	0.00000	0.00000	0.54124
0.68	0.65	0.59	2.12500	1.85714	0.00530	0.00570	0.87359	2.43500	0.98117	0.29904	0.74167
0.70	0.67	0.24	2.33333	2.03030	0.00267	0.00232	0.86998	2.68252	1.18428	0.33548	0.59900
0.89	0.87	0.65	8.09091	6.69231	0.00774	0.00639	0.82658	9.79490	6.88655	0.64708	0.92036

The extended Kelen–Tüdos plot reveals that the dependence of η versus ξ is linear as indicated by the R^2 parameter ($R^2 = 0.991$) and the linear fit allows the calculation of both reactivity ratios: $r_{DMAEA} = 0.81$ and $r_{tBocAEA} = 0.99$ (Figure III. 4). These closed r values confirm the random composition of these copolymers. The copolymerization is characteristic of an "ideal" copolymerization. Same behavior has been observed starting from DMAEA and methyl acrylate (MA) comonomers.10 When DMAEA is combined with an acrylamide monomer such as N,N-dimethylacrylamide,[24] 2-acrylamido-2-methyl-1-propanesulfonic acid,[25] and 3-aminopropylmethacrylamide,[26] the acrylamide possesses a much higher reactivity ratio and a higher tendency of homopropagation. Therefore, chain growth reaction proceeds predominantly by the addition of DMAEA monomer to polyacrylamide macroradicals yielding statistical copolymers.

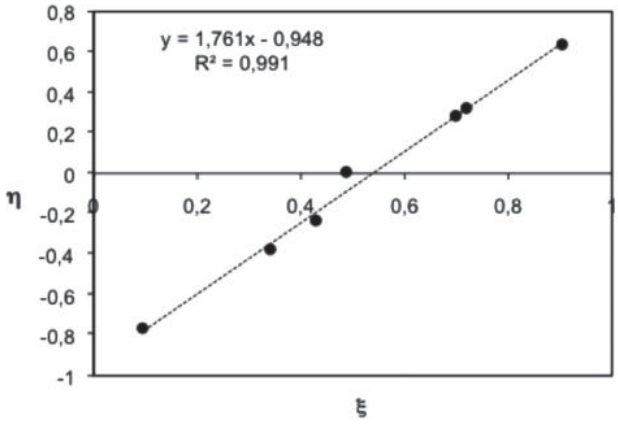

Figure III. 4. Kelen-Tüdos plot for the RAFT copolymerizations of DMAEA and *t*BocAEA at different loadings mediated by mPEO-CTA used as macromolecular chain transfer agent and ACVA used as the initiator in 1,4-dioxane at 70°C.

Another interesting feature in the RAFT copolymerization of DMAEA and tBocAEA is that the molar composition of statistical copolymers is equal to the molar composition of the feed comonomers whatever the conversion, as shown in Table III. 1. Therefore, the molar composition of statistical copolymers based on DMAEA and tBocAEA can be easily tuned.

B. RAFT copolymerization of DMAEA and *t*BocAEA using aPEO-CTA

The synthesis of aPEO-*b*-P(DMAEA-*co*-*t*BocAEA) copolymers with different DMAEA/*t*BocAEA molar ratios has been performed by RAFT copolymerization of DMAEA and *t*BocAEA using similar conditions than the one previously reported (Chapter 3 §I-A).

Polymerizations were performed using ACVA as the initiator in 1,4-dioxane and DMF at 70°C under argon (Scheme III. 2). The only difference is the use of the α-alkynyl,ω-dodecyltrithiocarbonate PEO (aPEO-CTA) (Chapter 2 §II-C-2) as the macromolecular chain transfer agent. The aPEO-CTA was used because of the alkyne group which is able to react with the thiol-group of the recognition ligand RGD.

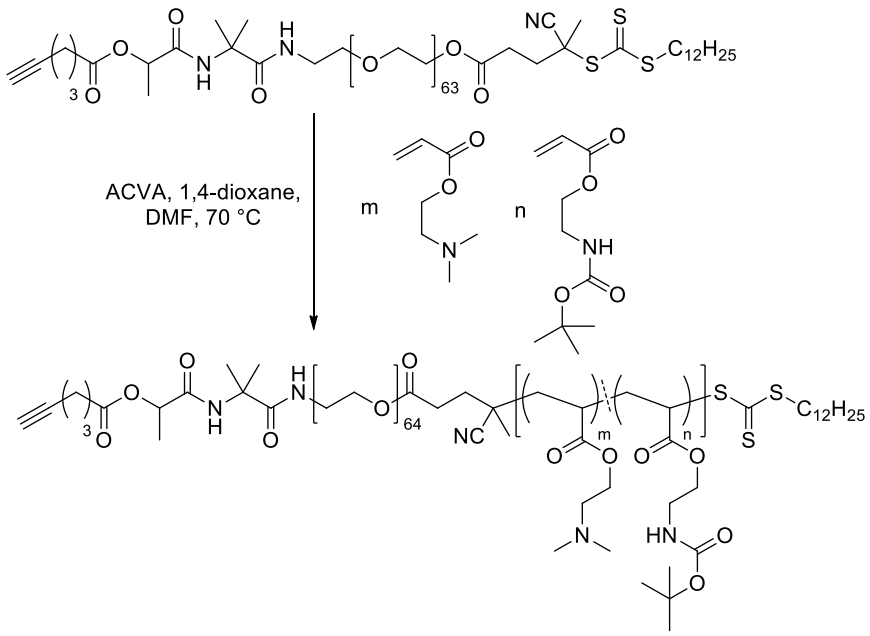

Scheme III. 2. RAFT copolymerization of *t*BocAEA and DMAEA mediated through ACVA used as the initiator and α-alkynyl,ω-dodecyltrithiocarbonate PEO (aPEO-CTA) used as the macromolecular chain transfer agent in 1,4-dioxane and DMF at 70°C (($[t\text{BocAEA}]_0+[\text{DMAEA}]_0)/[\text{aPEO-CTA}]_0/[\text{ACVA}]_0 = 100/1/0.2$).

A first RAFT polymerization of DMAEA and *t*BocAEA with the following initial molar ratio: $[\text{DMAEA}]_0/[t\text{BocAEA}]_0/[\text{aPEO-CTA}]/[\text{ACVA}]_0 = 50/50/1/0.2$ was launched at 70°C

under argon during 5h30. The aPEO-CTA chosen to this study has a $\overline{M_{n,SEC}}$ = 8200 g.mol^{-1} and a $Đ$ = 1.13. The total monomers conversion has been determined by ^{1}H NMR spectroscopy (Figure III. 5) by comparing the integration values of the alkene protons signals between 5.81 and 6.46 ppm (labeled b, c, d, e, f and g in Figure III. 5) at t_0 and at t_f using the methine *H*C(=O)NH $(CH_3)_2$ signal of DMF at 8.02 ppm as the reference (labeled a in Figure III. 5). The calculated conversion is equal to 24 %. The final product was purified by several precipitation and decantation in cold hexane/diethyl ether mixture (90/10, v/v). The purified copolymer was analyzed by FT-IR spectroscopy, ^{1}H NMR spectroscopy and SEC in DMF (LiBr 1 g.L^{-1}).

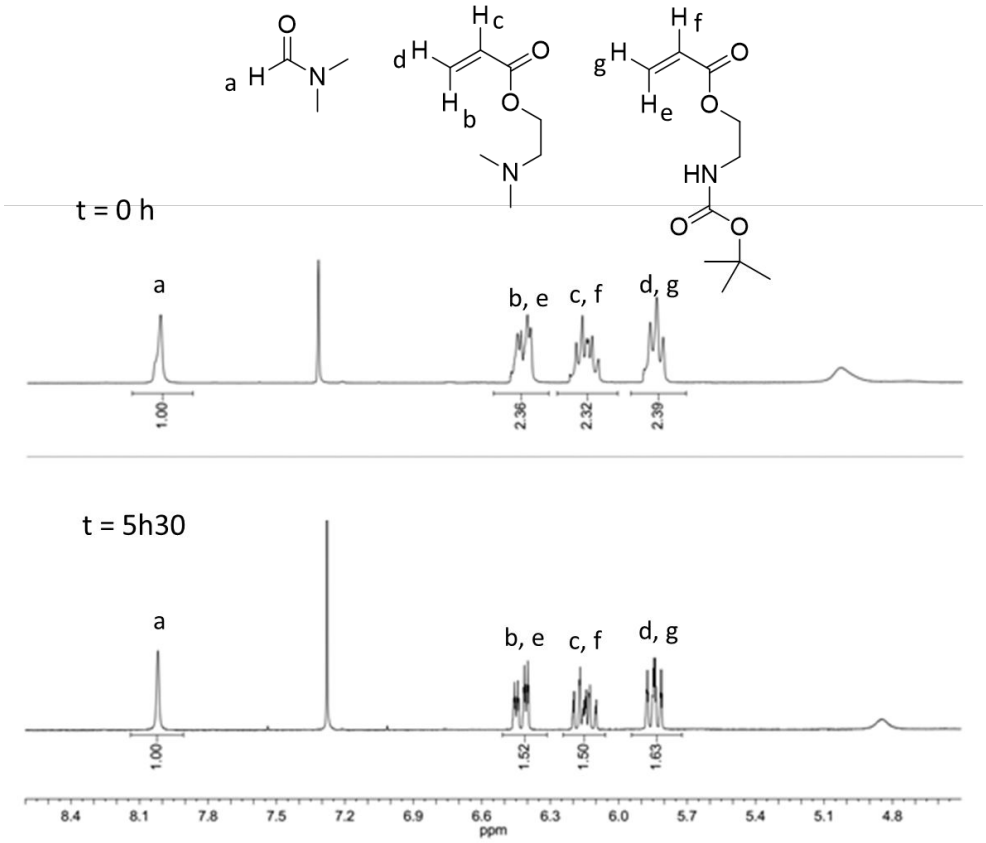

Figure III. 5. Overlaid of ^{1}H NMR spectra (400 MHz, $CDCl_3$) between 4.6 and 8.5 ppm of the crude mixture of RAFT copolymerization of DMAEA and *t*BocAEA using aPEO-CTA as the macromolecular chain transfer agent and ACVA as the initiator at 70°C in 1,4-dioxane and DMF using $[DMAEA]_0/[tBocAEA]_0/[aPEO\text{-}CTA]_0/[ACVA]_0$ = 50/50/1/0.2 (Run 9, Table III. 3)

The FT-IR spectrum of aPEO-*b*-P(DMAEA-*co*-*t*BocAEA) (Figure III. 6) shows the presence of the C-H stretching band at 2883 cm^{-1}, the signal at 1731 cm^{-1} relative to the C=O stretching band of the ester functions of acrylates repeating units, the C=O of carbamate stretching at 1518 cm^{-1} characteristic of the *t*BocAEA repeating unit and the C-O stretching band characteristic of the PEO at 1108 cm^{-1}.

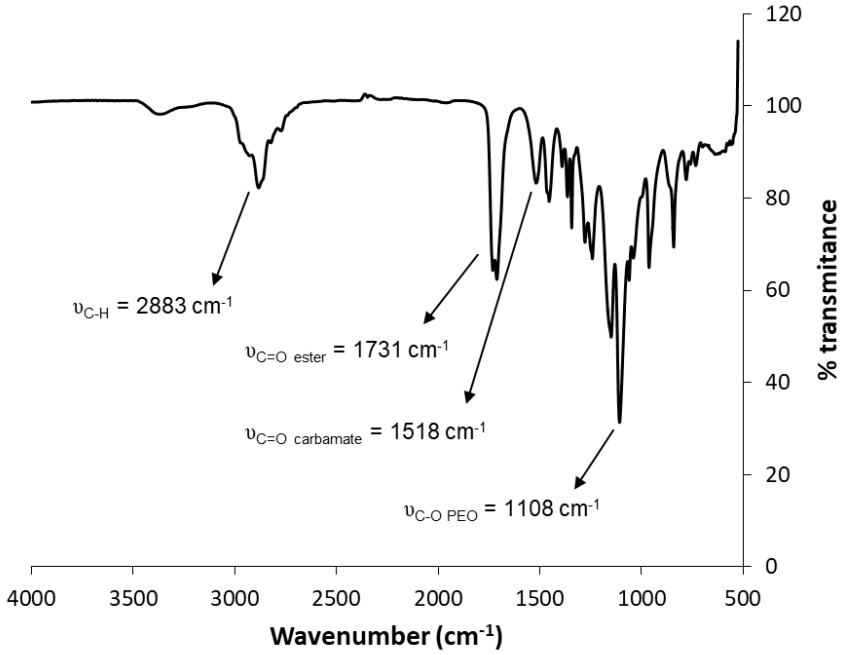

Figure III. 6. FT-IR spectrum of aPEO-*b*-P(DMAEA-*co*-*t*BocAEA) synthesized by RAFT copolymerization of DMAEA and *t*BocAEA using aPEO-CTA as the macromolecular chain transfer agent and ACVA as the initiator in 1,4-dioxane and DMF using $[DMAEA]_0/[t\text{BocAEA}]_0/[\text{aPEO-CTA}]_0/[ACVA]_0 = 50/50/1/0.2$.

The ^1H NMR spectrum (Figure III. 7) shows the characteristic signals of the methylene protons CH_2CH_2O (PEO units) at 3.65 ppm (labeled h in Figure III. 7), of the methyl protons of the $OCH_2CH_2N(CH_3)_2$ (DMAEA units) at 2.27 ppm (labeled o in Figure III. 7) and of the methyl protons $C(=O)OC(CH_3)_3$ (*t*BocAEA units) at 1.44 ppm (labeled r in Figure III. 7). The $\overline{DP_n}$ of P*t*BocAEA has been calculated by comparing the integration area values of the methine protons $CH_3CHC(=O)NH$ at 5.10 ppm (1 proton, labeled e in Figure III. 7) and of the

methylenes protons of $OCH_2CH_2NHC(=O)$ of *t*BocAEA units at 4.16 ppm and of $SCH_2(CH_2)_{10}CH_3$ at 3.35 ppm (26.79 protons, labeled q and s respectively in Figure III. 7). The $\overline{DP_n}$ of P*t*BocAEA is equal to 12. The $\overline{DP_n}$ of PDMAEA has been calculated by comparing the integration area values of the methine protons $CH_3CHC(=O)NH$ at 5.10 ppm (1 proton, labeled e in Figure III. 7) and of the methylene proton $CH_2CH_2OC(=O)$, of the $OCH_2CH_2N(CH_3)_2$ of DMAEA units and of OCH_2CH_2NHC of *t*BocAEA units (48.50 protons, labeled i, m and p respectively in Figure III. 10) The $\overline{DP_n}$ of PDMAEA is equal to 10. Both $\overline{DP_n}$ values are almost equal. This result is consistent with the results observed previously during reactivity ratios assessment.

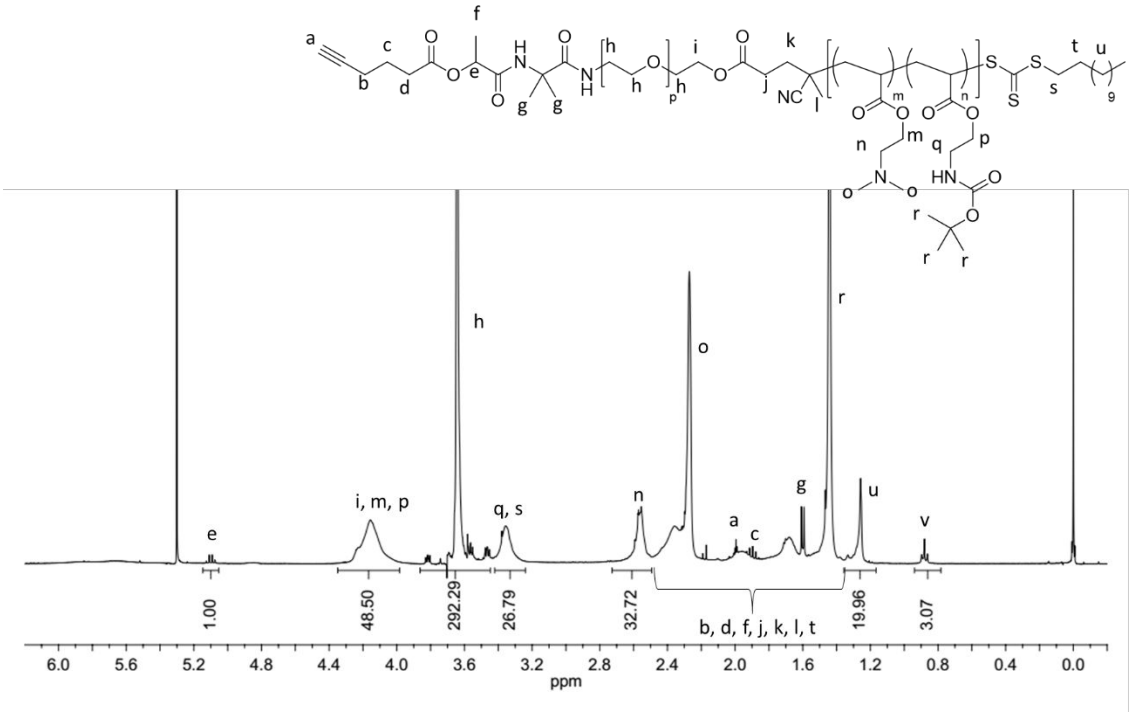

Figure III. 7. ^1H NMR spectrum (400 MHz, $CDCl_3$) of purified aPEO-*b*-P(DMAEA-*co*-*t*BocAEA) synthesized by RAFT copolymerization of DMAEA and *t*BocAEA using aPEO-CTA and ACVA at 70°C as the initiator in 1,4-dioxane and DMF using $[DMAEA]_0/[tBocAEA]_0/[aPEO\text{-}CTA]_0/[ACVA]_0 = 50/50/1/0.2$ (Run 9, Table III. 3).

The SEC was performed in DMF (LiBr 1 $g.L^{-1}$) (Figure III. 8). The overlaid SEC traces of aPEO-CTA and aPEO-*b*-P(DMAEA-*co*-*t*BocAEA) copolymer using RI detection shows a shift of the SEC trace of aPEO-CTA from higher retention times to lower retention times. This result shows the formation of the aPEO-*b*-P(DMAEA-*co*-*t*BocAEA) copolymer and the ability of aPEO-CTA to control the RAFT copolymerization of DMAEA and *t*BocAEA . The SEC trace of the purified copolymer shows a unimodal and narrow chromatogram ($\overline{M_{n,SEC}}$ = 11700 $g.mol^{-1}$ (equivalent PS) and $Đ$ = 1.31). The SEC traces using the UV-vis detection at 309 nm, characteristic wavelength of the trithiocarbonate group, show the covalent linkage of the trithiocarbonate moiety.

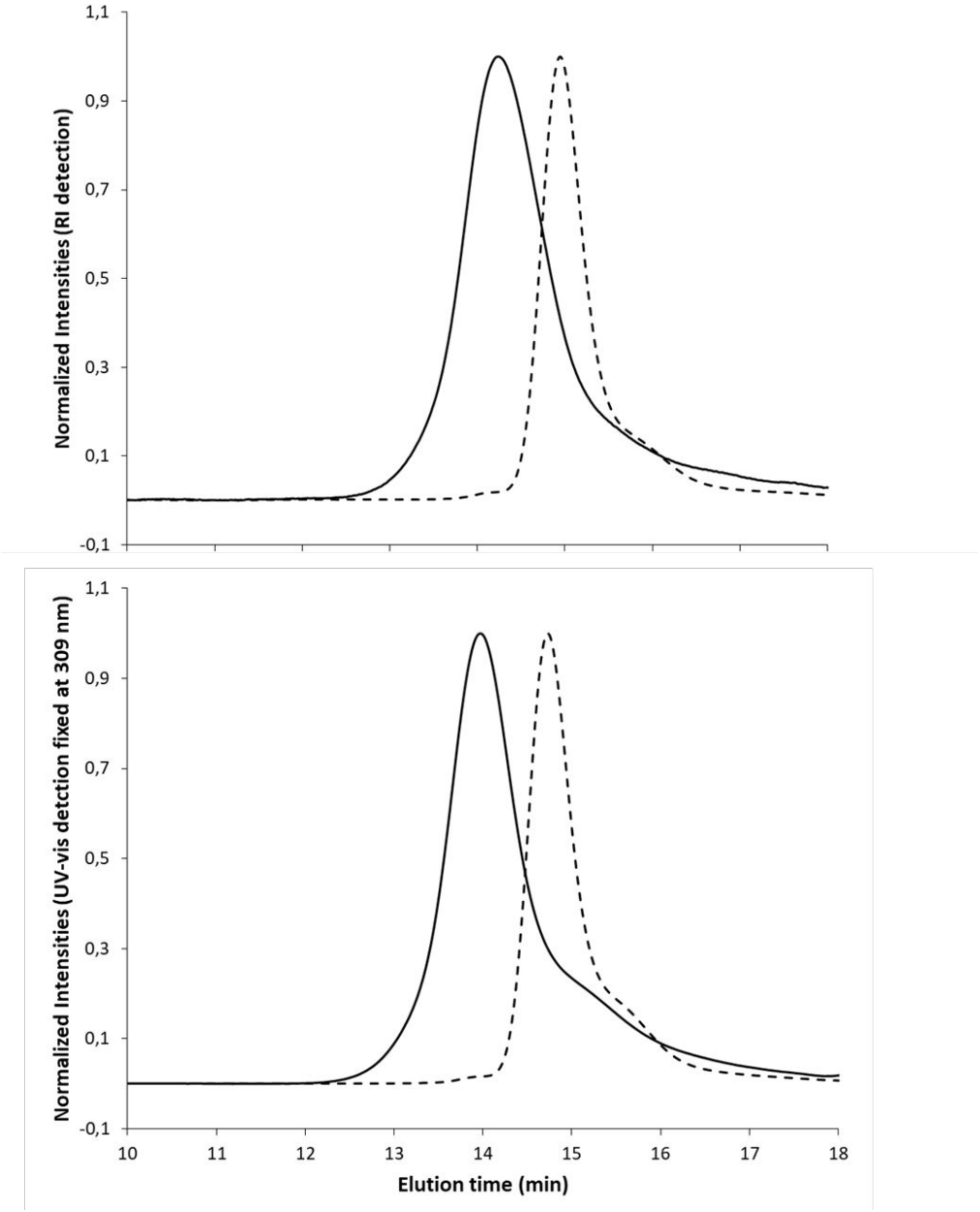

Figure III. 8. Overlaid SEC traces using RI detection (top) and UV-vis detection (fixed at 309 nm, bottom) of aPEO-CTA (dash line) and aPEO-*b*-P(DMAEA-*co*-*t*BocAEA) (solid line) synthesized by RAFT copolymerization of DMAEA and *t*BocAEA using aPEO-CTA as the macromolecular chain transfer agent and ACVA as the initiator at 70°C in 1,4-dioxane and DMF using $[DMAEA]_0/[tBocAEA]_0/[aPEO\text{-}CTA]_0/[ACVA]_0 = 50/50/1/0.2$.

The FT-IR, ^1H NMR spectroscopies and SEC in DMF (LiBr 1 $g.L^{-1}$) showed that the RAFT copolymerization of DMAEA and *t*BocAEA mediated through the α-alkynyl,ω-

dodecyltrithiocarbonate PEO used as the macromolecular chain transfer agent and ACVA used as the initiator allows to target a well-defined aPEO-*b*-P(DMAEA-*b*-*t*BocAEA).

Therefore, similar conditions have been used to synthesize copolymers with different DMAEA/*t*BocAEA molar ratios (Table III. 3).

Table III. 3. Macromolecular characteristics of aPEO-*b*-P(DMAEA-*co*-*t*BocAEA) synthesized by RAFT copolymerization of DMAEA and *t*BocAEA mediated through the aPEO-CTA as the macromolecular chain transfer agent and ACVA as the initiator under argon in 1,4-dioxane and DMF at 70°C using the following ratio: $([DMAEA]_0+[tBocAEA]_0)/[aPEO\text{-}CTA]_0/[ACVA]_0$ = 100/1/0.2.

Run	$[DMAEA]_0$/ $[tBocAEA]_0$	Time (h)	Conv (%) [a]	$\overline{DP_{n,\ PDMAEA}}$ [b]	$\overline{DP_{n,\ PtBocAEA}}$ [b]	$\overline{M_{n,NMR}}$ (g.mol^{-1}) [c]	$\overline{M_{n,SEC}}$ (g.mol^{-1}) [d]	$Đ$ [d]
1	50/50	18	23	11	9	7200	9900	1.48
	70/30	18	38	25	10	9400	11700	1.34
3	30/70	18	16	5	9	6400	11900	1.21
4	70/30	12.5	20	11	4	6100	11300	1.22
5	30/70	19	19	5	10	6600	11500	1.30
6	30/70	14	20	10	20	8700	13700	1.27
7	50/50	18	40	18	15	9500	12000	1.43
8	50/50	17	42	21	23	11500	11700	1.52
9	50/50	5.5	24	10	12	7500	11700	1.31

[a] Total monomers conversion monitored by ^{1}H NMR spectroscopy of the crude product (400 MHz, $CDCl_3$). [b] $\overline{DP_n}$ determined by ^{1}NMR spectroscopy of the purified polymer (400 MHz, $CDCl_3$). [c] $\overline{M_{n,NMR}}$ determined by ^{1}H NMR spectroscopy (400 MHz, $CDCl_3$) using the $\overline{DP_n}$ previously calculated, $\overline{M_{n,NMR}} = \overline{DP}_{n,PDMAEA} \times M_{DMAEA} + \overline{DP}_{n,tBocAEA} \times M_{tBocAEA} + \overline{M_{n,aPEO\text{-}CTA}}$

with $\overline{M_{n,aPEO\text{-}CTA}}$ = 3500 g.mol^{-1}, M_{DMAEA} = 143.2 g.mol^{-1} and $M_{tBocAEA}$ = 215.2 g.mol^{-1}. [d] Determined by SEC in DMF (LiBr 1 g.L^{-1}) using PS standards.

C. RAFT copolymerization of DMAEA and *t*BocAEA using PPEGA-CTA

In order to be able to study the influence of the PEO architecture and the DMAEA/AEA molar ratio onto pDNA complexation and onto resulting polyplexes cytotoxicity, different PPEGA-*b*-P(DMAEA-*b*-*t*BocAEA) are targeted. A first RAFT copolymerization of DMAEA and *t*BocAEA have been performed using the PPEGA-CTA (Chapter 2 §II-B-3) of $\overline{M_{n,SEC}}$ = 14700 g.mol^{-1} and $Đ$ = 1.26 as the macromolecular chain transfer agent and ACVA as the initiator at 70°C in 1,4-dioxane and DMF during 27 hours using the following initial molar ratio: $[DMAEA]_0/[t\text{BocAEA}]_0/[\text{PPEGA-CTA}]_0/[ACVA]_0$ = 50/50/1/0.2 (Scheme III. 3). The total monomers conversion has been determined by ^{1}H NMR spectroscopy (Figure III. 9) by comparing the integration values of the alkene protons signals between 6.52 and 5.79 ppm (labeled b, c, d, e, f and g in Figure III. 9) at t_0 and at t_f using the methine HC(=O)NH(CH$_3$)$_2$ signal of DMF at 8.02 ppm as the reference (labeled a in Figure III. 9). The calculated conversion is equal to 20 %. The product has been purified by several precipitation and decantation in cold hexane/diethyl ether mixture (90/10, v/v). The purified copolymer was analyzed by ^{1}H NMR spectroscopy and SEC in DMF (LiBr 1 g.L^{-1}).

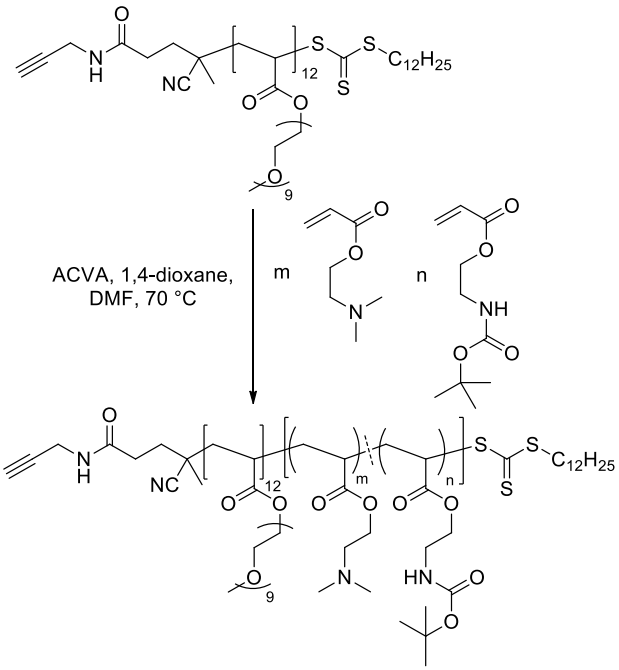

Scheme III. 3. RAFT copolymerization of *t*BocAEA and DMAEA mediated through ACVA used as the initiator and α-alkynyl,ω-dodecyltrithiocarbonate PPEGA (PPEGA-CTA) used as the macromolecular chain transfer agent in 1,4-dioxane and DMF at 70°C ($[t\text{BocAEA}]_0+[\text{DMAEA}]_0)/[\text{PPEGA-CTA}]_0/[\text{ACVA}]_0 = 100/1/0.2$.

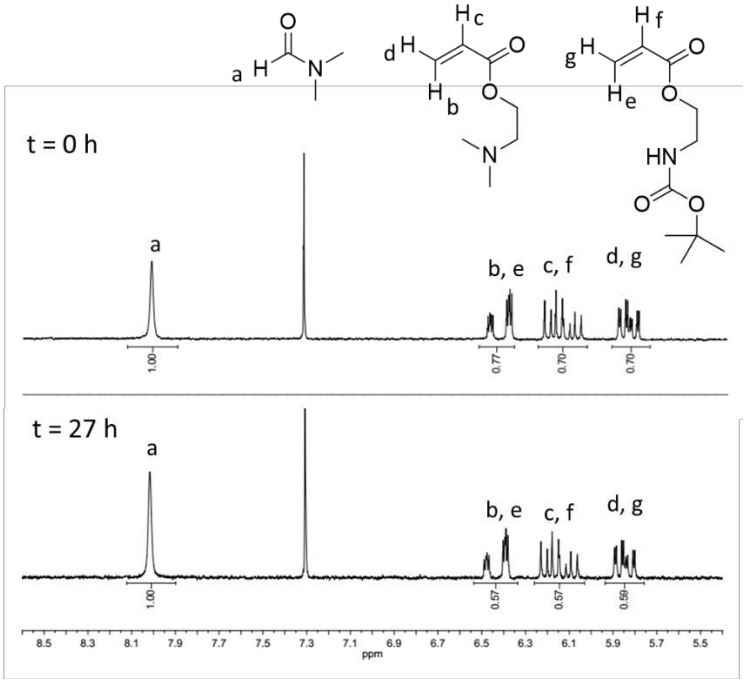

Figure III. 9. Overlaid ^{1}H NMR spectra (400 MHz, $CDCl_3$) between 5.4 and 8.6 ppm of the crude mixture of RAFT copolymerization of DMAEA and *t*BocAEA using PPEGA-CTA as the macromolecular chain transfer agent and ACVA as the initiator in 1,4-dioxane and DMF at 70°C using $[DMAEA]_0/[tBocAEA]_0/[PPEGA\text{-}CTA]_0/[ACVA]_0$ = 50/50/1/0.2 (Run 1, Table III. 4).

The ^{1}H NMR spectrum (Figure III. 10) shows the characteristic signals of the methylene protons C*H*$_2$C*H*$_2$O (PEGA units) at 3.65 ppm (labeled g in Figure III. 10), of the methyl protons of the $OCH_2CH_2N(CH_3)_2$ (DMAEA units) at 2.27 ppm (labeled k in Figure III. 10) and of the methyl protons NHC(=O)OC(C*H*$_3$)$_3$ (*t*BocAEA units) at 1.44 ppm (labeled n in Figure III. 10). The $\overline{DP_n}$ of P*t*BocAEA has been calculated by comparing the integration area values of the of the methylene protons C*H*$_2$C*H*$_2$O of PEGA repeating unit at 3.65 ppm (432.00 protons, labeled g in Figure III. 10) and of the methyl protons $(CH_2CH_2O)_9CH_3$ of PEGA units and methylene protons of OCH_2CH_2NH of *t*BocAEA units and of $SCH_2(CH_2)_{10}CH_3$ at 3.38 ppm (59.19 protons, labeled h, m and o in Figure III. 10). The $\overline{DP_n}$ of P*t*BocAEA is equal to 10. The $\overline{DP_n}$ of PDMAEA has been calculated by comparing the integration area values of the methylene

protons C*H*$_2$C*H*$_2$O of EO repeating unit at 3.65 ppm (432.00 protons, labeled g in Figure III. 10) and of the methylene protons of the *H*C≡CC*H*$_2$NH of the alkyne moiety, of the OC*H*$_2$CH$_2$O(CH$_2$CH$_2$O)$_8$ of PEGA units, of the OC*H*$_2$CH$_2$N(CH$_3$)$_2$ of DMAEA units, of the OC*H*$_2$CH$_2$NHC(=O) of *t*BocAEA units at 4.16 ppm (65.25 protons, labeled b, f, i and l in Figure III. 10) The $\overline{DP_n}$ of PDMAEA is equal to 9.

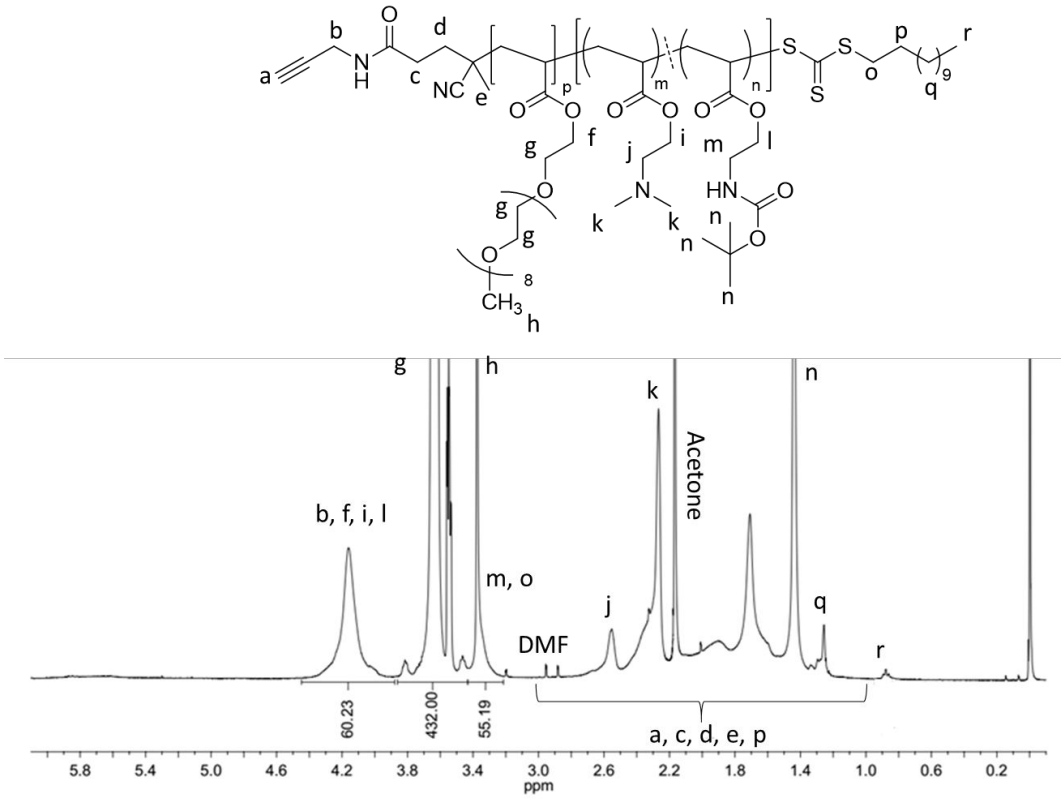

Figure III. 10. ^{1}H NMR spectrum (400 MHz, $CDCl_3$) of PPEGA-*b*-P(DMAEA-*co*-*t*BocAEA) synthesized by RAFT copolymerization of DMAEA and *t*BocAEA using PPEGA-CTA as the macromolecular chain transfer agent and ACVA as the initiator in 1,4-dioxane and DMF at 70°C with $[DMAEA]_0/[tBocAEA]_0/[PPEGA\text{-}CTA]_0/[ACVA]_0 = 50/50/1/0.2$ (Run 1, Table III. 4).

The SEC was performed in DMF (LiBr 1 g.L^{-1}) (Figure III. 11). The overlaid SEC traces of PPEGA-CTA and PPEGA-*b*-P(DMAEA-*co*-*t*BocAEA) copolymer using RI detection shows an insignificant shift of the SEC trace of PPEGA-CTA from higher retention times to lower

retention times. This result could be explained by a relative broad molar masses distribution of PPEGA-CTA ($Đ$ = 1.26). The SEC trace of the purified copolymer allowed to determine $\overline{M_{n,SEC}}$ = 11200 g.mol^{-1} (equivalent PS) and $Đ$ = 1.57. The SEC traces using the UV-vis detection at 309 nm, characteristic wavelength of the trithiocarbonate group, show the covalent linkage of the trithiocarbonate moiety.

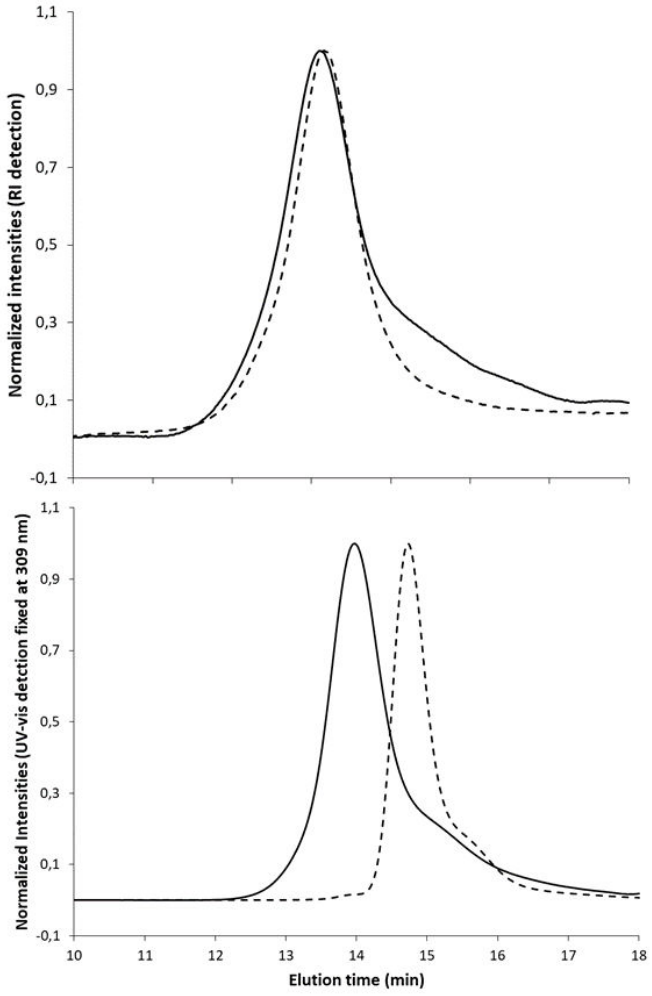

Figure III. 11. Overlaid of SEC traces using RI detection (top) and UV-vis detection (fixed at 309 nm, bottom) of PPEGA-CTA (dash line) and PPEGA-*b*-P(DMAEA-*co*-*t*BocAEA) (solid line) synthesized by RAFT copolymerization of DMAEA and *t*BocAEA using PPEGA-CTA as the macromolecular chain transfer agent and ACVA as the initiator in 1,4-dioxane and DMF at 70°C with $[DMAEA]_0/[tBocAEA]_0/[PPEGA\text{-}CTA]_0/[ACVA]_0$ = 50/50/1/0.2 (Run 1, Table III. 4).

The ^{1}H NMR spectroscopy and SEC in DMF (LiBr 1 g.L^{-1}) showed that the RAFT copolymerization of DMAEA and *t*BocAEA mediated through the α-alkynyl,ω-dodecyltrithiocarbonate PPEGA as the macromolecular chain transfer agent and ACVA as the initiator allows to target a PPEGA-*b*-P(DMAEA-*b*-*t*BocAEA) copolymers.

Therefore, similar conditions have been used to synthesize copolymers by RAFT polymerization using different DMAEA/*t*BocAEA molar ratios (Table III. 4).

Table III. 4. Macromolecular characteristics of PPEGA-*b*-P(DMAEA-*co*-*t*BocAEA) copolymers synthesized by RAFT copolymerization of DMAEA and *t*BocAEA using α-alkynyl,ω-dodecyltrithiocarbonate PPEGA (PPEGA-CTA) as the macromolecular chain transfer agent and ACVA as the initiator in 1,4-dioxane and DMF at 70°C.

Run	$[DMAEA]_0$/ $[t\text{BocAEA}]_0$	Time (h)	Conv (%)[a]	$\overline{DP_n}$ $_{PDMAEA}$[b]	$\overline{DP_n}$, $_{PtBocAEA}$[b]	$\overline{M_{n,NMR}}$ (g.mol^{-1})[c]	$\overline{M_{n,SEC}}$ (g.mol^{-1})[d]	$Đ$[d]
1	50/50	27	20	9	10	10100	11200	1.57
2	18/42	16	46	7	14	10700	9700	1.62
3	70/30	2	27	13	8	10300	10900	1.58

[a] Total monomers conversion monitored by ^{1}H NMR spectroscopy of the crude product (400 MHz, $CDCl_3$). [b] $\overline{DP_n}$ determined by ^{1}NMR spectroscopy of the purified polymer (400 MHz, $CDCl_3$). [c] $\overline{M_{n,NMR}}$ determined by ^{1}H NMR spectroscopy (400 MHz, $CDCl_3$) using the $\overline{DP_n}$ previously calculated, $\overline{M_{n,NMR}} = \overline{DP}_{n,PDMAEA} \times M_{DMAEA} + \overline{DP}_{n,PtBocAEA} \times M_{tBocAEA} + \overline{M_{n,PPEGA}}$.with $\overline{M_{n,PPEGA\text{-}CTA}}$ = 6700 g.mol^{-1}, M_{DMAEA} = 143.2 g.mol^{-1} and $M_{tBocAEA}$ = 215.2 g.mol^{-1}. [d] Determined by SEC in DMF (LiBr 1 g.L^{-1}) using PS standards.

In order to be able to study the influence of PEGylation of cationic P(DMAEA-*co*-*t*BocAEA) copolymers using lPEO and bPEO on pDNA complexation and onto resulting

polyplexes cytotoxicity, different cationic P(DMAEA-*co*-AEA) copolymers without PEO moiety were targeted.

D. RAFT copolymerization of DMAEA and *t*BocAEA using COPYDC

A first, P(DMAEA-*co*-*t*BocAEA) has been synthesized by RAFT copolymerization of DMAEA and *t*BocAEA mediated through COPYDC used as the chain transfer agent and ACVA used as the initiator in DMF at 70°C during 21 hours (Scheme III. 4) using the following initial molar ratio: $[DMAEA]_0/[tBocAEA]_0/[COPYDC]_0/[ACVA]_0$ = 50/50/1/0.2. The total monomers conversion has been determined by ^{1}H NMR spectroscopy (Figure III. 12) by comparing the integration values of the alkene protons signals between 6.52 and 5.79 ppm (labeled b, c, d, e, f and g in Figure III. 12) at t_0 and at t_f using the methine $HC(=O)NH(CH_3)_2$ signal of DMF at 8.02 ppm as the reference (labeled a in Figure III. 12). The calculated conversion is equal to 19 %. The product was purified by precipitation and decantation in diethyl ether/hexane mixture (10/90, v/v) and dried under vacuum. The purified polymer has been analyzed by ^{1}H NMR spectroscopy and SEC in DMF (LiBr 1 g.L^{-1}).

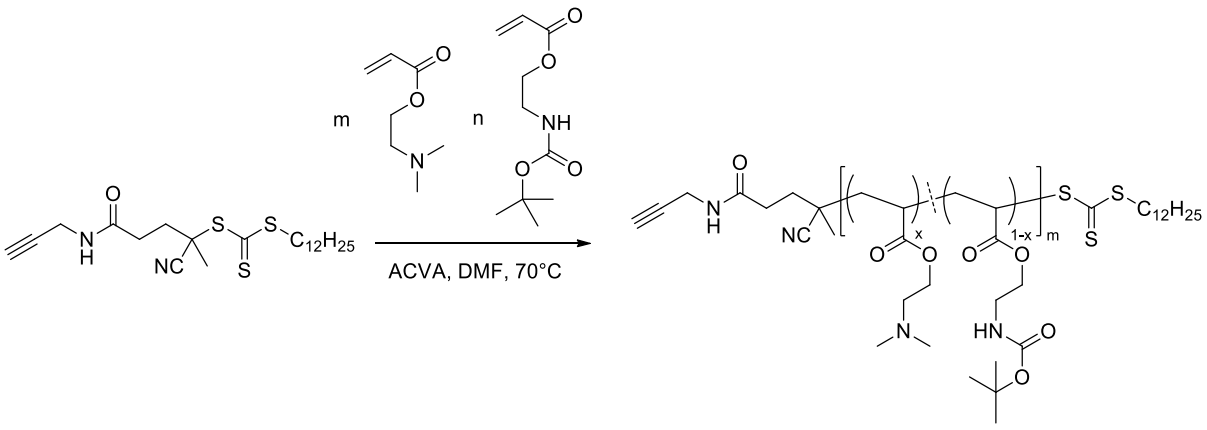

Scheme III. 4. RAFT copolymerization of DMAEA and *t*BocAEA mediated through COPYDC used as the chain transfer agent and ACVA used as the initiator in DMF at 70°C. $([DMAEA]_{0+}[tBocAEA]_0)/[COPYDC]_0/[ACVA]_0$ = 100/1/0.2.

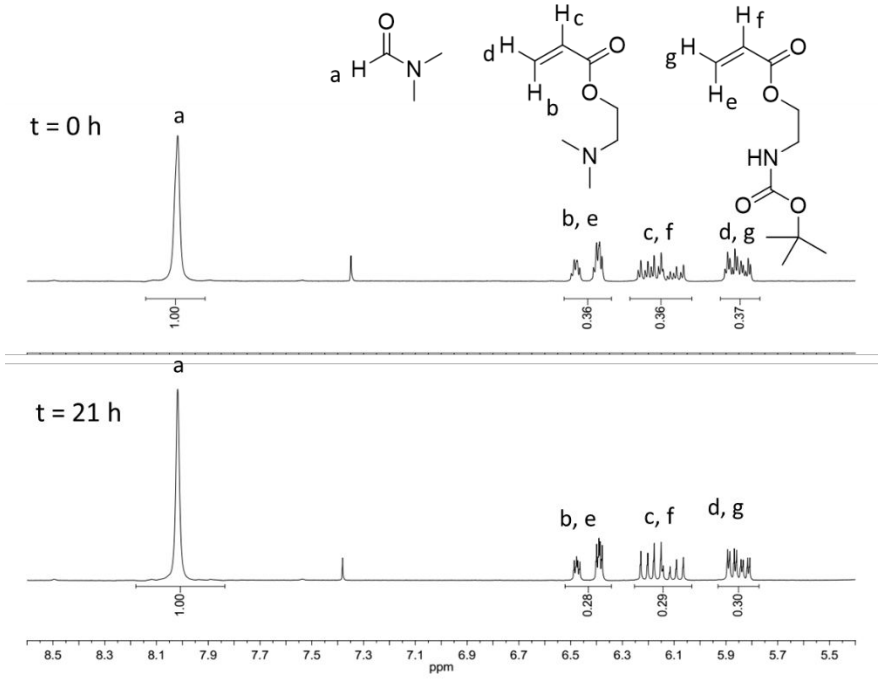

Figure III. 12. Overlaid of ^{1}H NMR spectra (400 MHz, $CDCl_3$) between 5.4 and 8.6 ppm of the crude mixture of RAFT copolymerization of DMAEA and *t*BocAEA using COPYDC as the chain transfer agent and ACVA as the initiator in 1,4-dioxane and DMF at 70°C using $[DMAEA]_0/[tBocAEA]_0/[COPYDC]_0/[ACVA]_0$ = 50/50/1/0.2 (Table III. 5, run 3).

The ^{1}H NMR spectrum (Figure III. 13) shows the characteristic signals of chain-ends: a singlet at 2.01 ppm of the methine proton $HC{\equiv}CCH_2NH$ (labeled a in Figure III. 13) and the triplet at 0.88 ppm of the methyl protons $SCH_2(CH_2)_{10}CH_3$ (labeled q in Figure III. 13). The signal at 2.27 ppm is characteristic of the methyl protons $OCH_2CH_2N(CH_3)_2$ of DMAEA repeating units (labeled i in Figure III. 13) and the signal at 1.44 ppm is characteristic of the $C(=O)OC(CH_3)_3$ of the *t*BocAEA repeating units (labeled m in Figure III. 13). The $\overline{DP}_n$ of P*t*BocAEA has been calculated by comparing the integration areas values of the methyl protons $SCH_2(CH_2)_{10}CH_3$ of the dodecyl chain-end at 0.88 ppm (3 protons, labeled q in Figure III. 13) and of the methylene protons at 3.36 ppm corresponding to OCH_2CH_2NH of *t*BocAEA repeating units and to the $SCH_2(CH_2)_{10}CH_3$ of the dodecyltrithiocarbonate moiety (26.91 protons, labeled k and n in Figure III. 13). The $\overline{DP}_n$ of *t*BocAEA is equal to 13. The $\overline{DP}_n$ of

PDMAEA has been calculated by comparing the integration areas values of the methyl protons $SCH_2(CH_2)_{10}CH_3$ of the dodecyl chain-end at 0.88 ppm (3 protons, labeled q in Figure III. 13) and the integration areas values of the methylene protons at 4.15 ppm corresponding to the methylene protons to $HC{\equiv}CCH_2NH$ of the α-chain-end, of the $OCH_2CH_2N(CH_3)_2$ of DMAEA units, and to the OCH_2CH_2NH of *t*BocAEA repeating units (45.37 protons, labeled b, g and j in Figure III. 13). The $\overline{DP}_n$ of DMAEA is equal to 9.

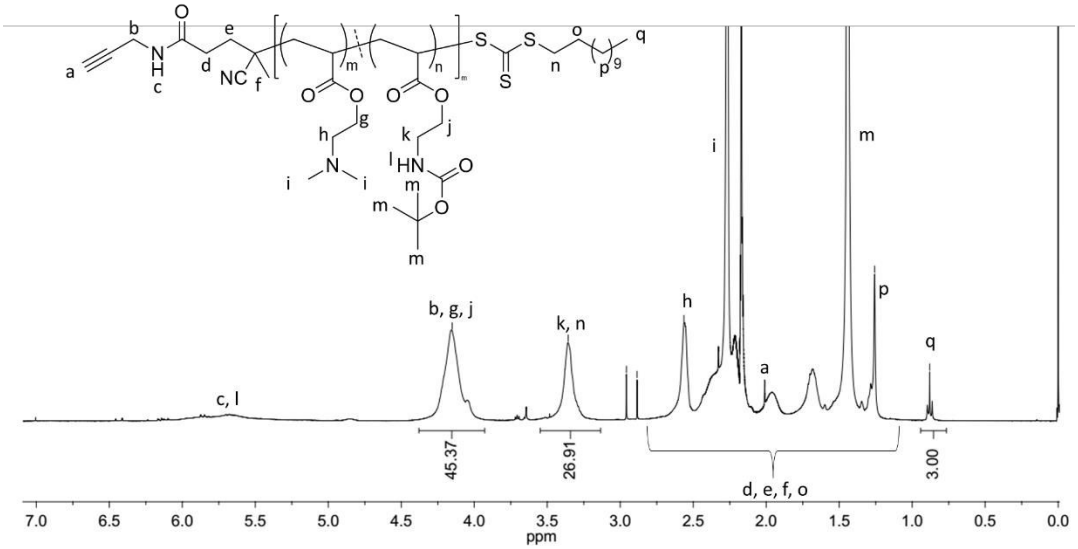

Figure III. 13. ^{1}H NMR spectrum (400 MHz, $CDCl_3$) of purified P(DMAEA-*co*-*t*BocAEA) synthesized by RAFT copolymerization of DMAEA and *t*BocAEA mediated through COPYDC as the chain transfer agent and ACVA as the initiator in DMF at 70°C using $[DMAEA]_0/[tBocAEA]_0/[COPYDC]_0/[ACVA]_0$ = 50/50/1/0.2 (Run 3, Table III. 5).

The SEC in DMF (LiBr 1 g.L^{-1}) using the RI detection shows a unimodal trace with a $\overline{M_{n,SEC}}$ = 5200 g.mol^{-1} (PS equivalents) and $Đ$ = 1.50 (Figure III. 14). The trace obtained with a UV-vis detector fixed at 309 nm (characteristic wavelength of the trithiocarbonate group) shows that the polymer absorbs at this wavelength. The shape of both SEC traces obtained with RI detection and UV-vis detection is not a Gaussian. Such behavior is probably due to the interactions of amine groups of the copolymer with SEC columns. This phenomenon, well-

known with aminoethyl acrylate-based polymers was attenuated when a PEO or a PPEGA was covalently linked to the aminoethyl acrylate-based copolymers.[27,28]

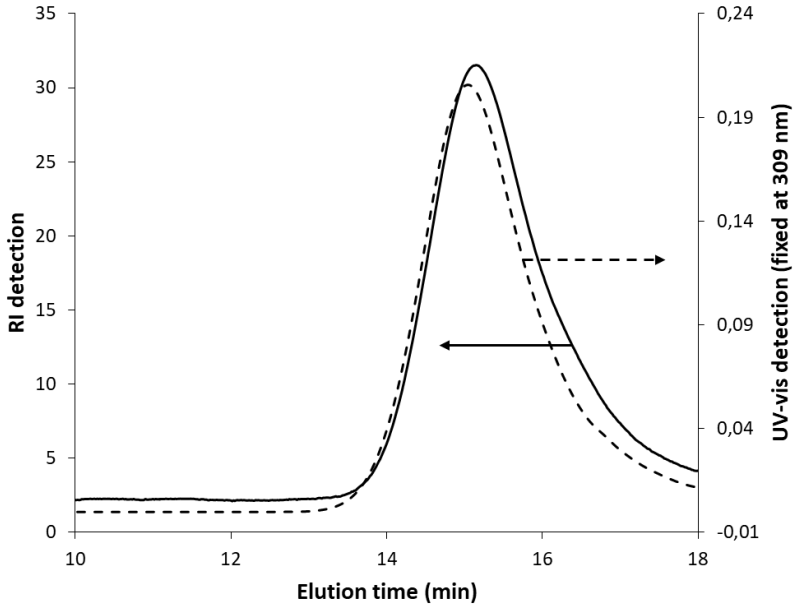

Figure III. 14. Overlaid SEC traces of purified P(DMAEA-*co*-*t*BocAEA) (solid line: RI response, dash line: UV-vis response at 309 nm) obtained by RAFT copolymerization of DMAEA and *t*BocAEA using COPYDC as the chain transfer agent and ACVA as the initiator in DMF at 70°C. $[DMAEA]_0/[tBocAEA]_0/[COPYDC]_0/[ACVA]_0 = 50/50/1/0.2$ (Run 3, Table III. 5).

The ^1H NMR spectroscopy and the SEC in DMF (LiBr 1 $g.L^{-1}$) showed the efficiency of the RAFT copolymerization of DMAEA and *t*BocAEA to target a well-defined P(DMAEA-*co*-*t*BocAEA) copolymers. The experimental conditions previously used for RAFT copolymerizations have been employed to synthesize several copolymers with different DMAEA/*t*BocAEA molar ratios (Table III. 5).

Table III. 5. Macromolecular characteristics of P(DMAEA-*co*-*t*BocAEA) synthesized by RAFT copolymerization of DMAEA and *t*BocAEA mediated through the COPYDC used as the chain transfer agent and ACVA used as the initiator in DMF at 70°C.

Run	$[DMAEA]_0/[tBocAEA]_0$	Time (h)	Conv (%) [a]	$\overline{DP_{n,PDMAEA}}$ [b]	$\overline{DP_{n,PtBocAEA}}$ [b]	$\overline{M_{n,NMR}}$ ($g.mol^{-1}$) [c]	$\overline{M_{n,SEC}}$ ($g.mol^{-1}$) [d]	$Đ$ [d]
1	70/30	4	26	10	4	7200	4300	1.20
2	18/42	38	19	4	14	9400	4200	1.23
3	50/50	21	19	9	13	6400	5200	1.50

[a] Total monomers conversion monitored by ^{1}H NMR spectroscopy of the crude product (400 MHz, $CDCl_3$). [b] $\overline{DP_n}$ determined by ^{1}NMR spectroscopy of the purified polymer (400 MHz, $CDCl_3$). [c] $\overline{M_{n,NMR}}$ determined by ^{1}H NMR spectroscopy (400 MHz, $CDCl_3$) using the $\overline{DP_n}$ previously calculated $\overline{M_{n,NMR}} = \overline{DP}_{n,PDMAEA} \times M_{DMAEA} + \overline{DP}_{n,PtBocAEA} \times M_{tBocAEA} + M_{COPYDC}$ with M_{COPYDC} = 440 $g.mol^{-1}$, M_{DMAEA} = 143.2 $g.mol^{-1}$ and $M_{tBocAEA}$ = 215.2 $g.mol^{-1}$. [d] Determined by SEC in DMF (LiBr 1 $g.L^{-1}$) using PS standards.

RAFT copolymerizations of DMAEA and *t*BocAEA using ACVA as the initiator and aPEO-CTA, PPEGA-CTA and COPYDC as the (macromolecular) chain transfer agents has led to well-defined aPEO-*b*-P(DMAEA-*co*-*t*BocAEA), PPEGA-*b*-P(DMAEA-*co*-*t*BocAEA) and P(DMAEA-*co*-*t*BocAEA), respectively. To target corresponding cationic copolymers able to complex pDNA, the amine deprotection of the *t*BocAEA repeating units is performed.

II. Amine deprotection of *t*BocAEA repeating units of aPEO-*b*-P(DMAEA-*co*-*t*BocAEA), PPEGA-*b*-P(DMAEA-*co*-*t*BocAEA) and P(DMAEA-*co*-*t*BocAEA)

*t*BocAEA units have been deprotected under acidic conditions to form aminoethyl acrylate (AEA) units. The deprotection of primary amines using trifluoroacetic acid (TFA) and CH_2Cl_2 has been widely used in peptide chemistry and organic chemistry.[29] Maynard and co-workers showed the efficiency of TFA in CH_2Cl_2 to deprotect a primary amine on the α-position of a PEO-*b*-Poly(oligo(ethylene glycol)methacrylate) (PPEGMA) and PEO-*b*-Poly((hydroxyethyl)methacrylate) (PHEMA) synthesized by ATRP and of a poly(*N*-isopropylacrylamide) PNIPAM synthesized by RAFT polymerization.[30,31] Moreover, our group showed the efficiency of TFA to deprotect *t*BocAEA.[17]

Same procedure is used to deprotect the amine of *t*BocAEA repeating units of aPEO-*b*-P(DMAEA-*co*-*t*BocAEA) copolymers, several PPEGA-*b*-P(DMAEA-*co*-*t*BocAEA) copolymers and several P(DMAEA-*co*-*t*BocAEA) copolymers in order to target corresponding cationic aPEO-*b*-P(DMAEA-*co*-AEA) copolymers, PPEGA-*b*-P(DMAEA-*co*-AEA) copolymers and P(DMAEA-*co*-AEA) copolymers, respectively.

Reactions are performed in CH_2Cl_2 at a concentration of copolymer equal to 50 $g.L^{-1}$ with 200 equivalents of TFA at room temperature during 5 hours (Scheme III.5). Copolymers were purified by several decantation and precipitation in cold diethyl ether/hexane mixture (50/50, v/v) and dried under vacuum. The purified copolymers were analyzed by FT-IR and ^1H NMR spectroscopies. Fully characterizations of aPEO-*b*-P(DMAEA-*co*-AEA), PPEGA-*b*-P(DMAEA-*co*-AEA) and P(DMAEA-*co*-AEA) are reported on following paragraphs A, B and C, respectively.

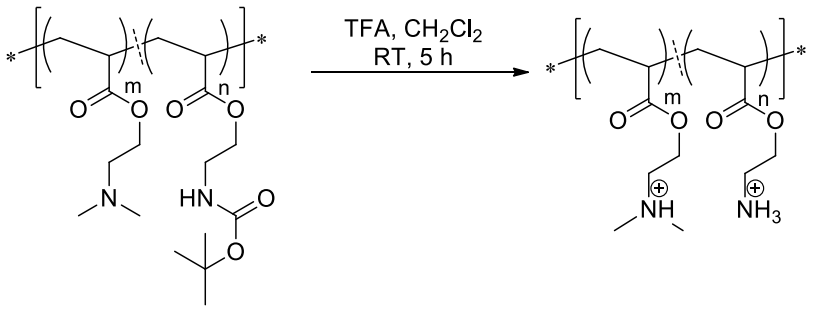

Scheme III. 5. Amine deprotection of *t*BocAEA repeating units mediated through TFA in CH_2Cl_2 at room temperature for 5 h.

A. Characterization of a cationic aPEO-*b*-P(DMAEA-*co*-AEA) copolymer

An aPEO-*b*-P(DMAEA-*co*-*t*BocAEA) with a $\overline{DP}_{n,PEO}$ = 64, $\overline{DP}_{n,PtBocAEA}$ = 4 and $\overline{DP}_{n,PDMAEA}$ = 11 (named $aPEO_{64}$-*b*-P($DMAEA_{11}$-*co*-*t*$BocAEA_9$), Run 1, Table III. 3) has been first analyzed by FT-IR spectroscopy (Figure III. 15) after *t*Boc deprotection under acidic media. Overlaid of FT-IR spectra of the $aPEO_{64}$-*b*-P($DMAEA_{11}$-*co*-*t*$BocAEA_4$) before and after deprotection shows the disappearance of the N-H amid bending band at 1518 cm^{-1} and the appearance of the amine N-H stretching band at 3400 cm^{-1}. This result shows the deprotection of the *t*BocAEA repeating units.

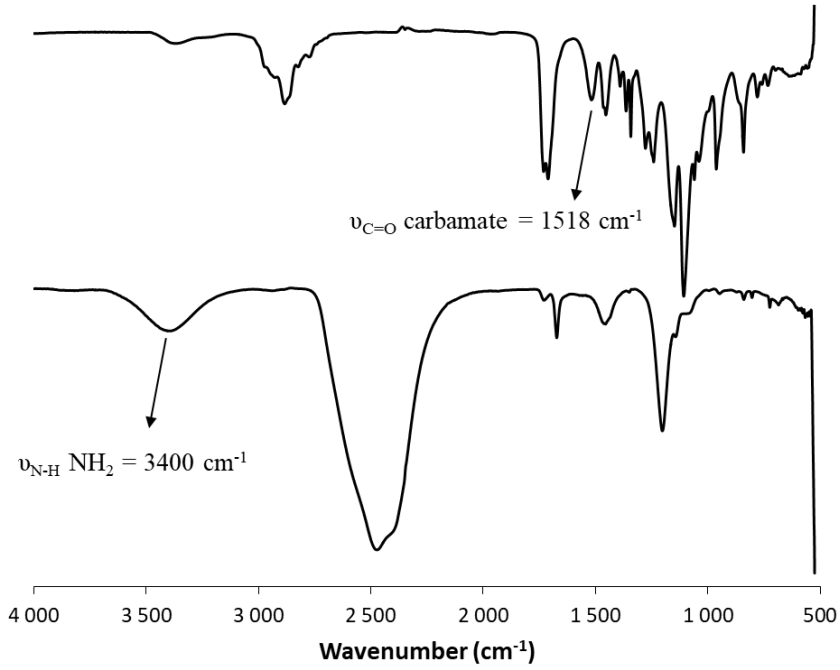

Figure III. 15. Overlaid of FT-IR spectra of aPEO$_{64}$-*b*-P(DMAEA$_{11}$-*co*-*t*BocAEA$_4$) (top) and aPEO$_{64}$-*b*-P(DMAEA$_{11}$-*co*-AEA$_4$) (bottom).

The deprotection of *t*BocAEA units in acidic medium has been investigated by ^{1}H NMR spectroscopy in dimethyl sulfoxyde (DMSO) d_6 (Figure III. 16). The overlaid ^{1}H NMR spectra of aPEO$_{64}$-*b*-(DMAEA$_{11}$-*co*-*t*BocAEA$_4$) and an aPEO$_{64}$-*b*-P(DMAEA$_{11}$-*co*-AEA$_4$) shows the disappearance of the signal at 1.37 ppm of the methyl protons C(=O)OC(C*H*$_3$)$_3$ of the *t*Boc group (labeled q in Figure III. 16). Moreover, the shift of the signal of methylene OCH$_2$C*H*$_2$N$^+$H(CH$_3$)$_2$ of DMAEA units, from 2.16 to 3.40 ppm (labeled m in Figure III. 16) and the shift of the signal of the methyl protons OCH$_2$CH$_2$N$^+$H(C*H*$_3$)$_2$ of DMAEA units, from 2.56 to 2.85 ppm (labeled n in Figure III. 16) prove the cationization of DMAEA units.

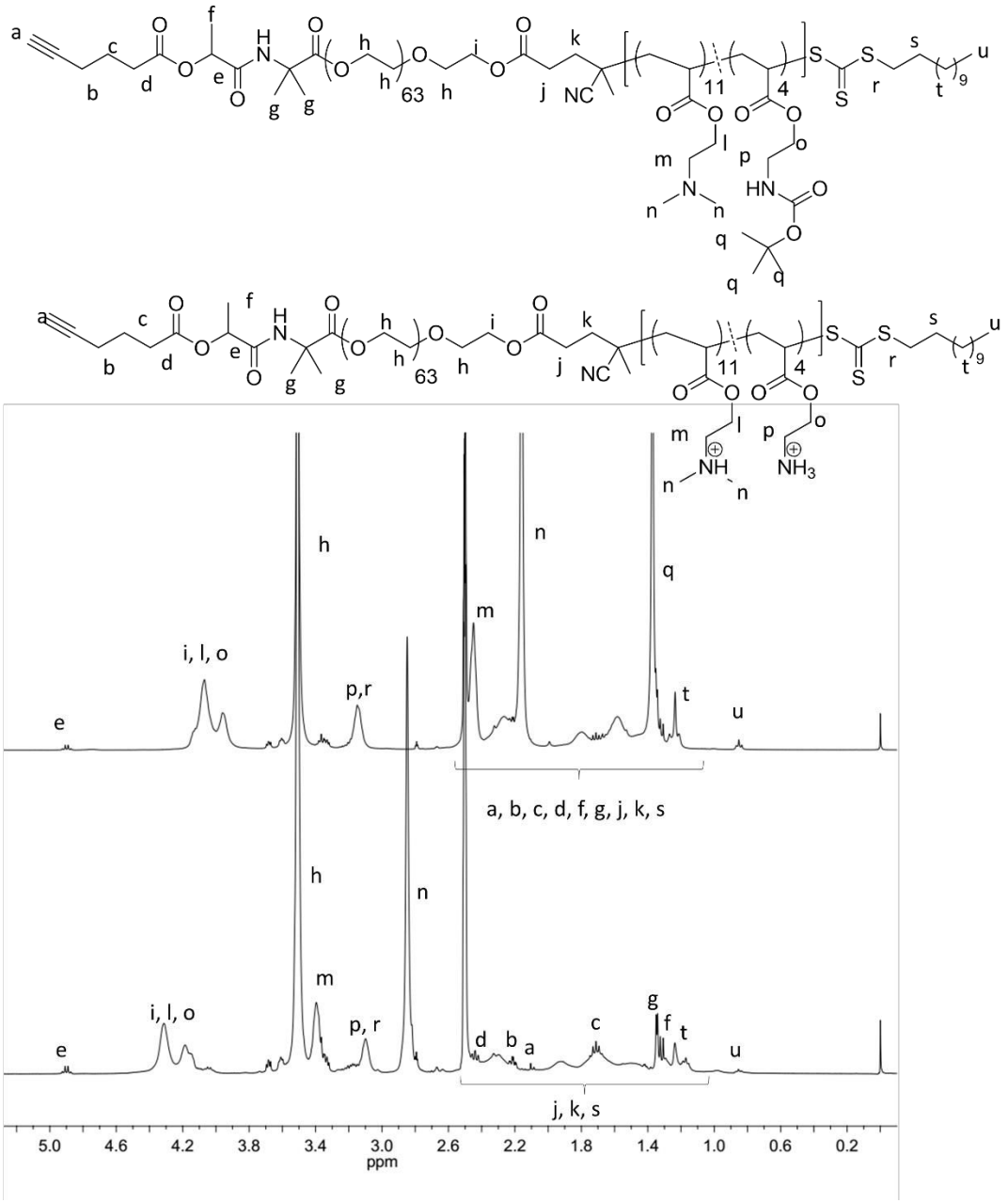

Figure III. 16. Overlaid of ^{1}H NMR spectra (400 MHz, DMSO d_6) of aPEO$_{64}$-*b*-P(DMAEA$_{11}$-*co*-*t*BocAEA$_4$) (top) and aPEO$_{64}$-*b*-P(DMAEA$_{11}$-*co*-AEA$_4$) (bottom).

^{1}H NMR spectra for aPEO$_{64}$-*b*-P(DMAEA$_{11}$-*co*-*t*BocAEA$_4$) and for an aPEO-*b*-P(DMAEA-*co*-AEA) have been both done in $CDCl_3$ and D_2O (Figure III. 17). The ^{1}H NMR spectra show the same result than with deuterated DMSO. The following ^{1}H NMR studies have been made by dissolving the copolymer before amine deprotection in $CDCl_3$ and after deprotection in D_2O.

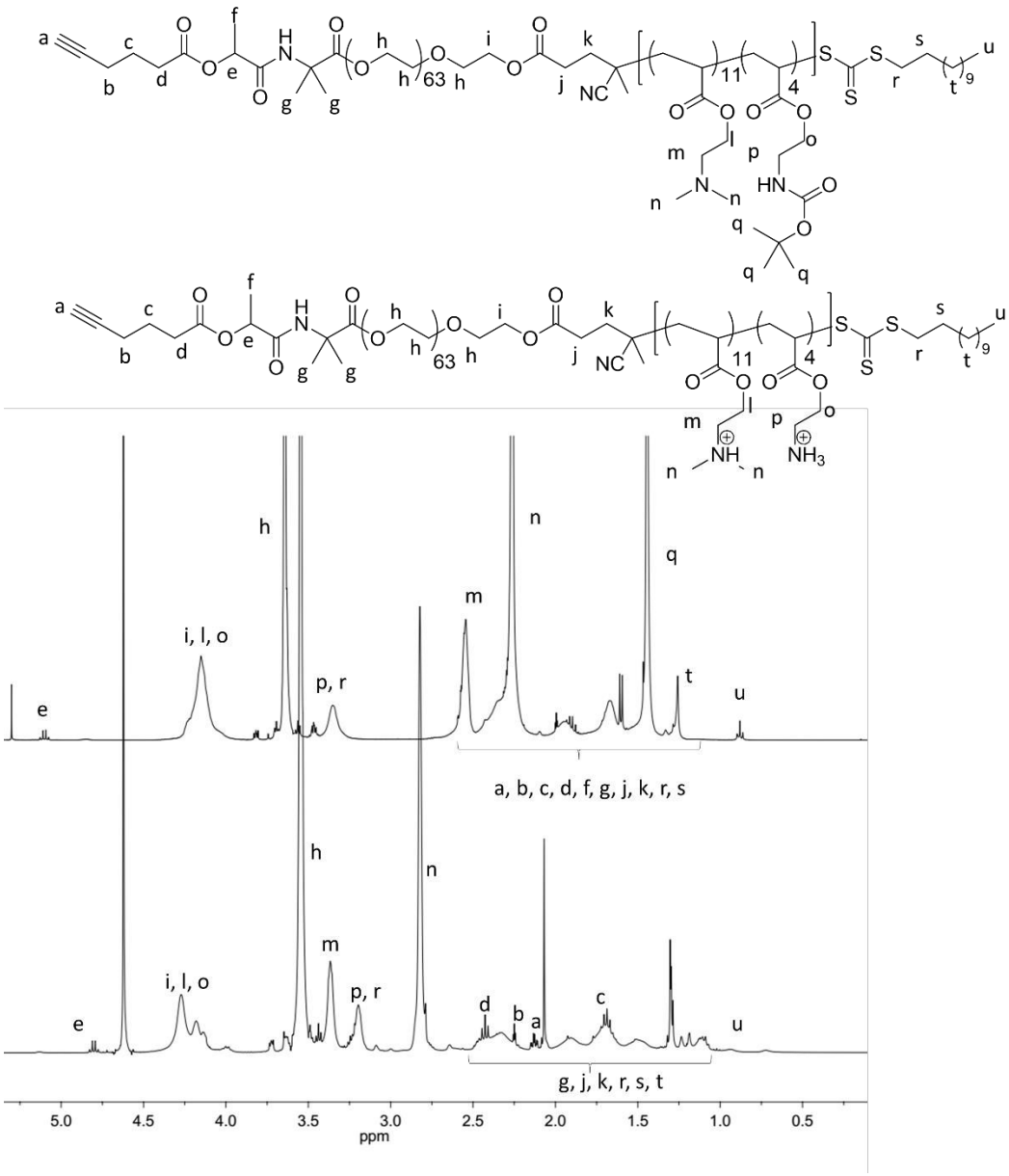

Figure III. 17. Overlaid of ^{1}H NMR spectra (400 MHz) of aPEO$_{64}$-*b*-P(DMAEA$_{11}$-*co*-*t*BocAEA$_{9}$) in $CDCl_3$ (top) and aPEO$_{64}$-*b*-P(DMAEA$_{11}$-*co*-AEA$_{9}$) in D_2O (bottom).

The FT-IR and the ^{1}H NMR analyses showed that the primary amine of deprotection and cationization of aPEO-*b*-P(DMAEA-*co*-*t*BocAEA) mediated through TFA is successful. Same primary amine deprotection has been performed on aPEO-*b*-P(DMAEA-*co*-*t*BocAEA) copolymers with different DMAEA/*t*BocAEA molar ratios.

B. Characterization of a cationic PPEGA-*b*-P(DMAEA-*co*-AEA) copolymer

A PPEGA-*b*-P(DMAEA-*co*-*t*BocAEA) with $\overline{DP}_{n,NMR}$ of PPEGA, PDMAEA and P*t*BocAEA equal to 12, 7 and 14 respectively (named $PPEGA_{12}$-*b*-P($DMAEA_7$-*co*-*t*$BocAEA_{14}$), Run 2, Table III. 4) has been analyzed by ^{1}H NMR spectroscopy after *t*Boc deprotection and cationization in acidic medium (Figure III. 18).

The overlaid ^{1}H NMR spectra of $PPEGA_{12}$-*b*-($DMAEA_7$-*co*-*t*$BocAEA_{14}$) and a $PPEGA_{12}$-*b*-P($DMAEA_7$-*co*-AEA_{14}) before and after deprotection shows the disappearance of the signal at 1.44 ppm of the methyl protons NHC(=O)OC(CH_3)$_3$ of the *t*Boc group (labeled n in Figure III. 18). Moreover, the shift of the signal of methylene $OCH_2CH_2N^+H(CH_3)_2$ of DMAEA units, from 2.56 to 3.43 ppm (labeled j in Figure III. 18) and the shift of the signal of the methyl protons $OCH_2CH_2N^+H(CH_3)_2$ of DMAEA, from 2.27 to 2.88 ppm (labeled k in Figure III. 15) demonstrate the cationization of DMAEA units.

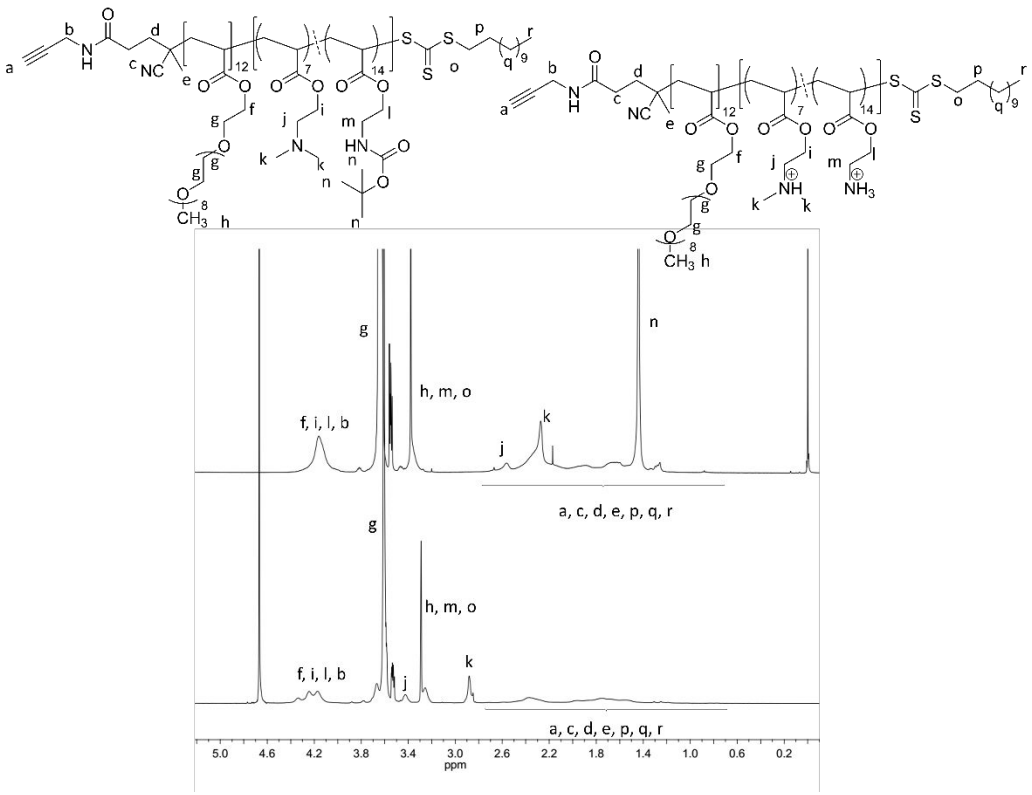

Figure III. 18. Overlaid ^{1}H NMR spectra (400 MHz) of PPEGA-*b*-P(DMAEA$_7$-*co*-*t*BocAEA$_{14}$) ($CDCl_3$, top) and PPEGA-*b*-P(DMAEA$_7$-*co*-AEA$_{14}$) (D_2O, bottom).

The ^{1}H NMR spectrum showed that the reaction of deprotection and cationization of PPEGA-*b*-P(DMAEA-*co*-*t*BocAEA) copolymers mediated through TFA leads to cationic PPEGA-*b*-P(DMAEA-*co*-AEA) copolymers. Same primary amine deprotection has been performed on PPEGA-*b*-P(DMAEA-*co*-*t*BocAEA) copolymers with different DMAEA/AEA molar ratios.

C. Characterization of a cationic P(DMAEA-*co*-AEA)

A P(DMAEA-*co*-*t*BocAEA) copolymer $\overline{DP}_{n,NMR}$ PDMAEA and P*t*BocAEA equal to 9 and 13 respectively (named P(DMAEA$_9$-*co*-*t*BocAEA$_{13}$), Run 3, Table III. 5) has been analyzed by ^{1}H NMR spectroscopy after *t*Boc deprotection and cationization in acidic medium (Figure III. 19).

The overlaid ^{1}H NMR spectra of P(DMAEA$_9$-*co*-*t*BocAEA$_{13}$) copolymers before and after deprotection shows the disappearance of the signal at 1.44 ppm of the methyl protons NHC(=O)OC(C*H*$_3$)$_3$ of the *t*Boc group (labeled k in Figure III. 19). Moreover, the shift of the signal of methylene protons OCH$_2$C*H*$_2$N$^+$H(CH$_3$)$_2$ of DMAEA units, from 2.56 to 3.52 ppm (labeled g in Figure III. 19) and the shift of the signal of the methyl protons OCH$_2$CH$_2$N$^+$H(C*H*$_3$)$_2$ of DMAEA units, from 2.27 to 2.99 ppm (labeled h in Figure III. 19) demonstrate the cationization of DMAEA units.

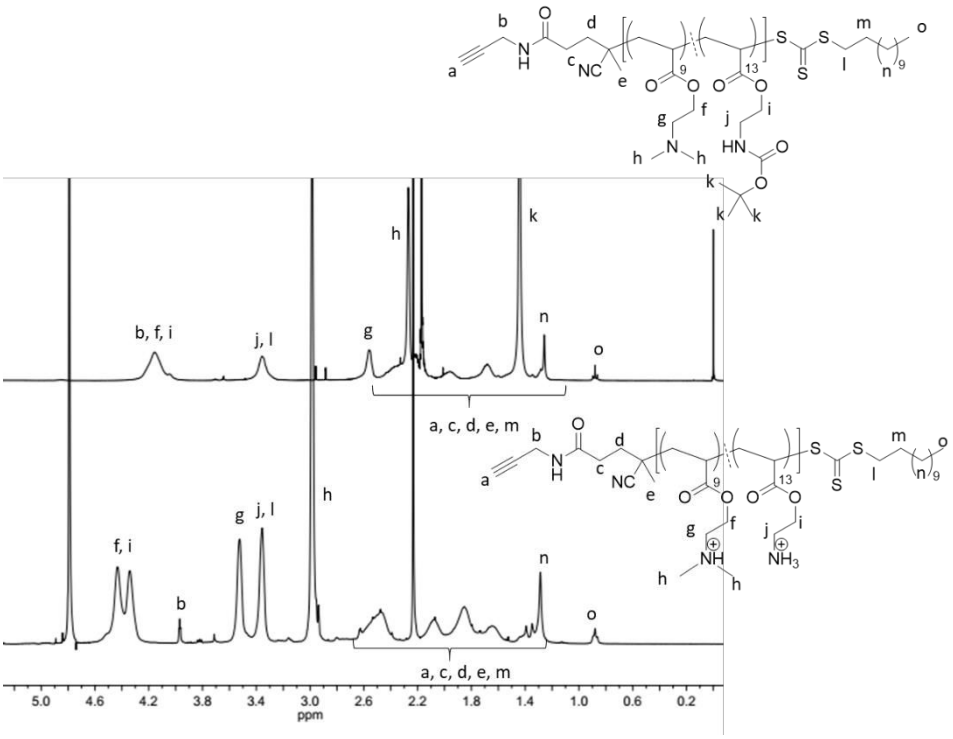

Figure III. 19. Overlaid ^{1}H NMR spectra (400 MHz) of P(DMAEA$_9$-*co*-*t*BocAEA$_{13}$) (top, CDCl$_3$) and P(DMAEA$_9$-*co*-AEA$_{13}$) (bottom, D$_2$O).

The ^{1}H NMR spectrum showed that the deprotection and the cationization of P(DMAEA-*co*-*t*BocAEA) is successful using TFA. Several cationic P(DMAEA-*co*-AEA) resulting from the cationization and deprotection reaction have been employed to complex pDNA.

The ^{1}H NMR spectra show the deprotection and cationization mediated through acidic media allows to obtain well-defined cationic polymer. Same primary amine deprotection has been performed on P(DMAEA-*co*-*t*BocAEA) copolymers with different DMAEA/AEA molar ratios.

Conclusion

Cationic copolymers based on protonated DMAEA and AEA units with different PEO architectures or without PEO have been successfully synthesized by sequential reactions.

In a first part, the RAFT copolymerization of DMAEA and *t*BocAEA has been studied using three different alkyne-base (macromolecular) chain transfer agents: the aPEO-CTA, the PPEGA-CTA and the COPYDC. An additional study on the determination of DMAEA and *t*BocAEA reactivity ratios exhibits r_{DMAEA} = 0.81 and $r_{tBocAEA}$ = 0.99 suggesting random monomer unit distribution resulting in "ideal" copolymers. Moreover it has been highlighted that the molar composition of random copolymers is equal to the molar composition of the feed comonomers whatever the conversion. Well-defined aPEO-*b*-(DMAEA-*co*-*t*BocAEA) copolymers ($6100 < \overline{M_{n,NMR}} < 11500$ and $1.21 < Đ < 1.52$), PPEGA-*b*-P(DMAEA-*co*-*t*BocAEA) copolymers ($10100 < \overline{M_{n,NMR}} < 10700$ and $1.57 < Đ < 1.62$) and P(DMAEA-*co*-*t*BocAEA) ($6400 < \overline{M_{n,NMR}} < 9400$ and $1.20 < Đ < 1.50$) copolymers with different DMAEA/AEA molar ratios have been successfully obtained through RAFT copolymerization using aPEO-CTA, PPEGA-CTA and COPYDC respectively as the (macromolecular) chain transfer agent using ACVA as the initiator at 70°C in 1,4-dioxane or/and DMF.

In a second part, the *t*Boc amine group of the copolymers previously synthesized have been deprotected using TFA in CH_2Cl_2 to form: cationic aPEO-*b*-(DMAEA-*co*-AEA) copolymers, cationic PPEGA-*b*-P(DMAEA-*co*-AEA) copolymers and cationic P(DMAEA-*co*-

AEA) copolymers. The efficiency of the deprotection and cationization reaction has been highlighted by FT-IR and ^{1}H NMR spectroscopies.

The resulting polymers will be used to study the impact of hydrophilic block architecture and DMAEA/AEA ratio on pDNA complexation and on cell viability.

Experimental part

A. Reagents

All reagents were purchased from Sigma-Aldrich unless otherwise noted. Trifluoroacetic acid (TFA, ≥ 98 %), 4,4-azobis(4-cyanolaveric acid) (ACVA, 98 %), hexane (≥ 95 %), 1,4-dioxane (≥ 99.8 %), *N,N*-dimethylformamide (DMF, ≥ 99.9 %), lithium bromide (LiBr, ≥99.9 %), aluminum oxide (basic activated), diethyl ether (99.8 %, Carlo Erba), Acetone (pure, Carlo Erba) and dichloromethane (CH_2Cl_2, 99.8 %, Carlo Erba) were used without purification. 2-(*N*,*N*-dimethylaminoethyl) acrylate (DMAEA, 98 %) was passed through a column of aluminum oxide prior to polymerization. *t*BocAEA has been synthesized following a reported procedure.[23] mPEO-CTA has been synthesized following a reported procedure ($\overline{M_{n,NMR}}$ = 2400 g.mol^{-1}, $Đ$ = 1.08).[32] COPYDC (M_{COPYDC} = 440 g.mol^{-1}), aPEO-CTA ($\overline{M_{n,NMR,aPEO\text{-}CTA}}$ = 3500 g.mol^{-1}) and PPEGA-CTA ($\overline{M_{n,NMR,PPEGA\text{-}CTA}}$ = 6700 g.mol^{-1}) have been synthesized following procedures reported in Chapter 2. All deuterated solvents were purchased from Euriso-top.

B. General characterization

Nuclear Magnetic Resonance (NMR) spectra were recorded on a Bruker DPX-200 and a Bruker AC-400 spectrometer for ^{1}H NMR (400 MHz) and ^{13}C NMR (100 MHz). Chemical shifts are reported in ppm relative to the deuterated solvent resonances.

The average molar masses (number-average molar mass $\overline{M_{n,SEC}}$, weight-average molar mass $\overline{M_{w,SEC}}$ and dispersity ($Đ$ = $\overline{M_{w,SEC}}/\overline{M_{n,SEC}}$) values were measured by Size Exclusion Chromatography (SEC) using DMF-LiBr (1 g.L^{-1}) as an eluent and carried out using a system equipped with a guard column (Polymer Laboratories, PL Gel 5 µm) followed by two columns (Polymer Laboratories, 2 PL gel 5 µm MIXED-D columns) and with a Waters 410 differential refractometer (RI) and a Waters 481 UV-Visible detector. The instrument operated at a flow

rate of 1.0 mL.min^{-1} at 60°C and was calibrated with narrow linear polystyrene (PS) standards ranging in molar mass from 580 g.mol^{-1} to 483 000 g.mol^{-1}. Molar masses and dispersities were calculated using Waters EMPOWER software.

FT-IR spectra of copolymers were recorded using a Nicolet iS5 FT-IR spectrometer operating with an attenuated total reflection (iD5 ATR Diamond) gate. Spectra were analyzed with the OMNIC software.

C. Copolymers based on DMAEA and *t*BocAEA units.

1. Determination of DMAEA and *t*BocAEA reactivity ratios.

In a successfull RAFT copolymerization procedure (Run 3, Table III. 1), a magnetic stir bar was charged to a round bottom flask together with *t*BocAEA (0.350 g, 1.63x10^{-3} mol), DMAEA (0.548 g, 3.83x10^{-3} mol), mPEO-CTA (0.130 g, 5.42x10^{-5} mol), ACVA (3 mg, 1.07x10^{-5} mol), 1,4-dioxane (3.0 mL) and DMF (0.10 mL) used as the internal reference. The mixture was deoxygenated by bubbling argon for 30 min. The solution was then immersed in an oil bath thermostatted at 70°C to allow the polymerization to occur. The reaction was stopped after 12 h by opening the reaction mixture to oxygen. Total conversion of DMAEA and *t*BocAEA were determined to be 24% by ^{1}H NMR spectroscopy by comparing the integration areas of vinylic proton of DMAEA and *t*BocAEA at 5.81-6.46 ppm and with the integral area value of the CH of DMF at 8.02 ppm. 1,4-Dioxane and DMF were removed under vacuum. The resulting product was then dissolve in acetone and precipitated several times in cold hexane/diethyl ether (90/10 v/v), filtered and dried under vacuum. The final product obtained as a yellow solid was characterized by ^{1}H NMR spectroscopy, FT-IR spectroscopy and SEC analysis.

$\overline{DP}_{n,PDMAEA}$ (= 18) and $\overline{DP}_{n,PtBocAEA}$ (= 9) were determined by comparing the integration area values of the signal of C*H*$_2$C*H*$_2$O units at 3.65 ppm, of the signal of C*H*$_3$O(CH$_2$CH$_2$O), of

$OCH_2CH_2NHC(=O)O$, of $SCH_2(CH_2)_{10}CH_3$ at 3.38-3.40 ppm, of the signal of $CH_2CH_2OC(=O)$, of OCH_2CH_2NH of *t*BocAEA and of $OCH_2CH_2N(CH_3)_2$ of the DMAEA at 4.15 ppm on ^1H NMR spectrum. $\overline{M_{n,NMR}}$ = 6910 g.mol^{-1}.

SEC in DMF (LiBr 1 g.L^{-1}): $\overline{M_{n,SEC}}$ = 9600 g.mol^{-1}; $Đ$ = 1.17.

FT-IR (ν, cm^{-1}): 3369 (m, N-H), 2928-2772 (C-H), 1732 (C=O ester), 1514 (C=O carbamate).

^1H NMR (400 MHz, $CDCl_3$, δ ppm): 0.89 (t, $SCH_2(CH_2)_{10}CH_3$), 1.26 (m, $SCH_2(CH_2)_{10}CH_3$), 1.42 (m, $C(=O)OC(CH_3)_3$), 1.45-2.65 (m, CH_2CH, $OCH_2CH_2N(CH_3)_2$, $NHC(=O)OC(CH_3)_2$), 2.55 (m, $OCH_2CH_2N(CH_3)_2$), 3.38-3.40 (m, $CH_3O(CH_2CH_2O)$, $OCH_2CH_2NHC(=O)O$ and $SCH_2(CH_2)_{10}CH_3$, 22.00 H), 3.65 (m, CH_2CH_2O, 176 H), 4.15 (m, $OCH_2CH_2N(CH_3)_2$, OCH_2CH_2NH and $CH_2CH_2OC(=O)$, 56.30 H).

2. RAFT copolymerization of DMAEA and *t*BocAEA using aPEO-CTA

In a successfull RAFT copolymerization (Run 9, Table III. 3) procedure, a magnetic stir bar was charged to a round bottom flask together with *t*BocAEA (0.4166 g, 1.93x10^{-3} mol), DMAEA (0.2758 g, 1.93x10^{-3} mol), aPEO-CTA (0.1350 g, 3.86x10^{-5} mol), ACVA (2.2 mg, 7.71x10^{-6} mol), 1,4-dioxane (4.1 mL) and DMF (0.07 mL) used as the internal reference. The mixture was deoxygenated by bubbling argon for 30 min. The solution was then immersed in an oil bath thermostatted at 70°C to allow the polymerization to occur. The reaction was stopped after 5h30 by opening the reaction mixture to oxygen. Total of conversion of DMAEA and *t*BocAEA were determined to be 24% by ^1H NMR spectroscopy by comparing the integration areas of vinylic proton of DMAEA and *t*BocAEA at 5.81-6.46 ppm and with the integral area value of the CH of DMF at 8.02 ppm. 1,4-Dioxane and DMF were removed under vacuum. The resulting product was then dissolve in CH_2Cl_2 and precipitated in cold hexane/diethyl ether

(90/10 v/v), filtered and dried under vacuum. The final product obtained as a yellow solid was characterized by ^{1}H NMR and FT-IR spectroscopies and SEC analysis.

$\overline{DP}_{n,PDMAEA}$ (= 10) and $\overline{DP}_{n,PtBocAEA}$ (= 12) were determined by comparing the integration area values of the signal of $CH_3CHC(=O)NH$ at 5.10 ppm, of the signal of OCH_2CH_2NH and of $SCH_2(CH_2)_{10}CH_3$ at 3.35 ppm and of the signal of $CH_2CH_2OC(=O)$, of $OCH_2CH_2N(CH_3)_2$ and of OCH_2CH_2NH at 4.16 ppm on ^{1}H NMR spectrum. $\overline{M_{n,NMR}}$ = 7500 g.mol^{-1}

SEC in DMF (LiBr 1 g.L^{-1}): $\overline{M_{n,SEC}}$ = 11700 g.mol^{-1}; $Đ$ = 1.31

FT-IR (υ, cm^{-1}): 3367 (N-H carbamate), 2883 (C-H), 1731 (C=O ester), 1518 (C=O carbamate), 1454 (C-H), 1108 (C-O).

^{1}H NMR (400 MHz, $CDCl_3$), δ (ppm): 0.88 ppm (t, $SCH_2(CH_2)_{10}CH_3$, 3.07 H), 1.21 (m, $SCH_2CH_2(CH_2)_9CH_3$, 19.96 H), 1.35-2.41 (m, $HC{\equiv}CCH_2CH_2CH_2$-, $CH_3CHO(C=O)NH$, $NHC(CH_3)_2C(=O)NH$, $CH_2CH_2C(CN)(CH_3)$, $(CH_2CH)_n$, $OCH_2CH_2N(CH_3)_2$, $C(=O)OC(CH_3)_3$, SCH_2CH_2, 293.06 H), 2.56 (m, $OCH_2CH_2N(CH_3)_2$, 32.72 H), 3.35 (m, OCH_2CH_2NHC, $SCH_2(CH_2)_{10}CH_3$, 26.79 H), 3.65 (m, CH_2CH_2O, 292.29 H), 4.16 (m, $CH_2CH_2OC(=O)$, $OCH_2CH_2N(CH_3)_2$, OCH_2CH_2NH, 48.50 H), 5.10 (q, $CH_3CHC(=O)NH$, 1.00 H).

3. RAFT copolymerization of DMAEA and *t*BocAEA using PPEGA-CTA

In a successfull RAFT copolymerization (Run 1, Table III. 4) procedure, a magnetic stir bar was charged to a round bottom flask together with *t*BocAEA (0.3958 g, 1.84x10^{-3} mol), DMAEA (0.2712 g, 1.89x10^{-3} mol), PPEGA-CTA (0.3340 g, 3.68x10^{-5} mol), ACVA (2.0 mg, 7.32x10^{-6} mol), 1,4-dioxane (10 mL) and DMF (0.3 mL) used as the internal reference. The mixture was deoxygenated by bubbling argon for 30 min. The solution was then immersed in an oil bath thermostatted at 70°C to allow the polymerization to occur. The reaction was stopped after 27 h by opening the reaction mixture to oxygen. Total conversion of DMAEA and

*t*BocAEA were determined to be 20% by ^{1}H NMR spectroscopy by comparing the integration areas of vinylic proton of DMAEA and *t*BocAEA at 5.79-6.52 ppm and with the integral area value of the CH of DMF at 8.02 ppm. 1,4-dioxane and DMF were removed under vacuum. The resulting product was then dissolve in CH_2Cl_2, precipitated several times in cold hexane/diethyl ether (90/10 v/v), centrifuged (7000 rpm, 5 min, 0°C) and dried under vacuum. The final product obtained as a yellow solid was characterized by ^{1}H NMR spectroscopy and SEC analysis.

$\overline{DP}_{n,PDMAEA}$ (= 9) and $\overline{DP}_{n,PtBocAEA}$ (= 10) were determined by comparing the integration area values of the signal of C*H*$_2$C*H*$_2$O units at 3.65 ppm, of the signal of $(CH_2CH_2O)_9CH_3$, of OCH_2CH_2NH, of $SCH_2(CH_2)_{10}CH_3$ at 3.38 ppm, and of the signal of $HC{\equiv}CCH_2NH$, of $OCH_2CH_2O(CH_2CH_2O)_8$ of $OCH_2CH_2N(CH_3)_2$, of $OCH_2CH_2NHC(=O)O$ at 4.16 ppm on ^{1}H NMR spectrum. $\overline{M_{n,NMR}}$ = 10100 g.mol^{-1}

SEC in DMF (LiBr 1 g.L^{-1}): $\overline{M_{n,SEC}}$ = 11200 g.mol^{-1} (PS equivalents); $Đ$ = 1.57

^{1}H NMR (400 MHz, $CDCl_3$), δ (ppm): 0.88 ppm (t, $SCH_2(CH_2)_{10}CH_3$, 3.60 H), 1.21-2.90 (m, *H*C≡CCH$_2$NH, C*H*$_2$C*H*$_2$C(CN)(C*H*$_3$), (C*H*$_2$C*H*)$_n$, OCH$_2$C*H*$_2$N(CH$_3$)$_2$, OCH$_2$CH$_2$N(C*H*$_3$)$_2$, NHC(=O)OC(C*H*$_3$)$_3$, SCH$_2$(C*H*$_2$)$_{10}$CH$_3$, 325.05 H), 3.38 (m, $(CH_2CH_2O)_9CH_3$, OCH$_2$C*H*$_2$NH, SC*H*$_2$(CH$_2$)$_{10}$CH$_3$, 55.19 H), 3.65 (m, (C*H*$_2$C*H*$_2$O), 432.00 H), 4.16 (m, HC≡CC*H*$_2$NH-, -OC*H*$_2$CH$_2$O(CH$_2$CH$_2$O)$_8$, OC*H*$_2$CH$_2$N(CH$_3$)$_2$, OC*H*$_2$CH$_2$NHC(=O)O, 60.23 H).

4. RAFT copolymerization of DMAEA and *t*BocAEA using COPYDC

In a successfull RAFT copolymerization (Run 3, Table III. 5) procedure, a magnetic stir bar was charged to a round bottom flask together with *t*BocAEA (3.6124 g, 1.68x10^{-2} mol), DMAEA (2.1602 g, 1.51x10^{-2} mol), COPYDC (0.1348 g, 3.07x10^{-4} mol), ACVA (8.4 mg, 3.00x10^{-5} mol), DMF (6.3 mL). The mixture was deoxygenated by bubbling argon for 30 min. The solution was then immersed in an oil bath thermostatted at 70°C to allow the

polymerization to occur. The reaction was stopped after 21h by opening the reaction mixture to oxygen. Total conversion of DMAEA and *t*BocAEA were determined to be 19 % by ^{1}H NMR spectroscopy by comparing the integration areas of vinylic proton of DMAEA and *t*BocAEA at 5.79-6.52 ppm and with the integral area value of the CH of DMF at 8.02 ppm. DMF were removed under vacuum. The resulting product was then dissolve in acetone, precipitated several times in cold hexane/diethyl ether (90/10 v/v), centrifugated (7000 rpm, 5 min, 0°C) and dried under vacuum. The final product obtained as a yellow oil was characterized by ^{1}H NMR spectroscopy and SEC analysis.

$\overline{DP}_{n,PDMAEA}$ (= 9) and $\overline{DP}_{n,PtBocAEA}$ (= 13) were determined by comparing the integration area values of the signal of $SCH_2(CH_2)_{10}CH_3$ at 0.88 ppm, of the signal of OCH_2CH_2NH, of $SCH_2(CH_2)_{10}CH_3$ at 3.36 ppm and of the signal of $HC{\equiv}CCH_2NH$, of $OCH_2CH_2N(CH_3)_2$, of CH_2CH_2NH at 4.15 ppm on ^{1}H NMR spectrum. $\overline{M_{n,NMR}}$ = 6400 g.mol^{-1}

SEC in DMF (LiBr 1 g.L^{-1}): $\overline{M_{n,SEC}}$ = 5200 g.mol^{-1} (PS equivalents); $Đ$ = 1.50

^{1}H NMR (400 MHz, $CDCl_3$), δ (ppm): 0.88 (t, $SCH_2(CH_2)_{10}CH_3$, 3.00 H), 1.00-2.80 (m, $HC{\equiv}CCH_2NH$-, $CH_2CH_2C(CN)(CH_3)$, $(CH_2CH)_n$, $(CH_2CH)_m$ $CH_2N(CH_3)_2$, $OCH_2CH_2N(CH_3)_2$, $C(=O)OC(CH_3)_3$, $SCH_2(CH_2)_{10}CH_3$, 381.05 H), 3.36 (m, OCH_2CH_2NH, $SCH_2(CH_2)_{10}CH_3$, 29.91 H), 4.15 (m, $HC{\equiv}CCH_2NH$, $OCH_2CH_2N(CH_3)_2$, OCH_2CH_2NH, 45.37 H).

D. Amine deprotection of *t*BocAEA repeating units of aPEO-*b*-P(DMAEA-*co*-*t*BocAEA), PPEGA-*b*-P(DMAEA-*co*-*t*BocAEA) and P(DMAEA-*co*-*t*BocAEA)

1. Characterization of a cationic aPEO-*b*-P(DMAEA-*co*-AEA) copolymer

In a typical procedure, 100.3 mg of aPEO-*b*-P(DMAEA-*co*-*t*BocAEA) ($13.9x10^{-5}$ mol) block copolymer was dissolved in dichloromethane (CH_2Cl_2, 2 mL). The TFA (214 µL, $2.78x10^{-3}$ moL) was added dropwise at 0°C. After completed addition, the solution was stirred during 5h at room temperature. The CH_2Cl_2 was then removed using a rotary evaporator and the polymer was dissolved in acetone, precipitated into diethyl ether/hexane (50/50 v/v), centrifuged (7000 rpm, 0°C, 5 min) and dried under vacuum. The product obtained was a yellow solid and analyzed by FT-IR and ^{1}H NMR spectroscopies.

FT-IR (υ, cm^{-1}): 3400 (N-H), 1673 (C=O ester), 1454 (C-H), 1203 (C-O), 840 (N-H), 659 (C-H, alkyne).

^{1}H NMR (DMSO d_6, 400 MHz), δ (ppm): 0.85 (t, $SCH_2(CH_2)_{10}CH_3$), 0.93-2.73 (m, $HC{\equiv}CCH_2CH_2CH_2$, $CH_3CHC(=O)NH$, $NHC(CH_3)_2C(=O)NH$, $CH_2CH_2C(CN)(CH_3)$, $SCH_2(CH_2)_{10}CH_3$), 2.85 (m, $OCH_2CH_2N^+H(CH_3)_2$), 3.10 (m, $OCH_2CH_2N^+H_3$, $SCH_2(CH_2)_{10}CH_3$), 3.40 (m, $OCH_2CH_2N^+H(CH_3)_2$), 3.51 (m, $(CH_2CH_2O)_{63}$), 4.24 (m, $OCH_2CH_2N^+H(CH_3)_2$, $OCH_2CH_2N^+H_3$, (m, $CH_2CH_2OC(=O)$), 4.91 (q, $CH_3CHC(=O)NH$)

^{1}H NMR (D_2O, 400 MHz), δ (ppm): 0.78 (t, $S(CH_2)_{11}CH_3$), 1.00-2.78 (m, $HC{\equiv}CCH_2CH_2CH_2$, $CH_3CHC(=O)NH$, $NHC(CH_3)_2C(=O)NH$, $CH_2CH_2C(CN)(CH_3)$, $SCH_2(CH_2)_{10}CH_3$), 2.88 (m, $OCH_2CH_2N^+H(CH_3)_2$), 3.25 (m, $OCH_2CH_2N^+H_3$, $SCH_2(CH_2)_{10}CH_3$), 3.42 (m, $OCH_2CH_2N^+H(CH_3)_2$), 3.61 (m, $(CH_2CH_2O)_{63}$), 4.29 (m, $OCH_2CH_2N^+H(CH_3)_2$, $OCH_2CH_2N^+H_3$, (m, $CH_2CH_2OC(=O)$), 4.87 (q, $CH_3CHC(=O)NH$)

2. Characterization of a cationic PPEGA-*b*-P(DMAEA-*co*-AEA) copolymer

In a typical procedure, 220.2 mg of PPEGA-*b*-P(DMAEA-*co*-*t*bocAEA) ($2.19x10^{-5}$ mol) block copolymer was dissolved in dichloromethane (CH_2Cl_2, 4.5 mL). TFA (500 µL, $6.51x10^{-3}$ moL) was added dropwise at 0°C. After complete addition, the solution was stirred 5 h at room temperature. The CH_2Cl_2 was then removed using a rotary evaporator and the polymer was dissolved in acetone, precipitated into diethyl ether/hexane (50/50 v/v), centrifuged (7000 rpm, 0°C, 5 min) and dried in a vacuum. The product obtained was a yellow solid and analyzed by ^{1}H NMR spectroscopy.

^{1}H NMR (D_2O, 400 MHz), δ (ppm): 0.60-2.81 (m, *H*C≡CCH$_2$NH, C*H$_2$*C*H$_2$*C(CN)(C*H$_3$*), $(CH_2CH)_n$, SCH$_2$(C*H$_2$*)$_{10}$C*H$_3$*), 2.88 (m, OCH$_2$CH$_2$N$^+$H(*CH$_3$*)$_2$), 3.32 (m, $(CH_2CH_2O)_8$C*H$_3$*, OCH$_2$C*H$_2$*N$^+$H$_3$, SC*H$_2$*(CH$_2$)$_{10}$CH$_3$), 3.43 (m, OCH$_2$C*H$_2$*N$^+$H(CH$_3$)$_2$), 3.61 (m, (C*H$_2$*C*H$_2$*O)$_9$), 4.24 (m, HC≡CC*H$_2$*, OC*H$_2$*CHO(CH$_2$CH$_2$O), OC*H$_2$*CH$_2$N$^+$H(CH$_3$)$_2$, OC*H$_2$*CH$_2$N$^+$H$_3$).

3. Characterization of a cationic P(DMAEA-*co*-AEA)

In a typical procedure, 500 mg of P(DMAEA-*co*-*t*bocAEA) ($9.7x10^{-5}$ mol) copolymer was dissolved in dichloromethane (CH_2Cl_2, 10 mL). TFA (1.5 mL, $1.93x10^{-2}$ moL) was added dropwise at 0°C. After complete addition, the solution was stirred 5 h at room temperature. The CH_2Cl_2 was then removed using a rotary evaporator and the polymer was dissolved in acetone, precipitated into diethyl ether/hexane (50/50 v/v), centrifuged (7000 rpm, 0°C, 5 min) and dried in a vacuum. The product obtained was a yellow solid and analyzed by ^{1}H NMR spectroscopy.

^{1}H NMR (D_2O, 400 MHz), δ (ppm): 0.88 (t, SCH$_2$(CH$_2$)$_{10}$C*H$_3$*), 1.10-2.73 (m, *H*C≡CCH$_2$NH, C*H$_2$*C*H$_2$*C(CN)(C*H$_3$*), $(CH_2CH)_n$, SCH$_2$(C*H$_2$*)$_{10}$C*H$_3$*), 2.99 (m, OCH$_2$CH$_2$N$^+$H(*CH$_3$*)$_2$), 3.36 (m, OCH$_2$C*H$_2$*N$^+$H$_3$, SC*H$_2$*(CH$_2$)$_{10}$CH$_3$), 3.52 (m, OCH$_2$C*H$_2$*N$^+$H(CH$_3$)$_2$), 3.97 (m, HC≡CC*H$_2$*), 4.39 (m, OC*H$_2$*CH$_2$N$^+$H(CH$_3$)$_2$, OC*H$_2$*CH$_2$N$^+$H$_3$).

References

(1) Samal, S. K.; Dash, M.; Van Vlierberghe, S.; Kaplan, D. L.; Chiellini, E.; van Blitterswijk, C.; Moroni, L.; Dubruel, P. Cationic Polymers and Their Therapeutic Potential. *Chemical Society Reviews* **2012**, *41* (21), 7147-7194.

(2) Mintzer, M. A.; Simanek, E. E. Nonviral Vectors for Gene Delivery. *Chemical Reviews* **2009**, *109* (2), 259–302.

(3) Al-Dosari, M. S.; Gao, X. Nonviral Gene Delivery: Principle, Limitations, and Recent Progress. *The AAPS Journal* **2009**, *11* (4), 671–681.

(4) Pouton, C. W.; Seymour, L. W. Key Issues in Non-Viral Gene Delivery. *Advanced Drug Delivery Reviews* **1998**, *34* (1), 3–19.

(5) Putnam, D.; Gentry, C. A.; Pack, D. W.; Langer, R. Polymer-Based Gene Delivery with Low Cytotoxicity by a Unique Balance of Side-Chain Termini. *Proceedings of the National Academy of Sciences* **2001**, *98* (3), 1200–1205.

(6) Zhu, C.; Jung, S.; Si, G.; Cheng, R.; Meng, F.; Zhu, X.; Park, T. G.; Zhong, Z. Cationic Methacrylate Copolymers Containing Primary and Tertiary Amino Side Groups: Controlled Synthesis via RAFT Polymerization, DNA Condensation, and in Vitro Gene Transfection. *Journal of Polymer Science Part A: Polymer Chemistry* **2010**, *48* (13), 2869–2877.

(7) Bauri, K.; Roy, S. G.; Pant, S.; De, P. Controlled Synthesis of Amino Acid-Based pH-Responsive Chiral Polymers and Self-Assembly of Their Block Copolymers. *Langmuir* **2013**, *29* (8), 2764–2774.

(8) McCool, M. B.; Senogles, E. The Self-Catalysed Hydrolysis of poly(N,N-Dimethylaminoethyl Acrylate). *European Polymer Journal* **1989**, *25* (7), 857–860.

(9) Zhang, K.; Fang, H.; Wang, Z.; Li, Z.; Taylor, J.-S. A.; Wooley, K. L. Structure-Activity Relationships of Cationic Shell-Crosslinked Knedel-like Nanoparticles: Shell Composition and Transfection Efficiency/Cytotoxicity. *Biomaterials* **2010**, *31* (7), 1805–1813.

(10) Cotanda, P.; Wright, D. B.; Tyler, M.; O'Reilly, R. K. A Comparative Study of the Stimuli-Responsive Properties of DMAEA and DMAEMA Containing Polymers. *Journal of Polymer Science Part A: Polymer Chemistry* **2013**, *51* (16), 3333–3338.

(11) Truong, N. P.; Jia, Z.; Burges, M.; McMillan, N. A. J.; Monteiro, M. J. Self-Catalyzed Degradation of Linear Cationic Poly(2-Dimethylaminoethyl Acrylate) in Water. *Biomacromolecules* **2011**, *12* (5), 1876–1882.

(12) Ahmed, M.; Narain, R. Progress of RAFT Based Polymers in Gene Delivery. *Progress in Polymer Science* **2013**, *38* (5), 767–790.

(13) Sprouse, D.; Reineke, T. M. Investigating the Effects of Block versus Statistical Glycopolycations Containing Primary and Tertiary Amines for Plasmid DNA Delivery. *Biomacromolecules* **2014**, *15* (7), 2616–2628.

(14) Rinkenauer, A. C.; Schubert, S.; Traeger, A.; Schubert, U. S. The Influence of Polymer Architecture on in Vitro pDNA Transfection. *Journal of Material Chemistry B* **2015**, *3* (38), 7477–7493.

(15) *Handbook of RAFT Polymerization*; Barner-Kowollik, C., Ed.; Wiley-VCH: Weinheim, 2008.

(16) Truong, N. P.; Jia, Z.; Burgess, M.; Payne, L.; McMillan, N. A. J.; Monteiro, M. J. Self-Catalyzed Degradable Cationic Polymer for Release of DNA. *Biomacromolecules* **2011**, *12* (10), 3540–3548.

(17) Ho, H. T.; Pascual, S.; Montembault, V.; Casse, N.; Fontaine, L. Innovative Well-Defined Primary Amine-Based Polyacrylates for Plasmid DNA Complexation. *Polymer Chemistry* **2014**, *5* (19), 5542.

(18) Fineman, M.; Ross, S. D. Linear Method for Determining Monomer Reactivity Ratios in Copolymerization. *Journal of Polymer Science Part A: Polymer Chemistry* **1950**, *5* (2), 259–262.

(19) Mayo, F. R.; Lewis, F. M. Copolymerization. I. A Basis for Comparing the Behavior of Monomers in Copolymerization; the Copolymerization of Styrene and Methyl Methacrylate. *Journal of the American Chemical Society* **1944**, *66* (9), 1594–1601.

(20) Kelen, T.; Tüdos, F. Analysis of the Linear Methods for Determining Copolymerization Reactivity Ratios. I. A New Improved Linear Graphic Method. *Journal of Macromolecular Science: Part A - Chemistry* **1975**, *9* (1), 1–27.
(21) Madruga, E. L. From Classical to Living/Controlled Statistical Free-Radical Copolymerization. *Progress in Polymer Science* **2002**, *27* (9), 1879–1924.
(22) Tüdos, F.; Kelen, T.; Földes-berezsnich, T.; Turcsányi, B. Analysis of Linear Methods for Determining Copolymerization Reactivity Ratios. III. Linear Graphic Method for Evaluating Data Obtained at High Conversion Levels. *Journal of Macromolecular Science: Part A - Chemistry* **1976**, *10* (8), 1513–1540.
(23) Ho, H. T.; Bohec, M. L.; Frémaux, J.; Piogé, S.; Casse, N.; Fontaine, L.; Pascual, S. Tuning the Molar Composition of "Charge-Shifting" Cationic Copolymers Based on 2-(N, N-Dimethylamino) Ethyl Acrylate and 2-(Tert-Boc-Amino) Ethyl Acrylate. *Macromolecular Rapid Communications* **2017**, *38* (5).
(24) Pooley, S. A.; Rivas, B. L.; Pizarro, G. D. C. Hydrogels Based on (Dimethylamino)ethylacrylate (DMAEA) and N,N'-dimethylacrylamide (NNDMAAM): Synthesis, Characterization and Swelling Behavior. *Journal of the Chilean Chemical Society* **2013**, *58*, 1597–1602.
(25) Kim, S.-H.; Lim, B.-K.; Sun, F.; Koh, K.; Ryu, S.-C.; Kim, H.-S.; Lee, J. Preparation of High Flexible Composite Film of Hydroxyapatite and Chitosan. *Polymer Bulletin* **2008**, *62* (1), 111-118.
(26) Ros, S.; Burke, N. A. D.; Stöver, H. D. H. Synthesis and Properties of Charge-Shifting Polycations: Poly[3-Aminopropylmethacrylamide-Co-2-(Dimethylamino)ethyl Acrylate]. *Macromolecules* **2015**, *48* (24), 8958–8970.
(27) Zhang, C.; Maric, M. Synthesis of Stimuli-Responsive, Water-Soluble Poly[2-(Dimethylamino)ethyl Methacrylate/Styrene] Statistical Copolymers by Nitroxide Mediated Polymerization. *Polymers* **2011**, *3* (4), 1398–1422.
(28) Topham, P. D.; Sandon, N.; Read, E. S.; Madsen, J.; Ryan, A. J.; Armes, S. P. Facile Synthesis of Well-Defined Hydrophilic Methacrylic Macromonomers Using ATRP and Click Chemistry. *Macromolecules* **2008**, *41* (24), 9542–9547.
(29) López, S. E.; Salazar, J. Trifluoroacetic Acid: Uses and Recent Applications in Organic Synthesis. *Journal of Fluorine Chemistry* **2013**, *156*, 73–100.
(30) Heredia, K. L.; Tolstyka, Z. P.; Maynard, H. D. Aminooxy End-Functionalized Polymers Synthesized by ATRP for Chemoselective Conjugation to Proteins. *Macromolecules* **2007**, *40* (14), 4772–4779.
(31) Vázquez-Dorbatt, V.; Tolstyka, Z. P.; Maynard, H. D. Synthesis of Aminooxy End-Functionalized pNIPAAm by RAFT Polymerization for Protein and Polysaccharide Conjugation. *Macromolecules* **2009**, *42* (20), 7650–7656.
(32) Ho, H. T.; Levere, M. E.; Pascual, S.; Montembault, V.; Casse, N.; Caruso, A.; Fontaine, L. Thermoresponsive Block Copolymers Containing Reactive Azlactone Groups and Their Bioconjugation with Lysozyme. *Polym. Chem.* **2013**, *4* (3), 675–685.

Chapter 4: Chain-ends Modification of (PEGylated) Aminoethyl-based Polyacrylates.

Introduction

The incorporation of new functionality or removal unwanted chain-end reactivity is a major theme and essential tool for polymer researchers. Several reviews and recent highlight have been published on established and emerging strategies for polymer-chain end modification.[1,2] More often, such strategies are focused on the most popular chain-growth processes included RDRP and post-polymerization modifications. When polymers for gene delivery are concerned for post-polymerization modification, soft reaction conditions (room temperature, aqueous solution) are necessary to maintain the integrity of the cationic polymer or/and the bio(macro)molecules structures. In this project the post-polymerization modification of cationic aPEO-*b*-P(DMAEA-*co*-*t*BocAEA) copolymers, PPEGA-*b*-P(DMAEA-*co*-*t*BocAEA) copolymers and P(DMAEA-*co*-*t*BocAEA) copolymers has been studied to both decrease cytotoxicity and increase transfection efficiency.

Among organic synthetic methods able to modify alkyne-based RAFT copolymers chain-end under mild conditions the photochemical-mediated trithiocarbonate removal, the thiol-yne coupling reaction and the thiol-disulfide exchange have been chosen. The first one has been studied to decrease polymer cytotoxicity and the two following ones has been employed to insert a recognition ligand to increase transfection efficiency.

Even though, it has been shown the cytotoxicity of trithiocarbonyl group is lower compared to dithioester group,[3] it is necessary to remove the thiocarbonylthio group of copolymers to use them in non-viral gene delivery. Indeed, the thiocarbonylthio moieties are sulfur analogs of esters designed to readily undergo radical homolysis and may also be prone to hydrolysis and polymer-polymer coupling.[3,4] Moreover, the removal of the thiocarbonylthio group is preferable to avoid side reactions between such group and thiol groups included in biological molecule.[5] Several reviews reported chain transfer agent removal procedures.[6,7]

Among click chemistry reactions, the thiol-yne coupling reaction does not need any metallic catalyst and is a robust tool for polymer modification.[8–11] Such reaction can proceed through nucleophilic addition or radical addition. To use the nucleophilic addition, the unsaturated bond has to be activated and sensible to nucleophilic reagents. When the unsaturated bond is not activated, the thiol-yne reaction has to be made through radical addition. One or two thiol-based molecules could be added by thiol-yne reaction depending on experimental conditions.[8–11]

The thiol-disulfide exchange reaction can be reduced by enzymes as gluthatione.[12,13] In non-viral gene delivery, the disulfide bond has been employed as a reducible cross-linker or moiety to decrease cytotoxicity by increasing the degradation into the cytoplasm.[14–16] Furthermore, the disulfide bond remains stable in extra-cellular media.

In this work, the radical-induced trithiocarbonate group removal was modeled using a PNIPAM under thermo-activation. Then, the reaction was performed using photochemical-activation on the cationic aminoethyl polyacrylates copolymers, in order to maintain the integrity of copolymers under softer conditions. After the trithiocarbonate removal, the addition of a thiol compound was modeled using the disulfide coupling exchange on α-pyridyldithio,ω-hydroxylPEO and the thiol-yne coupling reaction on a PNIPAM. The challenging "one-pot" cascade thiol-yne click reaction at the α-chain end and the trithiocarbonate removal at the ω-chain-end through radical mechanisms will be explored.

I. Trithiocarbonate removal

Several fast and facile trithiocarbonate group removal procedures have been reported that do not require expensive reagents or harsh conditions.[6,7] Perrier *et al.* suggested in 2005 an easy way to achieve the complete removal of trithiocarbonate end-group thanks to a radical initiator such as AIBN.[17] Furthermore, the trithiocarbonate moiety can be changed to a different group by using a functional radical initiator. The authors showed that using ACVA as radical initiator, it is possible to functionalize the ω-position of the polymer chain-end by a carboxylic acid group.[17]

The thermal-mediated trithiocarbonate removal reaction conditions used by Perrier *et al*.[17] are studied in our work on a PNIPAM used as a polymer model easy to characterize by ^{1}H NMR spectroscopy and MALDI-TOF mass spectrometry.[18]

A. PNIPAM used as a model polymer to trithiocarbonate removal[‡]

A PNIPAM has been first synthesized by RAFT polymerization using COPYDC as the chain transfer agent. Then, the trithiocarbonate has been removed using AIBN as the initiator at 80°C.

1. RAFT polymerization of NIPAM with COPYDC

A RAFT polymerization of NIPAM was launched with COPYDC as chain transfer agent and AIBN as initiator in DMF solvent at 70°C with $[NIPAM]_0/[COPYDC]_0/[AIBN]_0$ = 100/1/0.1 (Scheme IV. 1).

[‡]Le Bohec M., Pascual S., Piogé S., Fontaine L., Heterofunctional RAFT-derived PNIPAM *via* cascade trithiocarbonate removal and thiol-yne click coupling reaction. *Journal of polymer science Part A: Polymer chemistry* **2017**

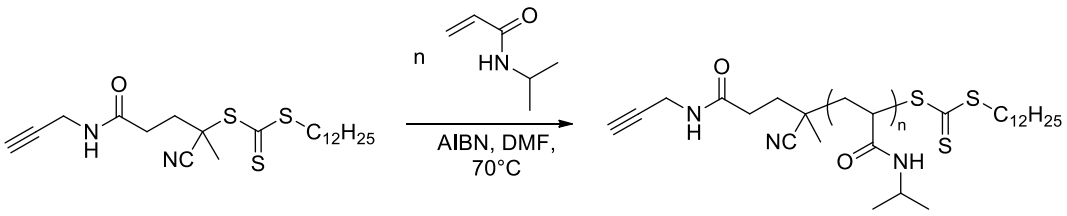

Scheme IV. 1. RAFT polymerization of NIPAM with COPYDC as chain transfer agent, initiated with AIBN in DMF at 70°C.

Samples were withdrawn to determine the NIPAM conversion by ^{1}H NMR spectroscopy and the number-average molar masses ($\overline{M_{n,SEC}}$) and dispersities ($Đ$) by SEC (Table IV. 1). Table IV.1 shows that NIPAM conversion increases with time. Moreover, this increase goes along with the increase of the $\overline{M_{n,SEC}}$ determined by SEC while the dispersity values remain low. When 70.3 % conversion was reached, the control was lost as the dispersity values increased (Entry 6, Table IV. 1). At low conversion, the SEC traces were unimodal and narrow while a second population with a higher molar mass appeared at high conversion (Figure IV. 1). This second population is due to polymer-polymer coupling at high conversion as evidenced also by the kinetic plot by a decrease of the slope of $\ln([M]_0/[M]_t)$ *vs* time (Figure IV. 2).[19] Moreover, the kinetic plot of $\overline{M_{n,SEC}}$ *vs* conversion is linear, this result shows the lack of unwanted transfer reaction during the RAFT polymerization (Figure IV. 3).

Table IV. 1. Monomer conversion and macromolecular characteristics of polymers obtained by RAFT polymerization of NIPAM with COPYDC as chain transfer agent and AIBN as initiator in DMF at 70°C. $[NIPAM]_0/[COPYDC]_0/[AIBN]_0 = 100/1/0.1$.

Entry	Time (min)	Conv. (%)[a]	$\overline{M_{n,th}}$ (g.mol^{-1})[b]	$\overline{M_{n,SEC}}$ (g.mol^{-1})[c]	$Đ$[c]
1	115	29.8	3810	7460	1.18
2	180	51.9	6309	11000	1.25
3	240	60.4	7270	13600	1.19
4	290	64.5	7730	14600	1.19
5	349	68.7	8200	15200	1.20
6	406	70.3	8380	14700	1.26

[a] Monomer conversion monitored by ^{1}H NMR spectroscopy by comparing the integration values of the formamide proton of DMF at 8.02 ppm, and of the alkene protons of NIPAM between 6.0 and 6.3 ppm. [b] $\overline{M_{n,th}} = \text{Conv.} \frac{[NIPAM]_0}{[COPYDC]_0} \times M_{NIPAM} + M_{EXT}$ where M_{NIPAM} is the molar mass of NIPAM (113.16 g.mol^{-1}) and M_{EXT} is the molar mass of the chain-ends (434.20 g.mol^{-1}). [c] Determined by SEC in DMF (LiBr 1 g.L^{-1}) using PS standards.

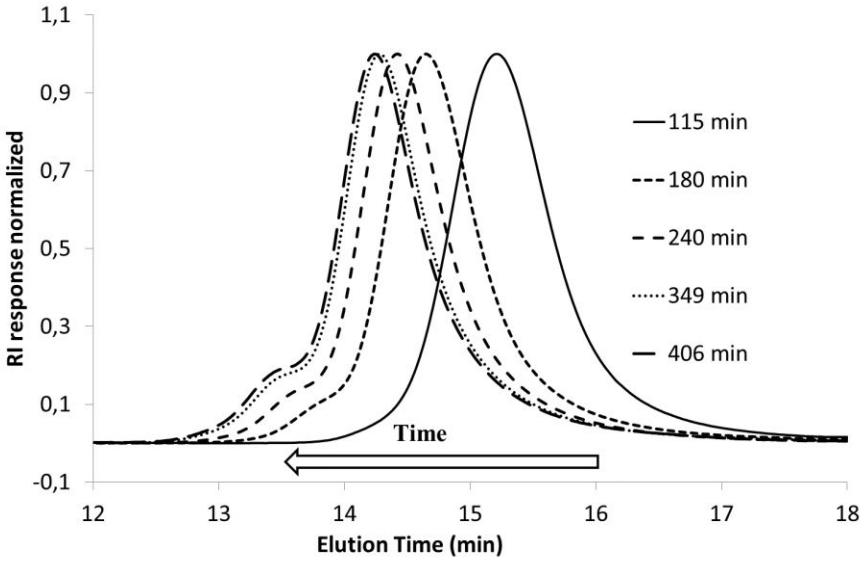

Figure IV. 1. Overlaid SEC traces of polymers obtained from the RAFT polymerization of NIPAM using COPYDC as chain transfer agent and initiated with AIBN in DMF at 70 °C. $[NIPAM]_0/[COPYDC]_0/[AIBN]_0 = 100/1/0.1$.

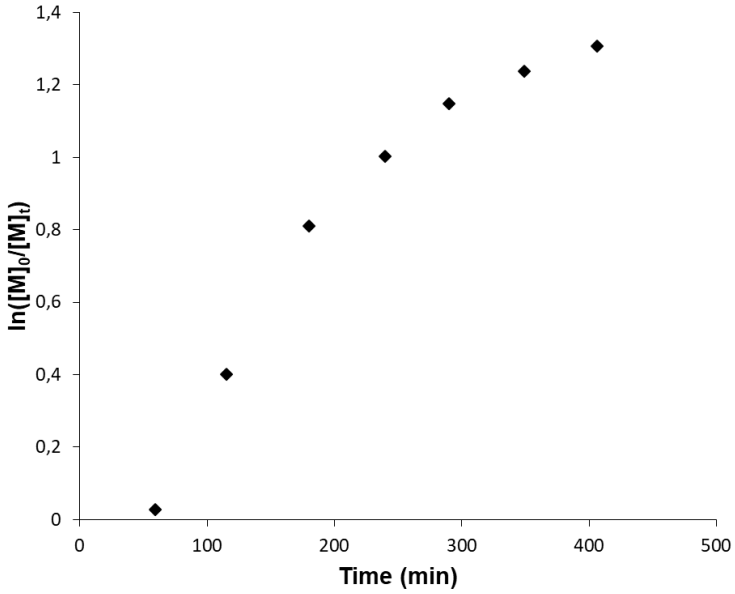

Figure IV. 2. $Ln([M]_0/[M]_t$ *vs.* time plot for the RAFT polymerization of NIPAM using COPYDC as chain transfer agent and AIBN as initiator in DMF at 70°C; $[NIPAM]_0/[COPYDC]_0/[AIBN]_0 = 100/1/0.1$.

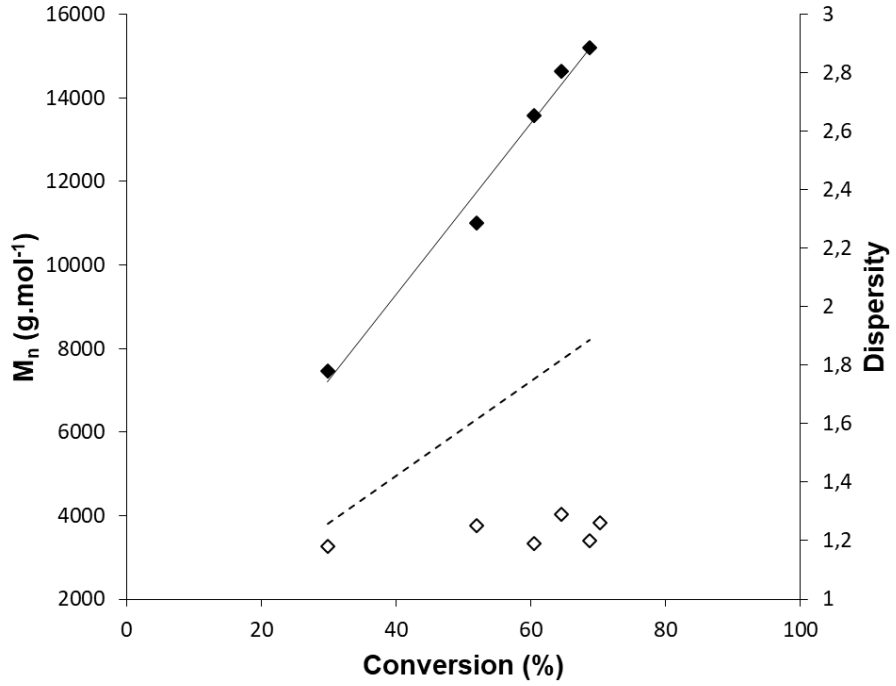

Figure IV. 3. $\overline{M_{n,SEC}}$ (filled marks, solid line: experimental values and dashed line: theoretical values) and *Đ* (empty marks) *vs.* conversion during the RAFT polymerization of NIPAM using COPYDC as chain transfer agent and AIBN as initiator in DMF at 70°C. $[NIPAM]_0/[COPYDC]_0/[AIBN]_0 = 100/1/0.1$.

A new batch of PNIPAM was synthesized using a similar $[NIPAM]_0/[COPYDC]_0/[AIBN]_0$ ratio of 100/1/0.1 while limiting the polymerization at a low conversion (40 % as determined by ^{1}H NMR spectroscopy analysis of the crude mixture) in order to prepare a well-defined PNIPAM with precise chain-ends. The polymer was purified by three precipitations in cold diethyl ether. The $\overline{DP_n}$ was determined by ^{1}H NMR spectroscopy (Figure IV. 4) by comparing the integration areas values of methyl protons $SCH_2(CH_2)_{10}CH_3$ of the dodecyl chain-end at 0.88 ppm (3 protons, labelled a in Figure IV. 4) and of methylene protons $HC{\equiv}CCH_2NH$ and of methine protons $NHCH(CH_3)_2$ of NIPAM repeating units 4.01 ppm (42.12 protons, labelled d and j in Figure IV. 4). The $\overline{DP_n}$ is equal to 40.

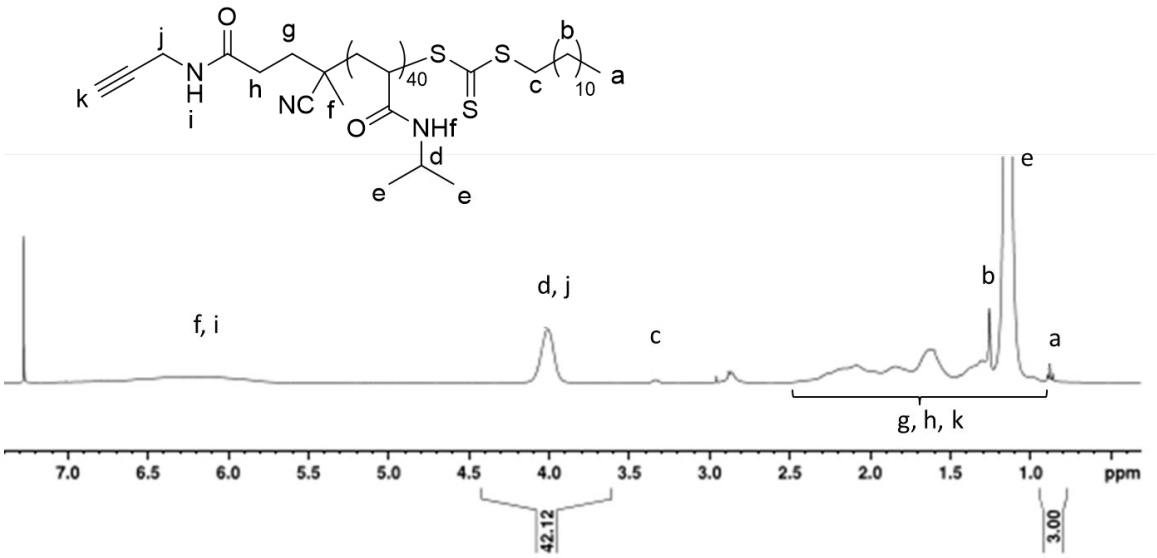

Figure IV. 4. ^{1}H NMR (400 MHz) spectrum in $CDCl_3$ of purified PNIPAM obtained from the RAFT polymerization of NIPAM using COPYDC as chain transfer agent and initiated with AIBN in DMF at 70°C using $[NIPAM]_0/[COPYDC]_0/[AIBN]_0 = 100/1/0.1$.

The SEC trace of the PNIPAM showed a narrow and unimodal signal with a dispersity value of 1.17 and a $\overline{M_{n,SEC}}$ = 11600 g.mol^{-1} (Figure IV. 5). The presence of the trithiocarbonate group was confirmed by the appearance of a peak at 309 nm, characteristic wavelength of the C=S bond on the SEC trace using UV detection (Figure IV. 5).

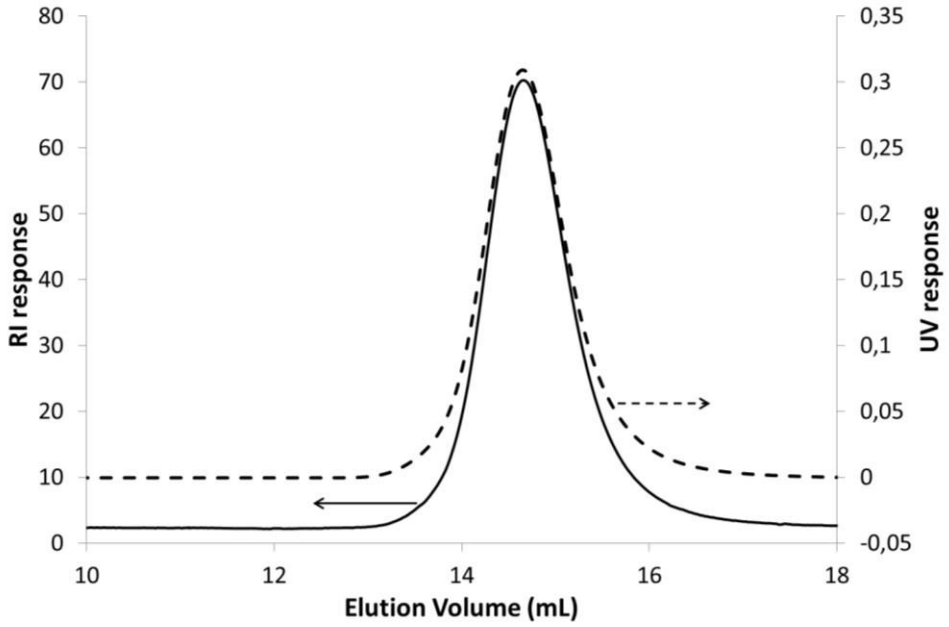

Figure IV. 5. Overlaid SEC traces of purified PNIPAM (solid line: RI response and dashed line: UV response at 309 nm) obtained from RAFT polymerization of NIPAM using COPYDC as chain transfer agent and AIBN as initiator in DMF at 70°C.

The PNIPAM structure was also evidenced by MALDI-TOF mass spectrometry (Figure IV. 6). The spectrum showed a single series of peaks separated by 113.136 Da, corresponding to the molar mass of the repeating unit (calculated value: 113.087 Da). The peak at 4081.987 Da corresponds to a polymer chain with 32 NIPAM units, a dodecyltrithiocarbonate moiety at ω-chain-end, a propargylamide group at α-chain-end, and a sodium entity as the atom responsible of the ionization (calculated value: 4081.886 Da).

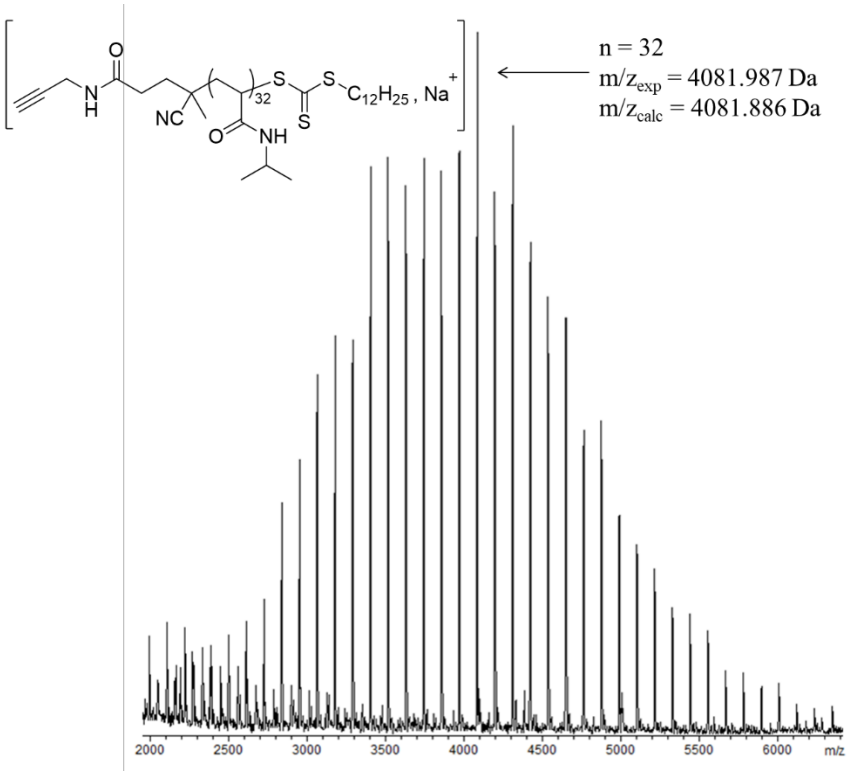

Figure IV. 6. MALDI-TOF mass spectrum of a PNIPAM synthesized by RAFT polymerization using the alkyne-based chain transfer agent COPYDC and AIBN as the initiator in DMF at 70°C. Matrix: DCTB, salt: Sodium trifluroacetate (NaTFA).

The ^{1}H NMR spectroscopy, the SEC in DMF (LiBr 1g.L^{-1}) and MALDI-TOF spectrometry showed that the alkyne-based chain transfer agent COPYDC efficiently mediates the RAFT polymerization to prepare well-defined heterofunctional PNIPAM. This PNIPAM is now used to model the reaction of trithiocarbonate removal using Perrier *et al.*[17] conditions.

2. Trithiocarbonate removal mediated through AIBN at 80°C

Methods for thiocarbonylthio group removal from polymers have been previously discussed in different reviews.[6,7] Among all the methods used to remove a trithiocarbonate,[6,7] the addition of an excess of radical initiator such as AIBN is a facile and efficient technique.[17] Hu *et al*. have shown that while this method is effective for removing chain-ends of polymers with a terminal methacrylate unit, it provides incomplete end group removal when applied to

polymers with a terminal acrylate or styrene unit.[20] When a polyacrylamide such as PNIPAM is considered, Zhang *et al.*[21] have shown that the dodecylthiocarbonylthio end group can be successfully removed by increasing the polymer concentration compare to Perrier's conditions.

In this work, the reaction was performed using a PNIPAM initial concentration of 0.012 mol.L^{-1} with 20 equivalents of AIBN in 1,4-dioxane at 80°C (Scheme IV. 2). Samples were withdrawn to follow the reaction by SEC using RI detection and UV-vis detection at 309 nm, the characteristic absorption wavelength of the trithiocarbonate group.

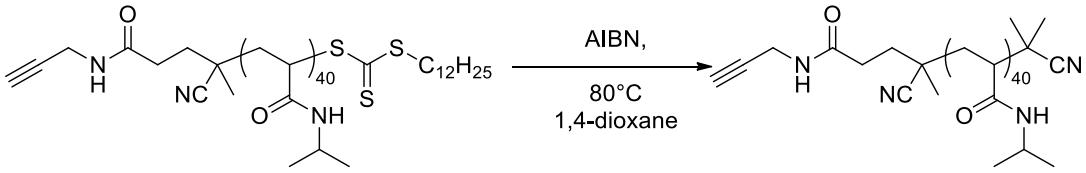

Scheme IV. 2. Removal of trithiocarbonate chain-end of α-alkynyl,ω-dodecyltrithiocarbonate PNIPAM using AIBN as radical initiator in 1,4-dioxane at 80°C.

SEC traces of crude mixtures showed that the UV-Vis signal at 309 nm corresponding to PNIPAM at an elution time of 14.4 min decreased with time (Figure IV. 7), evidencing the trithiocarbonate chain-end elimination. The trithiocarbonate removal was almost complete after 24 h with a conversion equals to 97 % (Table IV. 2) ($Đ \leq 1.17$).

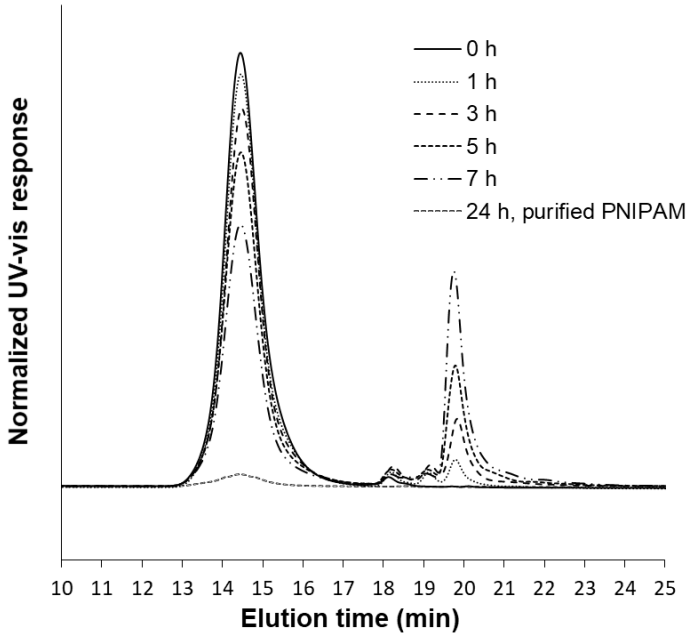

Figure IV. 7. Evolution with time of SEC traces obtained from crude mixtures and purified polymer resulting from the reaction of α-alkynyl,ω-dodecyl-trithiocarbonate PNIPAM with AIBN in 1,4-dioxane at 80°C (UV-vis detection at 309 nm).

Table IV. 2. Kinetic of the trithiocarbonate removal reaction of the α-alkynyl,ω-dodecyltrithiocarbonate PNIPAM using AIBN in 1,4-dioxane at 80°C.

Entry	Time (h)	$\overline{M_{n,SEC}}$ (g.mol^{-1})[a]	$Đ$[a]	Conv. (%)[b]
1	0	12300	1.14	0.0
2	1	12300	1.14	4.5
3	2	11900	1.14	12.8
4	3	11900	1.14	15.5
5	5	12400	1.14	23.4
6	7	12200	1.18	41.7
7	24	12800	1.17	97.0

[a] Determined by SEC in DMF with LiBr (1 $g.L^{-1}$) using PS standards. [b] Conversion calculated according to the following equation: conv. (%) = 100 - $\frac{[A_{t,UV}/A_{t,RI}]}{[A_{t0,UV}/A_{t0,RI}]}$ x 100 where $A_{t,RI}$ and $A_{t,UV}$ are peak areas at a given time (t) using respectively a RI detector and an UV-vis detector at 309 nm and $A_{t0,RI}$ and $A_{t0,UV}$ are peak areas before the reaction using respectively RI detector and UV-vis detector at 309 nm, respectively.

Efficient trithiocarbonate removal was also supported by discoloration of the polymer at the end of the reaction (Figure IV. 8).

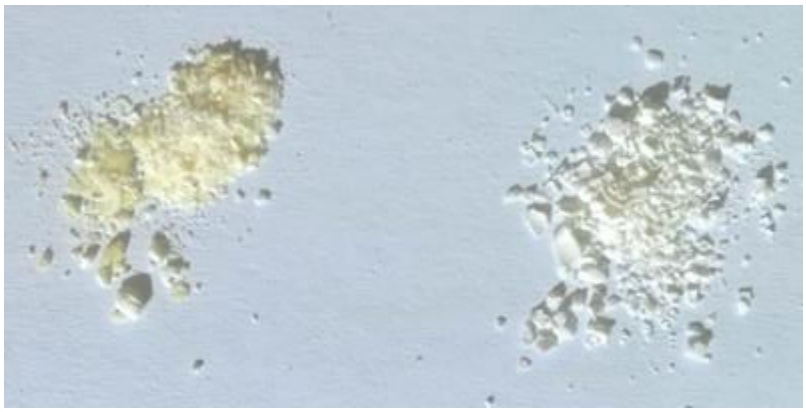

Figure IV. 8. Picture of α-alkynyl,ω-dodecyltrithiocarbonate PNIPAM before (left) and after (right) removal of the trithiocarbonate chain-end group using AIBN as radical initiator in 1,4-dioxane at 80°C.

The resulting polymer was further characterized by ^{1}H NMR spectroscopy after purification (Figure IV. 9). The spectrum showed the complete disappearance of the characteristic signals of the dodecyl chain-end (labelled a, b and c in Figure IV. 9). This result further confirms the success of the reaction. Furthermore, the purified polymer was characterized by SEC in DMF (LiBr 1 $g.L^{-1}$) (Figure IV. 7). The chromatogram showed the disappearance of the absorbance at 309 nm, with a low dispersity value ($Đ$ = 1.17). The low dispersity and the high conversion values demonstrate the absence of undesirable coupling reactions, and thus the efficiency of the reaction.

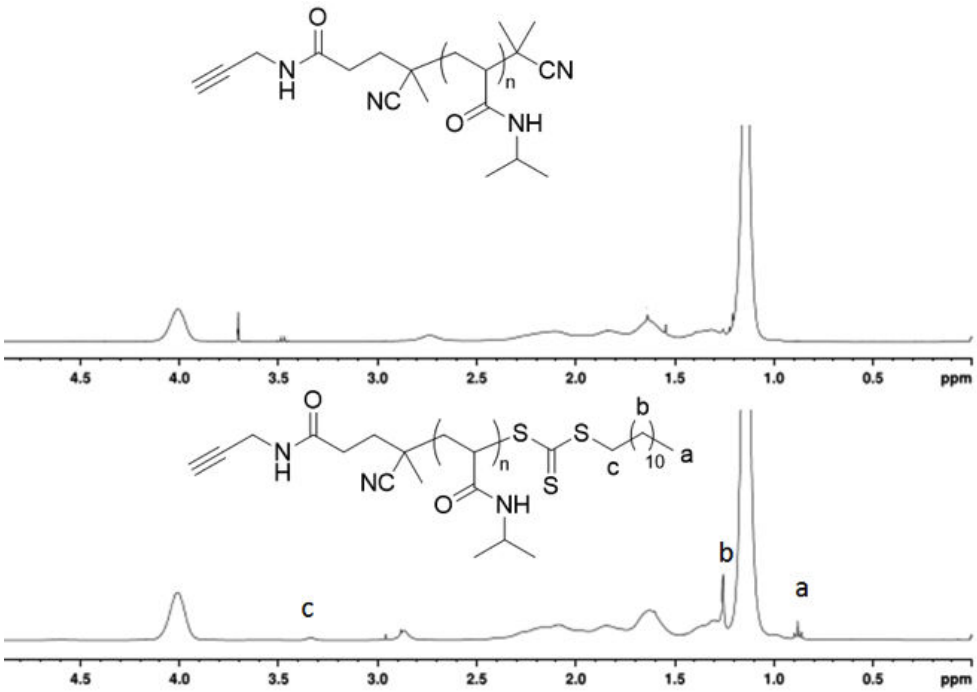

Figure IV. 9. ^{1}H NMR spectra (400 MHz, $CDCl_3$) of α-alkynyl,ω-dodecyltrithiocarbonate PNIPAM before (bottom) and after (top) trithiocarbonate removal reaction.

The ^{1}H NMR spectroscopy and the SEC analyses showed a complete trithiocarbonate removal in 24 hours. Experimental conditions used for the trithiocarbonate removal reaction with PNIPAM are then applied for the trithiocarbonate removal reaction on aPEO-*b*-P(DMAEA-*co*-*t*BocAEA) copolymer, and P(DMAEA-*co*-*t*BocAEA) copolymer using a photochemical-activation instead of thermal-activation. The photochemical-activation allowing the thiocarbonylthio removal in softer conditions than thermal one is studied in our work keeping AIBN as radical source.[22]

.

B. Trithiocarbonate removal on aPEO-*b*-P(DMAEA-*co*-*t*BocAEA) and P(DMAEA-*co*-*t*BocAEA) copolymers

A first reaction has been performed on an $aPEO_{64}$-*b*-$P(DMAEA_{11}$-*co*-*t*$BocAEA_4)$ using 20 equivalents of AIBN in ethanol activated with a mercury UV lamp of 125 W at 365 nm

(Scheme IV. 3). Ethanol was used because is a good solvent for the copolymer and is less cytotoxic than the 1,4-dioxane. Several samples were withdrawn to determine the conversion reaction by SEC in DMF (LiBr 1 $g.L^{-1}$) (Figure IV. 10).

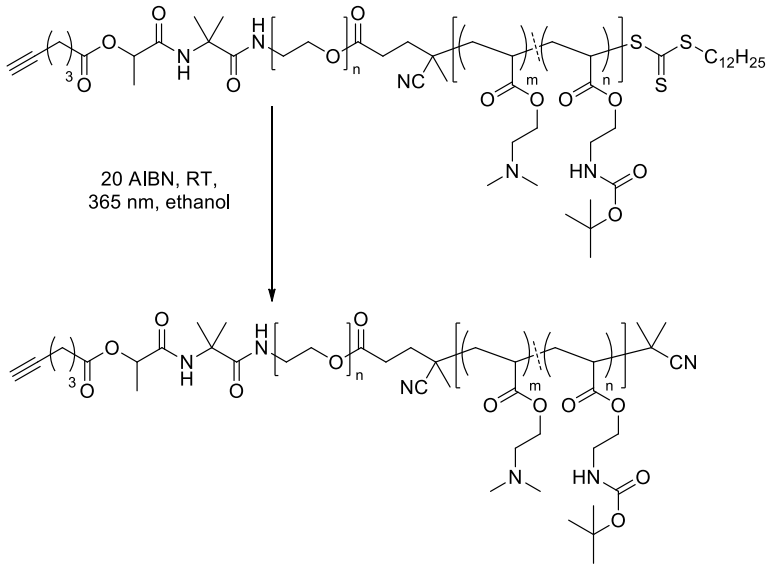

Scheme IV. 3. Removal of trithiocarbonate of a $aPEO_{64}$-*b*-P($DMAEA_{11}$-*co*-*t*$BocAEA_4$) mediated through 20 equivalents of AIBN in ethanol at room temperature using a UV lamp at 365 nm.

The Figure IV. 10 shows the decrease of SEC trace intensity of the copolymer with time using UV-vis detection at 309 nm. As for the model reaction using PNIPAM, the trithiocarbonate removal conversion was calculated by comparing the SEC trace areas of the copolymer at t = 0 and at t using UV-vis detection. Unlike the thermally activated reaction with PNIPAM, the reaction was launched during 2 weeks to finally reach a conversion of 89 % (Table IV. 3).

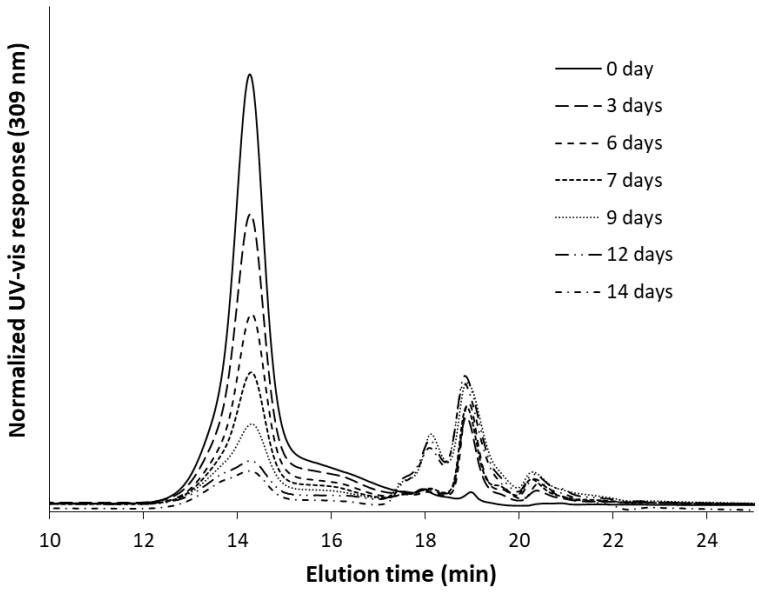

Figure IV. 10. Overlaid of SEC traces using the UV-vis detection fixed at 309 nm from crude mixtures resulting from the trithiocarbonate removal reaction of aPEO$_{64}$-*b*-P(DMAEA$_{11}$-*co*-*t*BocAEA$_4$) with AIBN in ethanol at room temperature using a UV lamp at 365 nm.

Table IV. 3. Kinetic of the trithiocarbonate removal reaction of aPEO$_{64}$-*b*-P(DMAEA$_{11}$-*co*-*t*BocAEA$_4$) using AIBN in ethanol under photochemical activation.

Entry	Time (days)	$\overline{M_{n,SEC}}$ (g.mol^{-1}) [a]	$Đ$ [a]	Conv. (%) [b]
t0	0	13500	1.19	0
t1	3	11700	1.32	37
t2	6	11600	1.31	56
t3	7	11900	1.31	68
t4	9	12600	1.25	78
t5	12	12200	1.36	87
t6	14	12300	1.31	89

[a] Determined by SEC in DMF with LiBr (1 $g.L^{-1}$) using PS standards. [b] Conversion calculated according to the following equation: conv. (%) = 100 - $\frac{[A_{t,UV}/A_{t,RI}]}{[A_{t0,UV}/A_{t0,RI}]}$ x 100 where $A_{t,RI}$ and $A_{t,UV}$ are peak areas at a given time (t) using respectively a RI detector and a UV-vis detector at 309 nm and $A_{t0,RI}$ and $A_{t0,UV}$ are peak areas before the reaction using respectively RI detector and UV-vis detector at 309 nm, respectively.

After 2 weeks of reaction, the reaction has been stopped and the resulting copolymer has been purified by several precipitation/decantation in cold diethyl ether/hexane mixture (50/50 v/v). The pure product was analyzed by ^{1}H NMR spectroscopy and SEC in DMF (LiBr 1 $g.L^{-1}$).

The overlaid ^{1}H NMR spectra of an $aPEO_{64}$-*b*-$P(DMAEA_{11}$-*co*-*t*$BocAEA_4)$ before and after trithiocarbonate removal shows the intensity decrease of the triplet at 0.88 ppm characteristic of the methyl protons $SCH_2(CH_2)_{10}CH_3$ of the dodecyl trithiocarbonate moiety (labelled v in Figure IV. 11). Moreover, the integration areas values of the methylene protons signal $CH_2CH_2OC(=O)$, $OCH_2CH_2N(CH_3)_2$ and OCH_2CH_2NH at 4.09 ppm (labelled i, m and p in Figure IV. 11) remain constant before and after the trithiocarbonate removal. The results show the trithiocarbonate removal together with the non-degradation of acrylate groups during reaction.

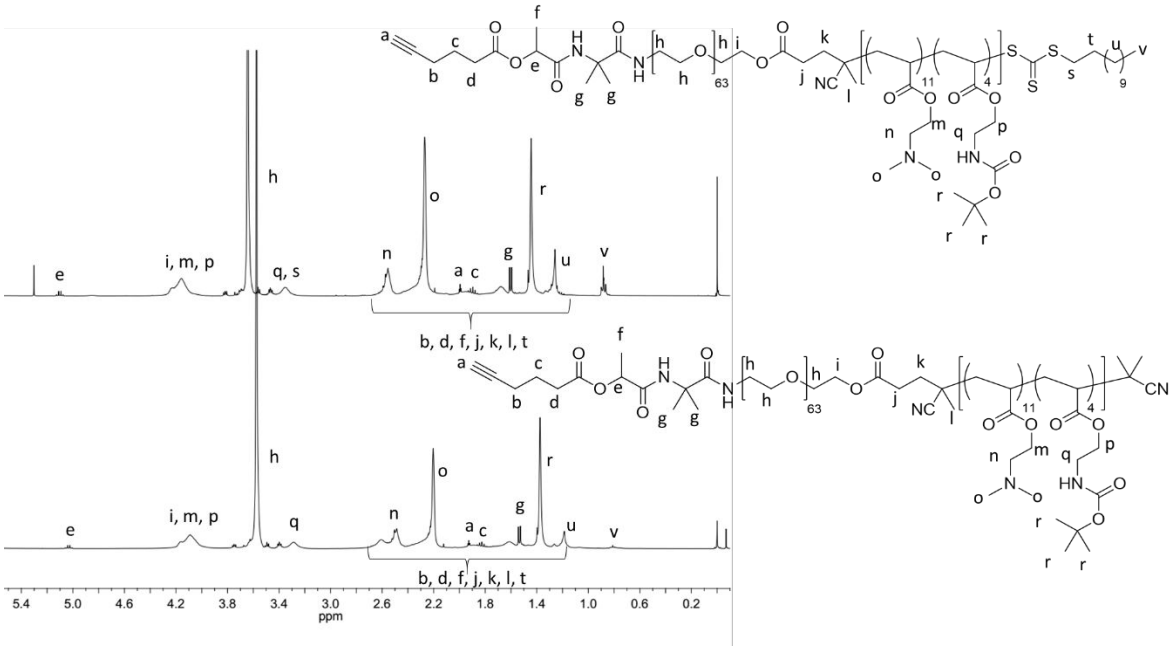

Figure IV. 11. ^{1}H NMR spectra (400 MHz, $CDCl_3$) of $aPEO_{64}$-*b*-$P(DMAEA_{11}$-*co*-*t*$BocAEA_4)$ before (top) and after (bottom) trithiocarbonate removal reaction mediated through AIBN in ethanol at room temperature and photo-activated using a UV lamp at 365 nm.

The SEC traces using the RI detection show a narrow and unimodal population before and after reaction (Figure IV. 12) with a low dispersity value after the reaction ($Đ$ = 1.19). Moreover, the overlaid SEC traces, using UV-vis detection at 309 nm, of $aPEO_{64}$-*b*-$P(DMAEA_{11}$-*co*-*t*$BocAEA_4)$ before and after trithiocarbonate removal shows drastic decrease of the absorbance after the reaction. This result confirms the efficiency of the reaction to remove trithiocarbonate by photo-activation.

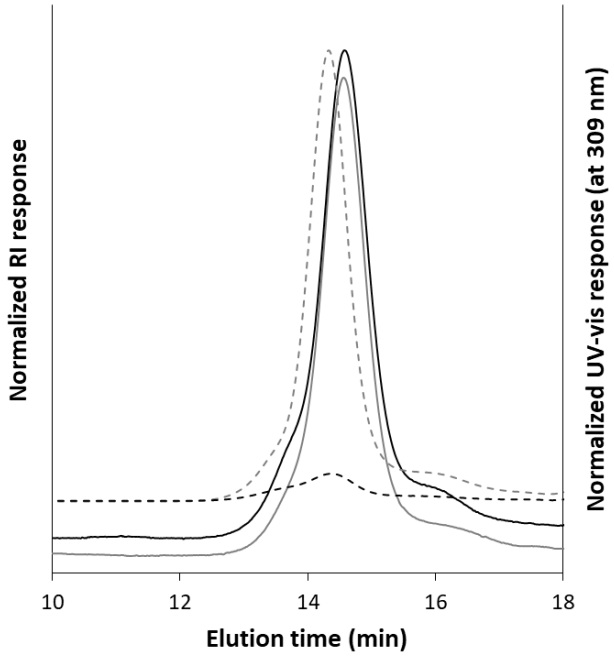

Figure IV. 12. Overlaid SEC traces of aPEO$_{64}$-*b*-P(DMAEA$_{11}$-*co*-*t*BocAEA$_4$) before (in grey) and after (in black) the trithiocarbonate removal reaction using RI detection (solid line) and UV-vis detection (fixed at 309 nm, dashed line).

The ^{1}H NMR spectra and the SEC in DMF (LiBr 1 g.L^{-1}) showed the efficiency to remove a trithiocarbonate by photo-activation. Moreover, the poly(aminoethyl acrylate)s were not degraded during the reaction. The reaction has been repeated on several aPEO-*b*-P(DMAEA-*co*-*t*BocAEA) copolymer and on several P(DMAEA-*co*-*t*BocAEA) copolymers with different DMAEA/*t*BocAEA molar ratios. Resulting copolymers have been cationized to study the impact of the dodecyltrithiocarbonate group on cytotoxicity (Table IV. 4). Because a lack of time, no trithiocarbonate group has been removed on PPEGA-*b*-P(DMAEA-*co*-*t*BocAEA) copolymers.

Table IV. 4. Macromolecular characteristics and trithiocarbonate removal conversion of aPEO-*b*-P(DMAEA-*co*-*t*BocAEA) and P(DMAEA-*co*-*t*BocAEA) copolymers using 20 equivalents of AIBN in ethanol mediated through photochemical-activation.

Polymer	PEO	$\overline{DP}_{n,PDMAEA}$	$\overline{DP}_{n,PtBocAEA}$	Trithiocarbonate Removal conv. % [a]
1	aPEO	25 [b]	10 [c]	90
2	aPEO	11 [b]	4 [c]	89
3	aPEO	5 [b]	10 [c]	89
4	aPEO	9 [b]	10 [c]	97
5	aPEO	5 [b]	11 [c]	82
6	None	9 [d]	13 [e]	81
7	None	4 [d]	14 [e]	89

[a] Conversion calculated according to the following equation: conv. (%) = 100 - $\frac{[A_{t,UV}/A_{t,RI}]}{[A_{t0,UV}/A_{t0,RI}]}$ x 100 where $A_{t,RI}$ and $A_{t,UV}$ are peak areas at a given time (t) using respectively a RI detector and an UV-vis detector at 309 nm and $A_{t0,RI}$ and $A_{t0,UV}$ are peak areas before the reaction using respectively RI detector and UV-vis detector at 309 nm, respectively. [b] Determined by ^{1}H NMR spectroscopy (400 MHz) in $CDCl_3$ by comparing integration area values of methine proton $CH_3CHC(=O)NH$ signals and methylene protons $OCH_2CH_2OC(=O)$, $OCH_2CH_2N(CH_3)_2$ and OCH_2CH_2NH [c] Determined by ^{1}H NMR spectroscopy (400 MHz) in $CDCl_3$ by comparing integration area values of methine proton $CH_3CHC(=O)NH$ signals and methylene protons OCH_2CH_2NH and $SCH_2(CH_2)_{10}CH_3$. [d] Determined by ^{1}H NMR spectroscopy (400 MHz) in $CDCl_3$ by comparing integration area values of the signal of the methyl proton $SCH_2(CH_2)_{10}CH_3$ and methylene protons $CH_2CH_2OC(=O)$, $OCH_2CH_2N(CH_3)_2$

and OCH_2CH_2NH. [e] Determined by ^1H NMR spectroscopy (400 MHz) in $CDCl_3$ by comparing integration area values of the signal of the methyl proton $SCH_2(CH_2)_{10}CH_3$ and methylene protons OCH_2CH_2NH and $SCH_2(CH_2)_{10}CH_3$.

II. Addition of a thiol based compound

To target specific cells, recognition ligands have been already added on polyplexes to increase their transfection efficiency.[23–25] In our work, the RGD has been chosen as recognition ligand due to its ability to target tumorous specific cells.[26,27] The RGD recognition ligand, as all peptides, is thermo-degradable.[28] Therefore, reactions able to be proceed in soft conditions (room temperature, aqueous solution, no by-products) were chosen to add the recognition ligand. As thiolated-RGD can be linked directly onto pyridyldithio and onto alkyne moieties, two strategies were studied: (i) by disulfide bond exchange using previously synthesized polymers containing the pyridyldithio-group at the α-position (Chapter 2 § I-A), and (ii) by thiol-yne coupling reaction using previously synthesized polymers containing the alkyne group at the α-position (Chapter 3 § I-B, C and D).

The thiol-disulfide coupling exchange has been modeled on an α-pyridyldithio,ω-hydroxylPEO synthesized in Chapter 2 I§A and the thiol-yne coupling reaction has been modeled on an α-alkynylPNIPAM synthesized in this Chapter (§I-A-2).

A. Thiol-disulfide coupling reaction

The reaction has been performed on the α-pyridyldithio,ω-hydroxylPEO ($\overline{M_{n,SEC}}$ = 8800 g.mol^{-1} and $Đ$ = 1.07) using 1.5 equivalent of *N*-acetylcysteine in phosphate buffering solution (pH = 7.5) (Scheme IV. 4). UV-vis spectrophotometry has been employed to determine the degree of functionalization.

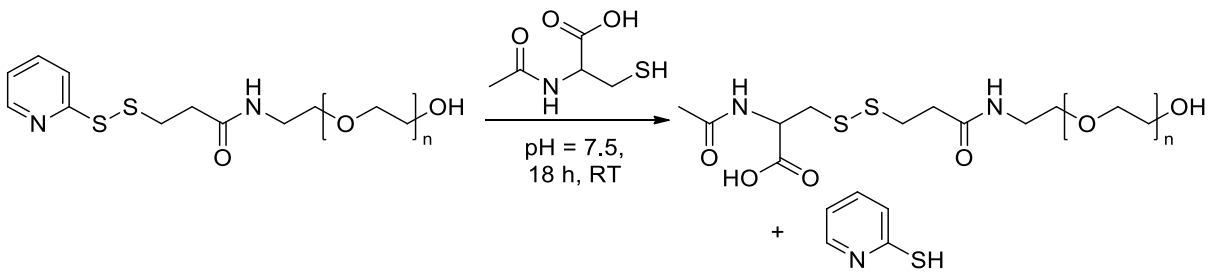

Scheme IV. 4. Thiol-disulfide coupling exchange reaction of α-pyridyldithio,ω-hydroxylPEO mediated through *N*-acetylcysteine in PBS (pH = 7.5) during 18 hours at room temperature.

The degree of functionalization of reaction has been calculated using 1 mL of media diluted by 10 and analyzed by UV-vis spectrophotometry (Figure IV. 13). A first band with a maximum wavelength at 272 nm corresponding to the α-pyridyldithio,ω-hydroxylPEO and a second band with a maximum wavelength at 343 nm corresponding to the 2-mercaptopyridine released during the reaction have been observed.

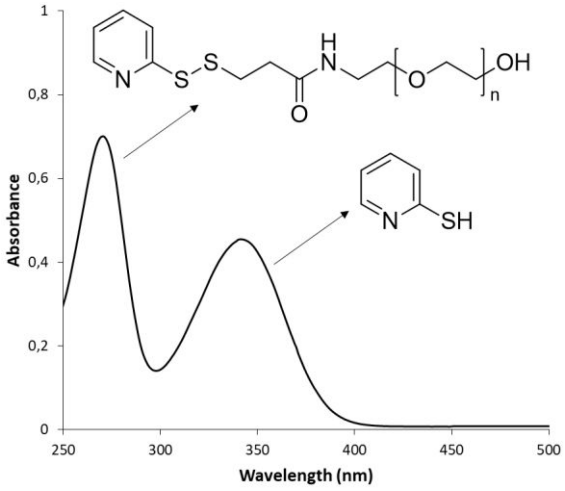

Figure IV. 13. UV-vis spectra of the crude mixture at t_f = 18 h of the disulfide coupling exchange reaction using *N*-acetylcysteine in PBS.

The degree of functionalization has been determined using the Beer-Lambert equation, initial concentration of α-pyridyldithio,ω-hydroxylPEO and the following equations.

$$\tau = 1 - \frac{C_{PEOt18h}}{C_{PEOt0}} \quad \text{Equation (IV. 1)}$$

$$C_{PEOt18h} = C_{PEOt0} - C_{MPt18h} \quad \text{Equation (IV. 2)}$$

$$\tau = \frac{C_{MPt18h}}{C_{PEOt0}} \quad \text{Equation (IV. 3)}$$

$$A_{343nm} = \frac{\varepsilon \times l \times C_{MPt18h}}{10} \quad \text{Equation (IV .4)}$$

$$\tau = \frac{A_{343nm} \times 10}{\varepsilon \times l \times C_{PEOt0}} \quad \text{Equation (IV. 5)}$$

Where, τ is the degree of functionalization, C_{PEOt18} is the molar concentration of α-pyridyldithio,ω-hydroxylPEO after 18 h of reaction, C_{PEOt0} is the intial molar concentration of α-pyridyldithio,ω-hydroxylPEO (C_{PEOt0} = 0.001 mmol.L^{-1}), C_{MPt18h} is the molar concentration of 2-mercaptopyridine after 18 h of reaction, A_{343nm} is the absorbance at 343 nm ($A_{343\ nm}$ = 0.4518), ε is the molar attenuation coefficient of 2-mercaptopyridine (ε = 8080 L.mol^{-1}.cm^{-1})[29,30] and l is the length of the UV-vis cell (l = 1 cm).

The degree of functionalization is equal to 56 %. The thiol-yne coupling reaction on α-alkynyl,ω-cyanoisopropylPNIPAM was then carried out in order to compare the functionalization degree obtained by the those two strategies.

B. Thiol-yne coupling reaction[‡]

The thiol-yne coupling reaction is performed using α-alkynyl,ω-cyanoisopropylPNIPAM and benzyl mercaptan as models using AIBN to generate radicals at 80°C in 1,4-dioxane (Scheme IV. 5). Benzyl mercaptan was used as a model molecule because it is easy to characterize by ^{1}H NMR spectroscopy thanks to the aromatic moiety leading to the characteristics signals between 7 and 8 ppm, and by SEC using UV-vis detection due to the characteristic absorption at 266.2 nm.

[‡]Le Bohec, M.; Pascual, S.; Piogé, S.; Fontaine, L.; Heterofunctional RAFT-derived PNIPAM *via* cascade trithiocarbonate removal and thiol-yne click coupling reaction. *Journal of Polymer Science Part A: Polymer chemistry* **2017**, accepted manuscript

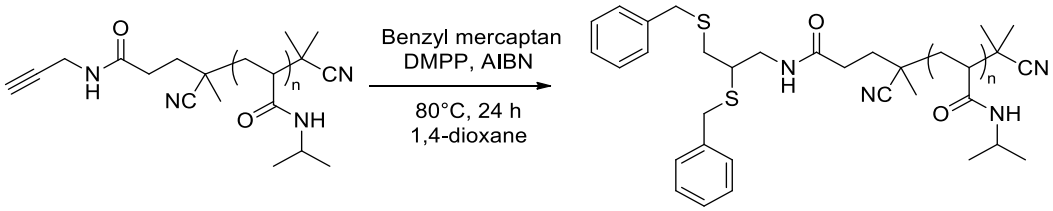

Scheme IV. 5. Thiol-yne coupling reaction of α-alkynyl-ω-cyanoisopropylPNIPAM with benzyl mercaptan using AIBN as radical initiator and dimethylphenyl phosphine (DMPP) as reducing agent in 1,4-dioxane at 80°C.

Different experimental conditions were tested in order to target a high thiol-yne coupling efficiency (Table IV. 5). The degree of functionalization was determined by SEC using UV-vis detection at 266.2 nm and confirmed by ^{1}H NMR spectroscopy. Results showed that the increase of the equivalent number of benzyl mercaptan leads to a better conversion: 6.2 % with 10 molar equivalents (Entry 1 in Table IV. 5) and 25 % with 20 equivalents (Entry 2 in Table IV. 5). Then, to increase the thiol-yne efficiency through the decrease of undesirable disulfide coupling reactions, DMPP was added as reducing agent.[31] Results showed that the addition of DMPP increased the conversion from 25 % to 39 % (Entries 2 and 3 in Table IV. 5).

Table IV. 5. Experimental conditions for the thiol-yne coupling reaction on α-alkynyl,ω-cyanoisopropylPNIPAM using benzyl mercaptan, DMPP as the reducing agent, and AIBN as the radical source in 1,4-dioxane at 80°C for 24 h.

Entry	Benzyl mercaptan (molar eq.)	DMPP (molar eq.)	τ (%)[a]
1	10	0	6.2
2	20	0	25
3	15	15	39

[a] τ: degree of functionalization determined by SEC using an UV-vis detector operating at 266.2 nm using the following equation: $\tau\ (\%) = \frac{[A_{t,UV}/A_{t,RI}]-[A_{t0,UV}/A_{t0,RI}]}{[A_{t0,UV}/A_{t0,RI}]}$ x 100 after purification with $A_{t,UV}$ and $A_{t,RI}$ peaks areas at a given moment using an UV-vis detector at 266.2 nm and a RI detector respectively and $A_{t0,UV}$ and $A_{t0,RI}$ are peaks areas a t = 0 using an UV-vis detector at 266.2 nm and a RI detector, respectively.

The PNIPAM resulting from optimal experimental conditions (Entry 3 in Table IV. 4) was purified and characterized by ^{1}H NMR (Figure IV. 14). The comparison of ^{1}H NMR spectra before and after thiol-yne coupling reaction showed the appearance of a signal corresponding to aromatics protons (labelled f, g and h in Figure IV.14) between 7 to 8 ppm. Moreover, the signal corresponding to the methylene protons S$CH_2C_6H_5$ appeared at 3.64 ppm (labelled e in Figure IV. 14). The thiol-yne reaction efficiency was determined by ^{1}H NMR spectroscopy using the integration area of the aromatic signal (C*H*=)$_2$CCH_2S at 7.52 ppm (labelled f in Figure IV. 14) and the integration area of SCH_2C*H*(S)CH_2NH protons and of NHC*H*$(CH_3)_2$ proton of the PNIPAM at 4.01 ppm (labelled d, c, b and a, respectively in Figure IV. 14) using the following equations. A 38 % conversion was thus calculated, in good agreement with the

conversion determined by SEC (39 %, Entry 3 in Table IV. 4). This low conversion is in agreement with the literature data. Indeed, previous reports have shown that thermally-induced hydrothiolation reactions give low degree of functionalization compare to photochemically-induced hydrothiolations which leads to higher degree of functionalization.[32,33]

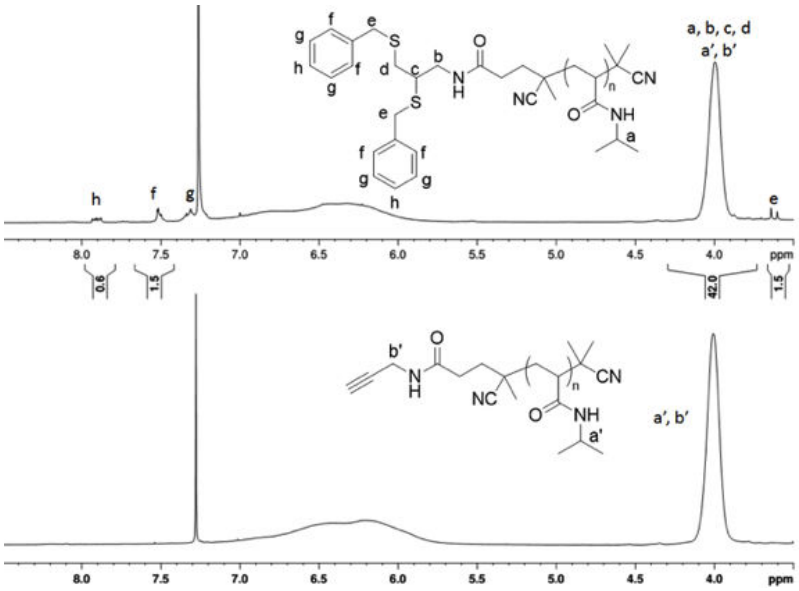

Figure IV. 14. ^{1}H NMR (400 MHz, $CDCl_3$) spectra between 3.5 ppm and 8.5 ppm of α-alkynyl,ω-cyanoisopropylPNIPAM before (bottom) and after (top) the thiol-yne coupling reaction.

The ^{1}H NMR spectrum and the SEC in DMF (LiBr 1 $g.L^{-1}$) show a functionalization degree of 38 % and 39 % of alkyne, respectively. This result shows the addition of 0.76 thiol group on one alkyne. The thiol-yne coupling reaction allows to add more thiol group than using the disulfide coupling reaction (0.56 thiol group on one α-pyridyldithio,ω-hydroxylPEO).

III. Tandem trithiocarbonate removal/thiol-yne reactions in a one-pot process[‡]

As previously shown, two steps are needed to be able to add thiol-based molecules onto RAFT polymers through a radical mechanism. The challenging one-pot radical mediated process *via* tandem thiol-yne/thiocarbonylthio chain-end removal reactions was studied.

This one-pot two-steps has been modeled using a α-alkynyl,ω-dodecyltrithiocarbonate-PNIPAM previously synthesized in this Chapter (§I-A-1) (Scheme IV. 6). Thus, such heterofunctional PNIPAM was first reacted with an excess of AIBN in 1,4-dioxane at 80°C for 24 hours; then 15 equivalents of benzyl mercaptan and 15 equivalents of DMPP were added and the reaction was continued for 24 hours (Scheme IV. 6). Samples were withdrawn to assess the trithiocarbonate removal efficiency using SEC with UV-Vis detection at 309 nm and the final sample was purified in order to determine the functionalization degree with the benzyl mercaptan by ^{1}H NMR spectroscopy analysis (Scheme IV. 6). Results are presented in Table IV. 6.

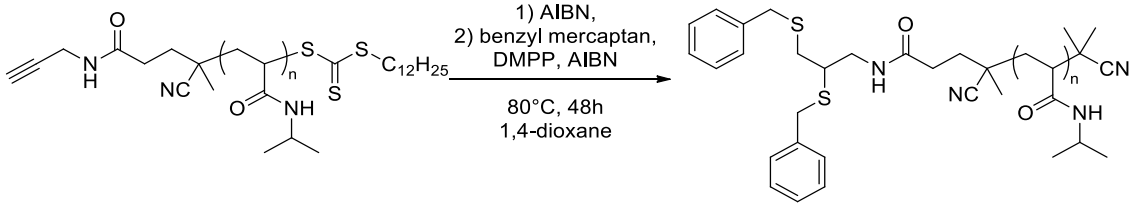

Scheme IV. 6. One-pot trithiocarbonate removal and thiol-yne coupling reactions of the α-alkynyl,ω-dodecyltrithiocarbonate PNIPAM using AIBN, benzyl mercaptan, and DMPP in 1,4-dioxane at 80°C.

[‡]Le Bohec, M.; Pascual, S.; Piogé, S.; Fontaine, L.; Heterofunctional RAFT-derived PNIPAM *via* cascade trithiocarbonate removal and thiol-yne click coupling reaction. *Journal of Polymer Science Part A: Polymer chemistry* **2017**, accepted manuscript

Table IV. 6. Conversions of trithiocarbonate removal/thiol-yne coupling during the one-pot reaction on the α-alkynyl,ω-dodecyltrithiocarbonate PNIPAM using AIBN, benzyl mercaptan and DMPP in 1,4-dioxane at 80°C.

Entry	Time (h)	Trithiocarbonate removal conv. (%) [a]	τ (%) [b]
1	24	99	0
2	48	97	40

[a] Conversion determined by SEC using UV-vis detection at 309 nm using the following equation: conv. (%) = $(1-\frac{[A_{t,UV}/A_{t,RI}]}{[A_{t0,UV}/A_{t0,RI}]})$x100 where $A_{t,UV\ nm}$ and $A_{t,RI}$ are peak areas at given time (t) using an UV-vis detector operating at 309 nm and a RI detector, respectively and $A_{t0,UV}$ and $A_{t0,RI}$ are peak areas before the reaction using an UV-vis detector operating at 309 nm and a RI detector, respectively. [b] τ: thiol-yne coupling degree of functionalitation determined by ^{1}H NMR spectroscopy (in CD_2Cl_2) analysis of purified PNIPAM using the following equation: τ (%) = $\frac{I_{7.25}\times(DP_n+2)}{10\times I_{3.90}-3\times I_{7.25}}\times 100$ where $I_{7.25}$ and $I_{3.90}$ are intensities of signals at 7.25 and 3.90 ppm, respectively.

Results showed that the trithiocarbonate moiety was completely removed after 24 hours of reaction (Entry 1 in Table IV. 6). The ^{1}H NMR spectrum (Figure IV. 15) of the purified PNIPAM shows a signal at 7.25 ppm corresponding to aromatic protons of the benzyl entity (labelled g in Figure IV. 15) and a signal at 3.54 ppm corresponding to methylene protons S$CH_2C_6H_5$ (labelled f in Figure IV. 15). The thiol-yne efficiency was determined by ^{1}H NMR spectroscopy using the signal at 3.90 ppm relative to methine protons of the PNIPAM units

(labelled b in Figure IV. 15), methylene and methine protons of the resulting ω-chain-end (labelled c, d and e in Figure IV. 15), and the signal at 7.25 ppm relative to aromatic protons (labelled g in Figure IV. 15). The degree of functionalization calculated was equal to 40 % (Entry 2 in Table 5). Such result is in good agreement with the first thiol-yne result (Entry 3, Table IV. 5).

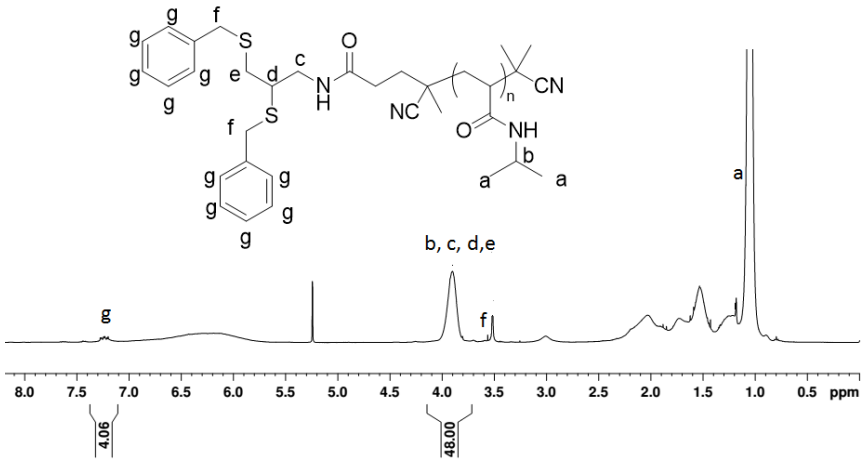

Figure IV. 15. ^{1}H NMR spectrum (400 MHz, CD_2Cl_2) of PNIPAM resulting from the one pot thrithiocarbonate removal/thiol-yne coupling reaction of the α-alkynyl,ω-dodecyltrithiocarbonate PNIPAM using AIBN, benzyl mercaptan and DMPP in 1,4-dioxane at 80°C.

In this one-pot reaction, while the trithiocarbonate removal conversion was high, the thiol-yne degree of functionalization remained limited. However, it should be noted that such a conversion allows for sufficient functionalization when applied to the bioconjugation of biologically active molecules or probes at polymer chain-end.[34,35]

As shown in I§B of this chapter, the trithiocarbonate removal reaction on aPEO-*b*-P(DMAEA-*co*-*t*BocAEA) copolymers, and P(DMAEA-*co*-*t*BocAEA) copolymers was used successfully through photochemical-activation. Therefore, the one-pot radical mediated process

via tandem trithiocarbonate removal/thiol-yne reactions will be employed using UV photochemical-activation in future work. This combination of reaction was never published and can be a good platform to introduce thiolated recognition ligand on RAFT copolymers through a radical process.

Conclusion

The incorporation of thiolated recognition ligand and the removal of unwanted trithiocarbonate group have been studied. Moreover, the combination of trithiocarbonate removal and thio-yne coupling reactions has been target *via* radical "one-pot" process.

The trithiocarbonate removal on aminoethyl acrylate based monomers was first modeled under thermo-activation using a PNIPAM. This PNIPAM was synthesized by RAFT polymerization using COPYDC as the chain transfer agent and AIBN as the initiator ($[NIPAM]_0/[COPYDC]_0/[AIBN]_0 = 100/1/0.1$). A conversion of 40 %, determined by ^{1}H NMR spectroscopy, was targeted to obtain a well-defined α-alkynyl,ω-dodecyltrithiocarbonate PNIPAM ($\overline{M_{n,SEC}}$ = 11600 g.mol^{-1}, $Đ$ = 1.17 and $\overline{DP_n}$ = 40). The structure was confirmed by MALDI-TOF mass spectrometry. Then the trithiocarbonate has been removed using 20 equivalents of AIBN as the radical source in 1,4-dioxane at 80°C. The reaction was followed by SEC using UV-vis detection at 309 nm. The conversion was equal to 97 % after 24 hours of reaction. This conversion was confirmed by ^{1}H NMR spectroscopy and SEC after purification. From this result and to maintain the integrity of the cationic polymer the trithiocarbonate removal of aminoethyl acrylate-based copolymers (aPEO-*b*-P(DMAEA-*co*-AEA) and P(DMAEA-*co*-AEA)) have been mediated through photochemical-activation using AIBN as the radical initiator. The reactions were followed by SEC and the conversions of trithiocarbonate removal were superior to 81 %. The ^{1}H NMR spectroscopy showed maintain of the integrity of the aminoethyl acrylate copolymers.

Two different pathways have been studied to covalently link a thiolated-recognition ligand. First, the thiol-disulfide exchange has been performed using an α-alkynyl,ω-hydroxylPEO and *N*-acetylcysteine as model (macro)molecules. The degree of functionalization was determined by UV-vis spectrophotometry and was equal to 0.56 thiol group per polymer chain. Then, the thiol-yne coupling reaction was studied using an α-alkynyl,ω-cyanoisopropylPNIPAM and benzyl mercaptan as the models (macro)molecules with AIBN as the radical initiator. The best conditions was obtained with 15 equivalents of benzyl mercaptan and 15 equivalents of DMPP leading to 0.76 thiol group per polymer chain, determined by ^{1}H NMR spectroscopy.

Then the "one-pot" cascade thiol-yne click reaction and radical-induced trithiocarbonate removal through radical mechanism was explored. The reaction was performed on an α-alkynyl,ω-dodecyltrithiocarbonate PNIPAM using AIBN to remove the trithiocarbonate on the ω-positions and AIBN, benzyl mercaptan and DMPP to functionalize the α-position by thiol-yne "click" chemistry. The SEC after 24 hours of reaction showed a complete removal of trithiocarbonate group and the ^{1}H NMR spectroscopy showed a degree of functionalization of 0.80 thiol molecule onto the alkyne bond, as shown ny ^{1}H NMR spectroscopy.

The aminoethyl acrylate-based copolymer after trithiocarbonate removal reaction will be cationized, deprotected and used to study the impact of the dodecyltrithiocarbonate on cytotoxicity and DNA binding affinity.

Experimental part

A. Reagents

All reagents were purchased from Aldrich unless otherwise noted. Sodium trifluoroacetate (NaTFA, ≥ 98 %), *trans*-2-[3-(4-*tert*-butylphenyl)-2-methyl-2-propenylidene]-malononitrile (DCTB, ≥ 98 %), *N*-isopropylacrylamide (NIPAM, ≥ 99 %), dimethylphenylphosphine (DMPP, 99 %), 1,4-dioxane (≥ 99.5 %), benzyl mercaptan (99 %), ethylenediaminetetraacetic acid (EDTA, 98 %), *N*-acetylcysteine (99 %), hexane (≥ 95 %), *N,N*-dimethylformamide (DMF), dibasic sodium phosphate ($Na_2H_2PO_4$, 99 %), basic sodium phosphate (Na_2HPO_4, Prolabo), diethyl ether (99.8 %, Carlo Erba), acetone (≥ 99.8 %, Carlo Erba) and ethanol (96 %, Carlo Erba). 2,2'-Azobis(2-methylpropionitrile) (AIBN, 98 %, Acros-Organics) was recrystallized from methanol once. COPYDC has been synthesized following procedure detailed in the Chapter 2 II§A. The α-pyridyldithio,ω-hydroxylPEO was synthesized in Chapter 2 §I-A ($\overline{M_{n,SEC}}$ = 8800 g.mol^{-1}, $Đ$ = 1.07). The aPEO$_{64}$-*b*-P(DMAEA$_{11}$-*co*-AEA$_4$) were synthesized in Chapter 3 §I-B ($\overline{M_{n,SEC}}$ = 11300 g.mol^{-1}, $Đ$ = 1.22). Dichloromethane (CH_2Cl_2, HPLC grade, Fisher Chemical) were dried over dry solvent stations GT S100. Ultra-pure water was obtained from a Millipore Direct Q system and had a conductivity of 18.2 MΩcm at 25°C. All deuterated solvent were purchased from Euriso-top.

B. General characterization

Nuclear Magnetic Resonance (NMR) spectra were recorded on a Bruker AC-400 spectrometer for ^{1}H NMR (400 MHz). Chemical shifts are reported in ppm relative to the deuterated solvent resonances.

The average molar masses (number-average molar mass $\overline{M_{n,SEC}}$, weight-average molar mass $\overline{M_{w,SEC}}$ and dispersity ($Đ = \overline{M_{w,SEC}}/\overline{M_{n,SEC}}$) values were measured by Size Exclusion

Chromatography (SEC) using DMF-LiBr (1 $g.L^{-1}$) as an eluent and carried out using a system equipped with a guard column (Polymer Laboratories, PL Gel 5 µm) followed by two columns (Polymer Laboratories, 2 PL gel 5 µm MIXED-D columns) and with a Waters 410 differential refractometer (RI) and a Waters 481 UV-Visible detector. The instrument operated at a flow rate of 1.0 $mL.min^{-1}$ at 60°C and was calibrated with narrow linear polystyrene (PS) standards ranging in molar mass from 580 $g.mol^{-1}$ to 483000 $g.mol^{-1}$. Molar masses and dispersities were calculated using Waters EMPOWER software.

MALDI-TOF Mass Spectrometry analyses were performed on a Bruker UltraFlex II instrument equipped with a nitrogen laser operating at 337 nm, pulsed ion extraction source and reflectron. Spectra were recorded in the reflectron mode with an acceleration voltage of 25 kV and a delay of 300 ns, 500 single shot aquisitions were summed to give the spectra and the data were analyzed using Bruker FlexAnalysis and Polytools softwares. Samples were prepared by dissolving the matrix (*trans*-2-[3-(4-*tert*-butylphenyl)-2-methyl-2-propenylidene]malononitrile, DCTB) in the solvent (CH_2Cl_2, 30 $mg.mL^{-1}$) and mixing with the polymer (10 $mg.mL^{-1}$) in the ratio 1/10 (v/v). 1 µL was spotted directly onto a thin layer of sodium trifluoroacetate (NaTFA) in acetone (concentration 19 $mg.mL^{-1}$) that had been deposited to act as a cationizing agent. UV-vis spectra of polymers were recorded using a VWR UV-3090PC. Spectra were analyzed with UV-vis Analyst software.

C. Trithiocarbonate Removal

1. PNIPAM used as a model polymer to trithiocarbonate removal

a) RAFT polymerization of NIPAM with COPYDC

A magnetic stir bar was charged to a round bottom flask together COPYDC (200.2 g, 0.455 mmol), AIBN (7.5 mg, 0.045 mmol), NIPAM (5.1354 g, 45.45 mmol) and DMF (8.63 mL). The solution was degassed during 30 minutes with argon then heated at 70°C The solution

was degassed with argon for 30 minutes and immersed in an oil bath thermostated at 70°C. Aliquots were withdrawn and are analyzed by ^{1}H NMR spectroscopy to determine NIPAM conversion and SEC in DMF (LiBr 1 g.L^{-1}) to determine the $\overline{M_{n,SEC}}$ and the *Đ*. The reaction was stopped by opening the reaction to the air and cooling the round bottom flask in liquid nitrogen. Conversion of NIPAM was determined to be 40 % by ^{1}H NMR spectroscopy by comparing the integration area values of the vinylic protons signals of NIPAM between 6.0 and 6.3 ppm and of the formamide proton signal of DMF used at internal standard at 8.02 ppm. The DMF was removed under vacuum and the polymer was dissolved in a minimum of CH_2Cl_2 and precipitated three times in cold diethyl ether. The solid obtained was dried under vacuum in the presence of P_2O_5. A yellow powder was obtained with a yield of 82 %. The final product was analyzed by ^{1}H NMR spectroscopy and SEC in DMF (LiBr 1g.L^{-1}).

^{1}H NMR (400 MHz, $CDCl_3$), δ (ppm): 0.88 (t, $SCH_2(CH_2)_{10}CH_3$, 3 H), 0.9-2.5 (m, *H*C≡CCH_2NH, C*H*$_2$C*H*$_2$C(CN)(CH_3), (C*H*$_2$C*H*)$_{40}$, NHCH(C*H*$_3$)$_2$, $SCH_2(CH_2)_{10}CH_3$), 3.35 (m, $SCH_2(CH_2)_{10}CH_3$), 4.01 (m, HC≡CC*H*$_2$NH and NHC*H*(CH_3)$_2$, 42.12 H), 6.33 (m, N*H*CH(CH_3)$_2$ and HC≡CCH_2N*H*).

SEC in DMF (LiBr 1 g.L^{-1}): $\overline{M_{n,SEC}}$ = 11600 g.mol^{-1}, Đ = 1.17.

b) Trithiocarbonate removal mediated through AIBN at 80°C.

A round bottom flask was charged with a stir bar together with PNIPAM (400.3 mg, 0.081 mmol), AIBN (264.6 mg, 1.611 mmol) and 1,4-dioxane (6.96 mL). The solution was degassed using argon during 15 minutes. The solution was heated at 80°C during 24 hours. Samples were withdrawn from reaction mixture at different times (0, 1, 2, 3, 5, 7 h) to follow the reaction kinetic by SEC. The conversion was calculated using the following equation and was equal to 97 %.

$$\text{Trithiocarbonate removal conversion (\%)} = 100 - \frac{A_{t,UV}/A_{t,\,RI}}{A_{t0,UV}/A_{t0,\,RI}} \times 100 \quad \text{Equation (IV. 6)}$$

where $A_{t,UV}$ and $A_{t,RI}$ represent peak areas at a given reaction time (t) using a UV-vis detector operating at 309 nm and a RI detector, respectively and where $A_{t0,UV}$ and $A_{t0,RI}$ represent peak areas at t = 0 using a UV-vis detector operating at 309 nm and a RI detector, respectively.

The solvent was evaporated from the final sample, the polymer was dissolved in a minimum of CH_2Cl_2 and precipitated dropwise three times in cold diethyl ether. The white solid was dried under vacuum at 40°C. The yield of 80 % was determined by gravimetry.

The trithiocarbonate removal conversion was also confirmed by ^{1}H NMR spectroscopy (400 MHz, $CDCl_3$) verifying the disappearance of the methyl signal at 0.88 ppm of the CH_3 of the dodecyl chain before and after reaction and purification. The product was characterized by ^{1}H NMR spectroscopy in $CDCl_3$ and by SEC in DMF (LiBr 1 g.L^{-1}).

^{1}H NMR (400 MHz, $CDCl_3$), δ (ppm): 0.9-2.5 (m, *H*C≡CCH$_2$NH, C*H*$_2$C*H*$_2$C(CN) (C*H*$_3$), (C*H*$_2$C*H*)$_{40}$, NHCH(C*H*$_3$)$_2$, CHCC(C*H*$_3$)$_2$(CN), 4.01 (m, HC≡CC*H*$_2$NH and NHC*H*(CH$_3$)$_2$), 6.33 (m, HC≡CCH$_2$N*H* and N*H*CH(CH$_3$)$_2$).

SEC in DMF (LiBr 1 g.L^{-1}): $\overline{M_{n,SEC}}$ = 12800 g.mol^{-1}, $Đ$ = 1.17.

2. Trithiocarbonate removal on PEO-*b*-P(DMAEA-*co*-*t*BocAEA) and P(DMAEA-*co*-*t*BocAEA) copolymers

In a typical procedure, a quartz round bottom flask was charged a stir bar together with PEO$_{64}$-*b*-P(DMAEA$_{11}$-*co*-*t*BocAEA$_4$) (150.7 mg, 0.0245 mmol), AIBN (80.2 mg, 0.489 mmol) in 7.4 mL of ethanol. The solution was degassed under argon and the reaction was launched at room temperature under UV-vis irradiation (365 nm) using a Philips HPR 125 W Hg lamp at 25 cm of the sample. Several aliquots were withdrawn to determine the conversion by SEC in

DMF (LiBr 1 g.L^{-1}). The conversion of 89 % was calculated by SEC by comparing peaks areas using a RI detector and a UV-vis detector (fixed at 309 nm) using the following equation:

$$\text{Trithiocarbonate removal conversion (\%)} = 100 - \frac{A_{t,UV}/A_{t,\,RI}}{A_{t0,UV}/A_{t0,\,RI}} \times 100 \quad \text{Equation (IV. 6)}$$

where $A_{t,UV}$ and $A_{t,RI}$ represent peak areas at a given reaction time (t) using a UV-vis detector operating at 309 nm and a RI detector, respectively and where $A_{t0,UV}$ and $A_{t0,RI}$ represent peak areas at t = 0 using a UV-vis detector operating at 309 nm and a RI detector, respectively.

The reaction was stopped after 14 days of reaction and the crude mixture was evaporated under vacuum. The crude oiled was dissolved in a minimum of acetone and precipitated in a cold mixture of hexane and diethyl ether (50/50 v/v), then the mixture was centrifuged (7000 rpm, 5 min, 0°C). The operation was repeated three times.

The solid obtained was dried under vacuum and analyzed by ^{1}H NMR spectroscopy and SEC in DMF (LiBr 1 g.L^{-1}).

^{1}H NMR spectroscopy (400 MHz, $CDCl_3$), δ (ppm): 0.88 (t, $SCH_2(CH_2)_{10}CH_3$, 2.70 H), 1.05-2.70 (m, $HC{\equiv}CCH_2CH_2CH_2$, $CH_3CHC(=O)NH$, $NHC(CH_3)_2C(=O)$, $CH_2CH_2C(CN)(CH_3)$, $(CH_2CH)_{15}$, $OCH_2CH_2N(CH_3)_2$, $OCH_2CH_2N(CH_3)_2$, $NHC(=O)OC(CH_3)_3$, $SCH_2(CH_2)CH_3$, 212.71 H), 3.29 (m, $CH_2NHC(=O)O$, 8.55 H), 3.57 (m, $(CH_2CH_2O)_{64}$, 254 H), 4.09 (m, $OCH_2CH_2OC(=O)$, $OCH_2CH_2N(CH_3)_2$, OCH_2CH_2NH, 32.77 H), 5.04 (q, $CH_3CHC(=O)NH$, 1.81 H).

SEC in DMF (LiBr 1 g.L^{-1}): $\overline{M_{n,SEC}}$ = 12600 g.mol^{-1}, $Đ$ = 1.19

D. Addition of a thiol based compound

1. Thiol-disulfide coupling reaction

A buffering solution of ethylenediaminetetraacetic acid (EDTA) (14.9 mg, 0.051 mmol), Na_2HPO_4 (433.1 mg, 3.05 mmol) and NaH_2PO_4 (168.2 mg, 1.17 mmol) at pH = 7.5 was prepared in 50 mL of ultra-pure water. In a round bottom flask, the α-pyridyldithio,ω-hydroxylPEO (25.1 mg, 0.0079 mmol) and the *N*-acetylcysteine (2.0 mg, 0.012 mmol) were dissolved in 8 mL of the PBS solution previously prepared. The reaction was launched at room temperature. A t= 18 h, 1 mL of media was withdrawn of an initial molar concentration equal to 0.001 mmol.L^{-1}, diluted by ten in PBS and analyzed by UV-vis spectrophotometry. The conversion of 56 % was calculated by UV-vis spectrophotometry using the following equations:

$$\tau = 1 - \frac{C_{PEOt18h}}{C_{PEOt0}} \quad \text{Equation (IV. 1)}$$

$$C_{PEOt18h} = C_{PEOt0} - C_{MPt18h} \quad \text{Equation (IV. 2)}$$

$$\tau = \frac{C_{MPt18h}}{C_{PEOt0}} \quad \text{Equation (IV. 3)}$$

$$A_{343nm} = \frac{\varepsilon \times l \times C_{MPt18h}}{10} \quad \text{Equation (IV .4)}$$

$$\tau = \frac{A_{343nm} \times 10}{\varepsilon \times l \times C_{PEOt0}} \quad \text{Equation (IV. 5)}$$

Where, τ is the degree of functionalization, C_{PEO} is the molar concentration of α-pyridyldithio,ω-hydroxylPEO after 18 h of reaction, C_{PEOt0} is the intial molar concentration of α-pyridyldithio,ω-hydroxylPEO (C_{PEOt0} = 0.001 mmol.L^{-1}), C_{MPt18h} is the molar concentration of 2-mercaptopyridine after 18 h of reaction, A_{343nm} is the absorbance at 343 nm (A_{343nm} = 0.4518), ε is the molar attenuation coefficient of 2-mercaptopyridine (ε = 8080 L.mol^{-1}.cm^{-1})[29,30] and l is the length of the UV-vis cell (l = 1 cm).

2. Thiol-yne coupling reaction.

To a round bottom flask were added α-alkynyl,ω-dodecyltrithiocarbonate PNIPAM (50 mg, 1.3×10^{-2} mmol, $\overline{M_{n,SEC}} = 11600$ g.mol^{-1}), AIBN (0.1 equivalent toward benzyl mercaptan), benzyl mercaptan (from 10 to 20 equivalents toward PNIPAM), DMPP (from 0 to 10 equivalents toward benzyl mercaptan) and 1,4-dioxane (0,9 mL). The solution was degassed with argon during 15 minutes and then heated at 80°C fot 24 hours. The solvent was evaporated, the polymer was dissolved with a minimum of CH_2Cl_2 and precipitated in cold diethyl ether three times. The solid obtained was dried under vacuum at 40°C. The degree of functionalization of the thiol-yne coupling reaction was determined by SEC comparing peaks areas using a RI detector and peaks areas using a UV-vis detector (fixed at 266.2 nm) using the following equation:

$$\tau\ (\%) = \frac{A_{t,UV}/A_{t,\ RI} - A_{t0,UV}/A_{t0,RI}}{A_{t0,UV}/A_{t0,\ RI}} \times 100 \quad \text{Equation (IV. 7)}$$

where τ is the degree of functionalization of thiol-yne coupling, $A_{t,UV}$ represents the peak area after the reaction using a UV-vis detector operating at 266.2 nm, $A_{t,RI}$ represents the peak area after the reaction using a RI detector, $A_{t0,UV}$ represents the peak area at $t = 0$ the reaction using a UV-vis detector operating at 266.2 nm and $A_{t0,RI}$ represents the peak area at $t = 0$ the reaction using a RI detector.

The degree of functionalization was also determined by ^{1}H NMR spectroscopy using the following set of equations:

$$I_{7.52} = 4 \times x \times y \quad \text{Equation (IV. 8)}$$

where $I_{7.52}$ is the intensity of the signal at 7.52 ppm, τ is the degree of functionalization, 4 is the number of aromatic protons at 7.52 ppm for a 100 % conversion and y is the integration coefficient.

$$I_{4.01} = (DP_n+2\,(1-x) + 5\,x) \times y \quad \text{Equation (IV. 9)}$$

where $I_{4.01}$ is the intensity of the signal at 4.01 ppm, DP_n is the number-average degree of polymerization of NIPAM, 2(1-x) is the number of methylene protons in α position of the alkyne bond according to the conversion and 5x is the number of protons for a 100 % conversion at 4.01 ppm.

$$x = \frac{I_{7.52} \times (DP_n+2)}{(4 \times I_{4.01} - 3 \times I_{7.52})} \quad \text{Equation (IV. 10)}$$

The product was characterized by ^{1}H NMR spectroscopy in $CDCl_3$ and by SEC in DMF (LiBr 1 $g.L^{-1}$). ^{1}H NMR (400 MHz, $CDCl_3$) δ (ppm) = 0.90-2.50 (m, C*H*$_2$C*H*$_2$C(C*H*$_3$)(CN), C*H*$_2$C*H*, *H*C≡CCH$_2$, NHCH(C*H*$_3$)$_2$, CHC(C*H*$_3$)$_2$(CN)), 3.64 (d, SC*H*$_2$C$_6$H$_5$, 1.5 H); 4.01 (m, SC*H*$_2$C*H*(S)C*H*$_2$NH, HC≡CC*H*$_2$NH and NHC*H*(CH$_3$)$_2$, 42.0 H), 6.33 (m, N*H*CH(CH$_3$)$_2$, N*H*CH$_2$CH), 7.30 (m, (C*H*CH=)$_2$CCH$_2$S), 7.52 (m, (CH=)$_2$CCHS, 1.5 H), 7.90 (m, C*H*(CHCH=)2CCH$_2$S, 0.6 H).

E. Tandem trithiocarbonate removal/thiol-yne reactions in a one-pot process.

In a round bottom flask a stir bar was charged together with PNIPAM (200.1 mg, 0.040 mmol), AIBN (132.2 mg, 0.806 mmol) and 1,4-dioxane (3.45 mL). This first solution was degassed with argon during 15 minutes and the reaction was launched at 80 °C for 24 hours. An aliquot was withdrawn to determine the trithiocarbonate removal reaction using SEC. A second solution previously degassed containing benzyl mercaptan (73.2 mg, 0.589 mmol), AIBN (9.7 mg, 0.059 mmol) and DMPP (85.0 mg, 0.615 mmol) was added to the first solution

under argon for further 24 h. The solution was precipitated in cold diethyl ether three times. The solid obtained was dried under vacuum at 40°C and analyzed by ^{1}H NMR spectroscopy in CD_2Cl_2 and by SEC in DMF (LiBr 1 g.L^{-1}). A white powder was obtained with a yield of 50 %. The conversion of the trithiocarbonate removal reaction was determined by SEC comparing peaks areas using a RI detector and a UV-vis detector operating at 309 nm. The degree of functionalization of the thiol-yne coupling reaction was determined by ^{1}H NMR spectroscopy using the following set of equations:

$$I_{7.25} = 10 \times x \times y \quad \text{Equation (IV. 11)}$$

where $I_{7.25}$ is the intensity of the signal at 7.25 ppm, 10 is the number of aromatic protons at 7.25 ppm for a 100 % conversion, x is the degree of functionalization and y is the integration coefficient.

$$I_{3.90} = (DP_n + 2\,(1-x) + 5\,x) \times y \quad \text{Equation (IV. 12)}$$

where $I_{3.90}$ is the intensity of the signal at 3.90 ppm, DP_n is the number-average degree of polymerization of NIPAM, 2(1-x) is the number of methylene protons in α-position of the alkyne bond according to the conversion and 5x is the number of protons at 3.90 ppm for a 100 % conversion.

$$x = \frac{I_{7.25} \times (DP_n + 2)}{(10 \times I_{3.90} - 3 \times I_{7.25})} \quad \text{Equation (IV .13)}$$

^{1}H NMR (400 MHz, CD_2Cl_2) δ (ppm) = 0.90-2.50 (m, C*H*$_2$C*H*$_2$C(C*H*$_3$)(CN), C*H*$_2$C*H*, *H*C≡CCH$_2$, NHCH(C*H*$_3$)$_2$, CHC(C*H*$_3$)$_2$(CN)), 3.54 (d, SC*H*$_2$C$_6$H$_5$); 3.90 (m, SC*H*$_2$C*H*(S)C*H*$_2$NH, HC≡CC*H*$_2$NH, NHC*H*(CH$_3$)$_2$, 48 H), 6.28 (N*H*CH(CH$_3$)$_2$, N*H*CH$_2$CH), 7.25 (C$_6$*H*$_5$, 4.06 H).

References

(1) Moldenhauer, F.; Theato, P. Sequential Reactions for Post-Polymerization Modifications. In *Multi-Component and Sequential Reactions in Polymer Synthesis*; Theato, P., Ed.; Springer International Publishing: Cham, **2015**; 133–162.

(2) Lunn, D. J.; Discekici, E. H.; Read de Alaniz, J.; Gutekunst, W. R.; Hawker, C. J. Established and Emerging Strategies for Polymer Chain-End Modification. *Journal of Polymer Science Part A: Polymer Chemistry* **2017**, *55* (18), 2903–2914.

(3) Pissuwan, D.; Boyer, C.; Gunasekaran, K.; Davis, T. P.; Bulmus, V. In Vitro Cytotoxicity of RAFT Polymers. *Biomacromolecules* **2010**, *11* (2), 412–420.

(4) Thomas, D. B.; Convertine, A. J.; Hester, R. D.; Lowe, A. B.; McCormick, C. L. Hydrolytic Susceptibility of Dithioester Chain Transfer Agents and Implications in Aqueous RAFT Polymerizations. *Macromolecules* **2004**, *37* (5), 1735–1741.

(5) Harrisson, S. Radical-Catalyzed Oxidation of Thiols by Trithiocarbonate and Dithioester RAFT Agents: Implications for the Preparation of Polymers with Terminal Thiol Functionality. *Macromolecules* **2009**, *42* (4), 897–898.

(6) Willcock, H.; O'Reilly, R. K. End Group Removal and Modification of RAFT Polymers. *Polymer Chemistry* **2010**, *1* (2), 149–157.

(7) Moad, G.; Rizzardo, E.; Thang, S. H. End-Functional Polymers, Thiocarbonylthio Group Removal/Transformation and Reversible Addition-Fragmentation-Chain Transfer (RAFT) Polymerization. *Polymer International* **2011**, *60* (1), 9–25.

(8) Lowe, A. B. Thiol-Yne "click"/Coupling Chemistry and Recent Applications in Polymer and Materials Synthesis and Modification. *Polymer* **2014**, *55* (22), 5517–5549.

(9) Lowe, A. B.; Harvison, M. A. Thiol-Based "Click" Chemistries in Polymer: Synthesis and Modification. *Australian Journal of Chemistry* **2010**, *63* (8), 1251.

(10) Yu, B.; Chan, J. W.; Hoyle, C. E.; Lowe, A. B. Sequential Thiol-Ene/Thiol-Ene and Thiol-Ene/Thiol-Yne Reactions as a Route to Well-Defined Mono and Bis End-Functionalized poly(N-Isopropylacrylamide). *Journal of Polymer Science Part A: Polymer Chemistry* **2009**, *47* (14), 3544–3557.

(11) Sprafke, J. K.; Spruell, J. M.; Mattson, K. M.; Montarnal, D.; McGrath, A. J.; Pötzsch, R.; Miyajima, D.; Hu, J.; Latimer, A. A.; Voit, B. I.; Aida, T.; Hawker, C. J. Revisiting Thiol-Yne Chemistry: Selective and Efficient Monoaddition for Block and Graft Copolymer Formation. *Journal of Polymer Science Part A: Polymer Chemistry* **2015**, *53* (2), 319–326.

(12) Wu, G.; Fang, Y.-Z.; Yang, S.; Lupton, J. R.; Turner, N. D. Glutathione Metabolism and Its Implications for Health. *The Journal of Nutrition* **2004**, *134* (3), 489–492.

(13) Pompella, A.; Visvikis, A.; Paolicchi, A.; Tata, V. D.; Casini, A. F. The Changing Faces of Glutathione, a Cellular Protagonist. *Biochemical Pharmacology* **2003**, *66* (8), 1499–1503.

(14) Lin, C.; Engbersen, J. F. The Role of the Disulfide Group in Disulfide-Based Polymeric Gene Carriers. *Expert Opinion on Drug Delivery* **2009**, *6* (4), 421–439.

(15) Zhang, L.; Li, Y.; Chen, Z. Dual-Degradable Disulfide-Containing PEI-Pluronic/DNA Polyplexes: Transfection Efficiency and Balancing Protection and DNA Release. *International Journal of Nanomedicine* **2013**, 3689-3701.

(16) Ou, M.; Wang, X.-L.; Xu, R.; Chang, C.-W.; Bull, D. A.; Kim, S. W. Novel Biodegradable Poly(disulfide Amine)s for Gene Delivery with High Efficiency and Low Cytotoxicity. *Bioconjugate Chemistry* **2008**, *19* (3), 626–633.

(17) Perrier, S.; Takolpuckdee, P.; Mars, C. A. Reversible Addition−Fragmentation Chain Transfer Polymerization: End Group Modification for Functionalized Polymers and Chain Transfer Agent Recovery. *Macromolecules* **2005**, *38* (6), 2033–2036.

(18) Ho, H. T.; Leroux, F.; Pascual, S.; Montembault, V.; Fontaine, L. Amine-Reactive Polymers Synthesized by RAFT Polymerization Using an Azlactone Functional Trithiocarbonate RAFT Agent. *Macromolecular Rapid Communications* **2012**, *33* (20), 1753–1758.
(19) *Handbook of RAFT Polymerization*; Barner-Kowollik, C., Ed.; Wiley-VCH: Weinheim, **2008**.
(20) Hu, N.; Ji, W.-X.; Tong, Y.-Y.; Li, Z.-C.; Chen, E.-Q. Synthesis of Diblock Copolymers Containing poly(N-Vinylcarbazole) by Reversible Addition-Fragmentation Chain Transfer Polymerization. *Journal of Polymer Science Part A: Polymer Chemistry* **2010**, *48* (20), 4621–4626.
(21) Zhang, X.; Li, J.; Li, W.; Zhang, A. Synthesis and Characterization of Thermo- and pH-Responsive Double-Hydrophilic Diblock Copolypeptides. *Biomacromolecules* **2007**, *8* (11), 3557–3567.
(22) Liu, Z.; Zhang, G.; Lu, W.; Huang, Y.; Zhang, J.; Chen, T. UV Light-Initiated RAFT Polymerization Induced Self-Assembly. *Polymer Chemistry* **2015**, *6* (34), 6129–6132.
(23) Plow, E. F.; Haas, T. A.; Zhang, L.; Loftus, J.; Smith, J. W. Ligand Binding to Integrins. *Journal of Biological Chemistry* **2000**, *275* (29), 21785–21788.
(24) Kim, W. J.; Yockman, J. W.; Lee, M.; Jeong, J. H.; Kim, Y.-H.; Kim, S. W. Soluble Flt-1 Gene Delivery Using PEI-G-PEG-RGD Conjugate for Anti-Angiogenesis. *Journal of Controlled Release* **2005**, *106* (1–2), 224–234.
(25) Qian, Y.; Zha, Y.; Feng, B.; Pang, Z.; Zhang, B.; Sun, X.; Ren, J.; Zhang, C.; Shao, X.; Zhang, Q.; Jiang, X. PEGylated poly(2-(Dimethylamino) Ethyl Methacrylate)/DNA Polyplex Micelles Decorated with Phage-Displayed TGN Peptide for Brain-Targeted Gene Delivery. *Biomaterials* **2013**, *34* (8), 2117–2129.
(26) Park, J.; Singha, K.; Son, S.; Kim, J.; Namgung, R.; Yun, C. O.; Kim, W. J. A Review of RGD-Functionalized Nonviral Gene Delivery Vectors for Cancer Therapy. *Cancer Gene Therapy* **2012**, *19* (11), 741–748.
(27) Pezzoli, D.; Tarsini, P.; Melone, L.; Candiani, G. RGD-Derivatized PEI-PEG Copolymers: Influence of the Degree of Substitution on the Targeting Behavior. *Journal of Drug Delivery Science and Technology* **2017**, *37*, 115–122.
(28) Buhlert, J.; Carle, R.; Majer, Z.; Spitzner, D. Thermal Degradation of Peptides and Formation of Acrylamide, Part 2. *Letters in Organic Chemistry* **2007**, *4* (5), 329–331.
(29) Stuchbury, T.; Shipton, M.; Norris, R.; Malthouse, J. P. G.; Brocklehurst, K.; Herbert, J. A. L.; Suschitzky, H. A Reporter Group Delivery System with Both Absolute and Selective Specificity for Thiol Groups and an Improved Fluorescent Probe Containing the 7-Nitrobenzo-2-Oxa-1,3-Diazole Moiety. *Biochemistry Journal* **1975**, *151* (2), 417.
(30) Boyer, C.; Liu, J.; Wong, L.; Tippett, M.; Bulmus, V.; Davis, T. P. Stability and Utility of Pyridyl Disulfide Functionality in RAFT and Conventional Radical Polymerizations. *Journal of Polymer Science Part A: Polymer Chemistry.* **2008**, *46* (21), 7207–7224.
(31) Nguyen, L.-T. T.; Devroede, J.; Plasschaert, K.; Jonckheere, L.; Haucourt, N.; Du Prez, F. E. Providing Polyurethane Foams with Functionality: A Kinetic Comparison of Different “click” and Coupling Reaction Pathways. *Polymer Chemistry* **2013**, *4* (5), 1546–1556.
(32) Türünç, O.; Meier, M. A. R. A Novel Polymerization Approach via Thiol-Yne Addition. *Journal of Polymer Science Part A: Polymer Chemistry.* **2012**, *50* (9), 1689–1695.
(33) Uygun, M.; Tasdelen, M. A.; Yagci, Y. Influence of Type of Initiation on Thiol–Ene “Click” Chemistry. *Macromolecular Chemistry and Physics* **2010**, *211* (1), 103–110.
(34) Dondoni, A.; Marra, A. Metal-Catalyzed and Metal-Free Alkyne Hydrothiolation: Synthetic Aspects and Application Trends: Metal-Catalyzed and Metal-Free Alkyne Hydrothiolation. *European Journal of Organic Chemistry* **2014**, (19), 3955–3969.
(35) Amir, R. J.; Albertazzi, L.; Willis, J.; Khan, A.; Kang, T.; Hawker, C. J. Multi-Functional Trackable Dendritic Scaffolds and Delivery Agents. *Angewandte Chemie (International ed. in English)* **2011**, *50* (15), 3425–3429.

Chapter 5: Cationic (PEGylated) aminoethyl-based polyacrylates: pDNA complexation and cytotoxicity.

Introduction

DNA-delivery mediated *via* cationic polymers is driven by several important parameters influencing transfection efficiency and/or cytotoxicity.

The effect of PEGylation on transfection efficiency and cytotoxicity has been widely studied on different non-viral gene delivery system including PEI or PLL (Chapter 1 §II).[1–3] The different studies showed a decrease of cytotoxicity and a decrease of transfection efficiency with the PEGylated polymers which has been explained by the "hiding" of the cationic charges leading to a limitation of polyplex instability under physiological conditions (salt, proteins) and by the aid to the decrease of cell binding affinity, respectively. Moreover, the influence of the PEO architecture was not signification as reported by Venkataraman *et al.* [4] Authors just noticed a slight better transfection efficiency of the PEO-*b*-PDMAEMA copolymers based polyplexes than the PPEGA-*b*-PDMAEAMA copolymers based polyplexes at high N/P ratios, 15 and 20.

Introducing protonable primary and tertiary entities and tuning their molar ratio improved transfection efficiency by modifying the pKa of cationic polymer. Zhu *et al.*[5] synthesized P(DMAEMA-*co*-AEMA) copolymers with different DMAEMA/AEMA molar ratios and they showed that a decrease of DMAEMA/AEMA molar ratio allowed to reduce of the N/P ratios to target full DNA complexation. However, such DMAEMA/AEMA molar ratio decreases led to a reduction of COS-7 cells viability.

As it mentioned in Chapter 4 §I-A the trithiocarbonate can be hydrolyzed leading to polymer-polymer coupling, even if, is more stable than dithioester groups. Moreover, it has been shown that the polymer chain-end can influence cytotoxicity. Akinc *et al.*[6] showed by replacing alcohol chain-end extremities by acrylate functions on PBAEA the drastic decreases of cell viability.

In this chapter, the influence of (i) the PEGylation, (ii) the DMAEA/AEA molar ratio and (iii) the chain-end nature within DMAEA and AEA based copolymers were studied on polyplex formation and cytotoxicity. A previous study of polyplex size and pDNA complexation has been previously done on a PEO-*b*-P(DMAEA-*co*-AEA). Gel retardation assays allow to evaluate the DNA/polymer binding affinity and to target optimal N/P ratios. *In vitro* cytotoxicity of cationic polymers has been evaluated using the 3-[4,5-dimethylthiazol-2-yl]-3,5-diphenyltetrazolium bromide (MTT) assay on three different cell lines (i) NIH-3T3, the most commonly used fibroblast cell lines, with a rapid response to external stimuli, (ii) endothelial umbilical vein cells (HUVEC) responds fast to external stimuli and is sensitive and (iii) murine macrophage-monocyte cells (J774.A1) which may highlight the cytotoxicity during the endocytosis process because of its key role in phagocytosis.

I. Size and zeta potential of a pDNA/aPEO-*b*-P(DMAEA-*co*-AEA) polyplex

The polyplex size plays a key role for cytotoxicity and transfection efficiency.[7] It has been shown that polyplexes with a sizes below 150 nm lead to non-cytotoxic sytem.[8] Moreover, Xu *et al.*[9] showed the pDNA/bPEI polyplex size impact the transfection efficiency of A549 cell line, Hela cell line, BGC-823, a human gastric adenocarcinoma cell line and Bel7402, human hepatocellular carcinoma, cell line. Authors, synthesized several polyplex with sizes ranging from, 38 nm to 167 nm. They showed the best that transfection efficiency was targeted with a size of polyplex ranging from below 87 nm.

The determination of the polyplex size and zeta potential has been done by dynamic light scattering (DLS) and zetametry, respectively. The analyses have been made on an $aPEO_{64}$-*b*-$P(DMAEA_{10}$-*co*-$AEA_{12})$ (Run 9, Table III. 3, Chapter 3) with a trithiocarbonate group. First, the optimal N/P ratio to obtain a fully complexed pDNA has been determined by gel retardation

assay; then the size and the zeta potential of the polyplex have been characterized using the polyplex obtained with this optimal N/P ratio.

The optimum N/P ratio has been determined using a pDNA containing 4631 base pairs. The electrophopherogram shows a migration of pDNA for N/P ratios of 0, 1 and 2 (Figure V. 1). At N/P ratios above 3 no migration was observed due to the fully complexation of pDNA.

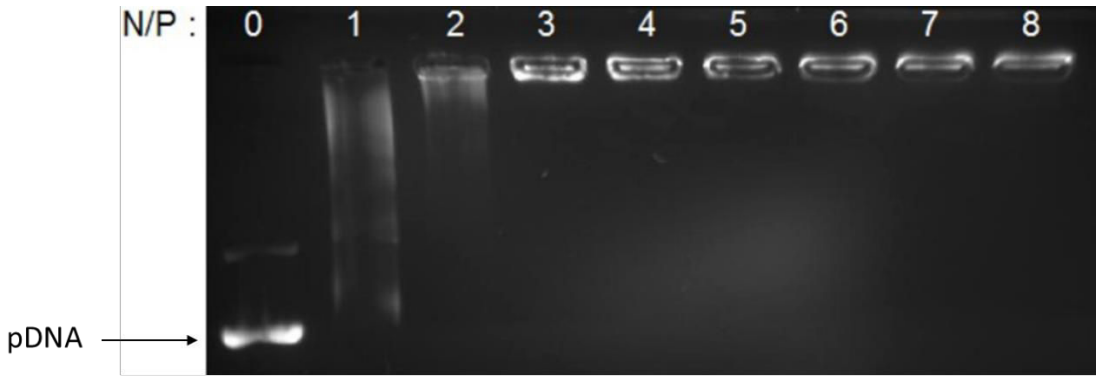

Figure V. 1. Agarose gel electropherogram of a pDNA/aPEO$_{64}$-*b*-P(DMAEA$_{10}$-*co*-AEA$_{12}$) polyplex obtained with different N/P ratios.

Further by DLS and zeta potential analyses were performed on the polyplex formed with a N/P = 3 to measure the hydrodynamic diameter (D_h), the size disperisity (PD) and zeta potential of the polyplex.

The formed polyplex was analyzed by DLS a D_h equal to 38 nm with a PD of 0.39 were observed. Moreover, it has been that shown the polyplex size below 87 nm leads to low cytotoxicity.[9] The zeta potential of a aPEO$_{64}$-*b*-P(DMAEA$_{11}$-*co*-AEA$_9$) cationic copolymer and associated polyplex has been compared.

The zeta potential of the cationic aPEO$_{64}$-*b*-P(DMAEA$_{11}$-*co*-AEA$_9$) copolymer is positive and equal to + 12 mV and the zeta potential of associated polyplex is around -1 mV. This result shows the neutralization of cationic charge during the complexation, the fully complexation of pDNA and the formation of the polyplex by electrostatic binding.

The aminoethyl acrylate-based cationic copolymers have been designed to study the influence of the PEGylation, DMAEA/AEA molar ratio and the chain-end nature.

II. Influence of the PEGylation of cationic DMAEA/AEA-based copolymers on pDNA binding and cell viability.

To study the influence of the PEGylation of cationic DMAEA/AEA based copolymers on polyplex formation, the behavior of polyplexes based on (i) pDNA/aPEO-*b*-P(DMAEA-*co*-AEA) copolymers (6100 g.mol^{-1} < $\overline{M_{n,SEC}}$ < 11500 g.mol^{-1} and 1.21 < Đ < 1.52), (ii) pDNA/PPEGA-*b*-P(DMAEA-*co*-AEA) copolymers (10100 g.mol^{-1} < $\overline{M_{n,SEC}}$ < 10700 g.mol^{-1} and 1.57 < Đ < 1.62) and pDNA/P(DMAEA-*co*-AEA) copolymers (6400 g.mol^{-1} < $\overline{M_{n,SEC}}$ < 9400 g.mol^{-1} and 1.20 < Đ < 1.50) were compared using gel retardation assays. The cell viability of these polymers were studied by cell viability tests.

A. Gel retardation assay

To study the influence of PEGylation a PPEGA$_{12}$-*b*-P(DMAEA$_7$-*co*-AEA$_{14}$) copolymer (Run 2, Table III. 4., Chapter 3) has been compared with a P(DMAEA$_9$-*co*-AEA$_{13}$) copolymer (Run 3, Table III. 5., Chapter 3).

Figure V. 2 shows electropherograms of a based on pDNA/P(DMAEA$_9$-*co*-AEA$_{13}$) polypex and a pDNA/PPEGA$_1$-*b*-(DMAEA$_7$-*co*-AEA$_{14}$) polyplex with different N/P ratios. A fully complexation has been obtained with a N/P ratio of 1 using the P(DMAEA$_9$-*co*-AEA$_{13}$) copolymer and of 4 using the PPEGA$_{12}$-*b*-(DMAEA$_7$-*co*-AEA$_{14}$). For the same PDMAEA/AEA ratio and the same P(DMAEA-*co*-AEA) length, the bPEO block PPEGA$_{12}$ the increases of the optimum N/P, from 1 to 4, can be explained by the increase of $\overline{M_n}$ copolymer and the decrease of complexation ability.

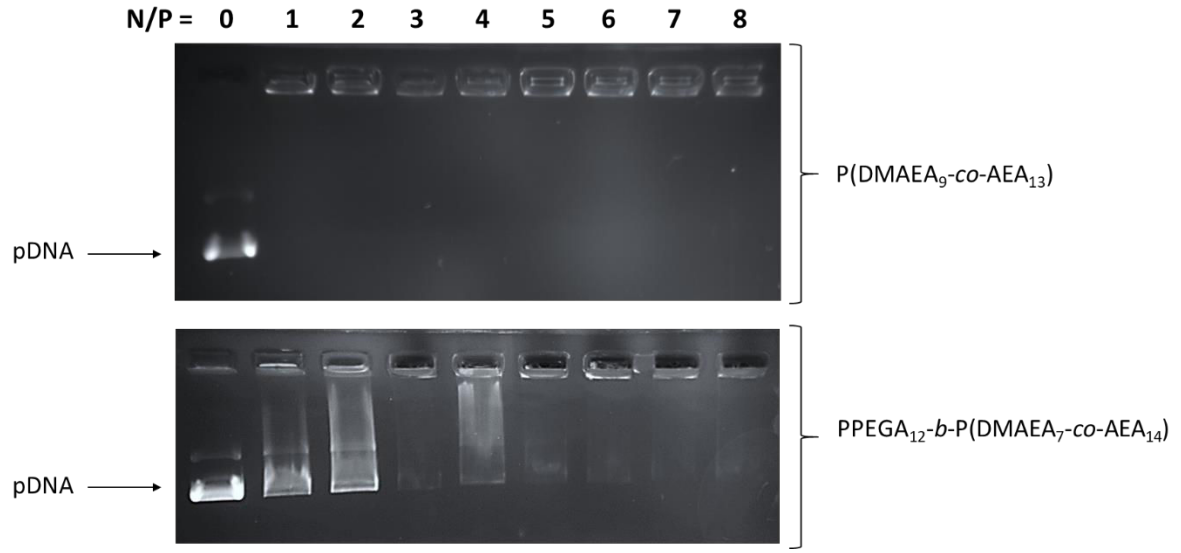

Figure V. 2. Agarose gel electropherogams of pDNA/P(DMAEA$_9$-*co*-AEA$_{13}$) polyplexes (top) and pDNA/PPEGA$_{12}$-*b*-P(DMAEA$_7$-*co*-AEA$_{14}$) polyplexes obtained with different N/P ratios.

To study the impact of the PEO architecture on the DNA complexation two polymers based on lPEO or bPEO have been compared, the aPEO$_{64}$-P(DMAEA$_{10}$-*co*-AEA$_{12}$) (run 9, Table III. 3, Chapter 3) with a lPEO and the PPEGA$_{12}$-P(DMAEA$_9$-*co*-AEA$_{10}$) (run 1, Table III. 4, Chapter 3) with a bPEO (Figure V. 3). The result obtained from gel retardation assay shows (Figure V. 3) a maximum N/P ratio equal to 3 for lPEO based cationic copolymer and a N/P ratio equal to 5 for bPEO based cationic copolymer to fully complex DNA. The decrease of the ability to complex DNA can be explained by the increase of the molar mass of the $\overline{M_n}$ of the PEO block, from 3000 g.mol^{-1} for the lPEO to 4800 g.mol^{-1} for the bPEO leading to a lower pDNA complexation ability.

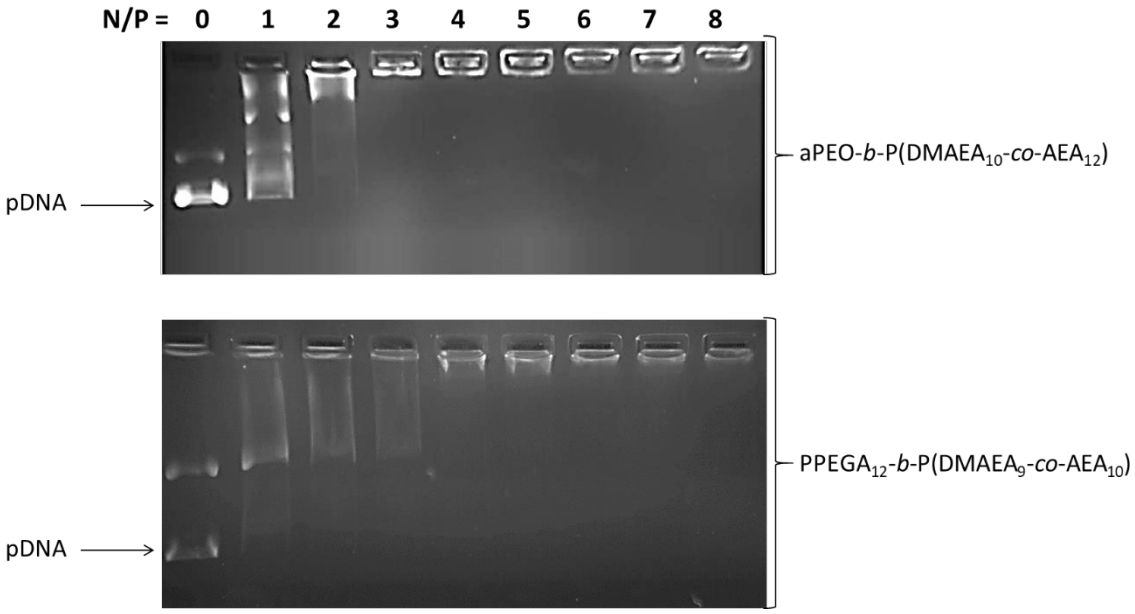

Figure V. 3. Agarose gel electropherograms of pDNA/aPEO$_{64}$-*b*-P(DMAEA$_{10}$-*co*-AEA$_{12}$) polyplexes (top) and pDNA/PPEGA$_{12}$-*b*-P(DMAEA$_9$-*co*-AEA$_{10}$) polyplexes (bottom) obtained with different N/P ratios.

The agarose gel electropherograms show that the addition of a PEO block leads to the decrease of pDNA binding affinity. Moreover, this decrease is more important for a bPEO compared to a lPEO.

B. Cell viability test

The influence of PEGylation on cell viability has been tested by comparing (i) a aPEO$_{64}$-*b*-P(DMAEA$_{11}$-*co*-AEA$_9$) copolymer and one aPEO$_{64}$-*b*-P(DMAEA$_5$-*co*-AEA$_{10}$) copolymer (Runs 1 and 5, respectively Table III. 3, Chapter3) with a P(DMAEA$_9$-*co*-AEA$_{13}$) copolymer (Run 3, Table III. 5, Chapter 3) and (ii) a P(DMAEA$_9$-*co*-AEA$_{13}$) copolymer with a PPEGA$_{12}$-*b*-P(DMAEA$_7$-*co*-AEA$_{14}$) (Run 2, Table III. 4, Chapter 3) copolymer on different cell lines, NIH-3T3, HUVEC and J774.A1 (Figure V. 4).

The MTT assays on NIH-3T3 cell lines (Figure V. 4(A)), contrary to HUVEC (Figure V. 4(B)) and J774.A1 cell lines (Figure V. 4 (C)), shows low or no cytotoxicity at 0.5 and 1 g.L^{-1}

(over 80 % of cell viability) for all copolymers. Moreover, at 2 $g.L^{-1}$ only the P($DMAEA_9$-*co*-AEA_{13}) shows cell viability of NIH-3T3 below 80 %

At a higher concentration (2 $g.L^{-1}$), the non-PEGylated P($DMAEA_9$-*co*-AEA_{13}) polymer induced a decrease of viability in all cell lines, revealing a greater sensibility of J774.A1 (22 % of cell viability, standard deviation of 2 %) compared to HUVEC (66 % of cell viability, standard deviation of 2 %) and NIH-3T3 cells (76 % of cell viability, standard deviation of 4 %).

The influence of PEO architecture has been studied on HUVEC cell line (Figure V. 4 (A)). The MTT assay using the aPEO_{64}-*b*-P($DMAEA_5$-*co*-AEA_{10}) shows a cell viability around 80 % for all tested concentrations, meanwhile the MTT assay of the P$PEGA_{12}$-*b*-P($DMAEA_7$-*co*-AEA_{14}) shows a decrease of cell viability from 1 $g.L^{-1}$ to 2 $g.L^{-1}$ (from 72 % to 58 %).

Cell viability decreased to 22 % when J774.A1 cells were incubated with the aPEO_{64}-*b*-P($DMAEA_{11}$-*co*-AEA_9). This lower cell viability could be explained taking into account the composition of copolymers, which will be further discussed in the following paragraphs.

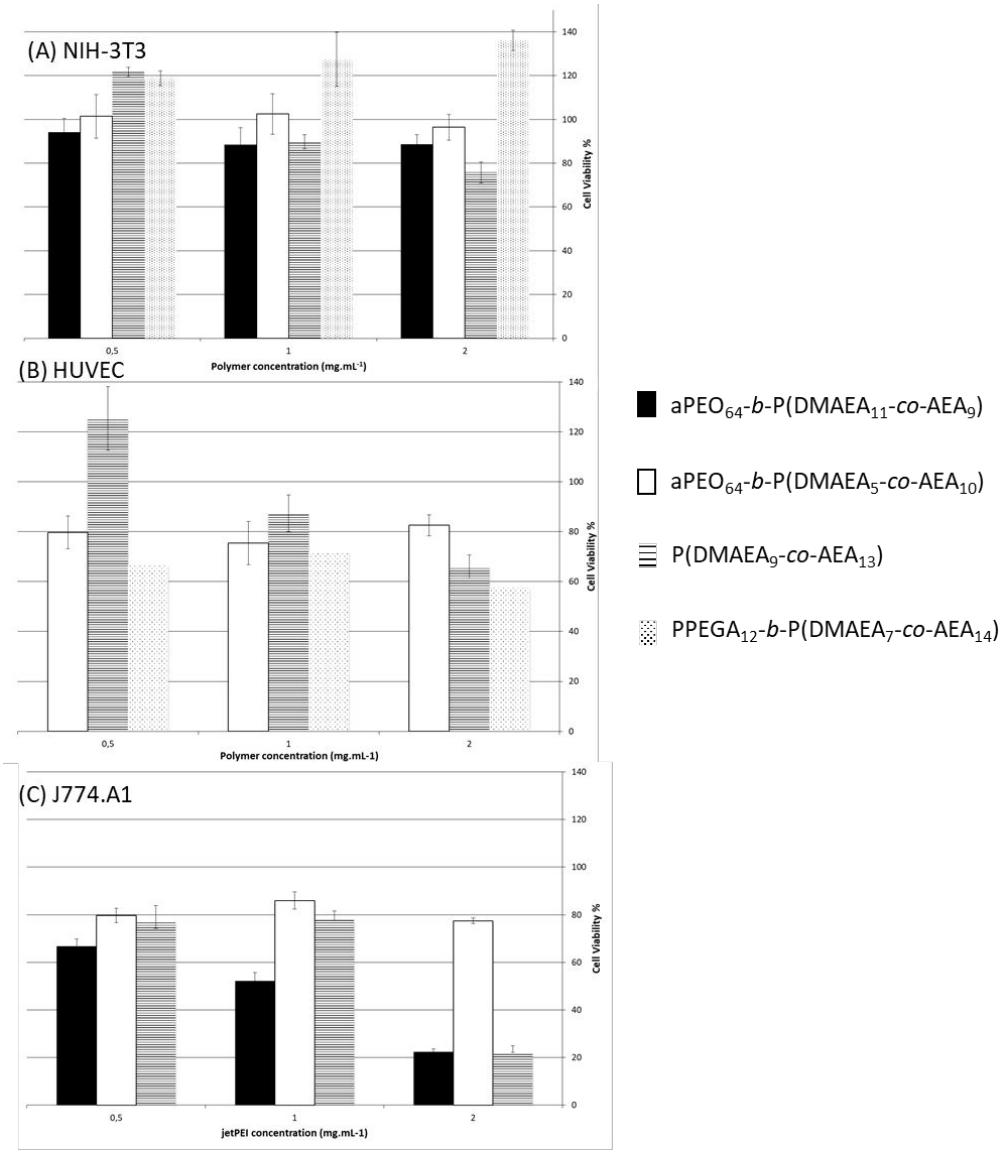

Figure V. 4. Cell viability (MTT assay) after incubation of (A) NIH-3T3 cells, (B) HUVEC cells (C) and J774.A1 cells with aPEO$_{64}$-*b*-P(DMAEA$_{11}$-*co*-AEA$_{9}$) (black graph), aPEO-$_{64}$-*b*-P(DMAEA$_{5}$-*co*-AEA$_{10}$) (white graph), P(DMAEA$_{9}$-*co*-AEA$_{13}$) (horizontal lines) and PPEGA-*b*-P(DMAEA$_{7}$-*co*-AEA$_{14}$) (pointed graph).

The MTT assays show a decrease of cell viability using PEGylated copolymer compare to non-PEGylated copolymer. The bPEO has been employed for PEGylation of P(PDMAEA-*co*-AEA), the copolymer is toxic just on HUVEC cells.

In conclusion of this part, the gel retardation assay shows a decrease of the complexation of pDNA with the PEGylation of the cationic P(DMAEA-*co*-AEA) copolymer. However, the PEGylation tends to decrease the cytotoxicity depending on the PEO architecture. lPEO is a better candidate than bPEO to decrease the cytotoxicity of P(DMAEA-*co*-AEA) copolymers.

III. Influence of the DMAEA/AEA molar ratios on pDNA binding and cell viability

The RAFT copolymerization of *t*BocAEA and DMAEA followed by the cationization and deprotection allow to tune efficiently the DMAEA/AEA molar ratios. The influence of the DMAEA/AEA ratio on pDNA binding and cell viability has been by gel retardation assay and MTT assay on NIH-3T3 cells, HUVEC cells and J774.A1 cells.

A. Gel retardation assays

The Figure V. 5 shows the comparison of gel retardation assay of pDNA polyplexes using an $aPEO_{64}$-P($DMAEA_{11}$-*b*-AEA_4) (Run 4, Table III. 3, Chapter 3) copolymer and an $aPEO_{64}$-P($DMAEA_5$-*co*-AEA_{10}) copolymer (Run 5, Table III. 3, Chapter 3). The gel retardation assays using an $aPEO_{64}$-P($DMAEA_{11}$-*b*-AEA_4) copolymer and an $aPEO_{64}$-P($DMAEA_5$-*co*-AEA_{10}) copolymer show an optimum N/P ratios above 8 and of 5, respectively to fully complex DNA. This results show the better pDNA binding affinity using copolymers with a higher amount of protonated primary amine AEA as shown with P(DMAEMA-*co*-AEMA) by Zhu *et al.*[5]

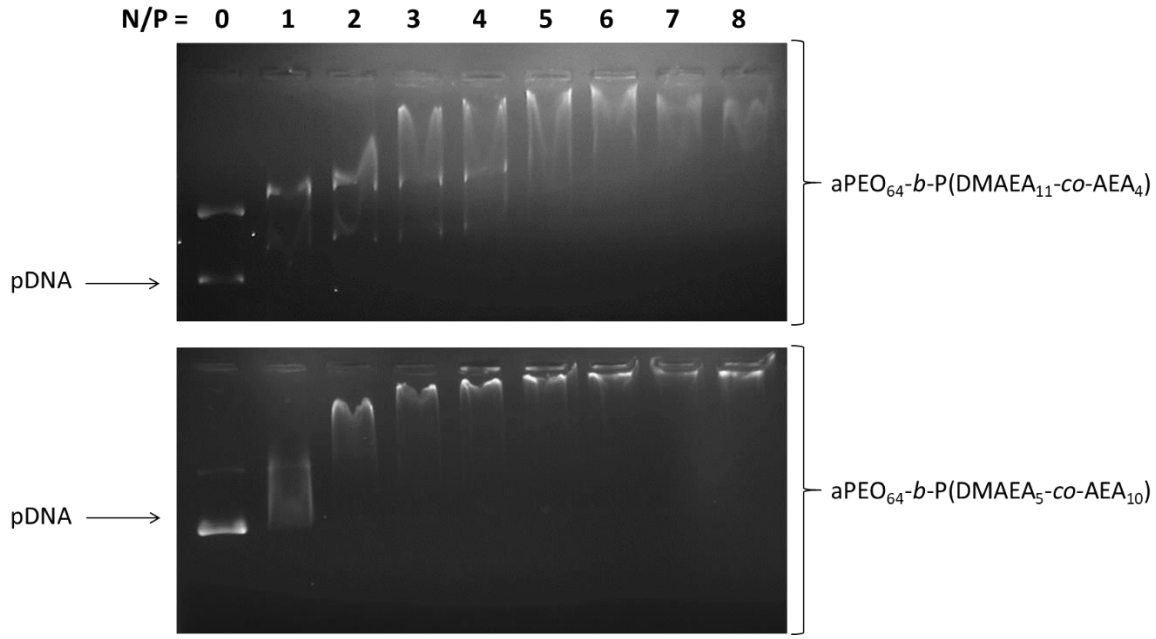

Figure V. 5. Agarose gel electropherograms of pDNA/aPEO$_{64}$-*b*-P(DMAEA$_{11}$-*b*-AEA$_4$) polyplexes (top) and pDNA/aPEO$_{64}$-*b*-P(DMAEA$_5$-*co*-AEA$_{11}$) polyplexes (bottom) obtained with different N/P ratios.

A similar behavior has been observed by comparing a PPEGA$_{12}$-*b*-P(DMAEA$_7$-*co*-AEA$_{14}$) copolymer with a PPEGA$_{12}$-*b*-P(DMAEA$_{13}$-*co*-AEA$_8$) (Run, Table III. 4, Chapter 3) copolymer to bind pDNA (Figure V. 6). N/P ratio of 5 is obtained to fully complex pDNA with PPEGA$_{12}$-*b*-P(DMAEA$_7$-*co*-AEA$_{14}$) copolymer. The optimum N/P ratio to fully complex pDNA using PPEGA$_{12}$-*b*-P(DMAEA$_{12}$-*co*-AEA$_8$) is above 8.

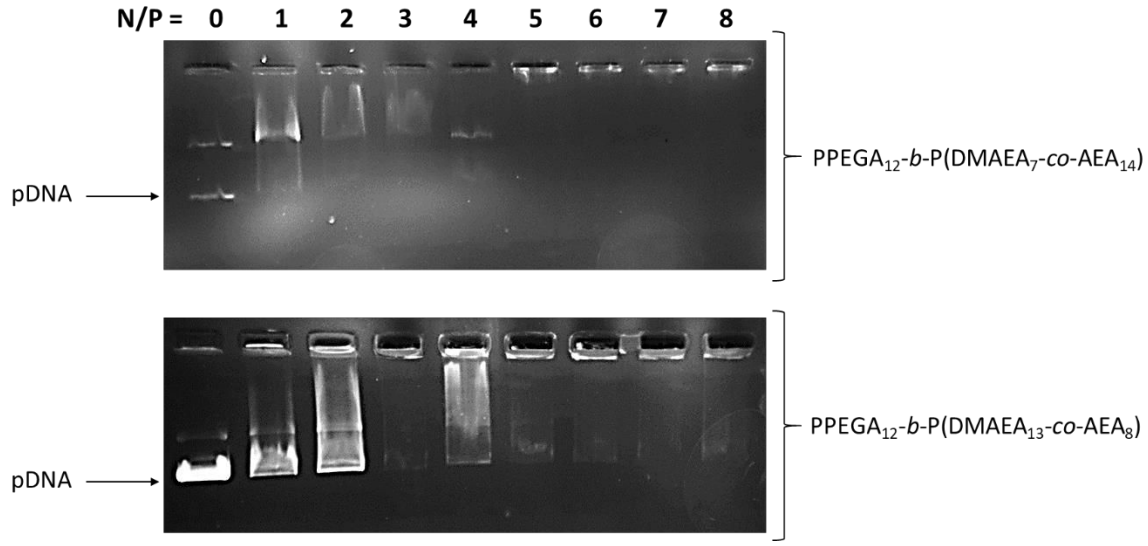

Figure V. 6. Agarose gel electropherograms of pDNA/PPEGA$_{12}$-*b*-P(DMAEA$_7$-*co*-AEA$_{14}$) polyplexes (top) and pDNA/PPEGA$_{13}$-*b*-P(DMAEA$_{13}$-*co*-AEA$_8$) polyplexes obtained with different N/P ratios

The gel retardation assays of pDNA/polyplexes using aPEO-*b*-P(DMAEA-*co*-AEA) copolymers and PPEGA-*b*-P(DMAEA-*co*-AEA) copolymers show that the increase of DMAEA/AEA molar ratio leads to the increase of the N/P ratio to fully complex pDNA due to a decrease of the protonated primary amine entities.

B. Cell viability test

The influence of cationic copolymer DMAEA/AEA molar ratio has been studied by comparing (i) an aPEO$_{64}$-*b*-P(DMAEA$_5$-*co*-AEA$_{10}$) copolymer (Run 5, Table III. 3, Chapter 3) with an aPEO$_{64}$-*b*-(DMAEA$_{11}$-*co*-AEA$_9$) copolymer (Run 1, Table III. 3, Chapter 3) and (ii) a PPEGA$_{12}$-*b*-(DMAEA$_7$-*co*-AEA$_{14}$) copolymer (Run 2, Table III. 4, Chapter 3) and a PPEGA$_{12}$-*b*-P(DMAEA$_{13}$-*co*-AEA$_8$) copolymer (Run 3, Table III. 4, Chapter 3).

The MTT assays of lPEO-based cationic copolymers did not show any significant differences on NIH-3T3 cells between aPEO$_{64}$-*b*-P(DMAEA$_5$-*co*-AEA$_{10}$) copolymer and the aPEO$_{64}$-*b*-(DMAEA$_{11}$-*co*-AEA$_9$) copolymer (Figure V. 7(A)). The influence of the

DMAEA/AEA molar ratio was evident also on J774.A1 cell lines. (Figure V. 7 (C)). The $aPEO_{64}$-*b*-P($DMAEA_{11}$-*co*-AEA_9) copolymer caused a dose-dependent reduction of the cell viability from 67 % (at 0.5 $g.L^{-1}$) to 22 % (at 2$g.L^{-1}$). No significant cytotoxicity was observed after incubation with the $aPEO_{64}$-*b*-P($DMAEA_5$-*co*-AEA_{10}) copolymer.

Higher viability was measured after NIH-3T3 exposure to the $PPEGA_{12}$-*b*-P($DMAEA_{13}$-*co*-AEA_8) copolymer (more than 100 % at 2 $g.L^{-1}$) compared to the $PPEGA_{12}$-*b*-P($DMAEA_7$-*co*-AEA_{14}) copolymer (49 % at 2 $g.L^{-1}$) (Figure V. 7(A)). A clear increase of the cytotoxicity was observed with the decrease of the DMAEA/AEA ratio. When tested on HUVEC cells (Figure V. 7 (B)), no differences were observed between the $PPEGA_{12}$-*b*-($DMAEA_7$-*co*-AEA_{14}) copolymer and the $PPEGA_{12}$-*b*-P($DMAEA_{13}$-*co*-AEA_8) copolymer, both responsible of a reduction of cell viability of ~50%.

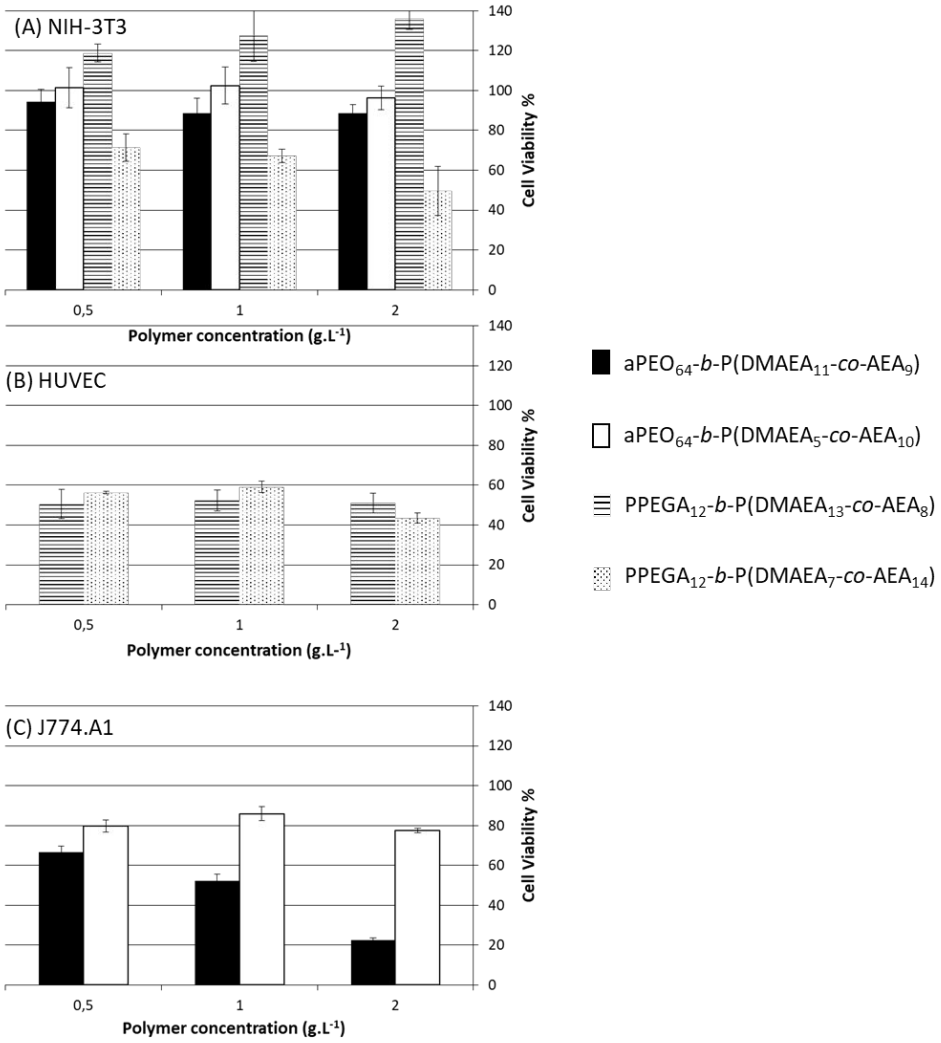

Figure V. 7. Cell viability (MTT assay) after incubation of (A) NIH-3T3 cells (B), HUVEC cells and (C) J774.A1 cells with aPEO$_{64}$-*b*-P(DMAEA$_{11}$-*co*-AEA$_9$) (black graph), aPEO$_{64}$-*b*-P(DMAEA$_5$-*co*-AEA$_{10}$) (white graph), PPEGA$_{12}$-*b*-(DMAEA$_7$-*co*-AEA$_{14}$) (horizontal lines) and PPEA$_{12}$-*b*-P(DMAEA$_{13}$-*co*-AEA$_8$) (pointed graph).

The gel retardation assay showed an increase of cell binding affinity with the decrease of DMAEA/AEA molar ratio. The cell viability showed opposites behaviors of the influence of DMAEA/AEA molar ratio between bPEO and lPEO depending of the cell lines. Further investigations will be made to evaluate more precisely the impact of DMAEA/AEA ratio on cytotoxicity.

IV. Influence of the trithiocarbonate chain-end on pDNA binding and cell viability

The trithiocarbonate has been removed efficiently on aPEO-*b*-P(DMAEA-*co*-*t*BocAEA) copolymers and P(DMAEA-*co*-*t*BocAEA) copolymers by a radical-mediated process through photochemical-activation. The influence of the dodecyltrithiocarbonate removal has been studied on associated cationic aPEO-*b*-P(DMAEA-*co*-AEA) copolymers and P(DMAEA-*co*-AEA) copolymers by gel retardation assay and cell viability assay (MTT).

A. Gel retardation assays

The influence of the dodecyltrithiocarbonate group on pDNA binding has been compared by gel retardation assay using the $aPEO_{64}$-P($DMAEA_{10}$-*co*-AEA_{12})-CTA copolymer with a dodecyltrithiocarbonate (-CTA) group and the $aPEO_{64}$-P($DMAEA_{11}$-*co*-AEA_{9}) (Run 9, Table III. 3, Chapter 3) copolymer without the dodecyltrithiocarbonate group (Figure V. 8). The comparison doesn't show any significant difference between the $aPEO_{64}$-P($DMAEA_{10}$-*co*-AEA_{12})-CTA and the $aPEO_{64}$-P($DMAEA_{10}$-*co*-AEA_{12}). Indeed, the optimum N/P ratio to fully complex pDNA for both copolymers is equal to 3. This result shows the presence of the trithiocarbonate doesn't lead to a better complexation of the pDNA.

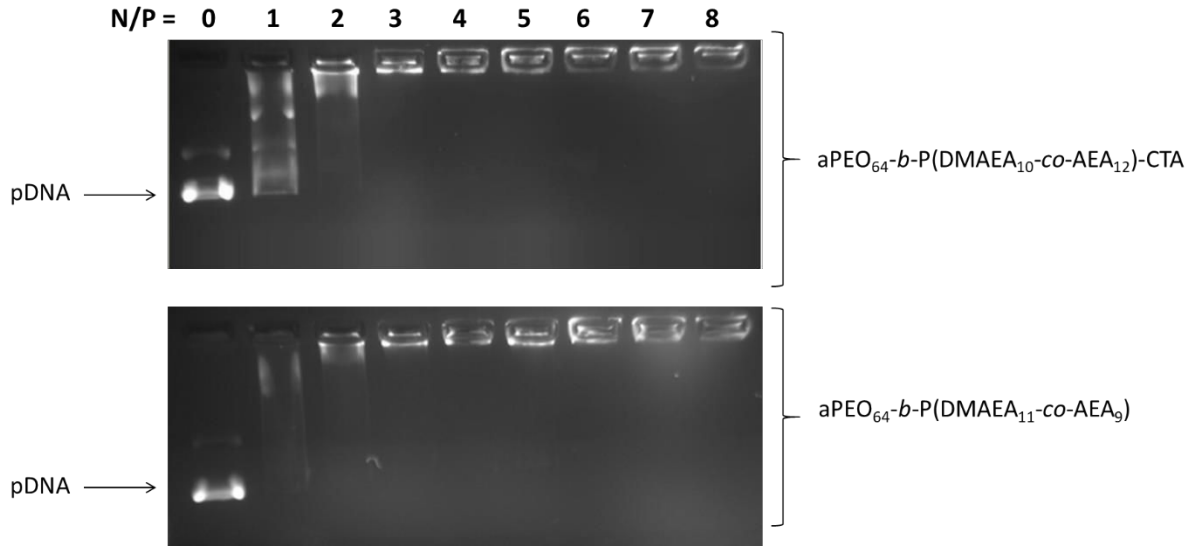

Figure V. 8. Agarose gel electopherograms of pDNA/aPEO$_{64}$-*b*-P(DMAEA$_{10}$-*co*-AEA$_{12}$)-CTA polyplexes (top) and pDNA/aPEO-*b*-P(DMAEA$_{11}$-*co*-AEA$_9$) polyplexes (bottom) obtained with different N/P ratios.

Even if the presence of the trithiocarbonate on copolymers did not show any effect on the pDNA complexation may plays a role in copolymers cytotoxicity.

B. Cell viability tests

The influence of the presence of the trithiocarbonate on the cytotoxicity have been measured on two cell lines: NIH-3T3 and HUVEC cell lines (Figure V. 9). On NIH-3T3 cells, the comparison between an aPEO$_{64}$-*b*-P(DMAEA$_{11}$-*co*-AEA$_9$)-CTA and an aPEO$_{64}$-*b*-P(DMAEA$_{11}$-*co*-AEA$_9$) shows a decrease of the cell viability from 89 % to 30 % when the trithiocarbonate has been removed (Figure V. 9(A)). Analogous results have been observed on NIH-3T3 and HUVEC cells when exposed to a P(DMAEA$_9$-*co*-AEA$_{13}$)-CTA and a P(DMAEA$_9$-*co*-AEA$_{13}$). At 2 g.L^{-1}, the P(DMAEA$_9$-*co*-AEA$_{13}$), cell viabilities was equal to 76 % and 66 % for NIH-3T3 and HUVEC cells, respectively. On the contrary a drop to ~50% in both cell lines was measured after incubation with the copolymer P(DMAEA$_9$-*co*-AEA$_{13}$)-CTA.

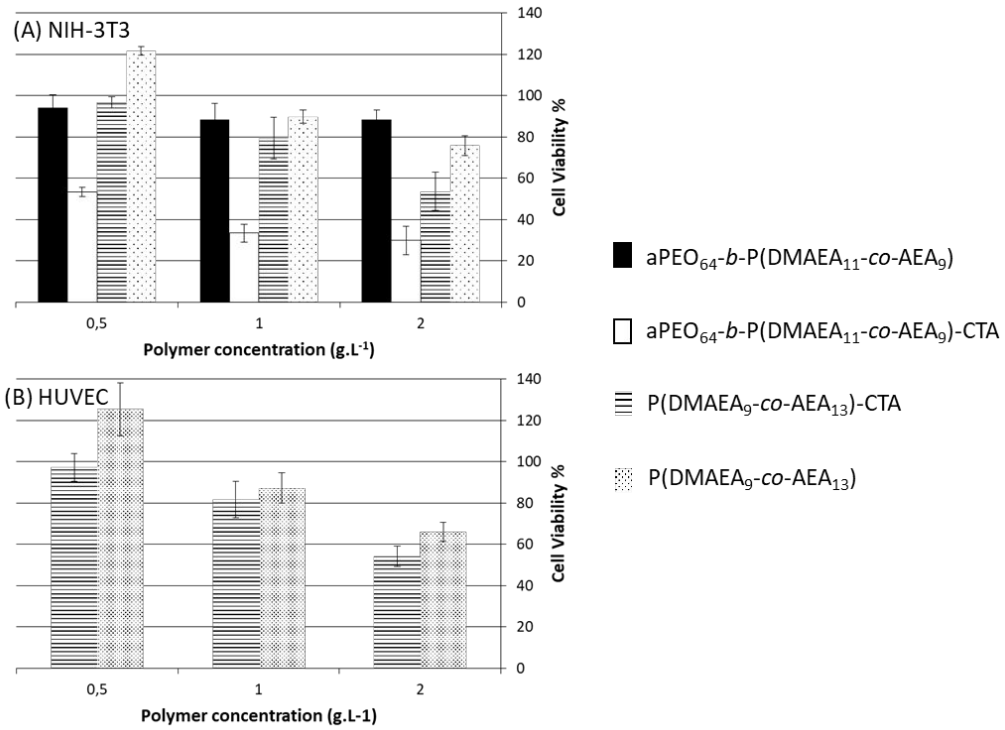

Figure V. 9. Cell viability (MTT assay) after incubation of (A) NIH-3T3 cells (B) and HUVEC cells with, aPEO$_{64}$-*b*-P(DMAEA$_{11}$-*co*-AEA$_9$) (black graph), aPEO$_{64}$-*b*-P(DMAEA$_{11}$-*co*-AEA$_9$)-CTA (white graph), P(DMAEA$_9$-*co*-AEA$_{13}$)-CTA (horizontal lines) and P(DMAEA$_9$-*co*-AEA$_{13}$) (pointed graph).

These results highlight the cytotoxocity due to the presence of dodecyltrithiocarbonate.

Conclusion

The pDNA polyplexes obtained from aPEO-*b*-P(DMAEA-*co*-AEA) copolymers, PPEGA-*co*-P(DMAEA-*co*-AEA) copolymers and P(DMAEA-*co*-AEA) copolymers with different DMAEA/AEA ratio with our without trithiocarbonate group have been characterized by gel retardation assay and MTT assays on three different cell lines.

In a preliminary study an aPEO$_{64}$-*co*-P(DMAEA$_{10}$-*co*-AEA$_{12}$) with a thrithiocarbonate function has been characterized by gel retardation assay. The electropherograms showed the

fully pDNA complexation with a N/P ratio of 3. The polyplex hydrodynamic diameter was equal to 38 nm with a size dispersity of 0.39, determined by DLS. The zetametry comparison between the aPEO$_{64}$-*co*-P(DMAEA$_{11}$-*co*-AEA$_9$) and its associated polyplex showed the neutralization of cationic charge after complexation, + 12 mV and – 1 mV, respectively.

The influence of the PEGylation has been studied by gel retardation assay. The gel retardation assays showed optimal N/P ratio of 4 for a pDNA/PPEGA$_{12}$-*b*-P(DMAEA$_7$-*co*-AEA$_{14}$) polyplex and N/P ratio of 1 for a pDNA/P(DMAEA$_9$-*co*-AEA$_{13}$) polyplex due to the addition of the bPEO block. The comparison between a bPEO based polyplex and a lPEO based polyplex with the same DMAEA/AEA molar ratio shows a fully complexation for a N/P of 5 and 3, respectively. This result is explained by the higher $\overline{M_n}$ of bPEO compare to the lPEO. Moreover, the MTT assays on three different cell lines showed a decrease of cytotoxicity on the three different cell lines after PEGylation using a lPEO. The cytotoxicity of bPEO based cationic copolymers is more important that lPEO based cationic copolymers but results are cell dependents.

The influence of DMAEA/AEA molar ratio has been studied. Electropherograms of pDNA/aPEO$_{64}$-*b*-P(DMAEA$_{11}$-*co*-AEA$_4$) polyplex and pDNA/aPEO$_{64}$-*b*-P(DMAEA$_5$-*co*-AEA$_{10}$) polyplex showed a decrease of optimal N/P with DMAEA/AEA molar ratio, from 8 to 5, due to the increase of primary amine ratio. Opposite behavior has been noticed using bPEO based polyplex.

The influence of the trithiocarbonate chain-end on the binding DNA affinity has been analyzed by gel retardation assay. The presence of this group did not show any significant differences on binding affinity. However, the MTT assay showed the high cytotoxicity of the trithiocarbonate, indeed using a lPEO based polyplex the cell viability of NIH-3T3 increases from 30 to 89 %, with and without dodecyltrithiocarbonate chain-end, respectively.

Further investigations on the influence of (i) DMAEA/AEA molar ratio (ii) the transfection efficiency, (iii) polyplex sizes and (iv) zeta potential will be made.

Experimental part

A. Reagents

Plasmid DNA (pDNA, pBR322, 0.5μg.μL^{-1}, EuroMEDEX), Trisacetate EDTA Buffer (TAE 50x, EuroMEDEX), agarose type D-5 (EuroMEDEX), 3-(4,5-dimethylthiazol-2-yl)-3,5-diphenyltetrazolium bromide (MTT, ≥ 97.5 %, sigma-Aldrich), Dulbecco's modified eagle medium (DMEM, Lonza), fetal bovine serum (FBS, Lonza), RPMI 1640 medium (Lonza), Dimethyl sulfoxide (DMSO, Pure, Carlo-Erba), Ethidium bromide (Sigma, molecular biology) were obtained and used as received.

B. General characterization

Zeta potential (ξ) and size measurements. ξ were performed using a dynamic light scattering instrument (Zetasizer Nano ZS, Malvern Instrument) equipped with a He-Ne laser beam at 658 nm. The average value was calculated from four replicate measurements. D_h of polyplex were calculated using multi narrow mode algorithm at a polyplex concentration of 0.5 μg.mL^{-1}.

C. Gel retardation assay

Cationic copolymers/pDNA polyplexes have been prepared by mixing pDNA (0.5 μg.L^{-1}) with a solution of copolymers in tris-HCl solution at pH = 7.4 (nitrogen concentration = 0.5 μg.μL^{-1}), DNA loading and completed with the pH buffering solution (Table V. 1). The solution was homogenized with a Vortex-2 Genie scientific industries. A gel agarose was prepared to characterize the polyplex (0.8 % of agarose in TAE 1 X buffer) with ethidium bromide. The gel retardation assay was carried out at 50 mV with running TAE 1 X buffer.

Table V. 1. Preparation of polyplexes at different N/P

N/P	V_{pDNA} (µL)	$V_{DNA\ loading}$ (µL)	$V_{pH\ buffering}$	$V_{copolymer\ solution}$ (µL)
0	2	2	7	0
1	2	2	5	2
2	2	2	3	4
3	2	2	1	6
4	2	2	0	8
5	2	2	0	10
6	2	2	0	12
7	2	2	0	14
8	2	2	0	16

D. Cells culture

Embryonic murine fibroblast (NIH-3T3) and human endothelial umbilical vein cells (HUVEC) were cultured in DMEM, supplemented with 50 $U.mL^{-1}$ penicillin, 50 $U.mL^{-1}$ streptomycin and 10% FBS. The J774.A1 murine macrophage-monocyte cell line was cultured in RPMI 1640 medium supplemented with 50 $U.mL^{-1}$ penicillin, 50 $U.mL^{-1}$ streptomycin, and 10% heat inactivated FBS. All cell lines were obtained from ATCC and maintained at 37 °C in a humidified 5% CO2 atmosphere.

E. MTT assay

The in vitro cytotoxic activity of the copolymers was evaluated on the three cell lines, using the MTT test. Cells were seeded in 100 µL of growth medium (HUVEC and J774.A1: 8

$\times$ 10^4 cells·mL^{-1}, NIH-3T3: 4 $\times$ 10^4 cells·mL^{-1}) in 96-well microliterplates (TPP) and preincubated for 24 h. After appropriate dilutions, 100 µL of copolymer solution in cell medium was added over the cells and incubated for 48 h (NIH-3T3) or 72 h (HUVEC and J774.A1). Initial cell density and incubation time were determined to allow cells to remain in exponential growth and to undergo two cell-doubling times during the assay. At the end of the incubation period, 20 µL of a 5 mg.mL^{-1} MTT solution in phosphate buffered saline was added to each well. After incubation, the culture medium was removed and replaced by 200 µL of DMSO, in order to solubilize the formazan crystals and obtain a purple solution. The absorbance of the solubilized dye was measured spectrophotometrically with a microplate reader (LAB System Original Multiscan MS) at 570 nm. The percentage of viable cells for each treatment was calculated from the ratio of the absorbance of the well containing the treated cells versus the average absorbance of the control wells (i.e., untreated cells). All experiments were repeated three times to determine means cell-viability and standard-deviations.

References

(1) Zhang, X.; Pan, S.-R.; Hu, H.-M.; Wu, G.-F.; Feng, M.; Zhang, W.; Luo, X. Poly(ethylene Glycol)-Block-Polyethylenimine Copolymers as Carriers for Gene Delivery: Effects of PEG Molecular Weight and PEGylation Degree. *Journal of Biomedical Materials Research Part A* **2008**, *84A* (3), 795–804.

(2) Fitzsimmons, R. E. B.; Uludag, H. Specific Effects of PEGylation on Gene Delivery Efficacy of Polyethylenimine: Interplay between PEG Substitution and N/P Ratio. *Acta Biomaterialia* **2012**, *8* (11), 3941–3955.

(3) Rungsardthong, U.; Deshpande, M.; Bailey, L.; Vamvakaki, M.; Armes, S. P.; Garnett, M. C.; Stolnik, S. Copolymers of Amine Methacrylate with Poly (Ethylene Glycol) as Vectors for Gene Therapy. *Journal of controlled release* **2001**, *73* (2), 359–380.

(4) Venkataraman, S.; Ong, W. L.; Ong, Z. Y.; Joachim Loo, S. C.; Rachel Ee, P. L.; Yang, Y. Y. The Role of PEG Architecture and Molecular Weight in the Gene Transfection Performance of PEGylated Poly(dimethylaminoethyl Methacrylate) Based Cationic Polymers. *Biomaterials* **2011**, *32* (9), 2369–2378.

(5) Zhu, C.; Jung, S.; Si, G.; Cheng, R.; Meng, F.; Zhu, X.; Park, T. G.; Zhong, Z. Cationic Methacrylate Copolymers Containing Primary and Tertiary Amino Side Groups: Controlled Synthesis via RAFT Polymerization, DNA Condensation, and in Vitro Gene Transfection. *Journal of Polymer Science Part A: Polymer Chemistry* **2010**, *48* (13), 2869–2877.

(6) Akinc, A.; Anderson, D. G.; Lynn, D. M.; Langer, R. Synthesis of Poly(β-Amino Ester)s Optimized for Highly Effective Gene Delivery. *Bioconjugate Chemistry* **2003**, *14* (5), 979–988.

(7) Mintzer, M. A.; Simanek, E. E. Nonviral Vectors for Gene Delivery. *Chemical Reviews* **2009**, *109* (2), 259–302.

(8) Cherng, J.-Y.; Schuurmans-Nieuwenbroek, N. M. E.; Jiskoot, W.; Talsma, H.; Zuidam, N. J.; Hennink, W. E.; Crommelin, D. J. A. Effect of DNA Topology on the Transfection Efficiency of Poly ((2-Dimethylamino) Ethyl Methacrylate)–plasmid Complexes. *Journal of controlled release* **1999**, *60* (2), 343–353.

(9) Xu, D.-M.; Yao, S.-D.; Liu, Y.-B.; Sheng, K.-L.; Hong, J.; Gong, P.-J.; Dong, L. Size-Dependent Properties of M-PEIs Nanogels for Gene Delivery in Cancer Cells. *International Journal of Pharmaceutics* **2007**, *338* (1–2), 291–296.

General Conclusion

The aim of this work was to synthesize a unique multi-structural copolymer with low cytotoxicity that can be used for efficient DNA delivery. To attain this goal, several heterofunctional PEGylated cationic polymers with different DMAEA and *t*BocAEA molar ratios with different PEO architectures (with or without a trithiocarbonate end-group) have been synthesized by RAFT polymerization. By using alkyne-based (macro)molecular chain transfer agents, well-defined P(DMAEA-*co*-*t*BocAEA), PEO-*b*-P(DMAEA-*co*-*t*BocAEA), PPEGA-*b*-P(DMAEA-*co*-*t*BocAEA), and P(DMAEA-*co*-*t*BocAEA) were successfully prepared. In parallel, a study was conducted to anchor a thiolated recognition ligand by thiol-yne coupling reaction and thiol-disulfide coupling reaction on model polymers (lPEO and PNIPAM). The associated cationic copolymers have been synthesized and characterized and their ability to complex DNA was studied by light scattering, zeta-potential and gel retardation assay. Cytotoxicity was evaluated using MTT assay on NIH-3T3, HUVEC and A1.J774 cell lines. The influence of (i) PEGylation, (ii) molar composition of cationic copolymer, and (iii) chain-end modification were investigated.

The synthesis of heterofunctional lPEO was studied first. Two different thiol-reactive groups, namely pyridyldithio and alkynyl groups, were covalently linked at the α-chain-end of lPEO. α-Pyridyldithio,ω-hydroxylPEO was obtain quantitatively by reacting commercial α-amino,ω-hydroxylPEO with an azlactone-based alkynyl linker under mild conditions. Then, a trithiocarbonate function was introduced by esterification at the ω-position of the so-obtained lPEO. The resulting PEO-based macro chain transfer agent was used to mediate the RAFT polymerization of aminoethyl acrylates.

Three different pathways were studied to anchor a chain-transfer agent on the lPEO: the esterification of lPEO with CDP was mediated through (i) an acyl chloride based on CDP, (ii) DMT-MM and (iii) DCC. The esterification of lPEO through the acyl choride based on CDP

and DMT-MM led to low degree of functionalization. Moreover, the esterification of the α-pyridyldithio,ω-hydroxylPEO using acyl chloride based on CDP and DMT-MM led to polymer-polymer disulfide coupling reaction. The esterification of lPEO with CDP with the α-pyridyditio,ω-hydroxylPEO mediated through DCC led to a low functionalization (53 %) but no polymer-polymer reactions occurred. The same pathway was used with the α-alkynyl,ω-hydroxylPEO allowing to obtain a fully functionalized and well-defined α-alkynyl,ω-dodecyltrithiocarbonate PEO (with a $\overline{M_{n,SEC}}$ = 8200 g.mol^{-1} and a $Đ$ = 1.13). The esterification mediated through DCC led to the best result with the α-pyridyditio,ω-hydroxylPEO and the α-alkynyl,ω-hydroxylPEO. Furthermore, this reaction led to a well defined α-alkynyl,ω-dodecyltrithiocarbonate PEO, this polymer was used to perform the RAFT polymerization of DMAEA and *t*BocAEA.

In order to study the influence of the PEO architecture on pDNA complexation and cytotoxicity, bPEO was synthesized by RAFT polymerization of PEGA using a new alkyne-based chain transfer agent (COPYDC). The optimal conditions were studied and was $[PEGA]_0/[COPYDC]_0/[ACVA]_0$ = 30/1/0.1. An α-alkynyl,ω-dodecyltrithiocarbonate PPEGA with a $\overline{DP_n}$ of 12 as calculated by ^{1}H NMR spectroscopy and a $\overline{M_{n,SEC}}$ = 14700 g.mol^{-1} and a $Đ$ = 1.26 was obtained for further study and used to copolymerize DMAEA and *t*BocAEA.

α-alkynyl,ω-dodecyltrithiocarbonate PEO (aPEO-CTA) and α-alkynyl,ω-dodecyltrithiocarbonate PPEGA (PPEGA-CTA) were then used for RAFT copolymerization of DMAEA and *t*BocAEA. Reactivity ratios determination led to r_{DMAEA} = 0.81 and $r_{t\text{BocAEA}}$ = 0.99, showing characteristics of an "ideal" copolymerization system.Moreover, the $\overline{DP_n}$ of DMAEA and *t*BocAEA units calculated by ^{1}H NMR spectroscopy shows that final DMAEA/AEA molar ratio in the copolymers are in agreement with the comonomer feeds. From these results the RAFT copolymerization of DMAEA and *t*BocAEA with different

DMAEA/AEA molar ratios has been performed mediated through aPEO-CTA, PPEGA-CTA and COPYDC used as (macromolecular) chain transfer agents to obtain several aPEO-*b*-(DMAEA-*co*-*t*BocAEA), PPEGA-*b*-P(DMAEA-*co*-*t*BocAEA) and P(DMAEA-*co*-*t*BocAEA) copolymers, respectively. Associated aPEO-*b*-P(DMAEA-*co*-AEA) cationic copolymers, PPEGA-*b*-P(DMAEA-*co*-AEA) cationic copolymers and P(DMAEA-*co*-AEA) cationic copolymers with different DMAEA/AEA ratios were obtained through the primary amine deprotection of *t*BocAEA units under acidic medium. The cationic (PEGylated) cation aminoethylacrylated were used to complex pDNA to form the polyplexes.

To increase the transfection efficiency and decrease the cytotoxicity, the incorporation of a thiolated recognition ligand and the trithiocarbonate removal have been studied. To avoid too much synthesis steps needed to target copolymers based on EO, DMAEA, and (*t*Boc)AEA units; the trithiocarbonate removal reaction has been first modeled. The PNIPAM has been chosen as a model polymer. The RAFT polymerization of NIPAM has been mediated using COPYDC as chain transfer agent and AIBN as the initiator leading to a well-defined α-alkynyl,ω-dodecyltrithiocarbonate PNIPAM with a $\overline{DP}_n$ of PNIPAM equal to 40. The trithiocarbonate removal reaction has been realized by thermal-activation (80°C) using 20 equivalents of AIBN, after 24 h the trithiocarbonate group was fully removed. The trithiocarbonate removal reaction has been adjust for the PEO-*b*-P(DMAEA-*co*-*t*BocAEA) and P(DMAEA-*co*-*t*BocAEA) copolymers using a photochemical-activation and the trithiocarbonate was fully removed in 2 weeks without aminoethyl polyacrylates modifications. The modification of chain end to anchor thiolated recognition ligand has been studied on the lPEO and the PNIPAM without trithiocarbonate. First, the thiol-disulfide exchange coupling reaction has been performed using an α-pyridyldithio,ω-hydroxylPEO and *N*-acetylcysteine as the thiol model molecule and the conversion was equal to 56 % in 18 hours. Then, the thiol-yne coupling reaction has been performed on a free trithiocarbonate PNIPAM using AIBN as the

radical initiator, benzyl mercaptan as the thiol model molecule and DMPP to reduce disulfide bonds during 24 hours. The highest functionalization degree has been obtained using a $[PNIPAM]_0/[AIBN]_0/[Benzyl\ mercaptan]_0$ initial molar ratio of 1/15/15, 0.78 aromatic group for 1 alkyne group. As the trithiocarbonate removal reaction and the thiol-yne coupling reaction have been performed in the same conditions the two reactions have been performed in one-pot two steps process. This combination led to the complete removal of the trithiocarbonate and the addition of 0.80 thiol group for 1 alkyne group. This reaction allow sufficient functionalization for bio-applications.[1,2] Moreover, the thiol-yne coupling reaction showed a better degree of functionalization than the thiol-disulfide coupling reaction.

The cationic aPEO-*b*-P(DMAEA-*co*-AEA) copolymers, PPEGA-*b*-P(DMAEA-*co*-AEA) copolymers and P(DMAEA-*co*-AEA) copolymers with and without trithiocarbonate group (CTA) have been characterized. First a PEO-*b*-P(DMAEA-*co*-AEA)-CTA and a $\overline{DP}_{n,PDMAEA}$ = 10 and a $\overline{DP}_{n,PtBocAEA}$ = 12 was used to complex DNA. Gel retardation assay showed an optimum ratio of N/P of 3. Then, zeta potentials of cationic PEO_{64}-*b*-P($DMAEA_{10}$-*co*-AEA_{12}) copolymer and the pDNA/PEO_{64}-*b*-P($DMAEA_{10}$-*co*-AEA_{12}) polyplex were compared. The zeta-potential showed a complete neutralization of cationic charge after complexation. Moreover, after complexation the hydrodynamic diameter of the polyplex was measured and equal to 38 nm. As shown in literature, this size led to non-toxic polyplex.[3]

The influence of the PEGylation, of the presence of the dodecyltrithiocarbonate group and the DMAEA/AEA ratio on pDNA binding affinity and cytotoxicity of cationic copolymers were studied. The gel retardation assay on PEGylated copolymers showed a complete pDNA complexation with a higher N/P ratio that non-PEGylated copolymer. Moreover, the MTT assay on three different cell lines showed an increase of cell viability using PEGylated copolymer. The comparison between the lPEO and the bPEO didn't show any significant differences on

cell viability. Gel retardation assays of different PEO-*b*-P(DMAEA-*co*-AEA) showed the decrease of optimal N/P ratios with the decrease of the DMAEA/AEA molar ratio due to the increase of primary amine ratio. The result has been confirmed with two bPEO-based aminoethyl polyacrylates. Furthermore, the decrease of the DMAEA/AEA ratio led to a decrease of cell viability using a lPEO as shown by MTT assay. Opposite behavior have been noticed using PPEGA based cationic polymer. The presence of the dodecyltrithiocarbonate group didn't play a role on pDNA binding affinity as shown by gel retardation assay. However, copolymer with dodecyltrithiocarbonate chain end exhibited higher cytotoxicity than without this group as shown by MTT assay. The best results were obtained using a PEGylated copolymer, to decrease cytotoxicity, with a low DMAEA/AEA ratio, to increase pDNA binding affinity and without trithiocarbonate chain-end.

To summarize, this work established efficient pathways to synthesize a small library of innovative PEGylated cationic copolymers containing primary and tertiary amine-based repeating units by combining efficient and versatile organic reactions with RAFT polymerization processes. The combination of a primary and tertiary amines entities allows to tune both the binding of pDNA affinity and cytotoxicity. Furthermore, PEGylation increases cell viability, leading to non-toxic cationic copolymers.

With these non-toxic poly(aminoethyl acrylates) copolymers in hand, investigation of the influence of PEGylation and DMAEA/AEA ratio on polymer degradation, zeta potential, polyplex size, and stability and transfection efficiency will be continued in the next future. Furthermore, it is expected that the addition of a recognition ligand will increase the transfection efficiency of these copolymers by increasing cellular uptake. Thanks to the methodologies implemented during this work and results using model reactions, the recognition ligand can be efficiently introduced into the non-toxic PEGylated cationic copolymer chains using photochemically-activated thiol-yne coupling.

References

(1) Dondoni, A.; Marra, A. Metal-Catalyzed and Metal-Free Alkyne Hydrothiolation: Synthetic Aspects and Application Trends: Metal-Catalyzed and Metal-Free Alkyne Hydrothiolation. *European Journal of Organic Chemistry* **2014**, *2014* (19), 3955–3969.

(2) Amir, R. J.; Albertazzi, L.; Willis, J.; Khan, A.; Kang, T.; Hawker, C. J. Multi-Functional Trackable Dendritic Scaffolds and Delivery Agents. *Angewandte Chemie (International ed. in English)* **2011**, *50* (15), 3425–3429.

(3) Xu, D.-M.; Yao, S.-D.; Liu, Y.-B.; Sheng, K.-L.; Hong, J.; Gong, P.-J.; Dong, L. Size-Dependent Properties of M-PEIs Nanogels for Gene Delivery in Cancer Cells. *International Journal of Pharmaceutics* **2007**, *338* (1–2), 291–296.

UNIVERSITE BRETAGNE LOIRE

Le Mans Université

Thèse de Doctorat

Maël LE BOHEC

Polyacrylates cationiques PEGylés pour la transfection : synthèse, caractérisation, complexation avec l'ADN et cytotoxicité

PEGylated cationic polyacrylates for transfection: synthesis, characterization, DNA complexation and cyotoxicity

Résumé

Le développement de la thérapie génique dépend des systèmes utilisés pour le transport de gènes vers les cellules eucaryotes. Les systèmes à base de virus sont les plus efficaces. Cependant, il est urgent de trouver une alternative à de tels systèmes viraux pathogènes et oncogènes. Les polymères cationiques sont des vecteurs synthétiques prometteurs ; toutefois, une question cruciale reste en suspens : quelle structure de polymère cationique visée pour une efficacité de transfection élevée et une faible cytotoxicité ? Face à ce questionnement scientifique, de nouveaux polymères cationiques offrant une grande flexibilité en termes de structure et de fonctionnalité sont développés dans cette thèse. Les différents paramètres structuraux pertinents étudiés sont : (i) des entités amines primaire et tertiaire pH-sensibles pour la complexation de l'ADN et pour la libération des polyplexes ADN/polymère, (ii) un groupe alcyne destiné à l'ancrage par chimie click de ligands capables de viser des récepteurs spécifiques de membrane cellulaire pour une reconnaissance efficace des cellules, (iii) des entités polyacrylates à « charge modulable » pour libérer l'ADN et diminuer la cytotoxicité du polymère et (iv) un poly(oxyde d'éthylène) (PEGylation) pour une meilleure stabilité en milieu physiologique et une meilleure biocompatibilté. L'élaboration de tels polymères cationiques est réalisée par combinaison de deux réactions : la polymérisation radicalaire contrôlée RAFT et la réaction click de couplage thiol-yne. Une bibliothèque de polymères cationiques possédant différents paramètres structuraux et différentes fonctionnalités a ainsi été élaborée dont les relations structure/complexation et structure/cytotoxicité ont été étudiées.

Mots clés
Polymères cationiques, Polyacrylates, PEGylation, Polymérisation RAFT, Chimie click thiol-yne, Cytotoxicité, Polyplexe ADN/polymére

Abstract

The clinical success of gene therapy is really dependent on the development of new efficient gene transfer systems. Viral-based gene transfer systems are remarkably efficient in transfecting body cells. However, viral-based systems raised some concerns in terms of immunogenicity, pathogenicity, and oncogenicity. Cationic polymers are promising candidates as they show low host immunogenicity, are cheaper and easier to produce in a large scale than viral ones. However, a crucial question is still pending: which cationic polymer structures and functionalities give the highest transfection efficiency and the lowest cytotoxicity? In dealing with this scientific issue, new cationic polymers with key structural parameters and functionalities were developped during this PhD thesis. The key structural features studied are : (i) pH sensitive primary and tertiary amine entities for DNA complexation and to ensure the endosomal escape, (ii) an alkyne group to attach ligands capable to target specific cell membrane receptors for an efficient cell recognition and receptor-mediated cellular uptake, (iii) "charge-shifting" amino-based polyacrylates for DNA release and to decrease cytotoxicity and (iv) PEG chains (PEGylation) to achieve high stability, longer circulation in physiological conditions and a better biocompatibility. The synthesis of such multi-structural cationic polymers has been achieved through the combination of RAFT polymerization and thiol-yne click coupling reaction. The structure/complexation and the structure/cells viability relationships have been investigated during this work.

Key Words
Cationic polymers, Polyacrylates, PEGylation, RAFT polymerization, Thiol-yne click chemistry, Cytotoxicity, Polyplex DNA/polymer